E I S A
European Institute for Sciences and Their Applications

Workshop on Connecting Insights in Fundamental Physics:

Standard Model and Beyond

August 31 - September 11, 2019

Highlights from ATLAS

Louis FAYARD (LAL Orsay)

on behalf of the ATLAS Collaboration

- ♪ ***Historical introduction , Setting the stage***
- ♪ ***Results from (****Run-1 and* ***) Run-2***
- ♪ ***Future of ATLAS , Run-3 , HL-LHC***
- ♪ ***Conclusions***
- ♪ ***Backup***

see also recent conferences

Presentation by Andreas Hoecker

LP2019

Presentation by Pierre Savard

Large number of results !

I will be selective with only few details !

For more results : look at backup and references

I will insist more on raw results (less on phenomenological interpretations)

Rien n'est cru si fermement que ce que l'on sait le moins

Nothing is believed more strongly that which we know the least

Montaigne, Essais

- ***Historical introduction , Setting the stage***
- ***Results from (run 1 and) run 2***
- ***Future of ATLAS , run 3 , HL-LHC***
- ***Conclusions***
- ***Backup***

Spontaneous Symmetry breaking

The Brout-Englert-Higgs mechanism

The LHC

in a 

1950 Ginzburg-Landau (Meissner-Ochsenfeld effect → London penetration length ~ W mass
→ Pippard coherence length ~ H mass)

1959 Nambu
1960 Goldstone, Gell-Mann Levy, NJL
1961 Schwinger
1962 Anderson
1964 Brout, Englert, Higgs, Guralnik,Hagen,Kibble
1967 Weinberg, Salam Faddeev,Popov
1970 Glashow, Iliopoulos,
Maiani, 't Hooft, Veltman, BRST…..

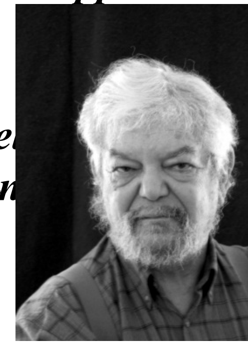


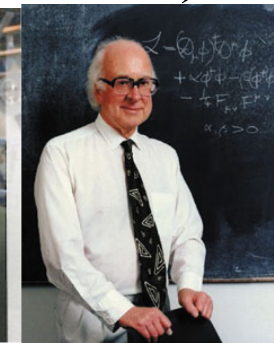

particles of mass $\sqrt{-2\mu_0^2}$

1983 Rubbia, van der M… discovery of W and Z at CERN
1984 Spi… Lausanne


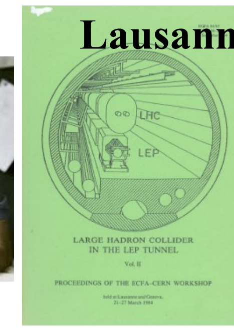

1989 constructi…
beginning…

1992 LOI of 'la…
1994 TP of ATL…
1995 discovery …)
1996 approval o…
1998
approval o… ALICE)
1999 ATLAS Ph… LEP data ended in
2000
2006
2008 CMS Phys…
2010 ATLAS E…
start-up a…
2012 4th July discovery of boson (m ~ 125 GeV) Tevatron data ended in Sept 2011
2013 boson like properties Nobel prize to Englert and Higgs
2014

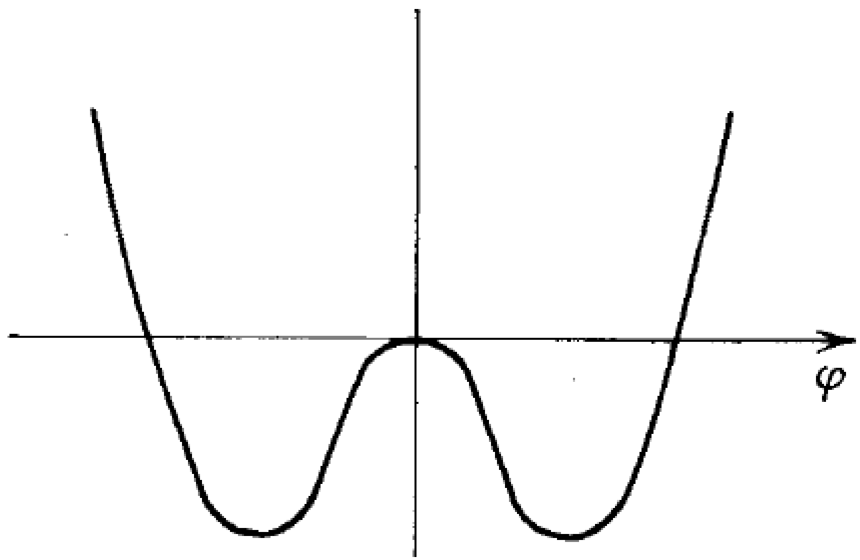

$$\frac{\mu_0^2}{2}\varphi^2 + \frac{\lambda_0}{24}\varphi^4$$

2008

10th september 2008 : first beams around
19th september 2008 : incident

14 months of major repairs and consolidation
New Quench Protection system

2009

20th november 2009 : first beams around (again)
december 2009 : collisions at 2.36 TeV cms

January 2010 : decided scenario 2010-11 7 TeV cms
instead of 14 TeV

2010

30th march 2010 : first collisions at 7 TeV cms
august 2010 : luminosity of 10^{31} cm^{-2} s^{-1}

may 2011 : luminosity > 10^{33} cm^{-2} s^{-1}
november 2011 : integrated luminosity ~ 5 fb^{-1}
13^{th} december 2011 : first 'signal' around 126 GeV

2011

march 2012 : start again at 8 TeV
(50 ns between bunches)
4^{th} July 2012 : evidence for a new boson
(8 TeV integrated luminosity ~ 6 fb^{-1})

2012

2013

(Standard-Model) boson-like properties
peak luminosity 7 10^{33} cm^{-2} s^{-1}
integrated luminosity ~ 5+ 20 fb^{-1}

end of Run-1

Muon Spectrometer ($|\eta|<2.7$) : air-core toroids (B ~ 0.5 / 1T in barrel/ end-cap) with gas-based muon chambers Muon trigger and measurement with momentum resolution < 10% up to E_μ ~ 1 TeV

run 1 ATLAS detector

Length : ~ 46 m
Radius : ~ 12 m
Weight : ~ 7000 tons
~10^8 electronic channels
3000 km of cables

3-level trigger reducing the rate from 40 MHz to ~200 Hz

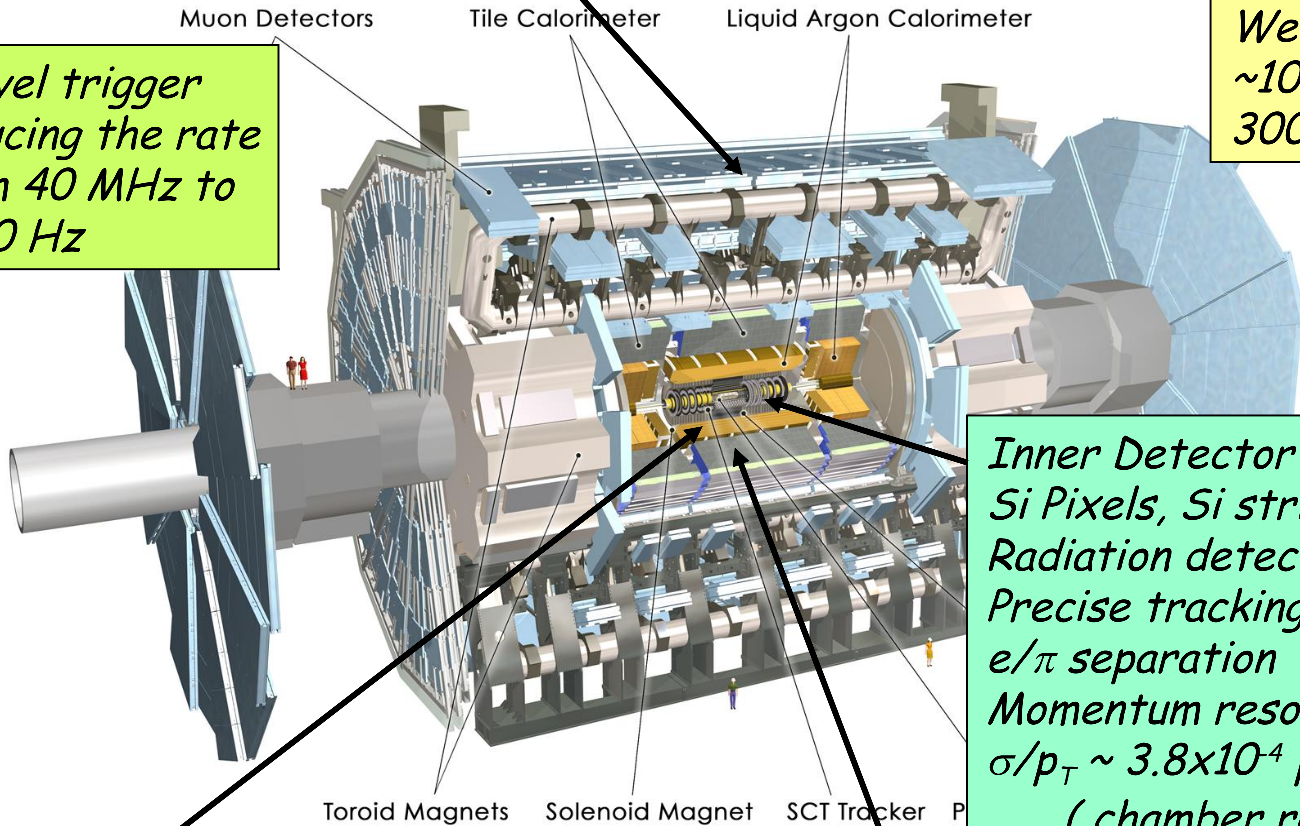

Inner Detector ($|\eta|<2.5$, B=2T):
Si Pixels, Si strips, Transition Radiation detector (straws)
Precise tracking and vertexing,
e/π separation
Momentum resolution:
$\sigma/p_T \sim 3.8\times10^{-4}\, p_T(\text{GeV}) \oplus 0.015$
(chamber resolution ⊕ MS)

EM calorimeter: Pb-LAr Accordion
e/γ trigger, identification and measurement
E-resolution: $\sigma/E \sim 10\%/\sqrt{E}$

HAD calorimetry ($|\eta|<5$): segmentation, hermeticity
Fe/scintillator Tiles (central), Cu/W-LAr (fwd)
Trigger and measurement of jets and missing E_T
E-resolution: $\sigma/E \sim 50\%/\sqrt{E} \oplus 0.03$

C

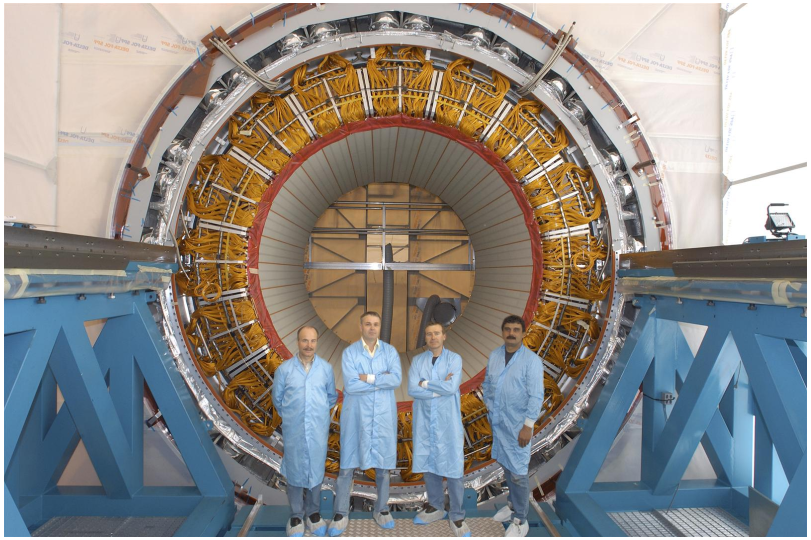

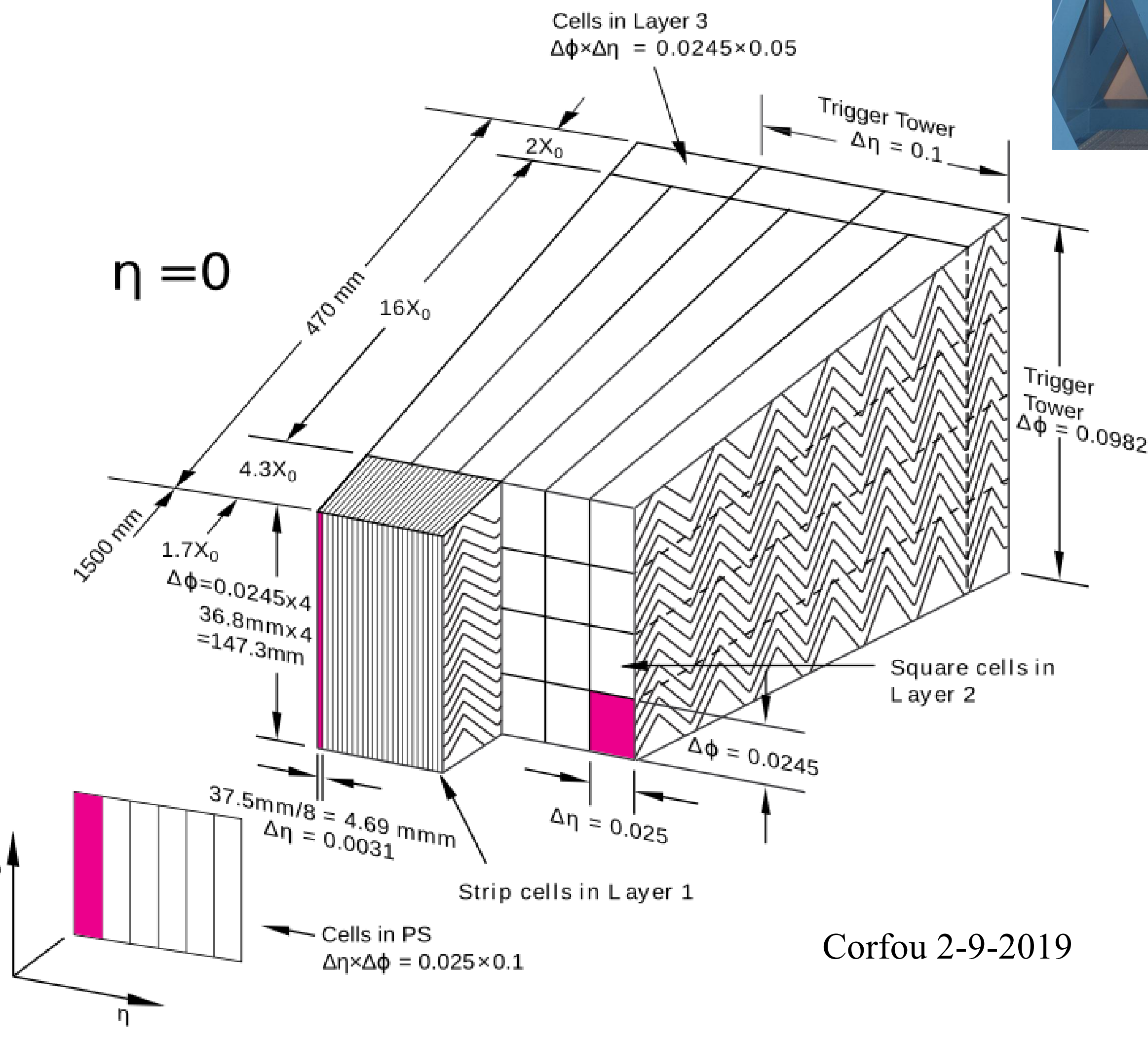

transverse and longitudinal segmentation of the EM ATLAS (Liquid Argon) accordion calorimeter (very stable - about 200 000 channels)

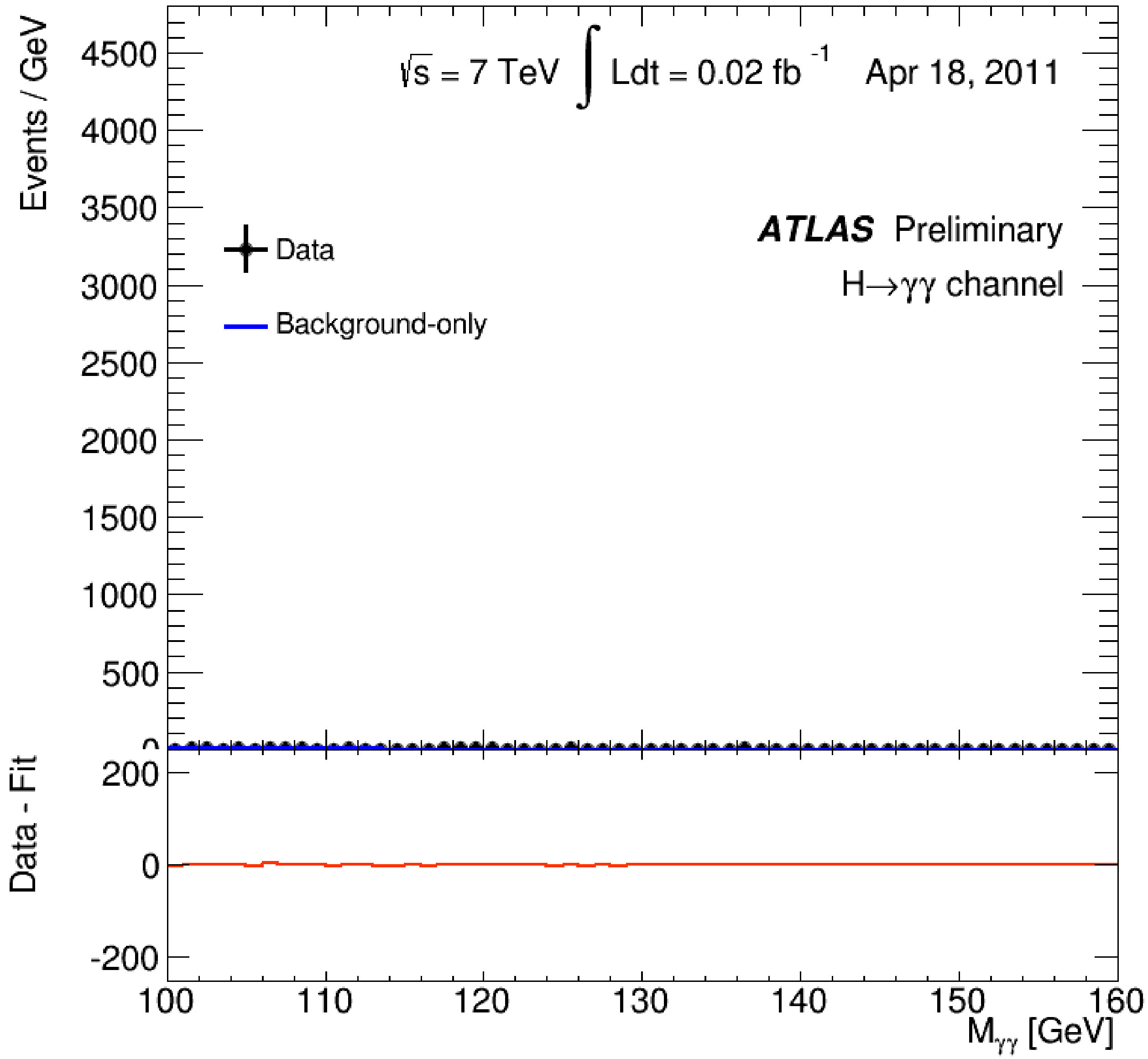

Events / GeV
4500
4000
3500
3000
2500
2000
1500
1000
500
0
$\sqrt{s}$ = 7 TeV $\int$ Ldt = 0.02 fb^{-1} Apr 18, 2011
Data
Background-only
ATLAS Preliminary
H→γγ channel
Data - Fit
200
0
-200
100
110
120
130
140
150
160
$M_{\gamma\gamma}$ [GeV]

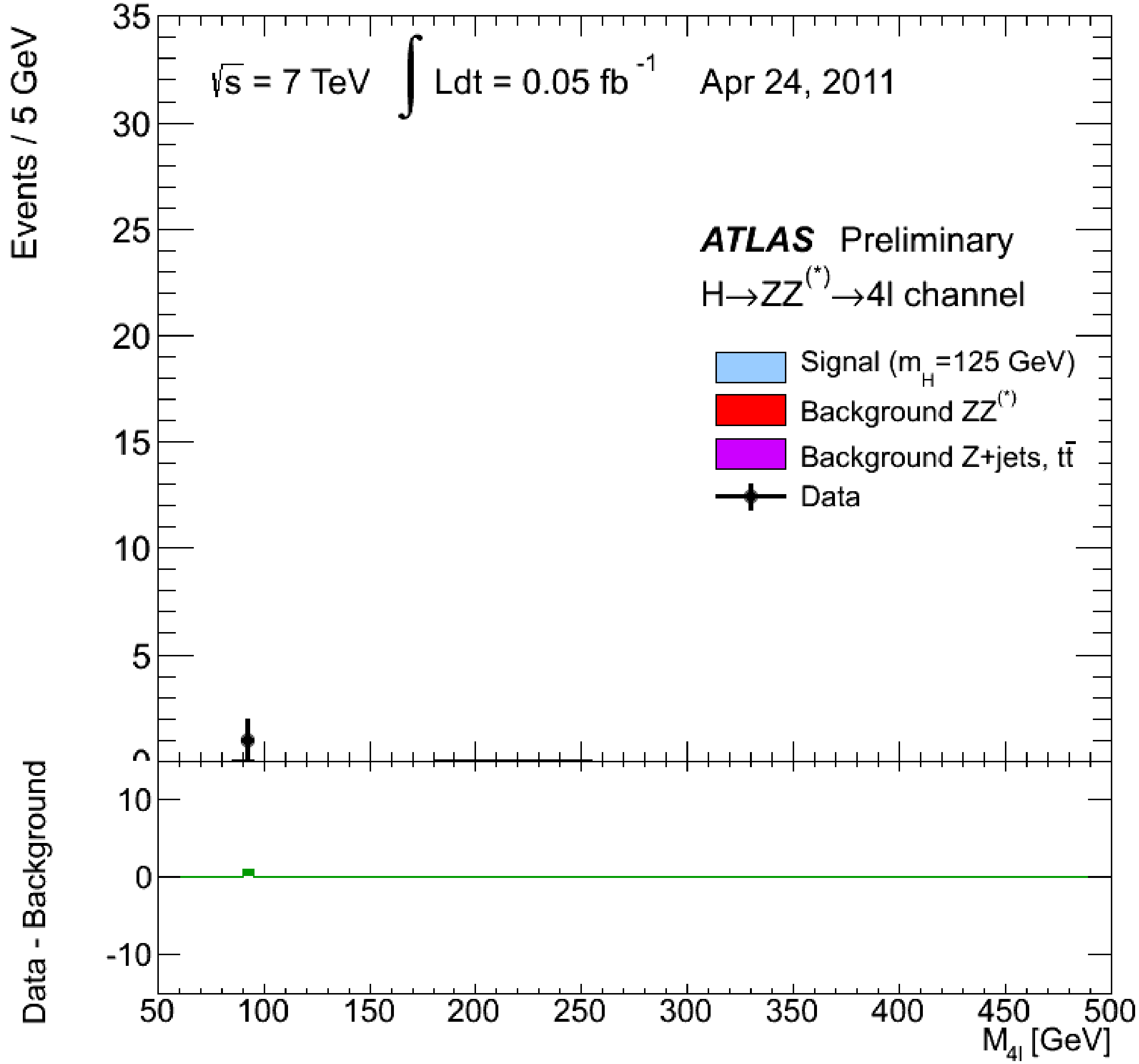

Events / 5 GeV
$\sqrt{s}$ = 7 TeV
$\int$ Ldt = 0.05 fb^{-1}
Apr 24, 2011
ATLAS Preliminary
H→ZZ$^{(*)}$→4l channel
Signal (m_H=125 GeV)
Background ZZ$^{(*)}$
Background Z+jets, $t\bar{t}$
Data
Data - Background
M_{4l} [GeV]

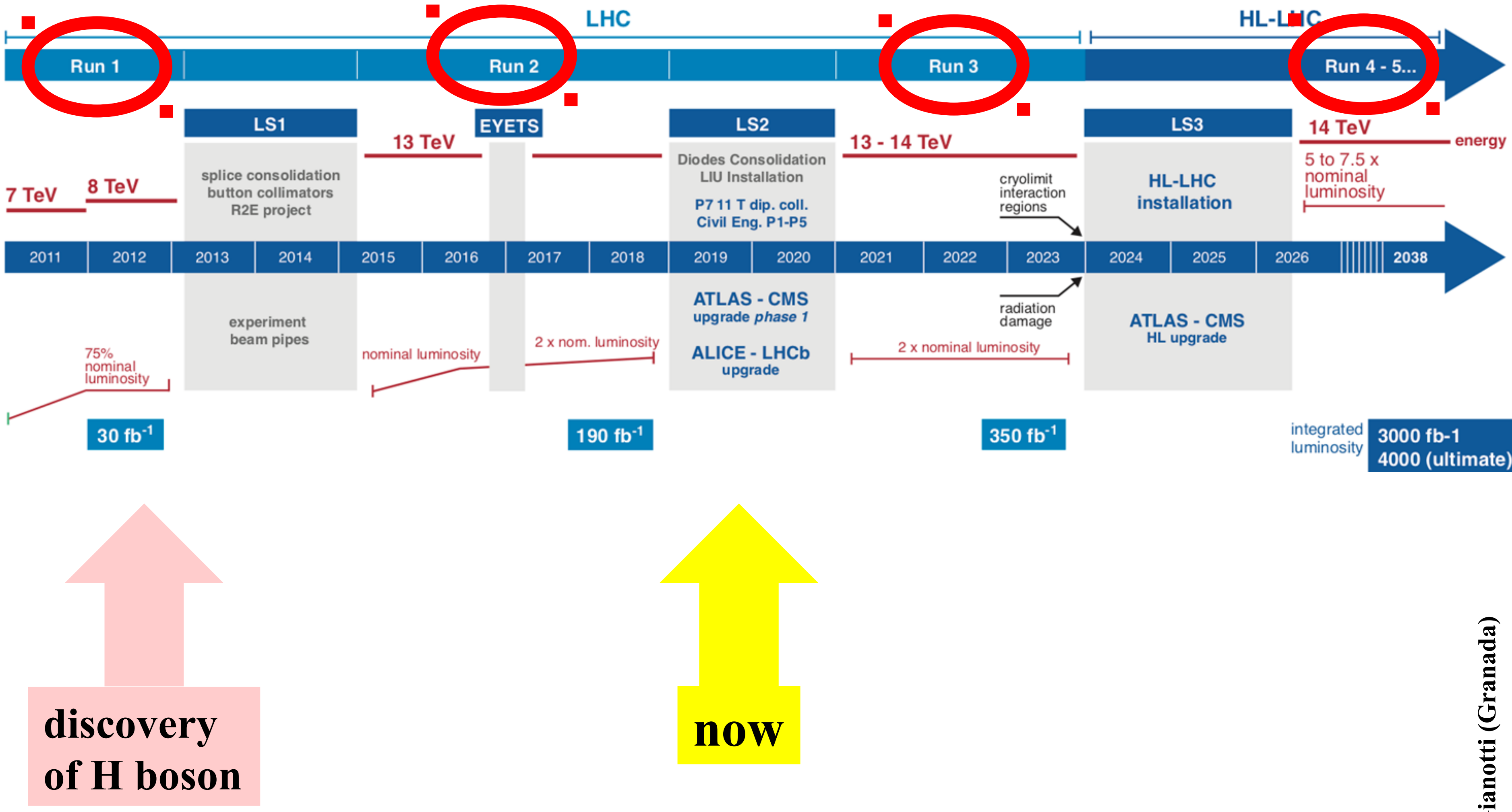
LHC
HL-LHC
Run 1
Run 2
Run 3
Run 4 - 5...
LS1
EYETS
LS2
LS3
7 TeV
8 TeV
13 TeV
13 - 14 TeV
14 TeV
energy
splice consolidation
button collimators
R2E project
Diodes Consolidation
LIU Installation
P7 11 T dip. coll.
Civil Eng. P1-P5
cryolimit
interaction
regions
HL-LHC
installation
5 to 7.5 x
nominal
luminosity
2011
2012
2013
2014
2015
2016
2017
2018
2019
2020
2021
2022
2023
2024
2025
2026
2038
experiment
beam pipes
ATLAS - CMS
upgrade phase 1
ALICE - LHCb
upgrade
radiation
damage
ATLAS - CMS
HL upgrade
75%
nominal
luminosity
nominal luminosity
2 x nom. luminosity
2 x nominal luminosity
30 fb-1
190 fb-1
350 fb-1
integrated
luminosity
3000 fb-1
4000 (ultimate)
discovery
of H boson
now

- ♪ ***Historical introduction , Setting the stage***
- ♪ ***Results from (****Run-1 and* ***) Run-2***
- ♪ ***Future of ATLAS , Run-3 , HL-LHC***
- ♪ ***Conclusions***
- ♪ ***Backup***

♪ ***Results from (*** *Run-1 and* ***) Run-2***

- ***detector***
- ***SM***
- ***BSM***
- ***(B-E)H***
- ***Vector-boson scattering***

short summary

1 > No new physics (yet) *outside the discovery of the H boson*

2> We are entering precision physics area

Large sample of various particles produced in Run-2

W bosons	**$12\ 10^9$**
Z bosons	**$3\ 10^9$**
Top	**$300\ 10^6$**
B quarks	**$40\ 10^{12}$**
BEH bosons	**$8\ 10^6$**

♪ ***Results from (run 1 and) run 2***

- ***detector***
- ***SM***
- ***BSM***
- ***(B-E)H***
- ***Vector-boson scattering***

ATLAS in Run-2

New detectors in Run-2:

- Innermost pixel layer IBL, 3.4cm from interaction point
- Forward proton detectors (one arm in 2016, 210m from IP)

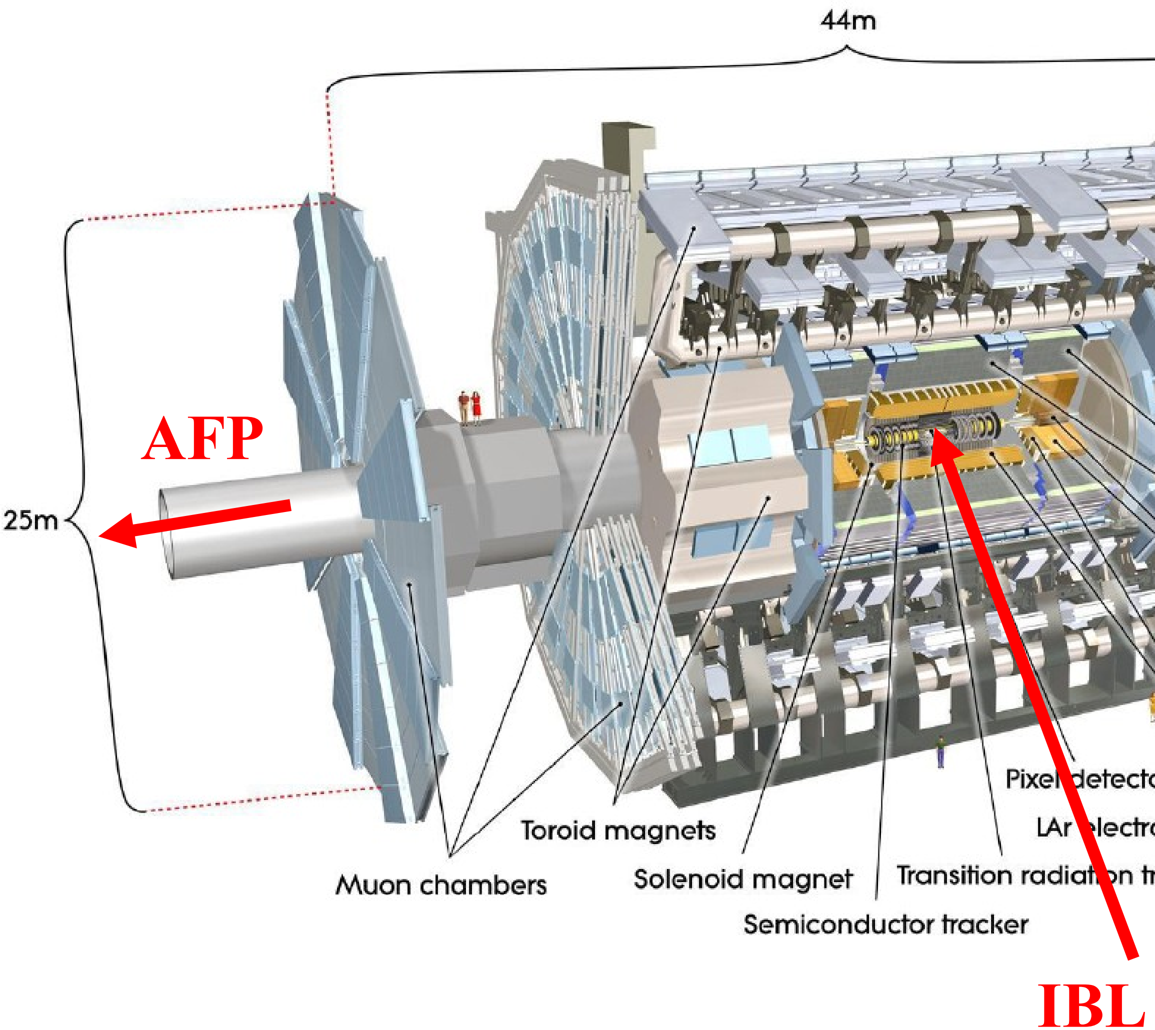

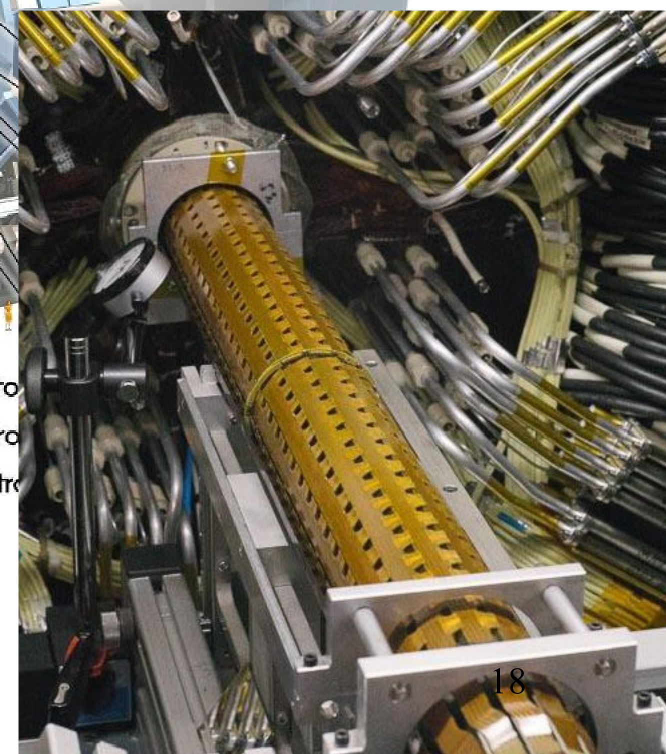

Integrated pp luminosity during Run-2

Also collected Pb-Pb p-Pd Xe-Xe data

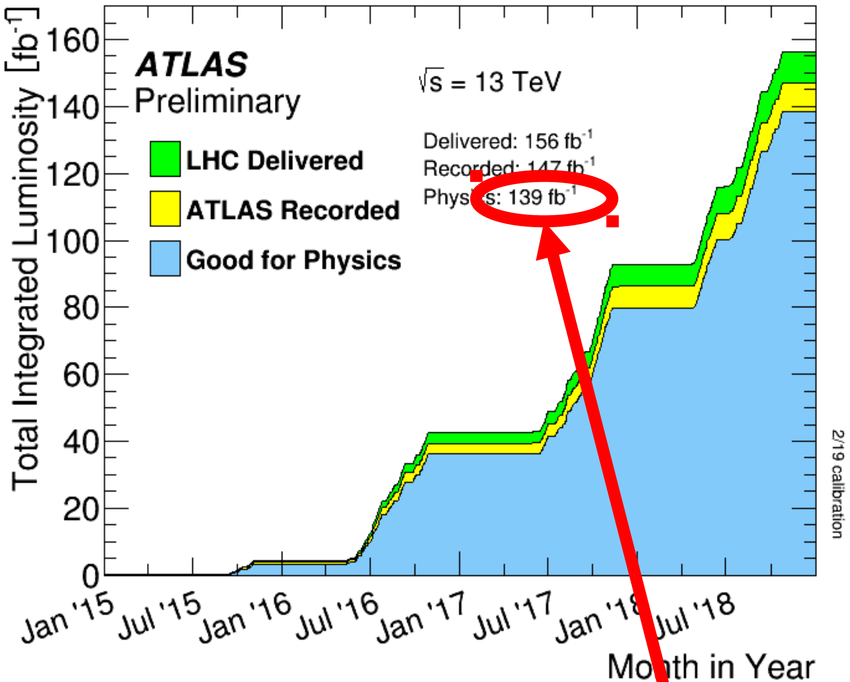

measured to 1.7% precision

(ATLAS-CONF-2019-021)

low μ data for high precision W physics

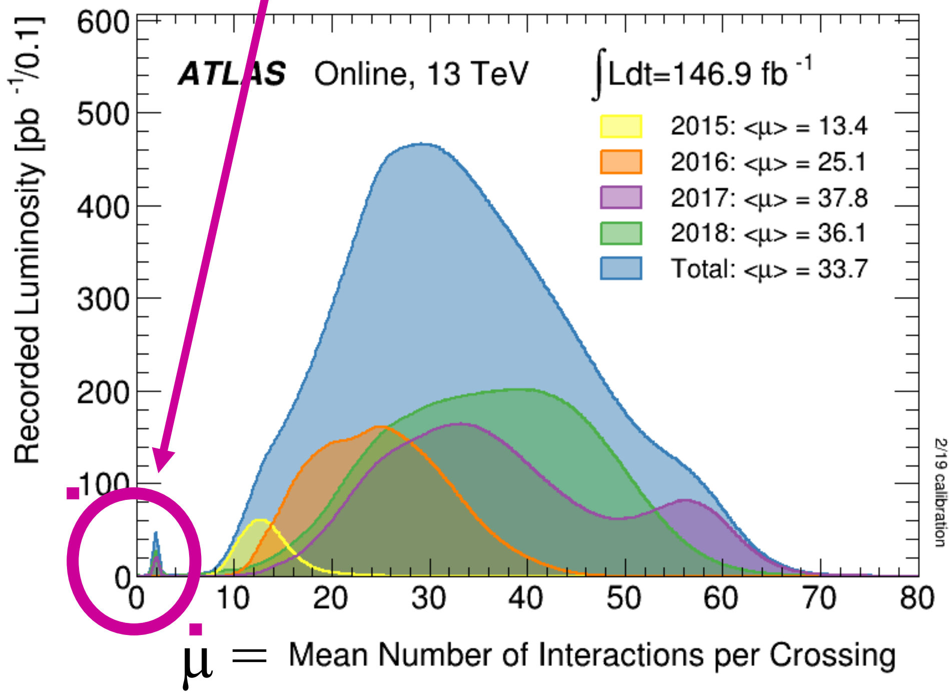

High-luminosity comes with a challenge

All dogmas need to be revisited

Like the fact that the response of the calorimeter is constant w.r.t time

(there are also short time-scale variations due to T change)

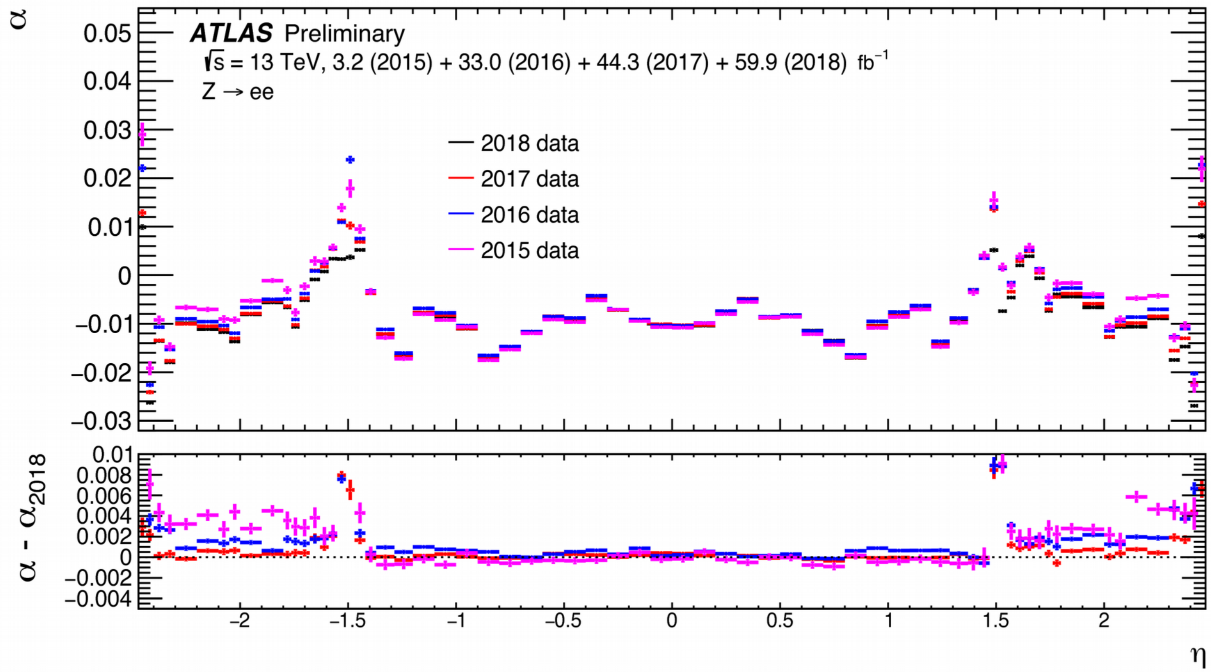

energy mis-calibration defined by α_i: $E^{\mathrm{data}} = E^{\mathrm{MC}}(1+\alpha_i)$

We have a lot of data in order to make precise calibrations

But the needs for precision physics are very important !

https://atlas.web.cern.ch/Atlas/GROUPS/PHYSICS/PLOTS/EGAM-2019-01/fig_02a.png

♪ ***Results from (run 1 and) run 2***

- ***detector***
- ***SM***
- ***BSM***
- ***(B-E)H***
- ***Vector-boson scattering***

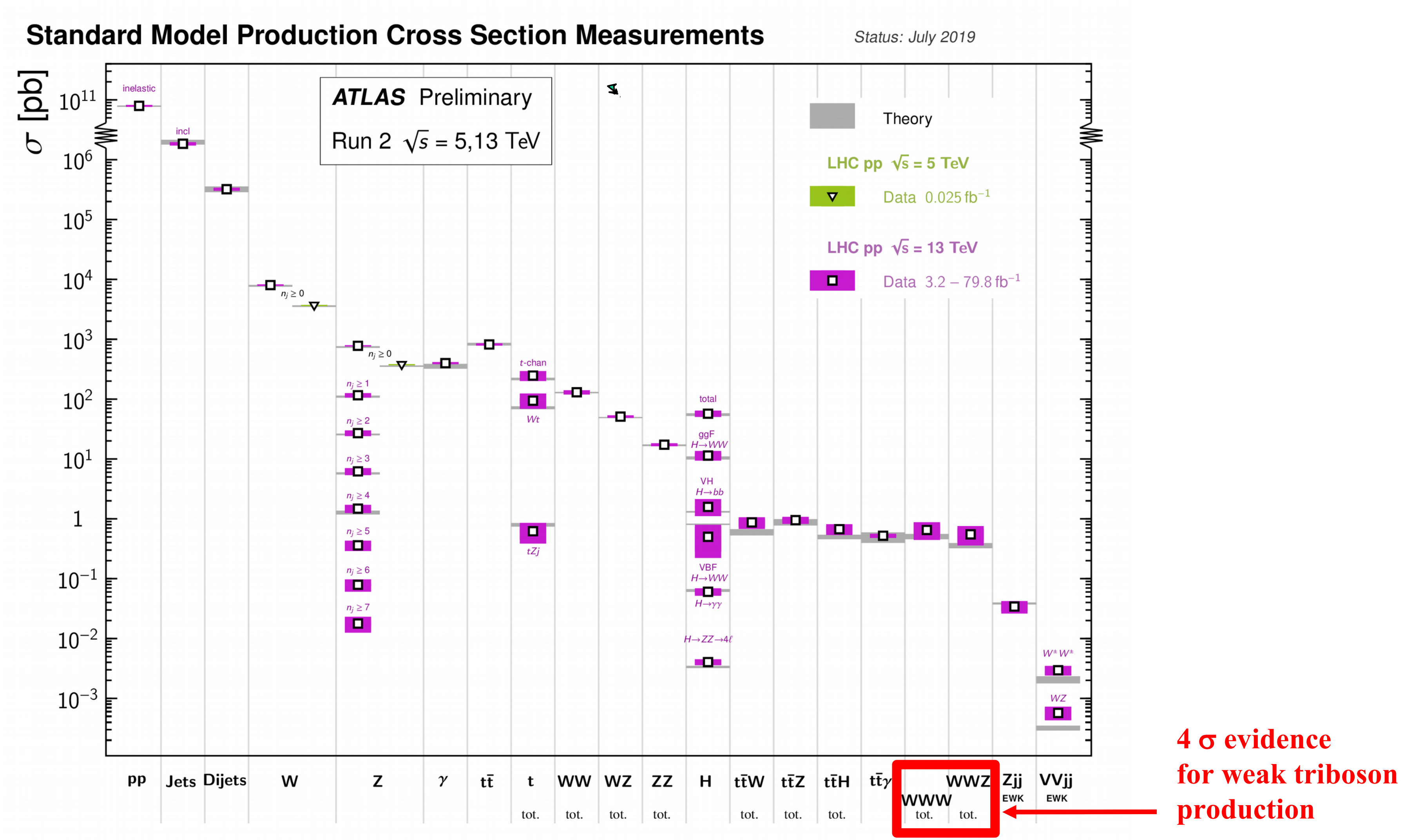

https://atlas.web.cern.ch/Atlas/GROUPS/PHYSICS/PUBNOTES/ATL-PHYS-PUB-2019-024/fig_05.png

Theory agrees so far with the measured cross sections on 15 orders of magnitude

4σ evidence for weak triboson production using 2015-2017 data

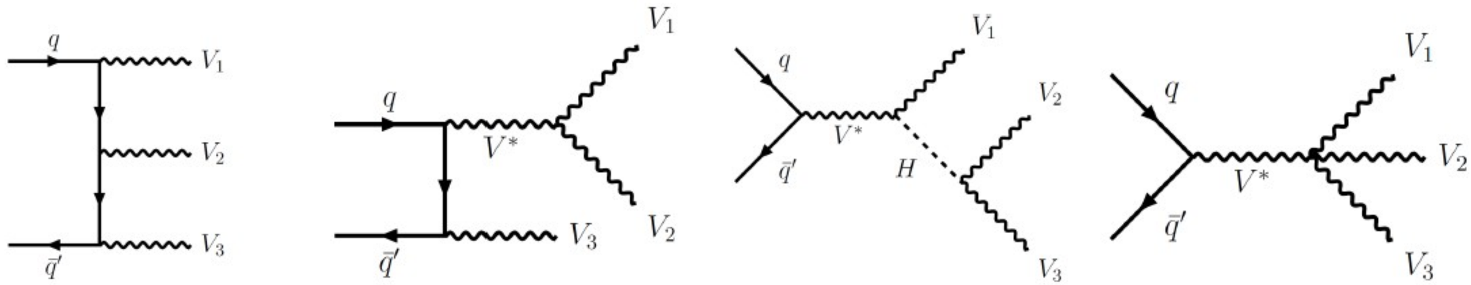

arXiv:1903.10415

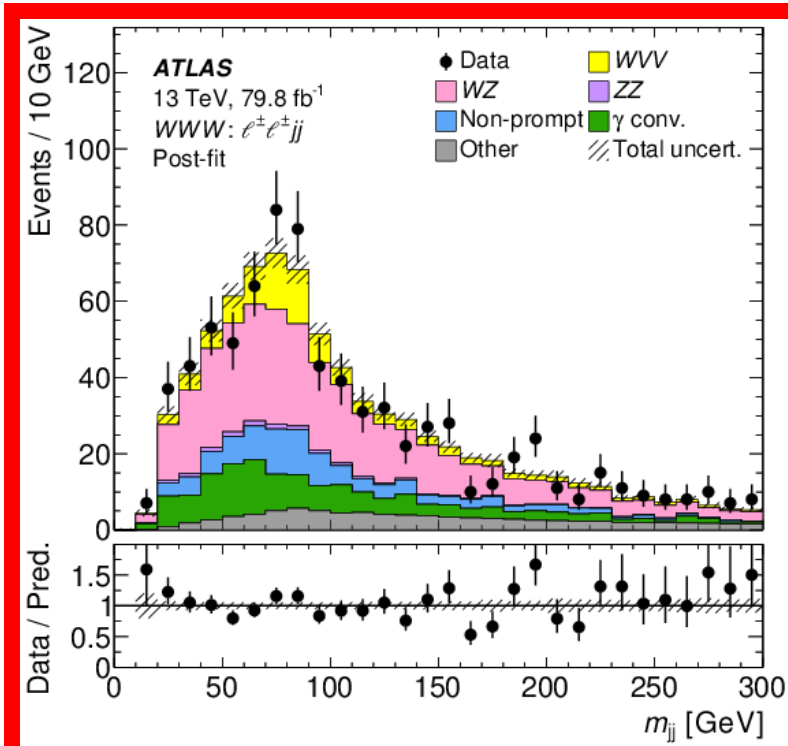

Decay channel	Significance Observed	Significance Expected
WWW combined	3.2σ	2.4σ
$WWW \to \ell\nu\ell\nu qq$	4.0σ	1.7σ
$WWW \to \ell\nu\ell\nu\ell\nu$	1.0σ	2.0σ
WVZ combined	3.2σ	2.0σ
$WVZ \to \ell\nu qq\ell\ell$	0.5σ	1.0σ
$WVZ \to \ell\nu\ell\nu\ell\ell/qq\ell\ell\ell\ell$	3.5σ	1.8σ
WVV combined	4.1σ	3.1σ

For different center-of-mass energies

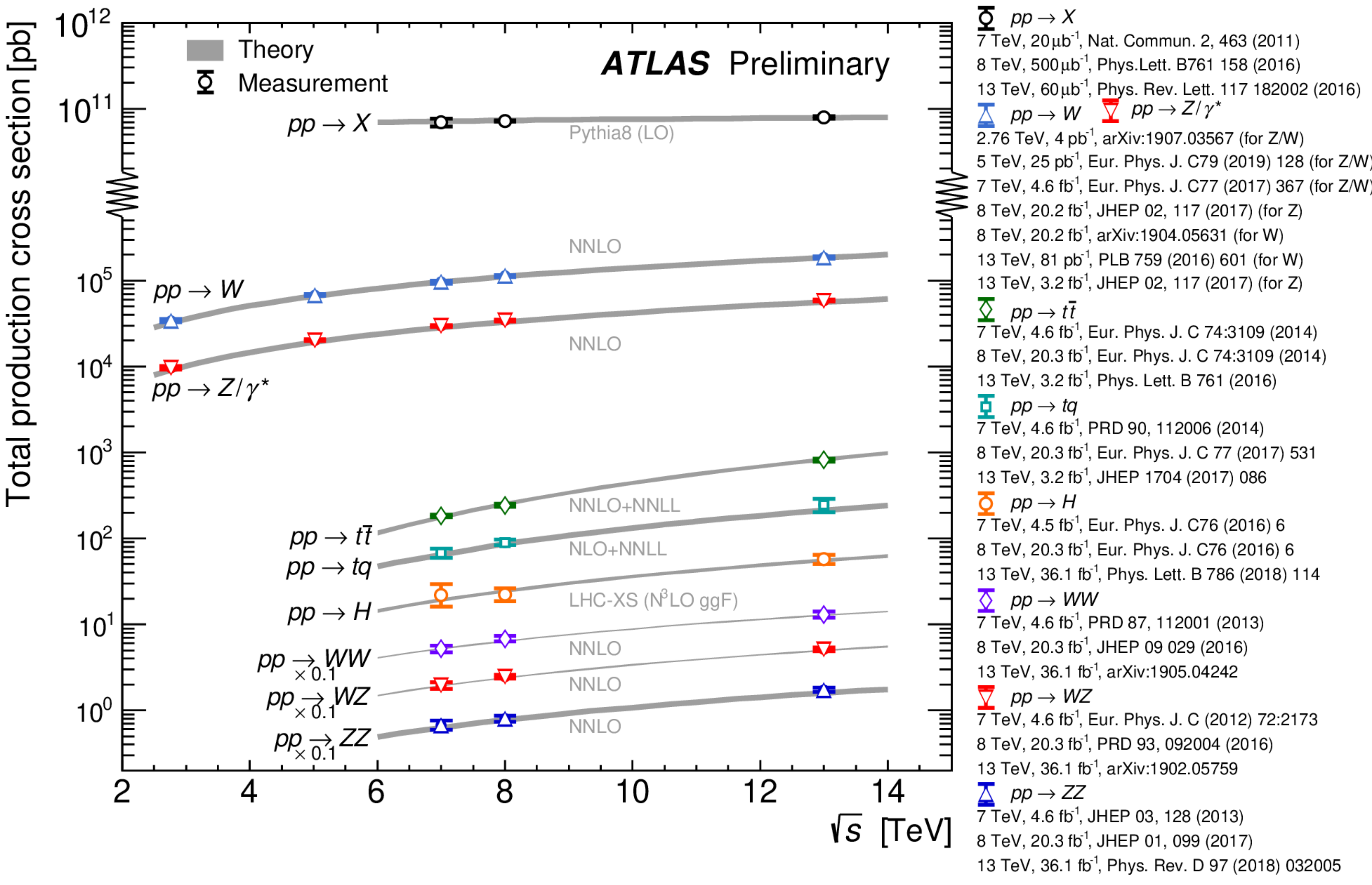

https://atlas.web.cern.ch/Atlas/GROUPS/PHYSICS/PUBNOTES/ATL-PHYS-PUB-2019-024/fig_24.png

Measurement of fiducial and differential W+ W- production cross-sections at √s=13 TeV with the ATLAS detector

Suppress top-quark background

⇒

events containing jets with a transverse momentum exceeding 35 GeV are not included in the measurement phase space

$$WW \rightarrow e^{\pm}\nu\mu^{\mp}\nu$$

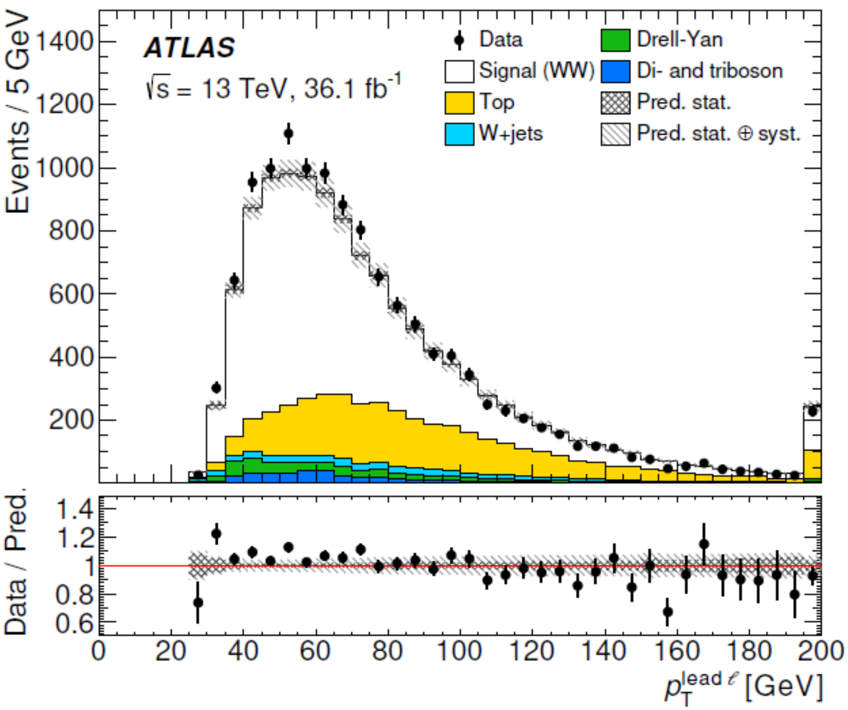

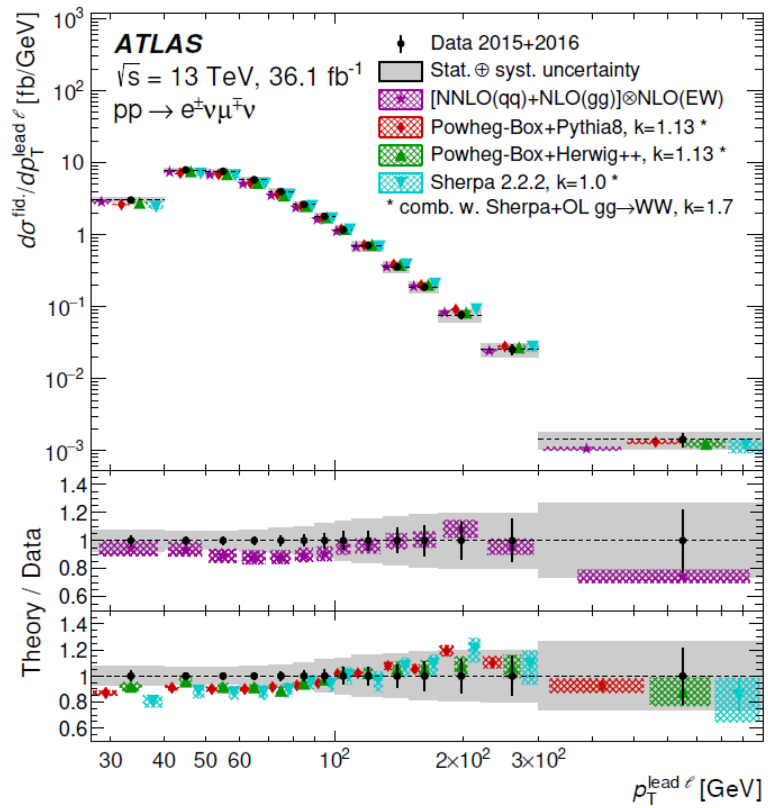

arXiv:1905.04242

Measurement of Z(→l+l-) γ differential cross-sections in pp collisions at √s= 13 TeV with the ATLAS detector

Full Run-2

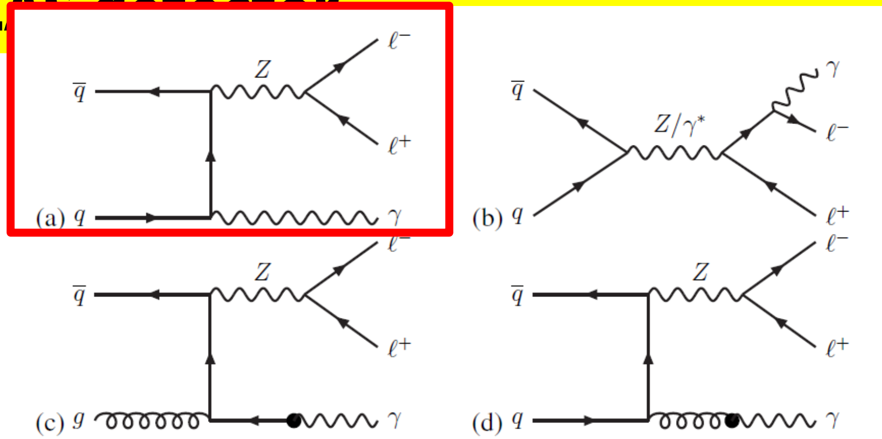

FSR and quark/gluon fragmentation removed (isolation)

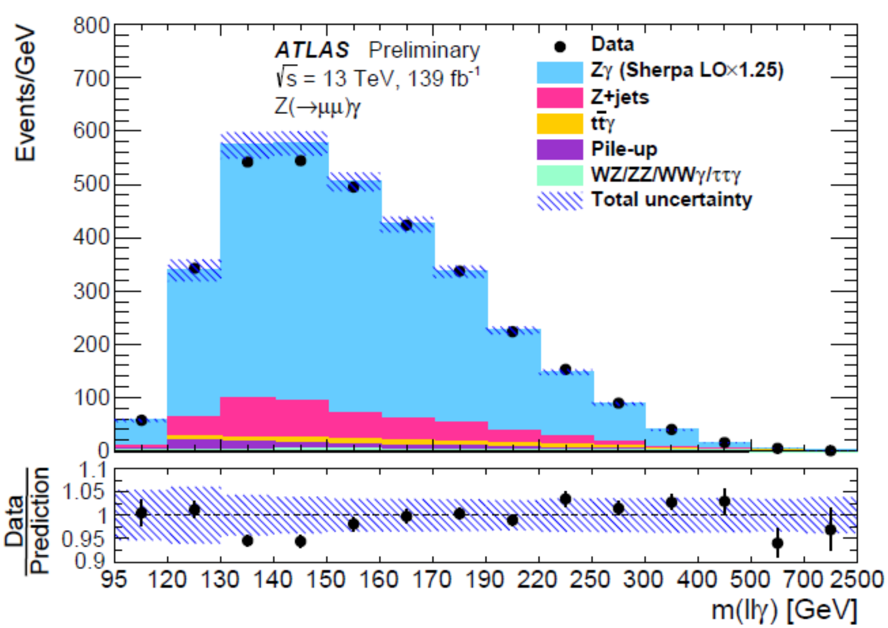

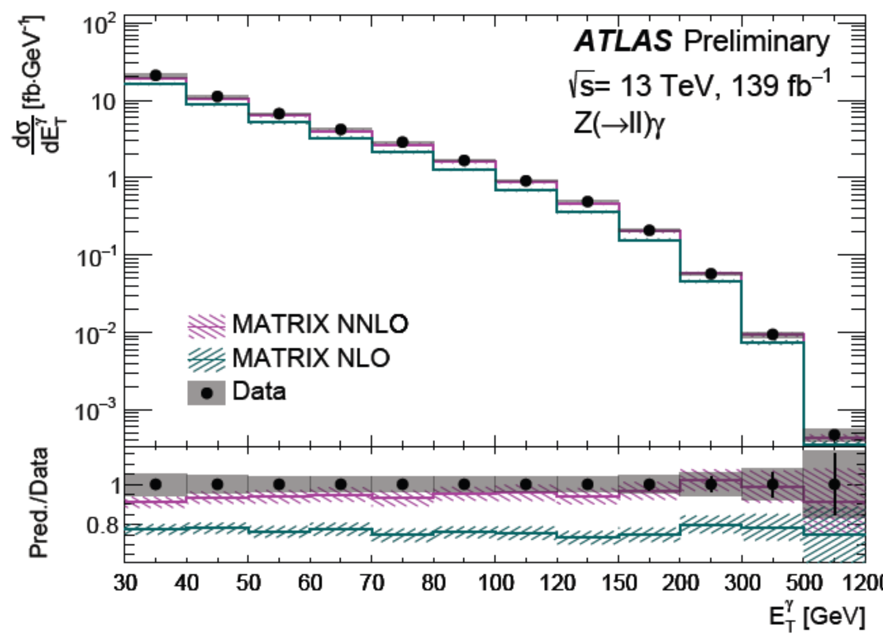

ATLAS-CONF-2019-034

Inclusive and differential measurements of the charge asymmetry in $t\bar{t}$ events at 13 TeV with the ATLAS detector

Full Run-2

a (Tevatron-inspired) central-forward charged asymmetry is defined

$$A_C = \frac{N(\Delta|y| > 0) - N(\Delta|y| < 0)}{N(\Delta|y| > 0) + N(\Delta|y| < 0)}$$

$$\Delta|y| = |y_t| - |y_{\bar{t}}|$$

different from 0 because of interference at NLO

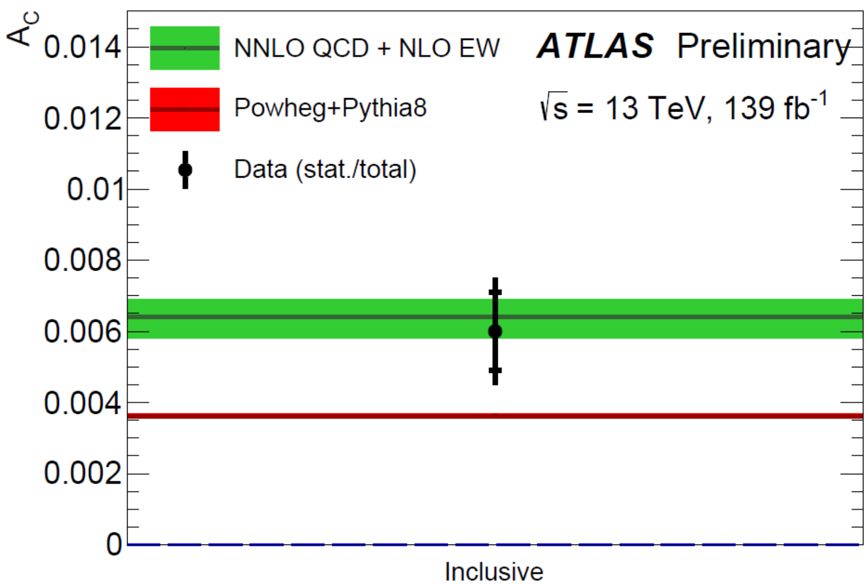

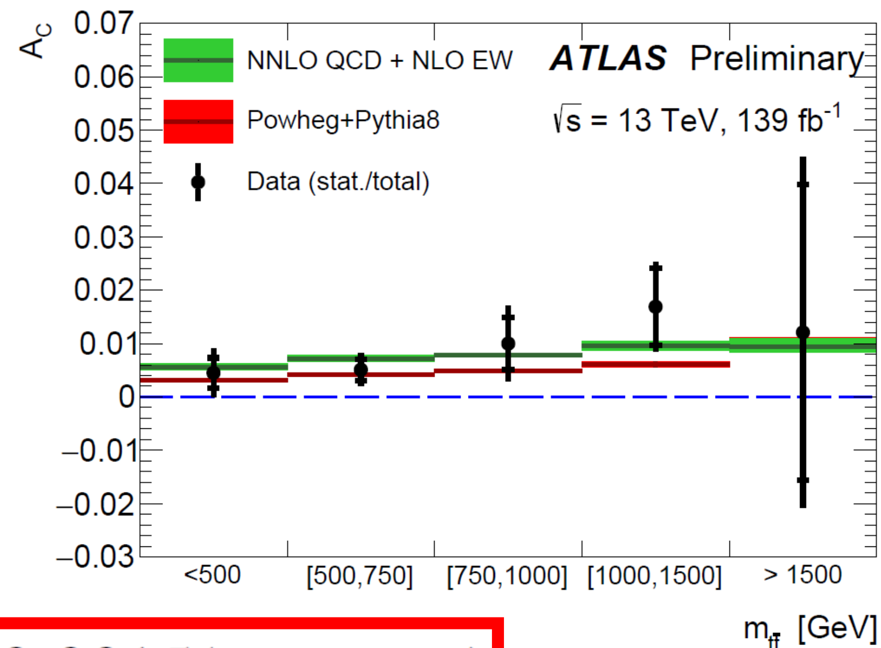

ATLAS-CONF-2019-026

$$A_C = 0.0060 \pm 0.0015(\text{stat+syst.})$$

FCNC (Flavour-Changing Neutral Current)

window for new physics

tqγ 80 fb^{-1} 13 TeV

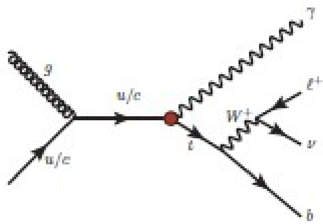

topology
1 e/μ, 1 γ
1 b-jet, MET

B(t→γc) < 2.2 10^{-4} (2.7 10^{-4} exp)
B(t→γu) < 2.8 10^{-5} (4.0 10^{-5} exp)

NN to separate S and B

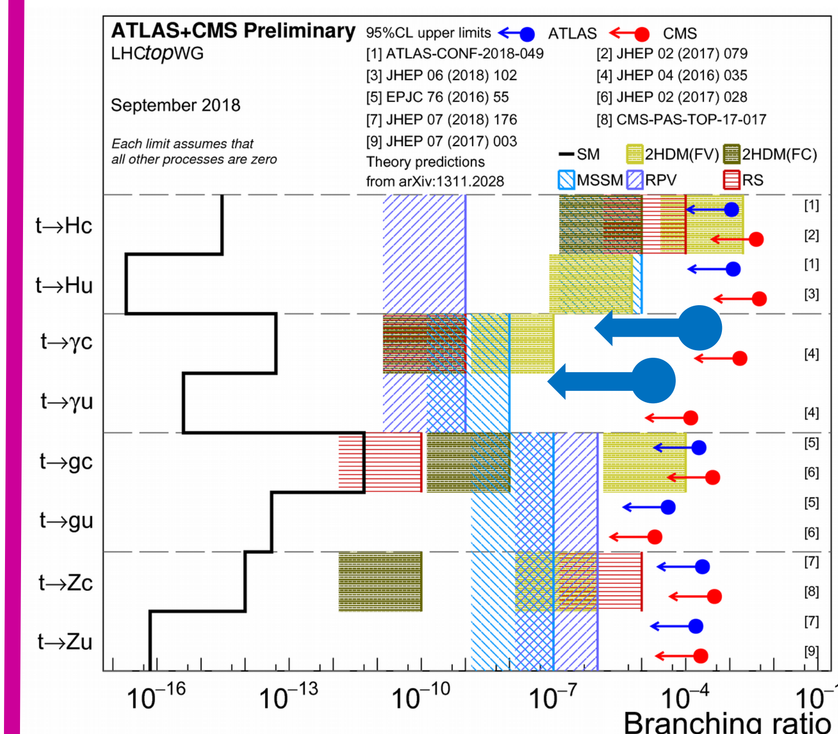

arXiv:1908.08461

t→ Hq 36fb^{-1}

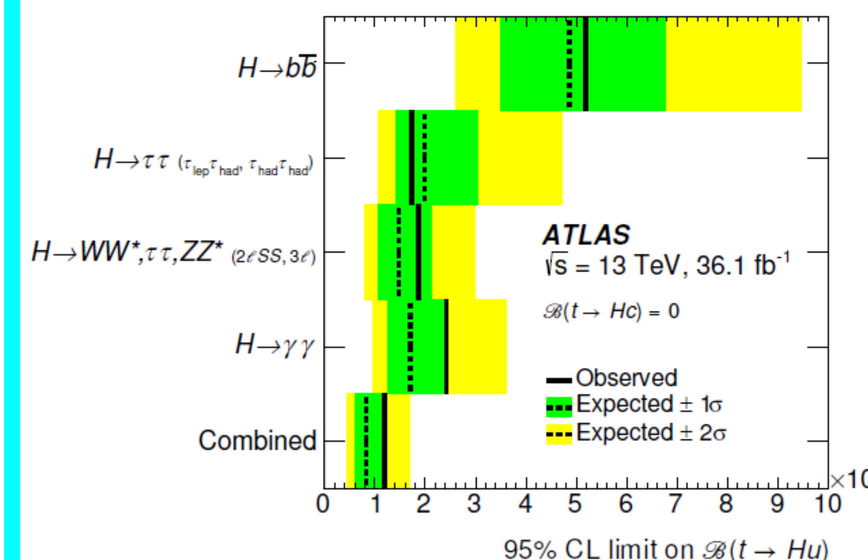

B(t→Hu) < 1.2 10^{-3} (0.8 10^{-4} exp)

JHEP 1905 (2019) 123

Observation of light-by-light scattering in ultraperipheral Pb+Pb collisions with the ATLAS detector

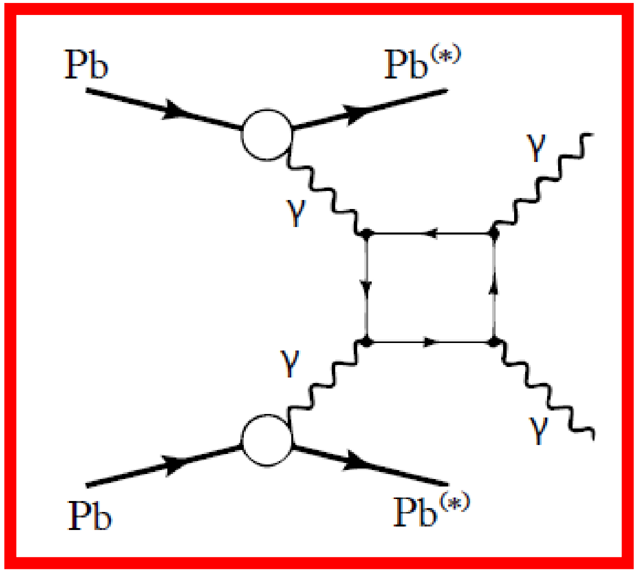

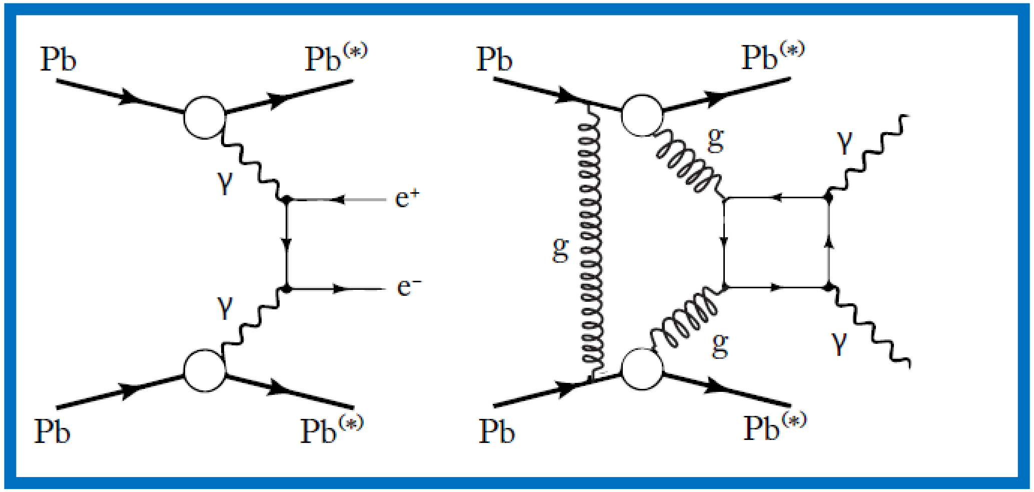

backgrounds

Signal :2 photons with very low $p_T(\gamma\gamma)$
: *< 1 GeV/c* and no further activity in the detector

Field strength up to 10^{25} V/m

γγ luminosity ~ Z^4 ~ 5 10^7

Phys.Rev.Lett. 123 (2019) no.5, 052001

Look at low-energy back-to-back photon pairs with no additional activity in detector

small acoplanarity

$$A_\phi = (1 - |\Delta\phi_{\gamma\gamma}|/\pi) < 0.01$$

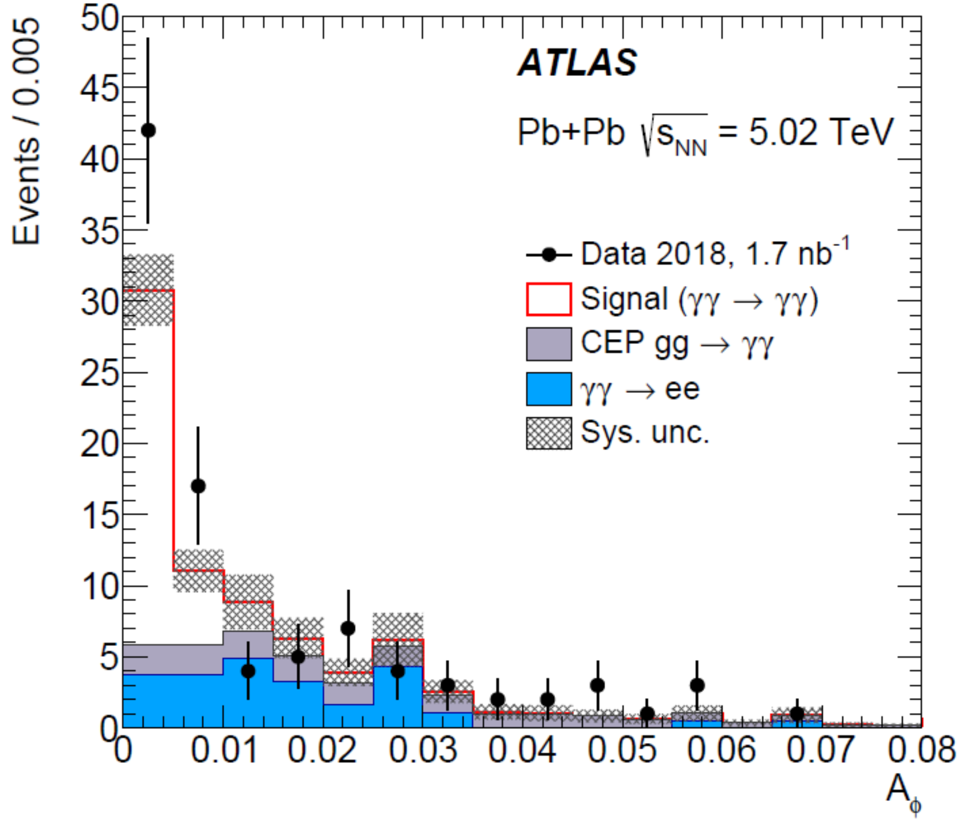

Phys.Rev.Lett. 123 (2019) no.5, 052001

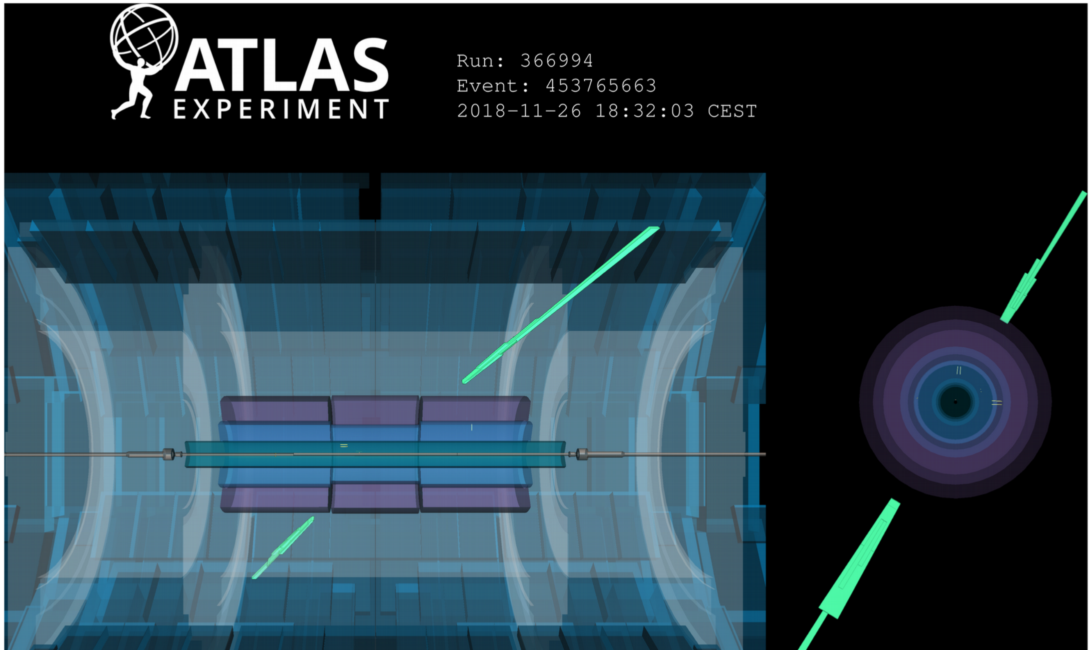

no additional activity in the detector

Event display for an exclusive $\gamma\gamma \to \gamma\gamma$ candidate.

Two back-to-back photons ($E_T^{\gamma 1}$ = 11 GeV and $E_T^{\gamma 2}$ = 10 GeV) with
$m_{\gamma\gamma}$ = 29 GeV, A_φ =0.002
$P_T^{\gamma\gamma}$=1.2 GeV

59 $\gamma\gamma \to \gamma\gamma$ events observed with an expected background of 12±3 (8.2 σ)

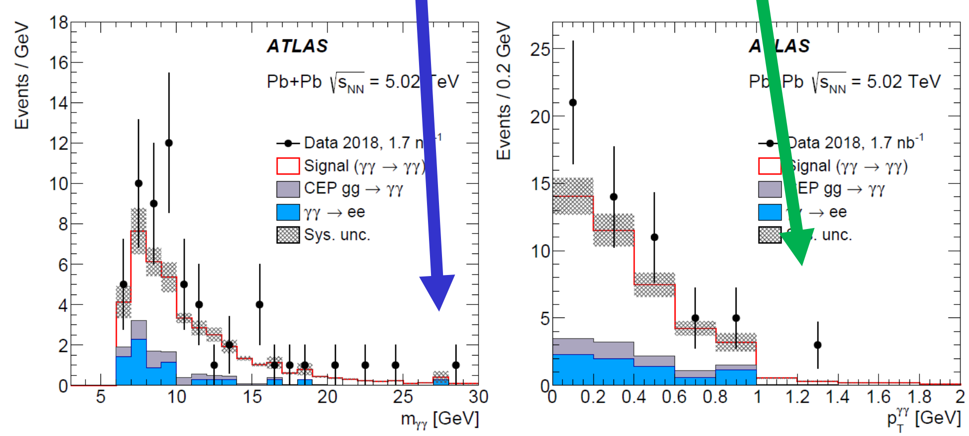

(a) (b)

Phys.Rev.Lett. 123 (2019) no.5, 052001

ATL-CONF-2018-037

EW precision measurements

Weak angle $\sin^2\theta^l_{eff}$ — W mass m_W

8 TeV data — **7 TeV data**

Eur.Phys.J. C78 (2018) no.2, 110, Erratum: Eur.Phys.J. C78 (2018) no.11, 898

One wants to have measurements with uncertainties close to the results of the EW fit $\sin^2\theta^l_{eff} = .23153 \pm .00006$ $m_W = 80354 \pm 7$ MeV

arXiv:1803.01853

F-B asymmetry $q\bar{q} \rightarrow Z/\gamma^* \rightarrow \ell^+\ell^-$

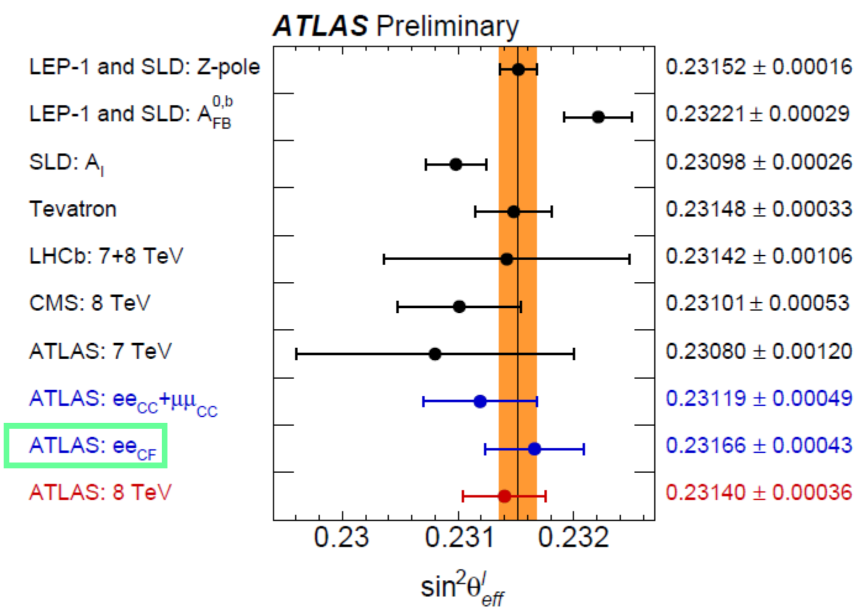

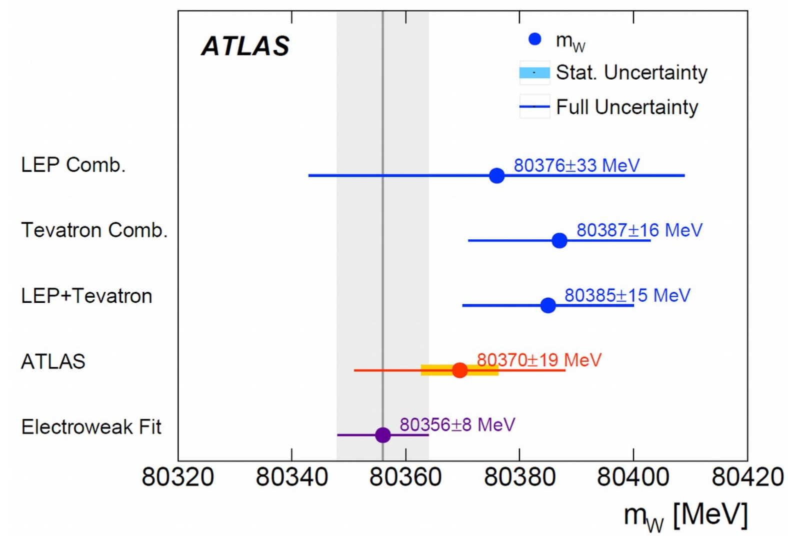

B physics

Run-1 + 26fb[-1] of Run-2

$$\mathcal{B}(B_s^0 \to \mu^+\mu^-) = \left(2.8^{+0.8}_{-0.7}\right) \times 10^{-9}$$

$$\mathcal{B}(B^0 \to \mu^+\mu^-) < 2.1 \times 10^{-10} \quad 95\%\ \text{CL}$$

JHEP 04 (2019) 098

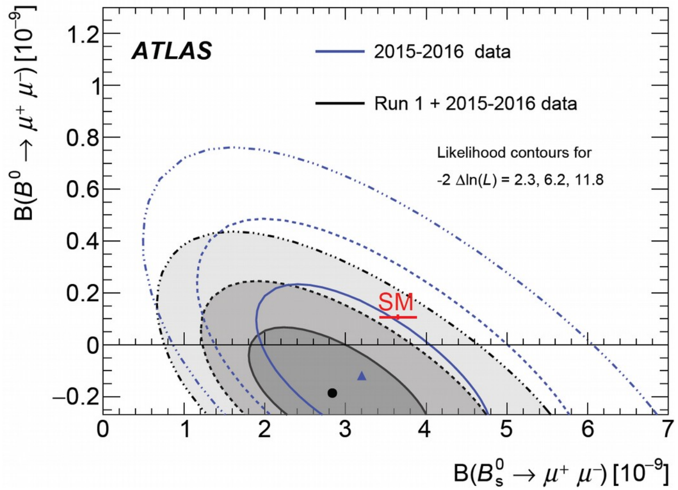

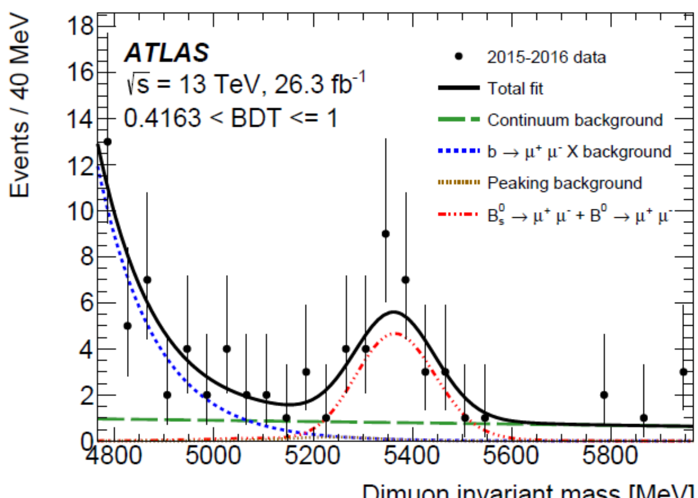

$B_s^0 \to J/\psi\phi$

Measurement of CP-violating phase ϕ_s

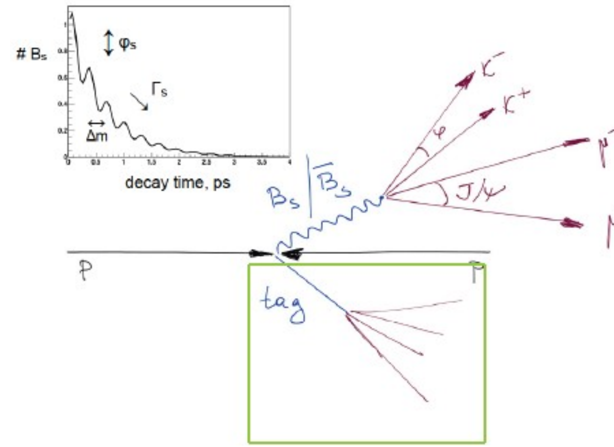

$$\phi_s = -0.076 \pm 0.034\ (\text{stat.}) \pm 0.019\ (\text{syst.})\ \text{rad}$$

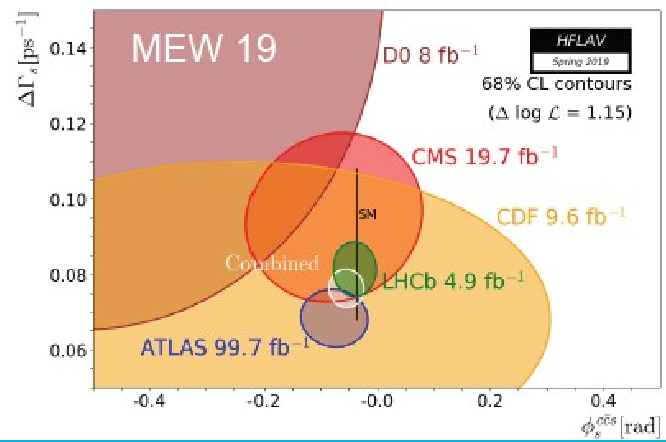

ATLAS-CONF-2019-009 Albrecht@EPS2019

♪ Results from (run 1 and) run 2

* ***detector***
* ***SM***
* ***BSM***
* ***(B-E)H***
* ***Vector-boson scattering***

interlude

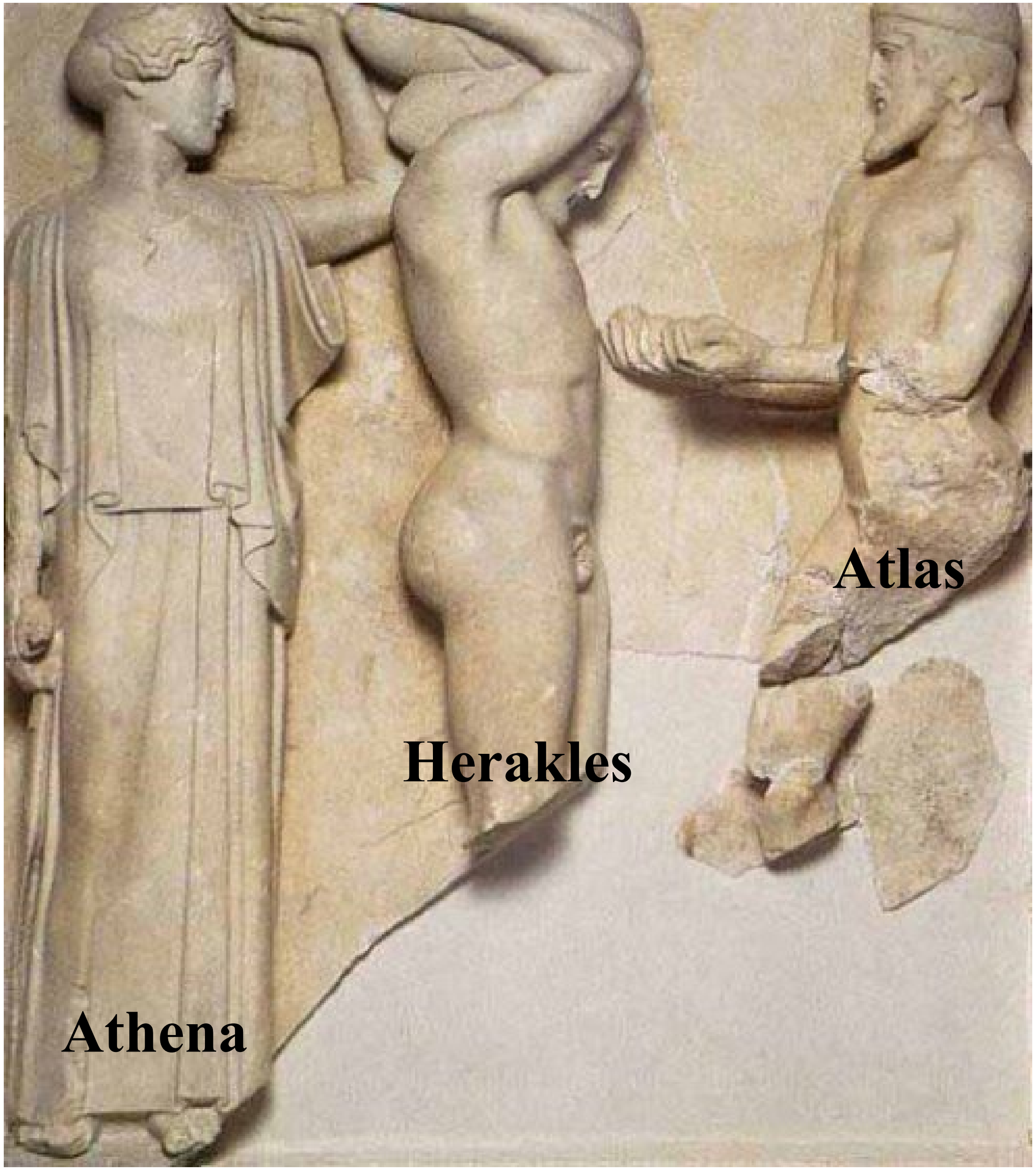

Search for Physics BSM (Beyond the Standard Model)

Some (temporary) rest

in a lot of places
Full Run-2 results

Search for Physics BSM (1)

A vast programme covering searches for high and low mass particles, small couplings, long lived particles, forbidden decays, …

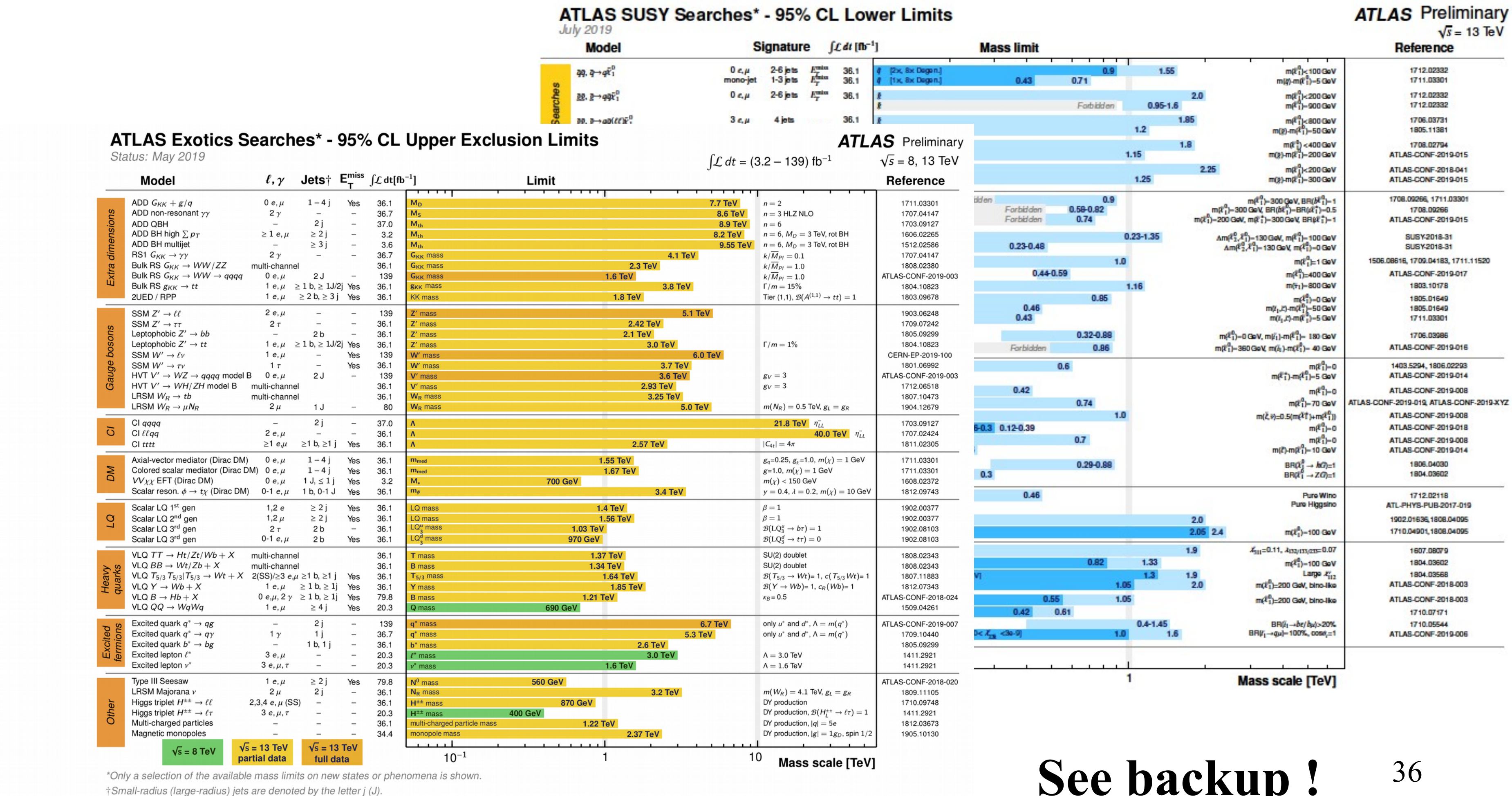

See backup !

Search for Physics BSM (2)

Full Run-2

highest-mass dijet event
the two central high-p_T jets each have p_T of 3.74 TeV their invariant mass is 8.02 TeV.

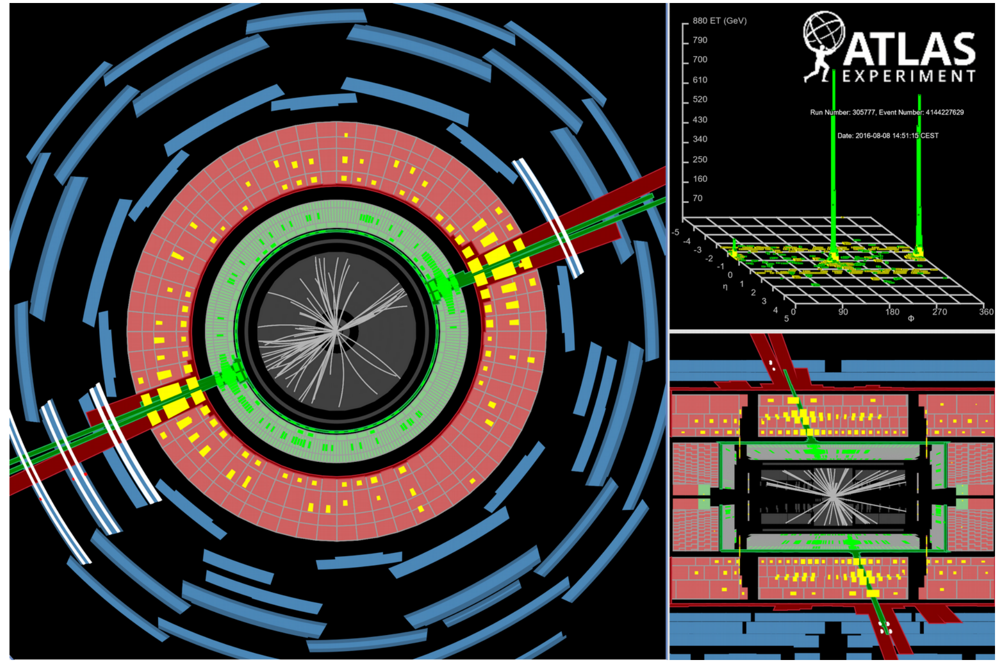

ATLAS-CONF-2019-007

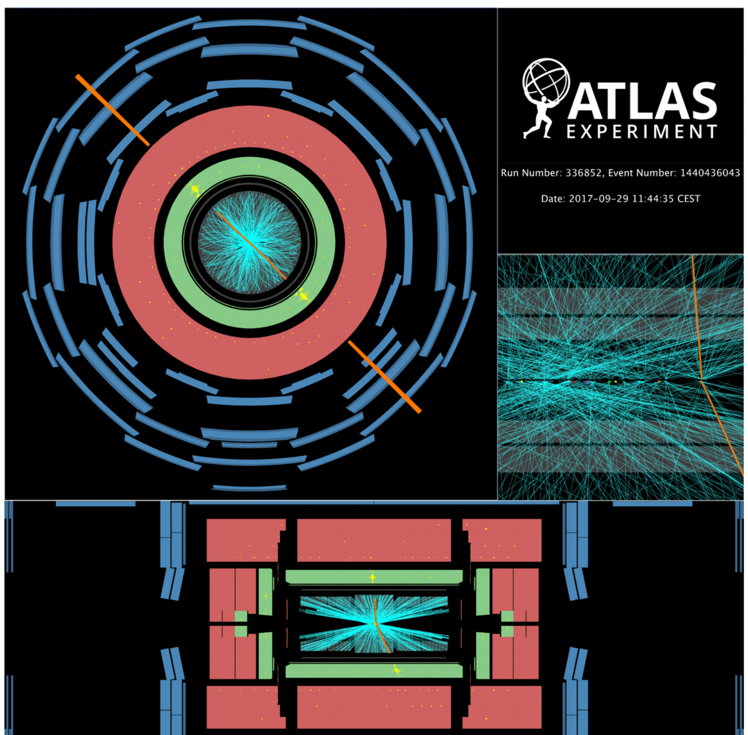

dielectron candidate with the highest invariant mass in the 2015-2018 data taking period with m_{ee} = 4.06 TeV
search for Z' and W'

arXiv:1903.06248 arXiv:1906.05609

Search for Physics BSM (3)

Full Run-2

Analysis and detector improvements very important !

2 b-jets

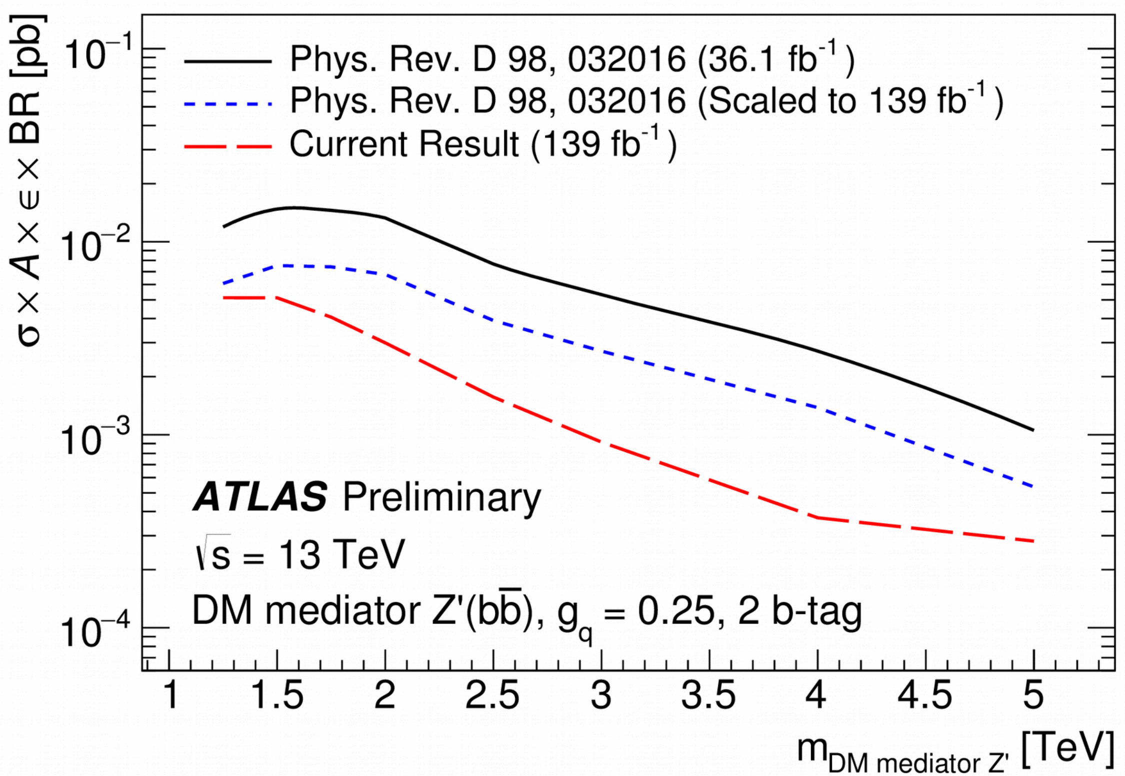

To be published soon see P.Savard @LP

width/mass = 3%

©Nishu priv com

Significant improvement in b-tagging performance at high p_T

Search for Physics BSM (4)

Full Run-2

arXiv:1906.08589

Resonances decaying to VV (WW, WZ, ZZ)

The diboson system is reconstructed using pairs of high transverse momentum, large-radius jets

diboson resonances with masses greater than 1.3 TeV

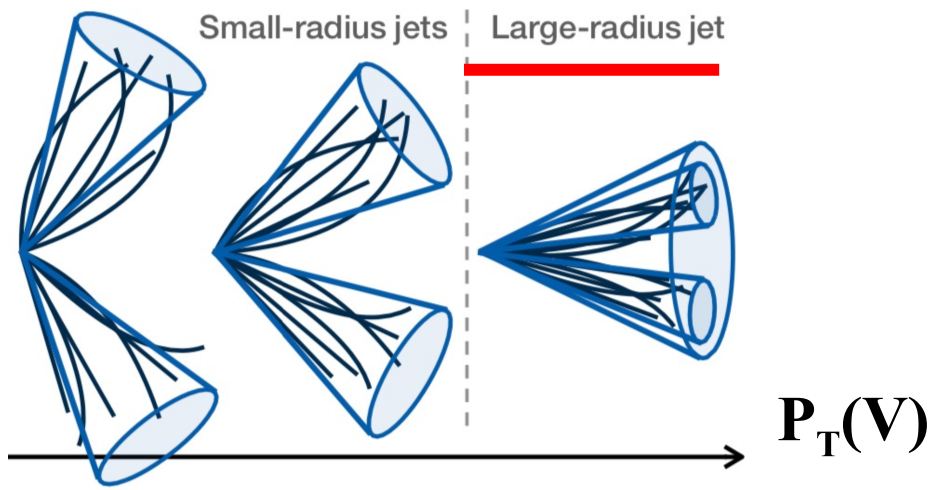

Highest m_{JJ}(=4440 GeV) diboson candidate

The leading (*subleading*) jet has a p_T of 2136 GeV (*2291 GeV*), a mass of 89.5 GeV (*62.5 GeV*)

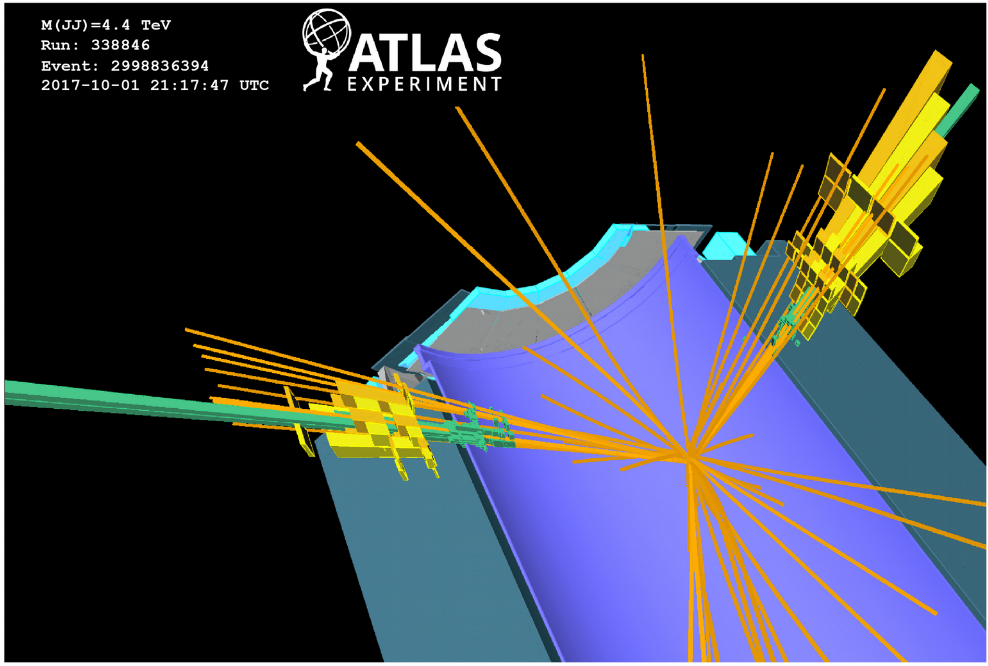

Search for Physics BSM (5)

SUSY Electroweak production (could dominate if squarks and gluinos heavy)

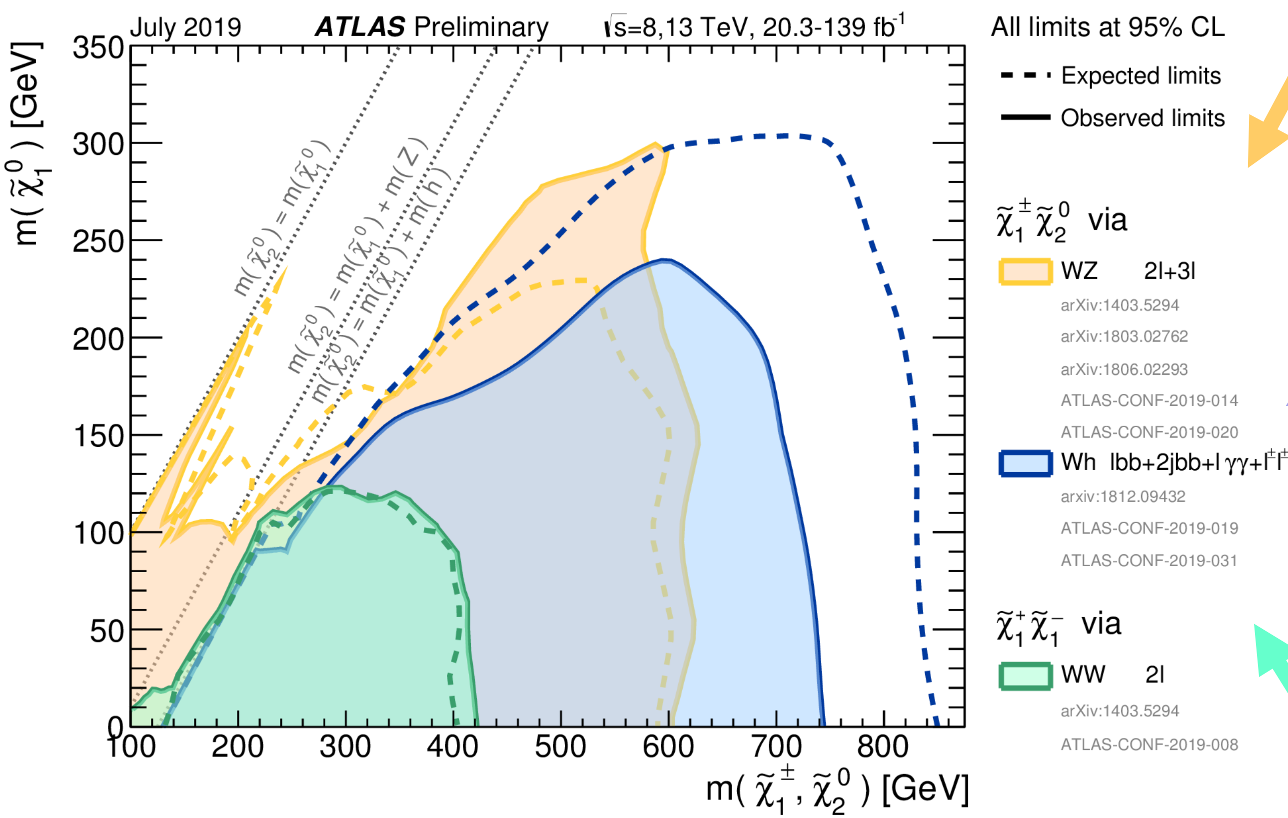

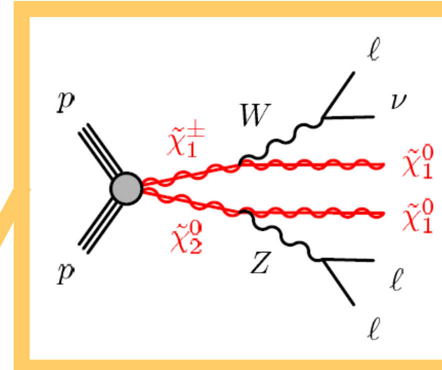

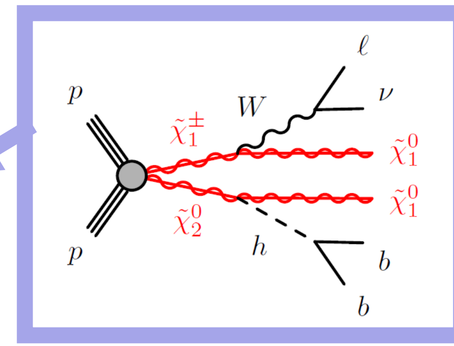

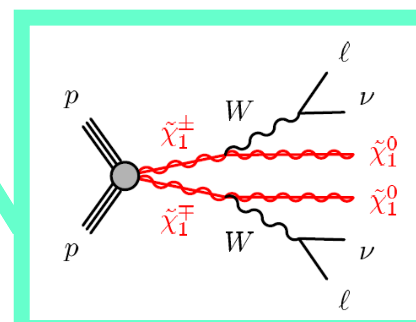

Example : weak-boson-mediated decays

Search for Physics BSM (6)

Full Run-2

SUSY Strong production of Squarks and Gluinos   Golden mode

Sensitive searches for squarks and gluinos (in R-parity conserving scenarios) with neutralino as LSP (*no leptons*)

Many different scenarios investigated

with cut-based analyses and BDTs

$$M_{eff} = \text{sum } (p_T\text{jets} > 50 \text{ GeV} + E_T^{miss})$$

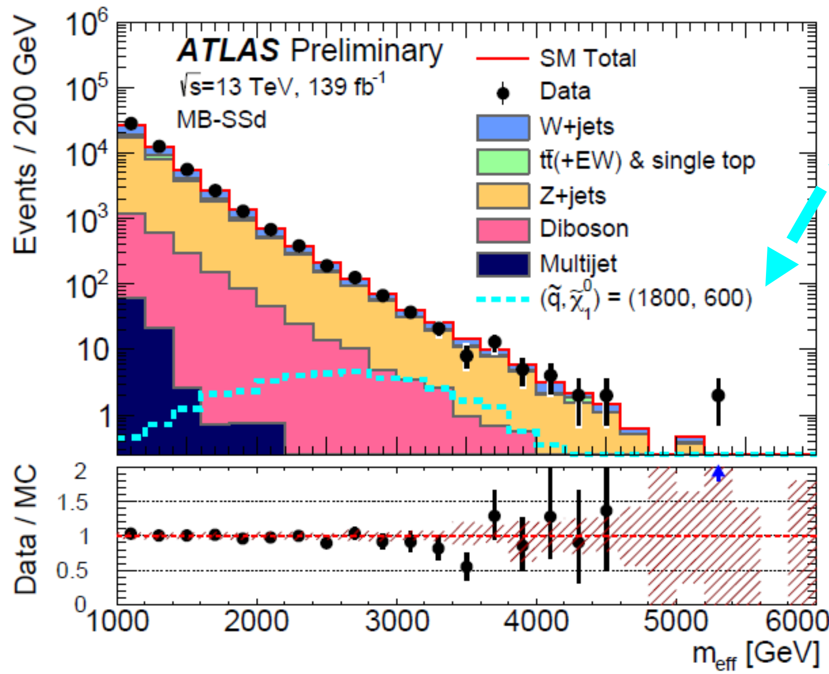

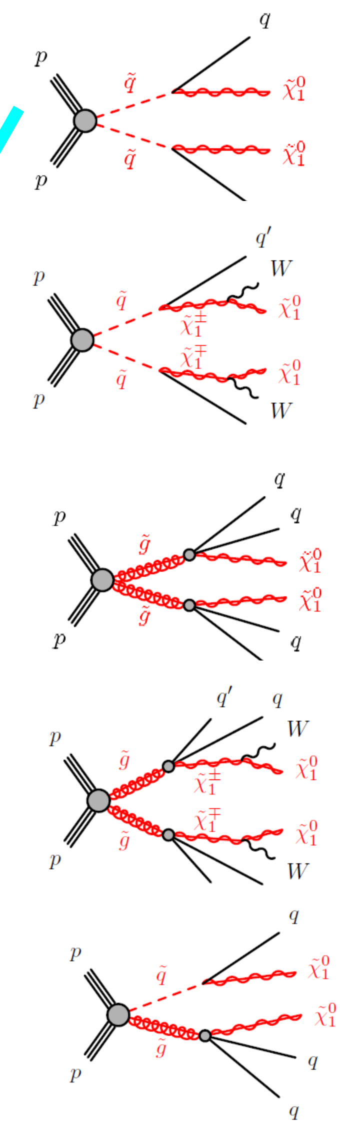

ATLAS-CONF-2019-040

Search for Physics BSM (7)

ATLAS-CONF-2019-040

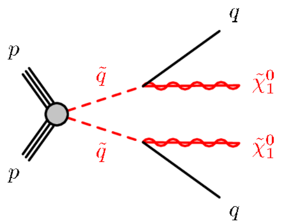

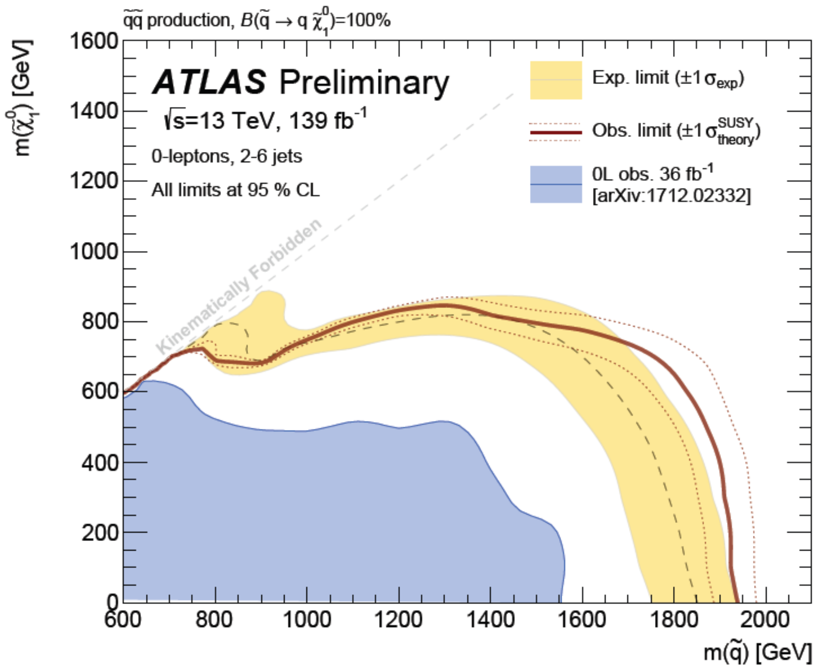

Used simplified scenarios

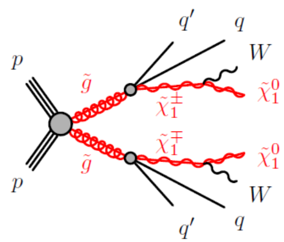

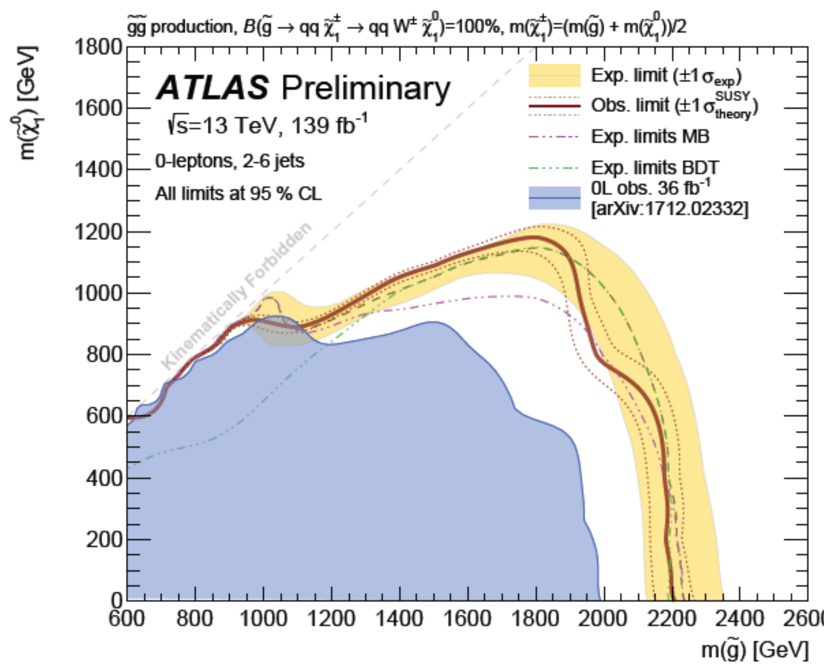

Search for Physics BSM (8)

Fluctuation reported in $m_{\mu\mu}$ spectrum

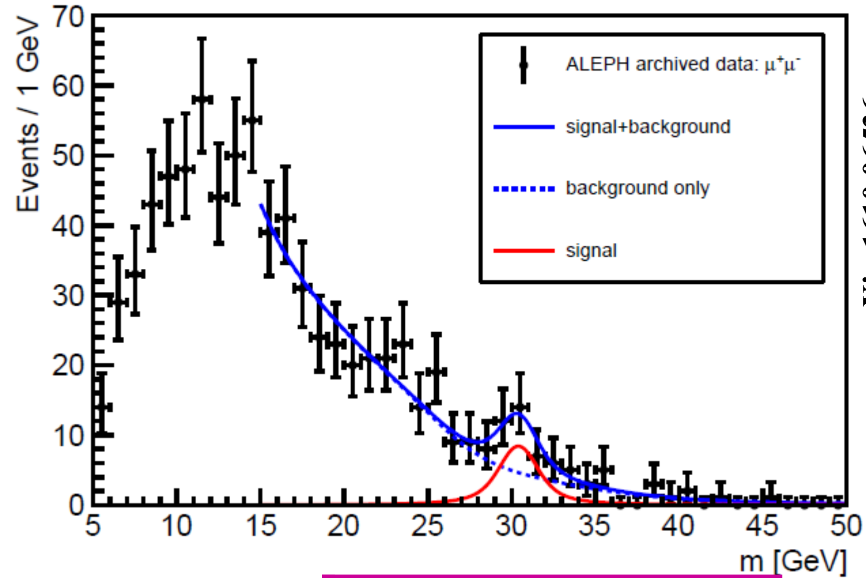

arXiv:1610.06536

$m_{\mu\mu}$ spectrum obtained from analysis of archived ALEPH data (with b bbar)

CMS JHEP 1811 (2018) 161

8TeV *19.7 fb^{-1}*

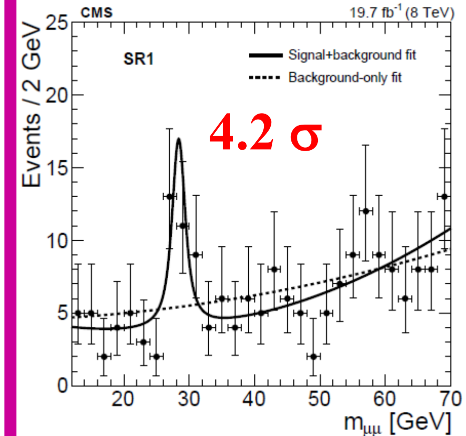

central-forward

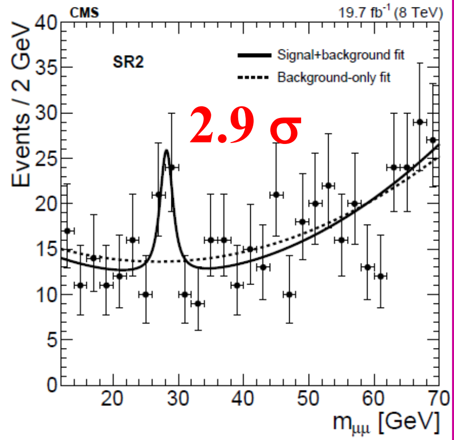

2 central

13TeV *35.9 fb^{-1}*

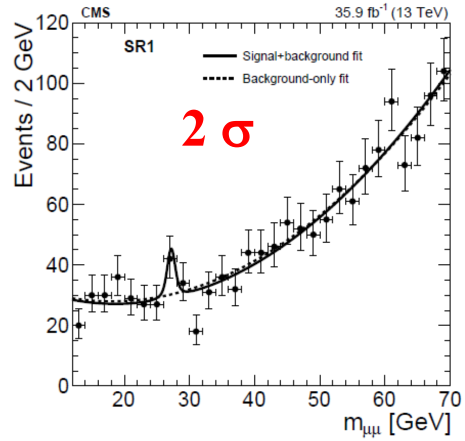

central-forward

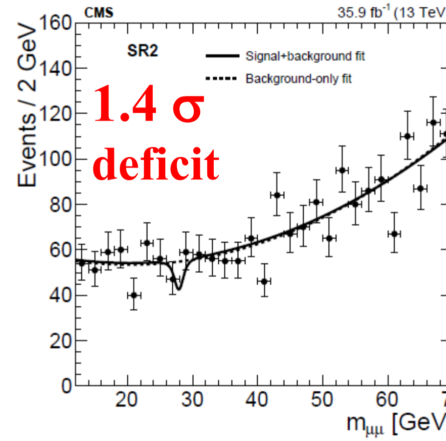

2 central

Search for Physics BSM (8)

Full Run-2 ~ same cuts than CMS

ATLAS-CONF-2019-036

8TeV

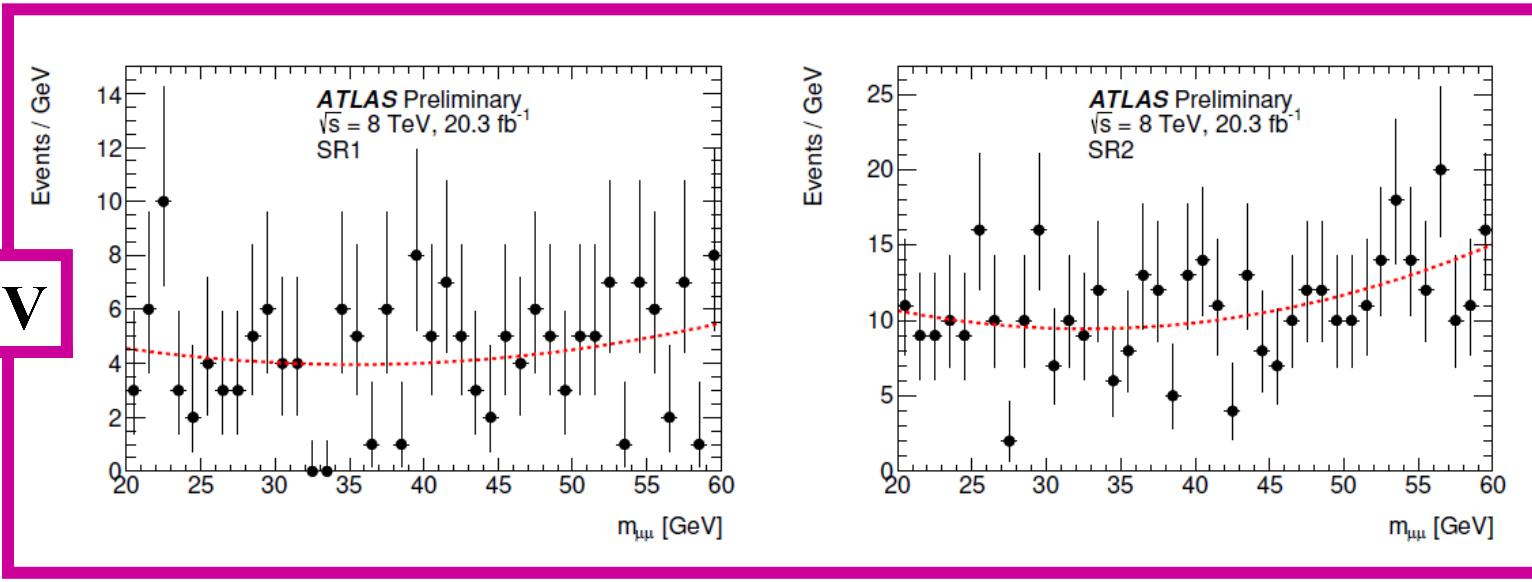

13TeV

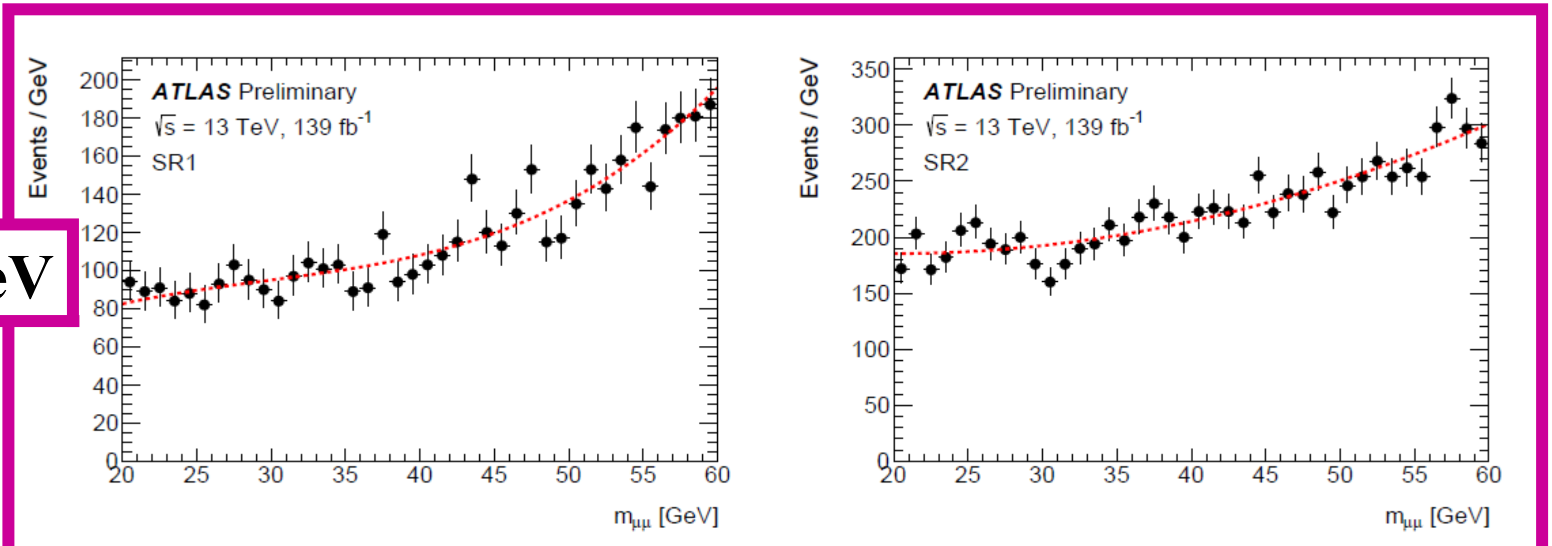

no significant excess observed

Multiple reasons to be long lived .. *small couplings .. intermediate states*

many challenging signatures

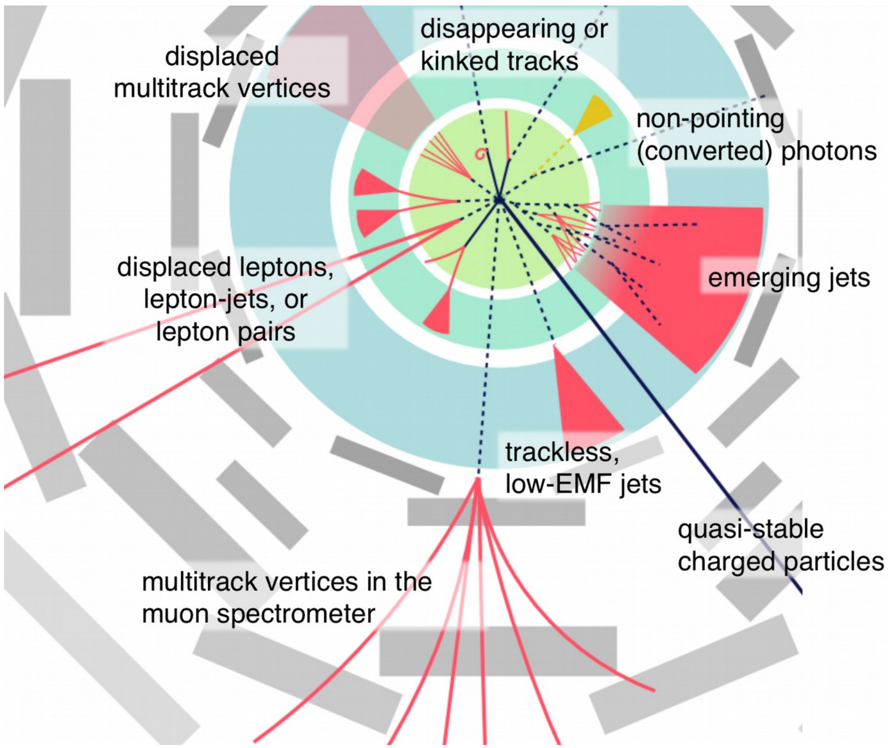

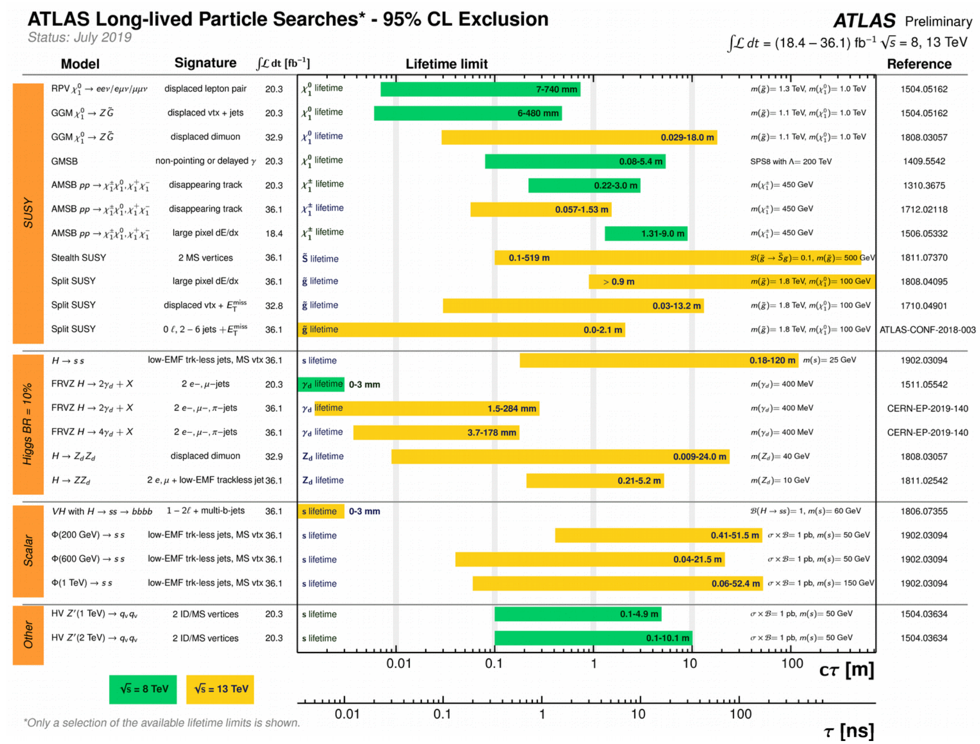

©M.H.Genest EPS2019

♪ ***Results from (run 1 and) run 2***

- ***detector***
- ***SM***
- ***BSM***
- ***(B-E)H***
- ***Vector-boson***

The (Brout-Englert-) Higgs = BEH boson(s)

1 Additional BEH bosons

2 The SM BEH boson

3 Search for a pair of BEH bosons

1 Additional BEH bosons (1)

General recipe : SM Higgs Doublet + Additional Field = Additional H bosons

SM + 1 additional H doublet = 2HDM (Two Higgs Doublet Model) that corresponds to 5 physical Higgs bosons

h, H, A, H^+, H^-

Four va … s

Coupling scale factor	Type I	Type II	Lepton-specific	Flipped
κ_V	$\sin(\beta-\alpha)$			
κ_u	$\cos(\alpha)/\sin(\beta)$			
κ_d	$\cos(\alpha)/\sin(\beta)$	$-\sin(\alpha)/\cos(\beta)$	$\cos(\alpha)/\sin(\beta)$	$-\sin(\alpha)/\cos(\beta)$
κ_ℓ	$\cos(\alpha)/\sin(\beta)$	$-\sin(\alpha)/\cos(\beta)$	$-\sin(\alpha)/\cos(\beta)$	$\cos(\alpha)/\sin(\beta)$

JHEP 1511 (2015) 206

MSSM ⊂ type II HDM .. Numerous benchmark models like hMSSM

1 Additional BEH bosons (2)

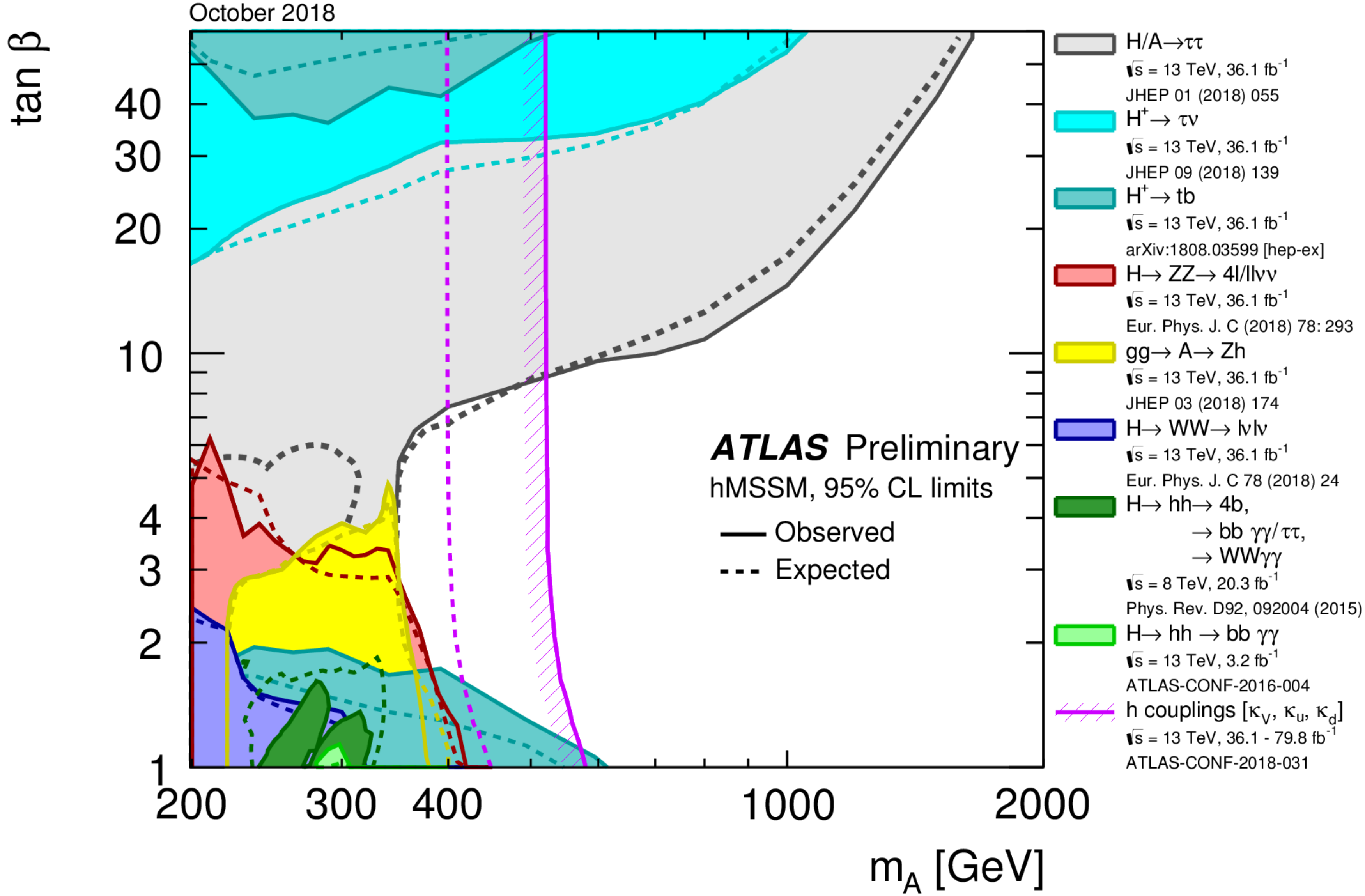

https://atlas.web.cern.ch/Atlas/GROUPS/PHYSICS/CombinedSummaryPlots/HIGGS/

1 Additional BEH bosons (3) γγ excess at 95 GeV

comparison between CMS and ATLAS results (*Sven Heinemeyer*)

CMS PAS HIG-17-013

20 fb^{-1} (8 TeV) + 36 fb^{-1} (13 TeV)

ATLAS-CONF-2018-025

80 fb^{-1} (13 TeV)

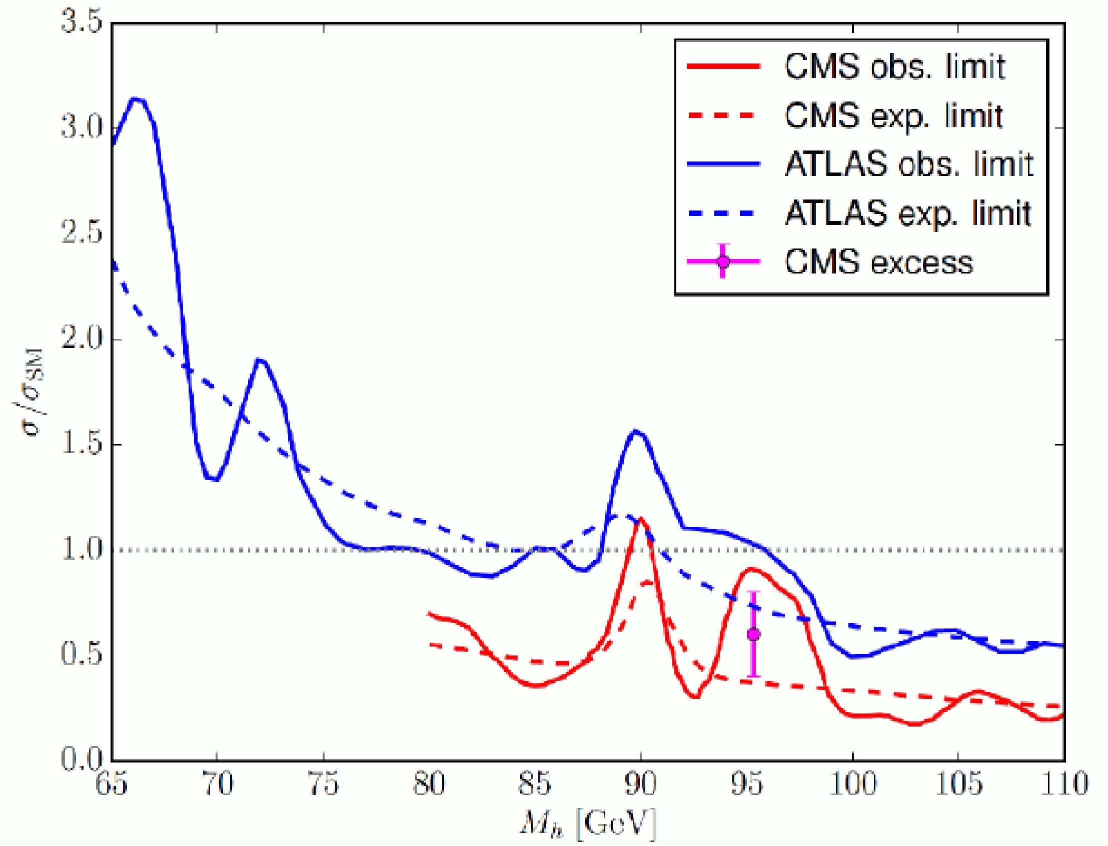

2 The SM BEH boson (1) executive summary

7 years after the discovery we have now a much clearer picture of the BEH boson properties

♠It is spin 0 and its interactions with bosons are mainly CP-even

♠ We know its mass at 0.2% accuracy

BEH boson couples to mass ➔ couplings to be measured

Increasing precision in all measurements

- **bosonic sector : inclusive measurement at ~10% precision differential measurements probing extended phase space with increasing accuracy**
- **fermionic sector : 3rd generation (τ, t, b) established with uncertainties approaching ~ 20% level . Most promising channel for 2nd generation is $H \rightarrow \mu\mu$**

2 The SM BEH boson (2)

A.Djouadi Phys.Rept.457:1-216

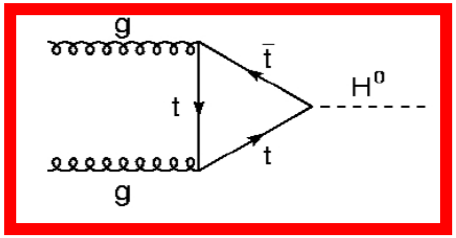

GF **H → WW , ZZ , γγ , (bb),ττ**

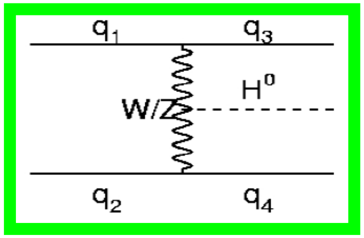

VBF **H → WW, ZZ , γγ , bb, ττ**

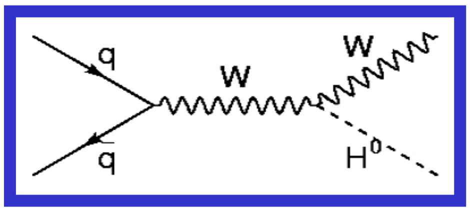

H → WW, γγ, bb

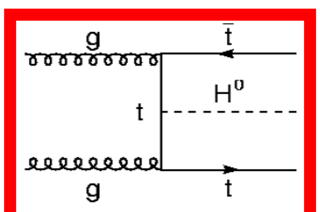

H → WW, γγ, ττ, ZZ, bb

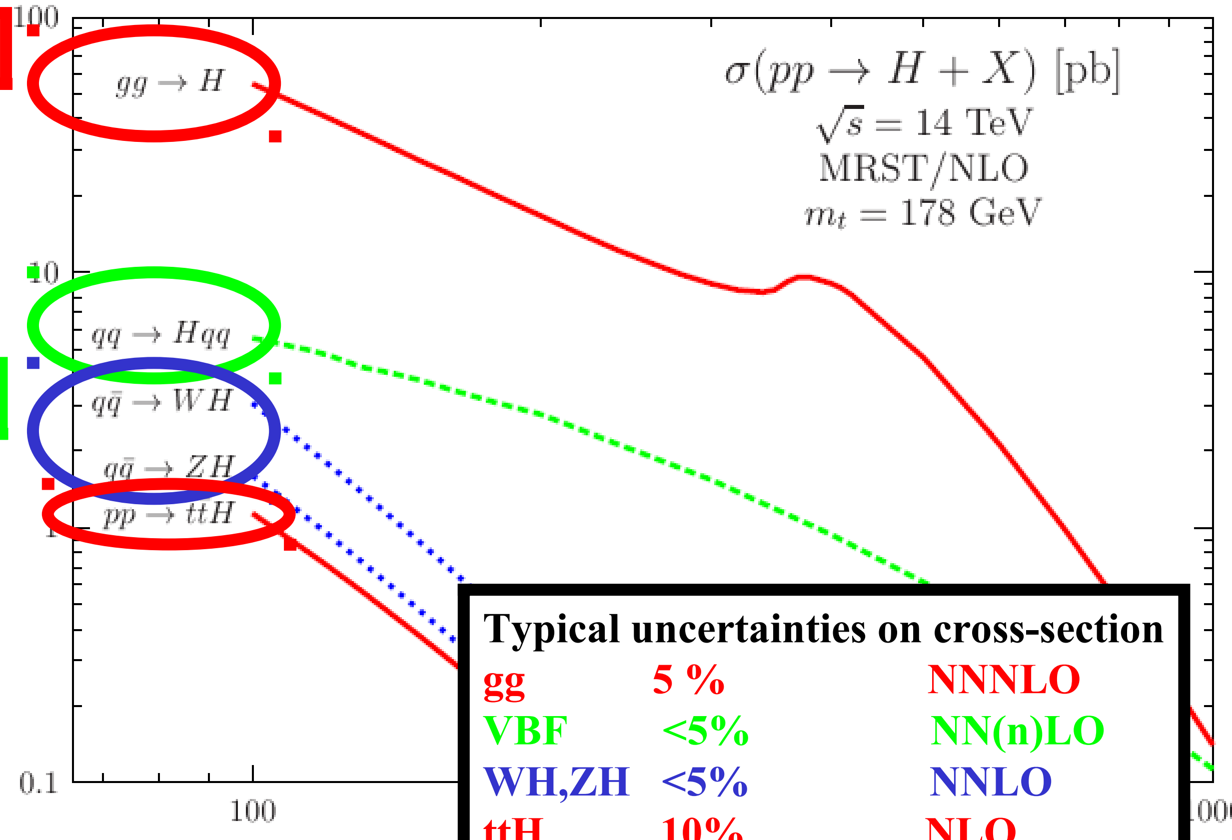

Typical uncertainties on cross-section

gg	5 %	NNNLO
VBF	<5%	NN(n)LO
WH,ZH	<5%	NNLO
ttH	10%	NLO

These production cross sections have to be used with the decays **bb , ττ , WW , ZZ , γγ**

channels with good mass resolution

2 The SM BEH boson (3)

A.Djouadi Phys.Rept.457:1-216

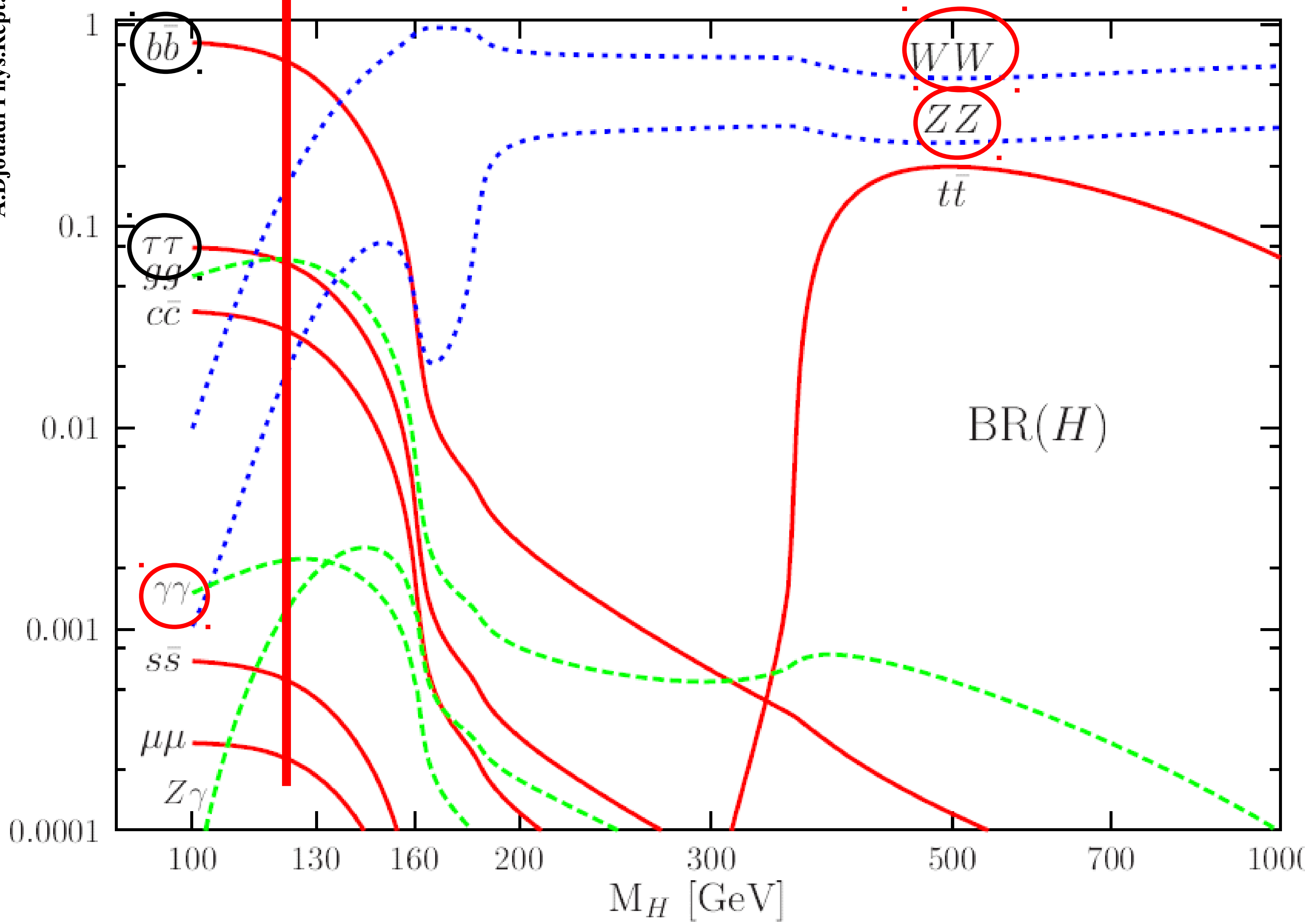

2 The SM BEH boson (4) The H mass

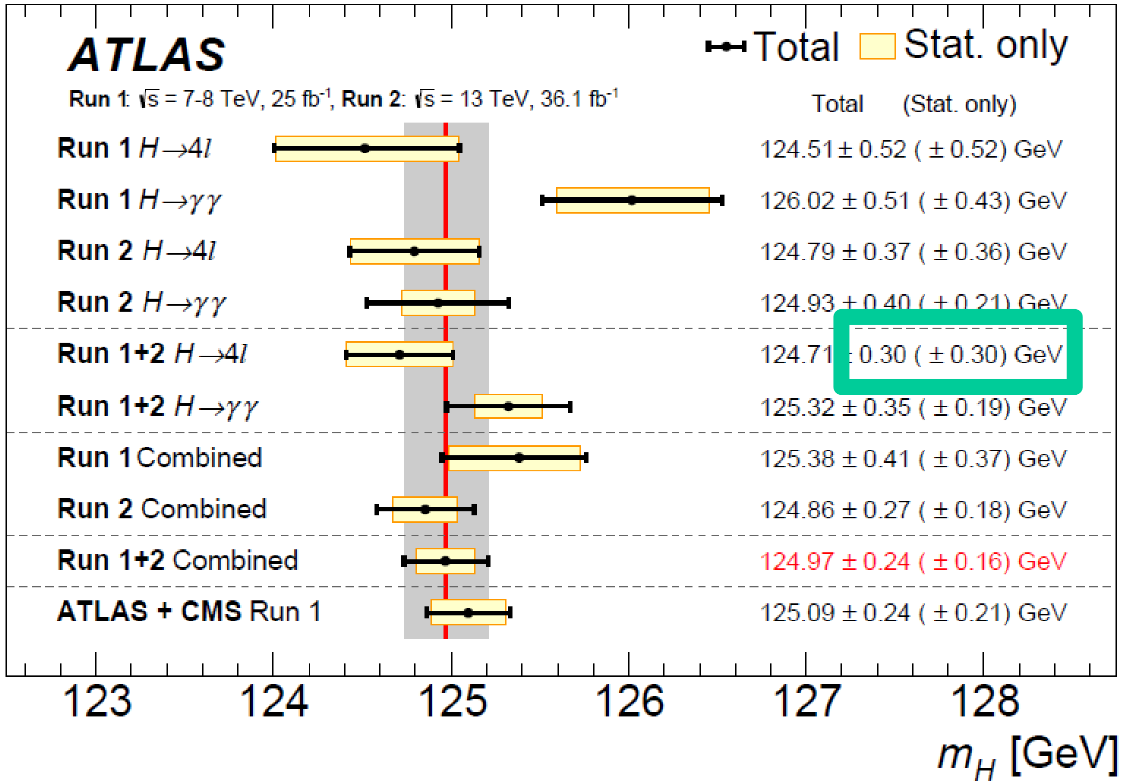

Phys. Lett. B 784 (2018) 345

uncertainty on mass < 0.2 %

Remember ATLAS has an uncertainty on W mass of 19 MeV Eur.Phys.J. C78 (2018) no.2, 110

note that $\Delta\, m_H = 0.1$ GeV → Δ (BR(H→ ZZ)) / BR(H→ ZZ) ~ 1%

At longer term uncertainty will be dominated by 4l

(for H→ γγ : need to extrapolate from e to γ !)

2 The SM BEH boson (5) Interference in $\gamma\gamma$ (between signal and background)

start to be sensitive to subtle effects like interference (between signal and background) in $\gamma\gamma$

Martin, Dixon and Li Phys.Rev.Lett. 111 (2013) 11180

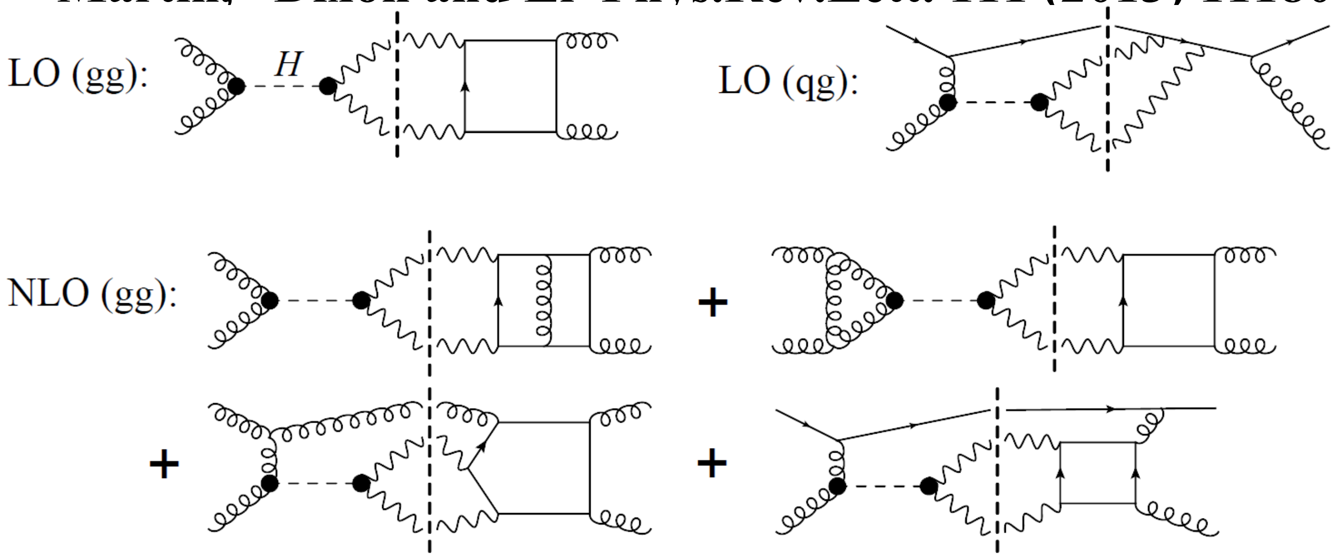

Interference depends of S/B , therefore is <u>smaller at high p_T(H)</u> where S/B is larger

some work can be done at high pT (H+2j) see for instance Phys.Rev. D92 (2015) no.1, 013004

2 The SM BEH boson (6) Mass shift

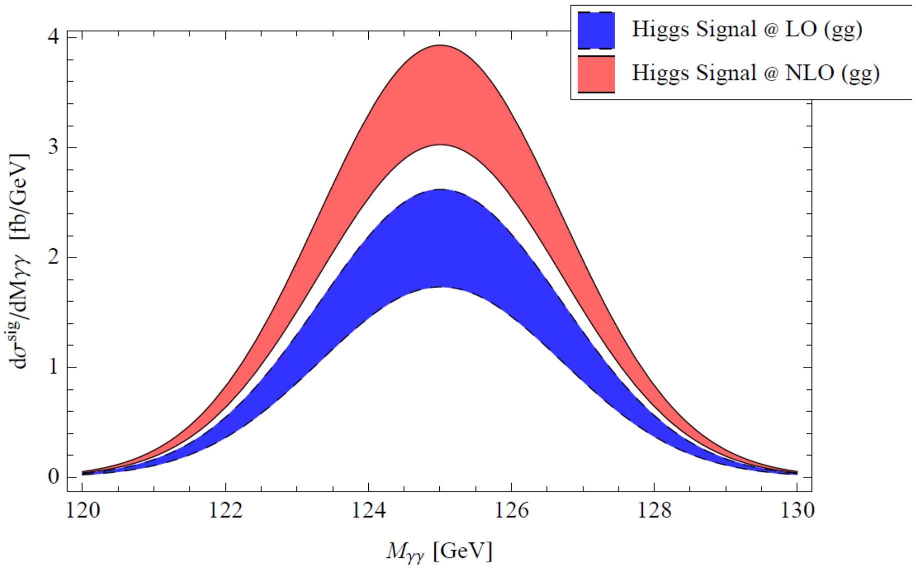

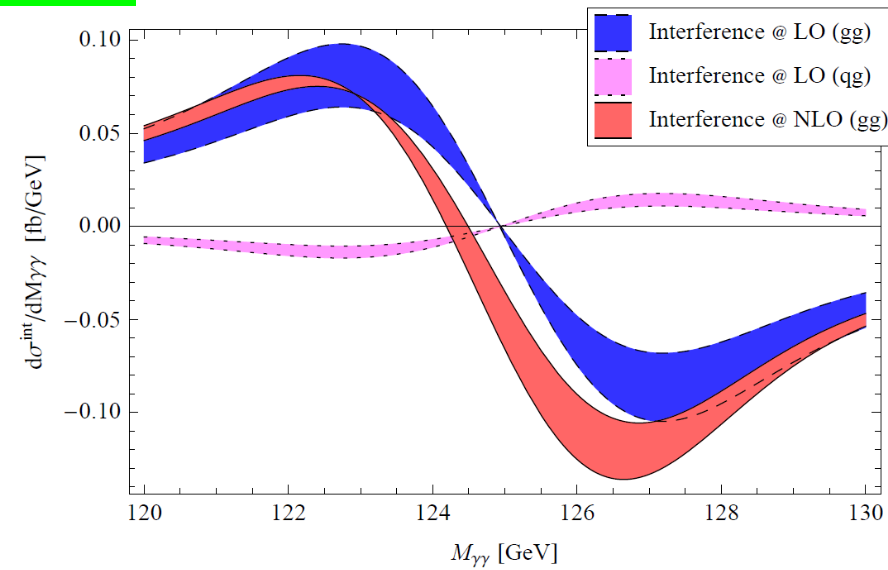

L.Dixon and Y.Li Phys.Rev.Lett. 111 (2013) 111802

The expected median mass shift is found to be $\Delta m_H = -35 \pm 9$ MeV assuming a Standard Model width of 4 MeV for the Higgs boson

ATL-PHYS-PUB-2016-009

However the effect is larger for larger H width
→ could constrain the H width

There is also an effect on the cross-section measurement (few %) to be taken into account

2 The SM BEH boson (7) definition of μ

$$\mu = (\sigma \,.\, BR) / (\sigma \,.\, BR)_{SM}$$

2 The SM BEH boson (8) some fermionic results

H→ττ

Analysis targets VBF and gg→Hj production

Three decay channels

$\tau_{lep}\tau_{had}$, $\tau_{lep}\tau_{lep}$, $\tau_{had}\tau_{had}$

Phys. Rev. D 99, 072001 (2019)

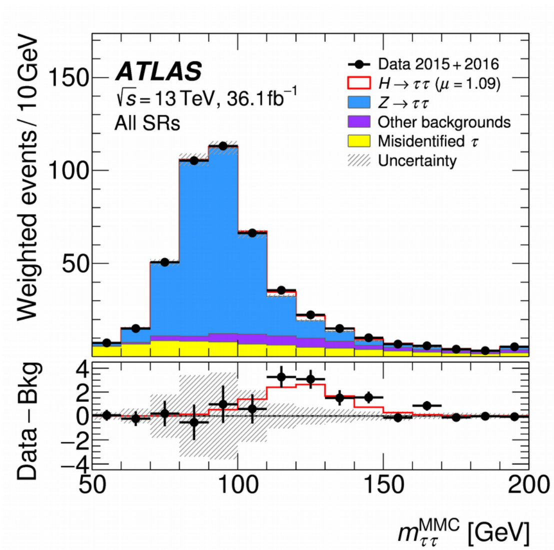

Observation of H→ττ (6.4 σ obs - 5.4 σ exp) when combined with Run-1

H→bb

Main analysis is targetting VH but also start to look at ggH and VBF modes

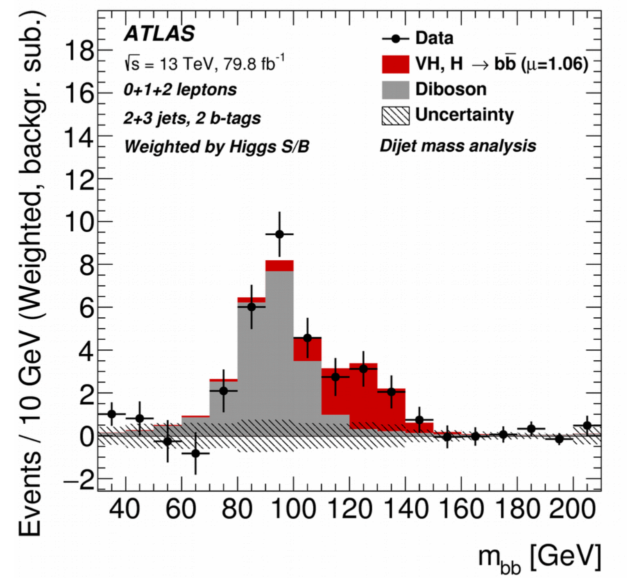

Phys.Lett. B786 (2018) 59-86

H→bb : 5.4 σ obs 5.5 σ exp

$$\mu = 1.01 \pm 0.12(\text{stat.})^{+0.16}_{-0.15}(\text{syst.})$$

Combination of VH channels gives significance obs(exp) of 5.3 σ (4.8 σ)

2 The SM BEH boson (9) ttH

Observation of ttH (june 2018)

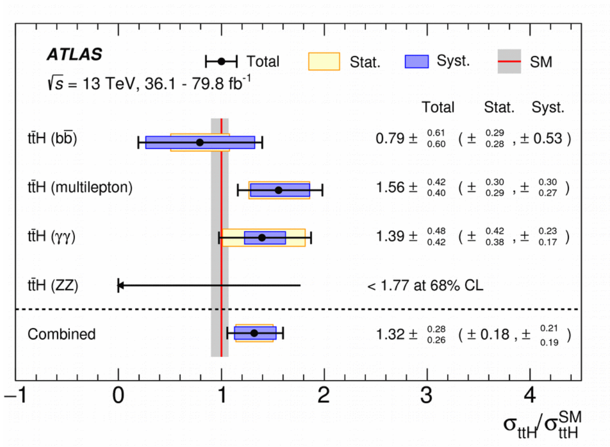

Phys.Lett. B784 (2018) 173-191

Combined with Run-1 obs(exp) significance of 6.3 (5.1) σ

Full Run-2

ttH(→γγ) full Run-2

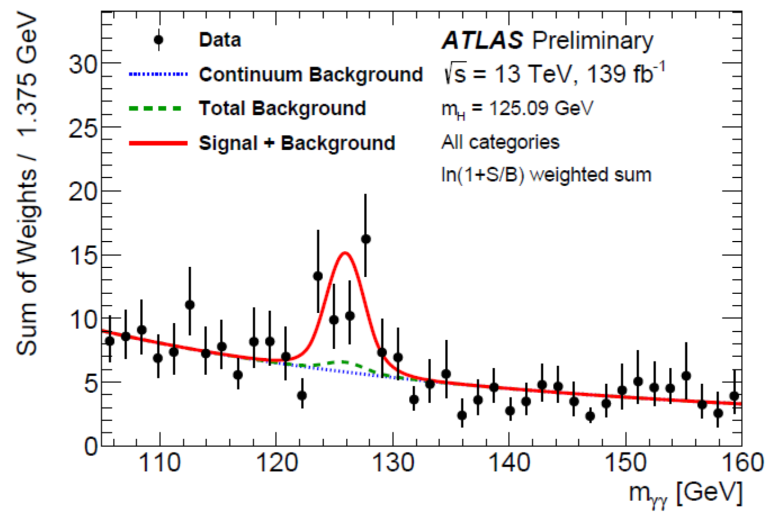

ATLAS-CONF-2019-C

Observed (exp) significance of 4.9(4.2) σ

2 The SM BEH boson (10) dileptons

Full Run-2

H→μμ

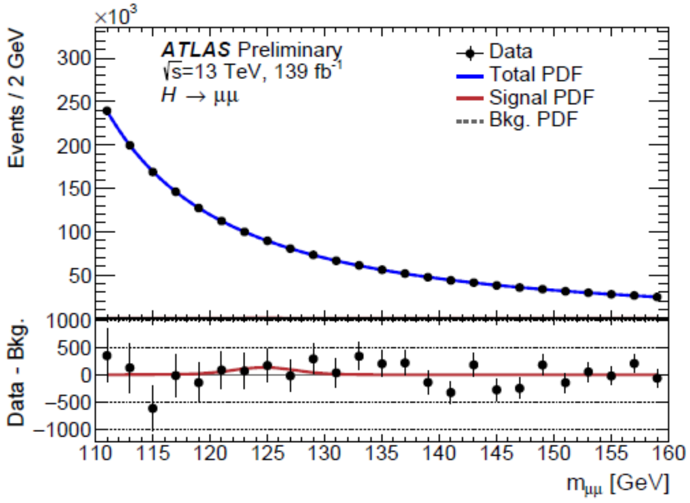

$\mu = 0.5 \pm 0.7$

ATLAS-CONF-2019-028

several categories

H→ee, eμ, eτ, τμ

no evidence for H→ee ☺

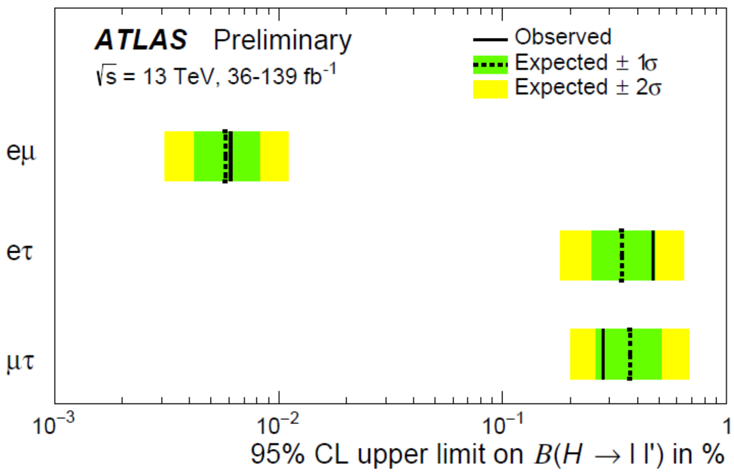

arXiv:1907.06131

ATLAS-CONF-2019-037

BR(H→ee) < 3.6 (3.5) 10^{-4}

obs exp

2 The SM BEH boson (11) H→ cc

Phys.Rev.Lett. 120 (2018) no.21, 211802

H→cc

in mode $Z(\to l^+l^-)H$

observed (expected) upper limit on μ at the 95% CL of 110 (150^{+80}_{-40})

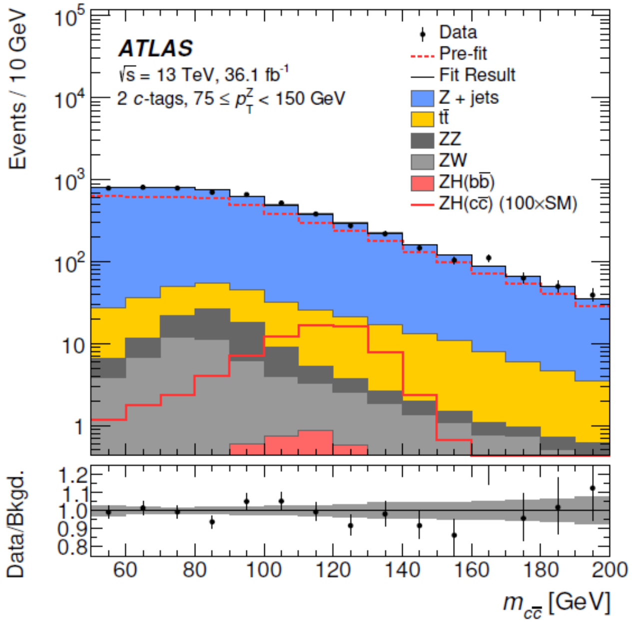

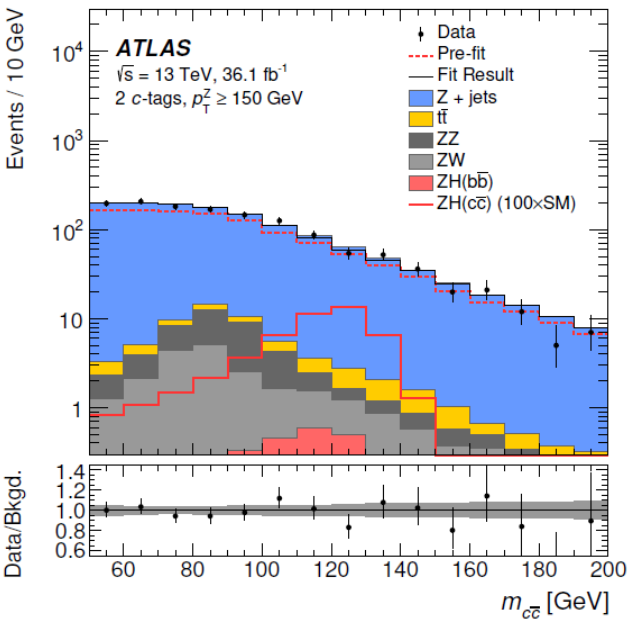

also H → J/ψ γ

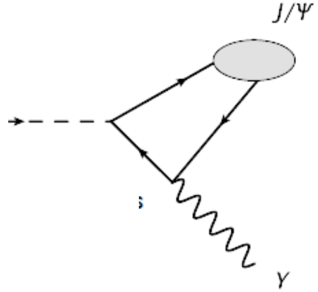

2 The SM BEH boson (12) invisible H decays

Invisible H

Upper limit at 95% CL on
BR(H→inv) obs(exp) 0.26(0.17)

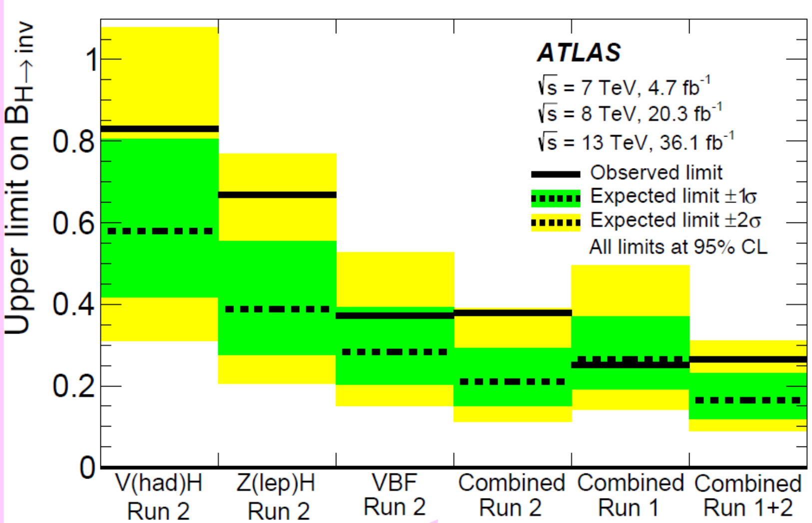

Comparison with direct detection experiments

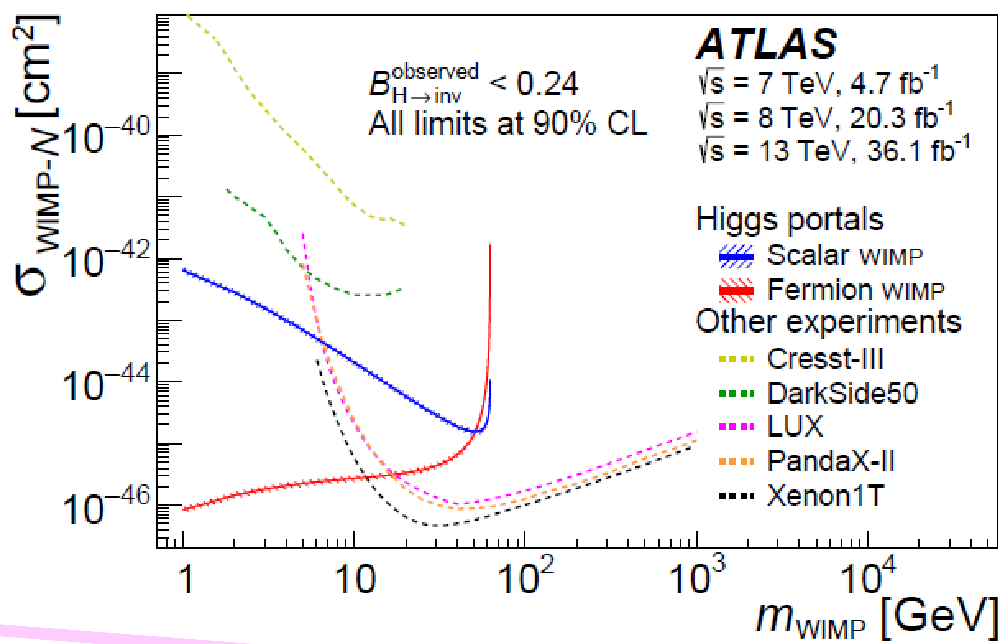

Phys.Rev.Lett. 122 (2019) no.23, 231801

SM BR(H→4ν) ~ 1.2 10^{-3}

E_T^{miss} + 2 jets

2 The SM BEH boson (13) H→ 4l H→γγ

Full Run-2

H→4l

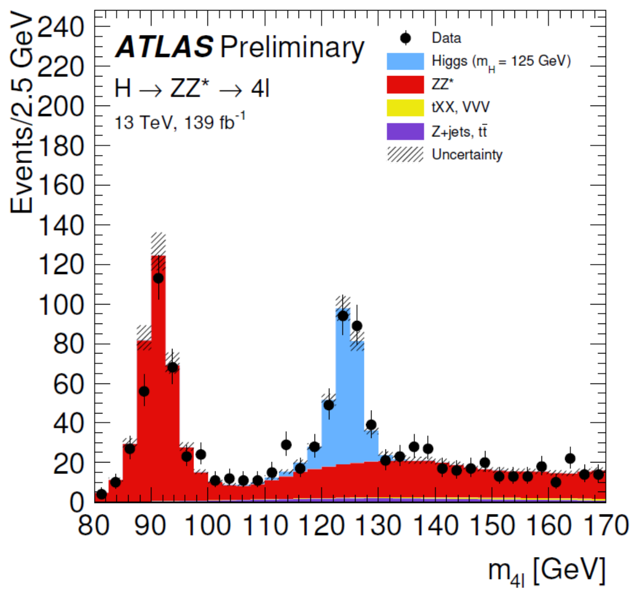

$$\mu = 1.04^{+0.09}_{-0.08}(\text{stat.})^{+0.04}_{-0.03}(\text{exp.})^{+0.06}_{-0.05}(\text{th.}) = 1.04^{+0.12}_{-0.10}$$

ATLAS-CONF-2019-025

Full Run-2

H→γγ

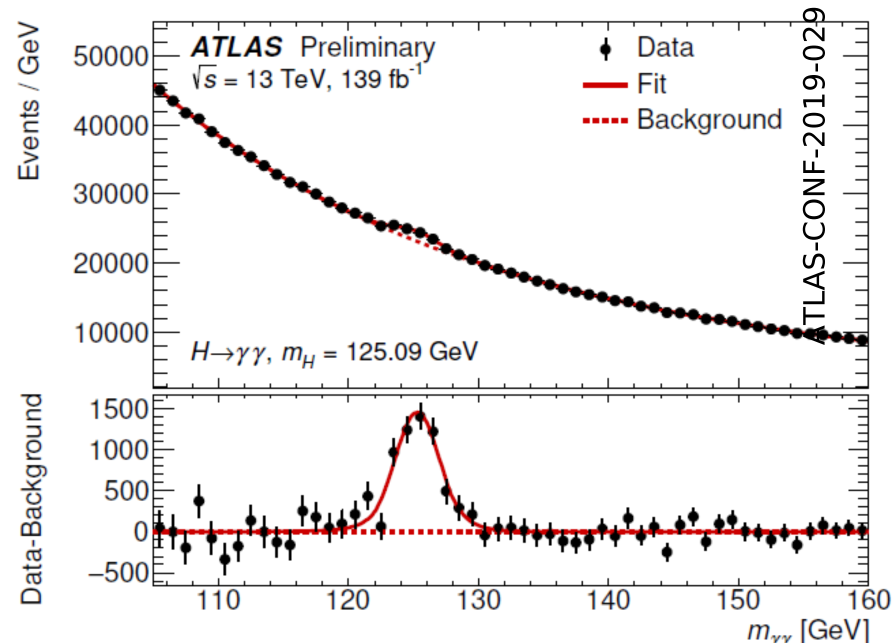

$\sigma_{\text{fid}} = 65.2 \pm 4.5\,(\text{stat.}) \pm 5.6\,(\text{syst.}) \pm 0.3\,(\text{theo.})$ fb

SM expectation of 63.6 ± 3.3 fb

constraint on charm coupling through pT distribution (see also next slide)

(gg→ H and $\bar{cc}$→ H)

Coefficient	Observed 95% CL limit	Expected 95% CL limit
κ_c	[−19, 24]	[−15, 19]

syst (background modelling + energy resolution + …. > stat !

2 The SM BEH boson (14) combined H→ 4l and H→γγ

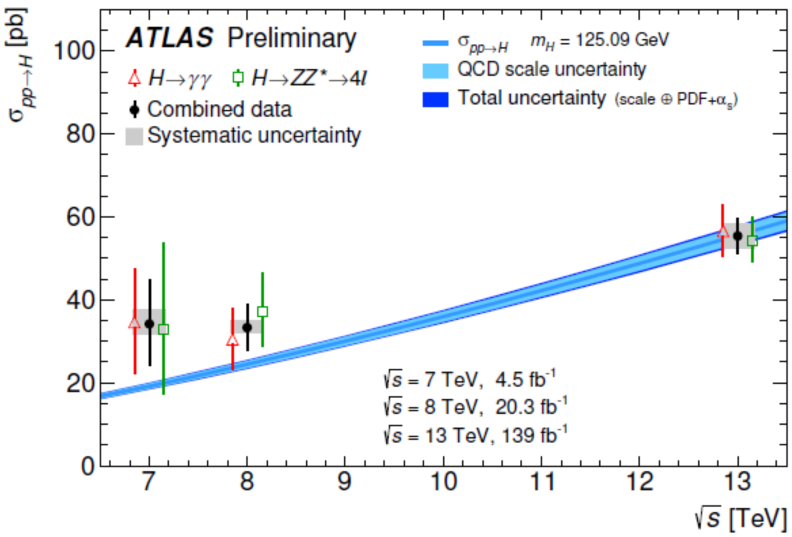

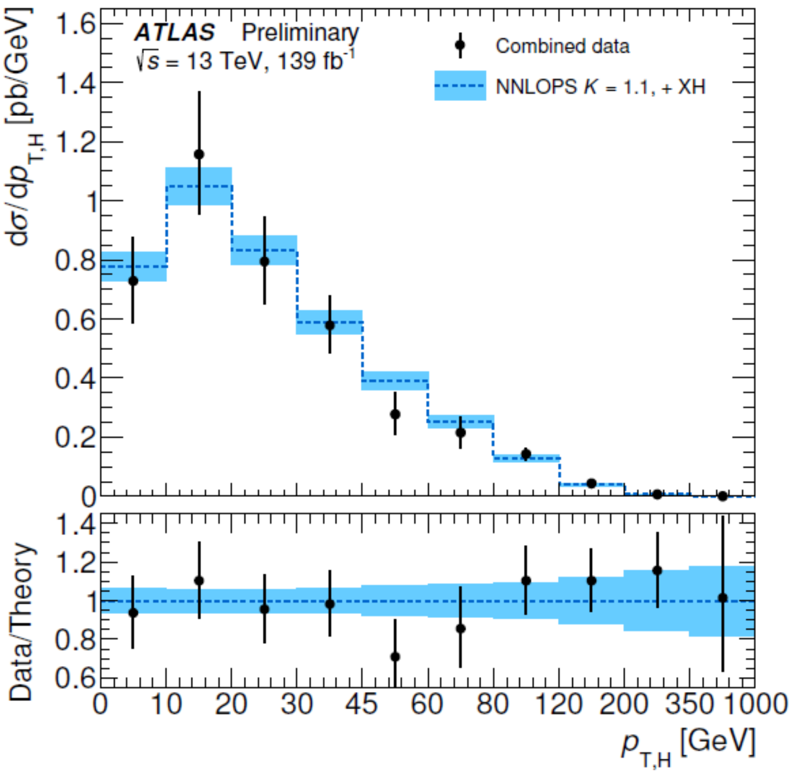

ATLAS-CONF-2019-032

Combined inclusive pp→H cross section

$$55.4^{+4.3}_{-4.2} \text{ pb } (\pm 3.1(\text{stat.}) \; ^{+3.0}_{-2.8}(\text{sys.}))$$

$$\text{SM} = 55.6 \pm 2.5 \text{ pb}$$

2 The SM BEH boson (15) H combination

$$\mu = 1.11^{+0.09}_{-0.08} = 1.11 \pm 0.05\,(\text{stat.})\,^{+0.05}_{-0.04}\,(\text{exp.})\,^{+0.05}_{-0.04}\,(\text{sig. th.}) \pm 0.03\,(\text{bkg. th.})$$

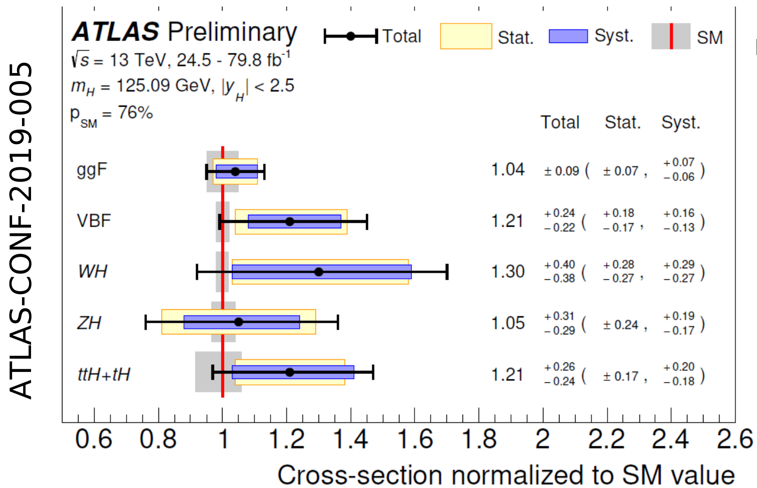

assumption of SM branching fractions

13 TeV
up to 80 fb^{-1}

iconic H plot

The SM BEH mechanism predicts relations between couplings and masses

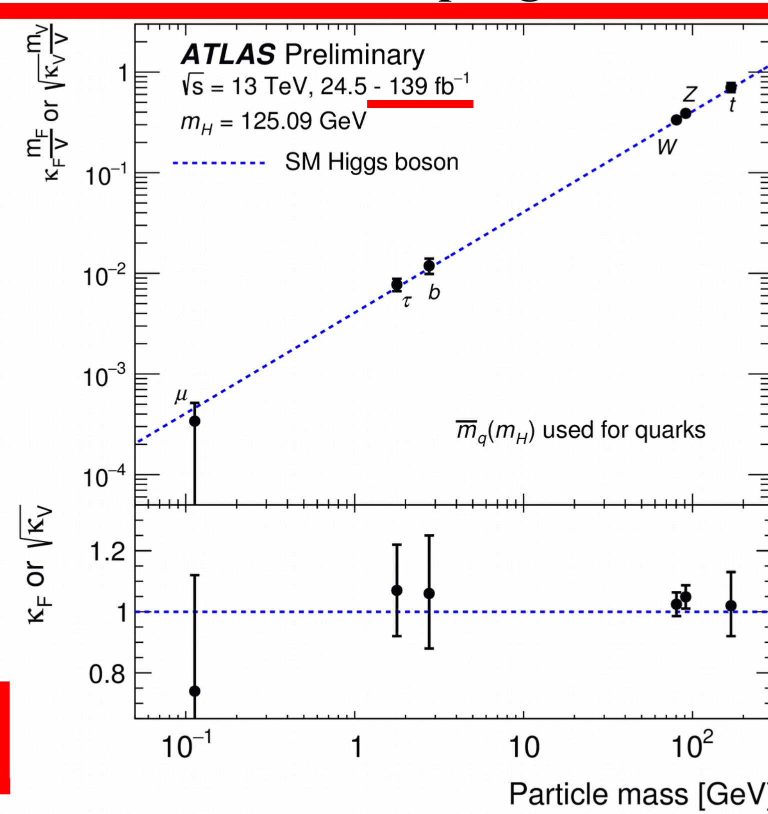

checked

3 Search for a pair of BEH bosons (1)

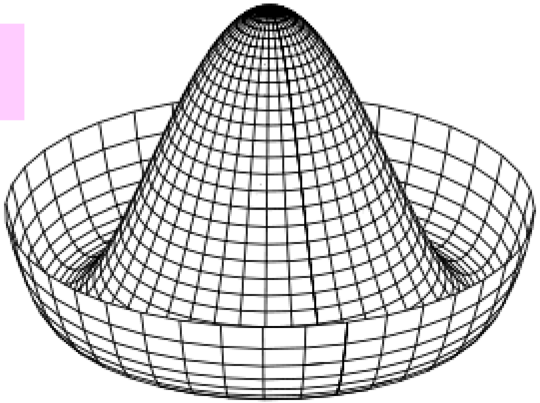

After discovering the Higgs boson, the ultimate probe of the Standard Model is to fully measure the Higgs potential.

$\Phi \rightarrow v + h$

$$V(\phi) = \frac{1}{2}\mu^2\phi^2 + \frac{1}{4}\lambda\phi^4 = \lambda v^2 h^2 + \lambda v h^3 + \frac{1}{4}\lambda h^4$$

mass term

$\frac{1}{2} m_h^2 h^2$

self coupling terms

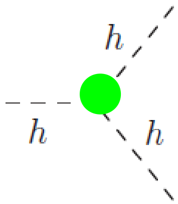

3 Search for a pair of BEH bosons (2)

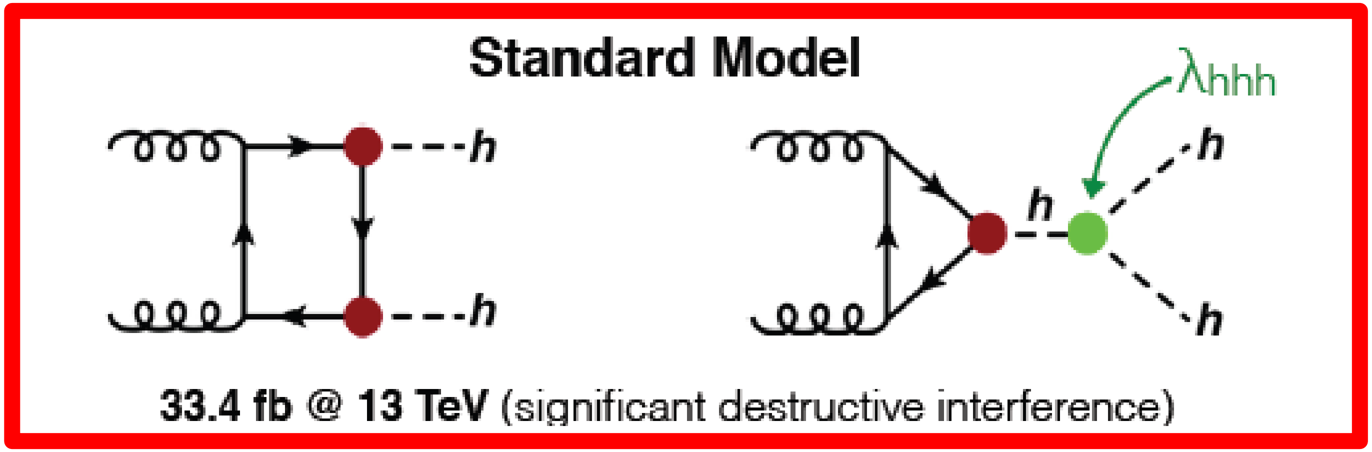

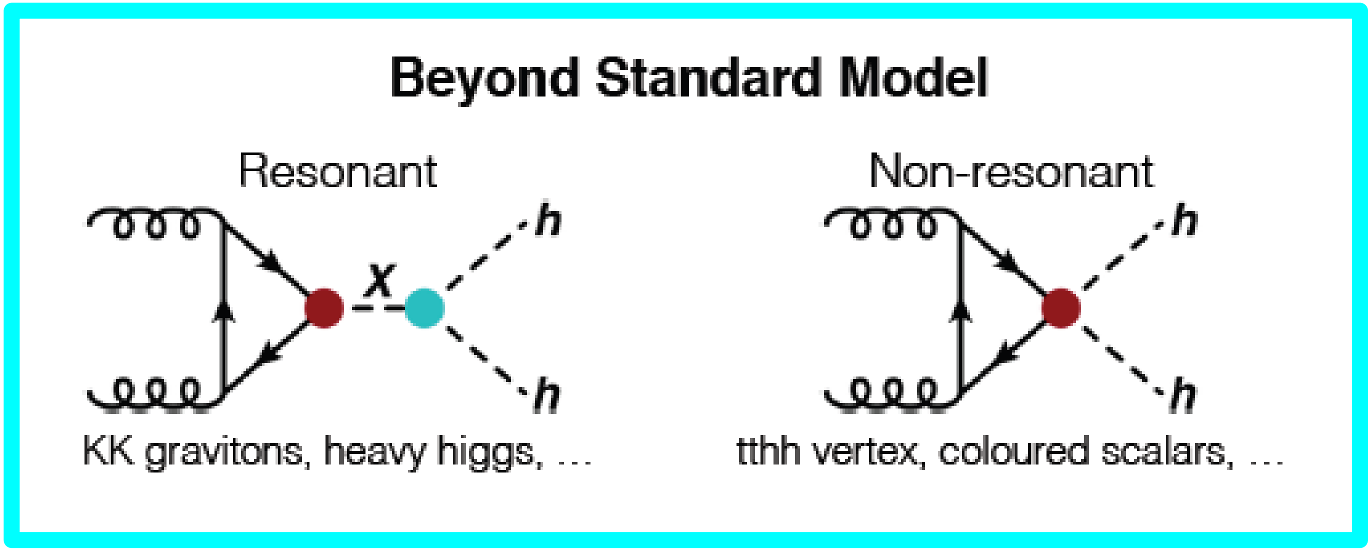

3 Search for a pair of BEH bosons (3)

arXiv:1906.02025

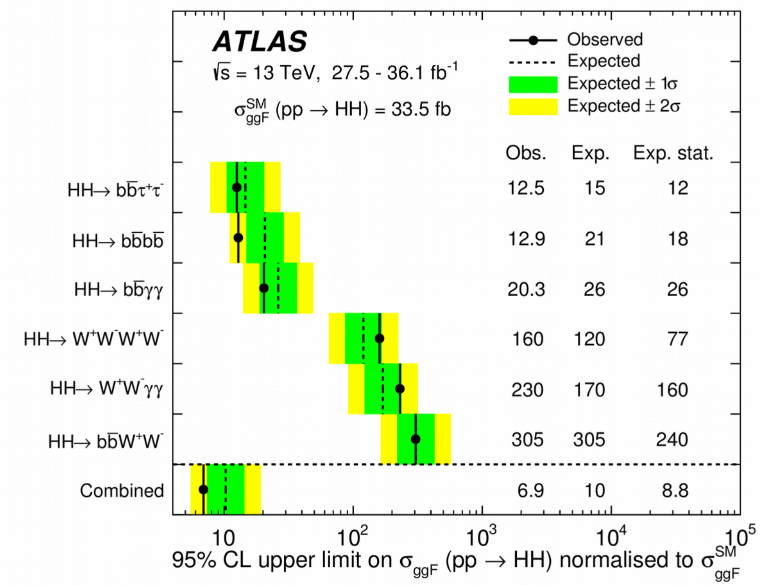

95% CL limit for $\kappa_\lambda = 1$:

6.9 (10) X SM obs. (exp.)

$$\kappa_\lambda = \lambda_{HHH} / \lambda_{HHH}^{\mathrm{SM}}$$

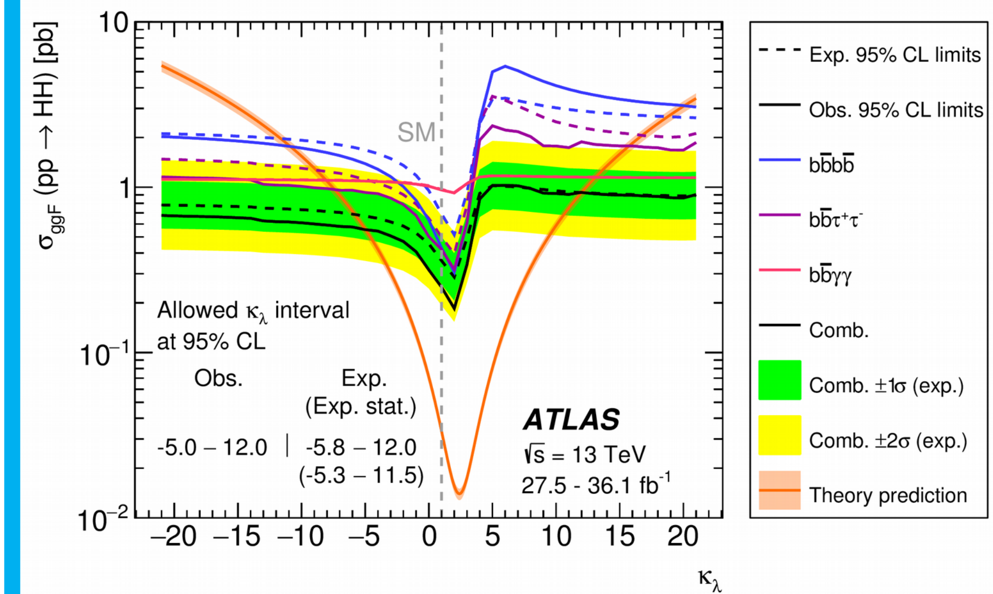

95% CL confidence intervals:

κ_λ: obs. [-5,12] (exp. [-5.8, 12])

see also new result on 4b channel (VBF) *ATLAS-CONF-2019-030*
and (better) new result on bblνlν *arXiv:1908.06765*

3 Search for a pair of BEH bosons (4) constraint of the H self-coupling from H differential production and decay mesurements

The Higgs boson cross sections, the branching fractions and the Higgs boson kinematics are affected by the Higgs-boson self coupling contribution through next to leading order electroweak corrections.

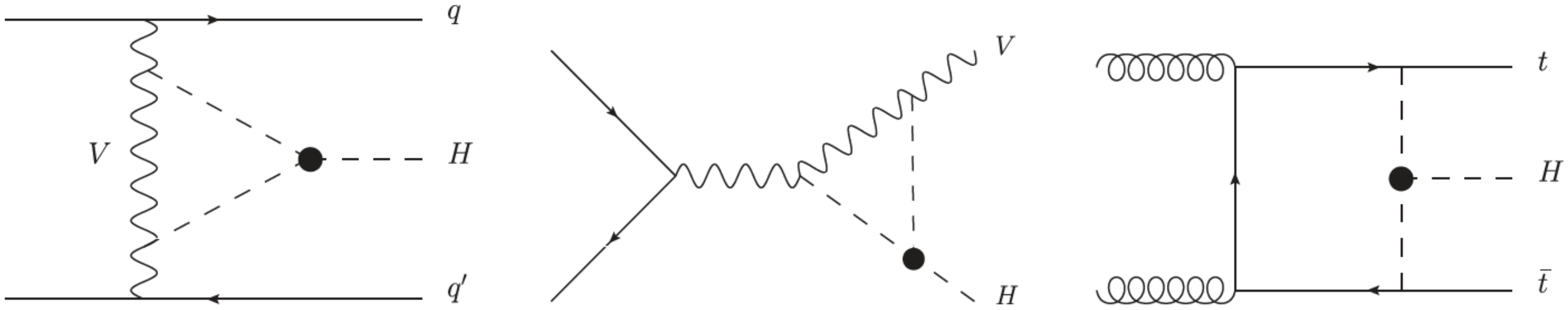

With the assumption that new physics affects only the Higgs boson self-coupling (λ_{HHH}), the ratio $\lambda_{HHH}/\lambda_{HHH}^{SM}$ is determined to be $\lambda_{HHH}/\lambda_{HHH}^{SM} = 4.0^{+4.3}_{-4.1}$, excluding values outside the interval $-3.2 < \lambda_{HHH}/\lambda_{HHH}^{SM} < 11.9$ at the 95% C.L.

Results similar to di-Higgs direct search

Theory :JHEP 1612 (2016) 080 Eur.Phys.J. C77 (2017) no.12, 887

♪ *Results from (run 1 and) run 2*

- ***detector***
- ***SM***
- ***BSM***
- ***(B-E)H***
- ***Vector-boson scattering***

EW weak boson scattering

Full Run-2

ATLAS-CONF-2019-033

H boson regularizes the EW weak boson scattering at high energies

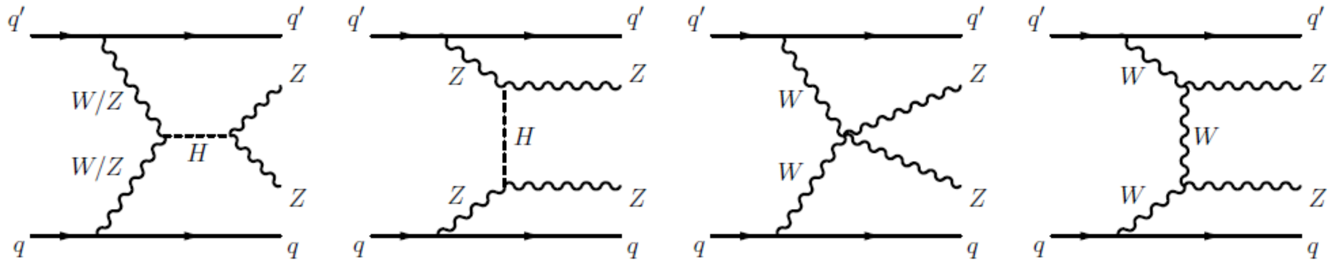

ZZ scattering

MVA to separate EW from QCD

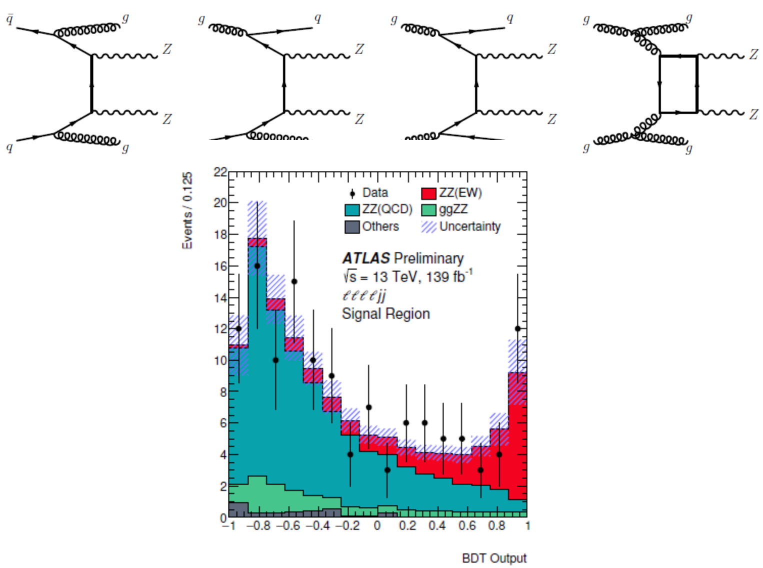

Observed (expected) significance for EW production: 5.5σ (4.3σ)

$\sigma_{fid}(EW) = 0.82 \pm 0.21$ fb

SM pred.= 0.61 ± 0.03 fb

arXiv:1812.09740

ATLAS observed vector boson scattering at:

- 6.9σ in WW channel
- 5.3σ in WZ channel

arXiv:1906.03203

WW ZZ WZ observed

also EW Zγ ATLAS-CONF-2019-039

- ♪ *Historical introduction , Setting the stage*
- ♪ *Results from (run 1 and) run 2*
- ♪ ***Future of ATLAS , run 3 , HL-LHC***
- ♪ *Conclusions*
- ♪ *Backup*

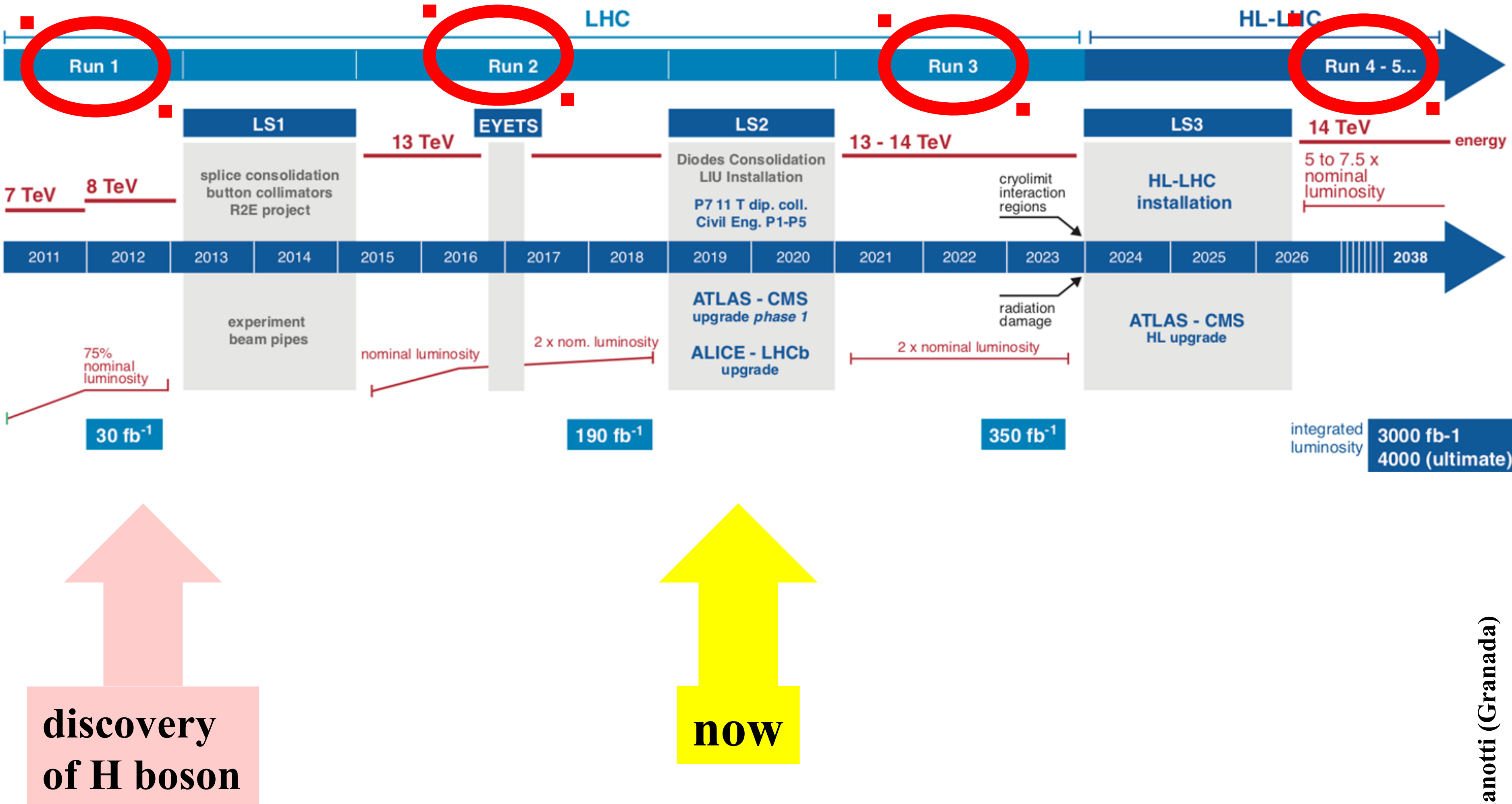
LHC
HL-LHC
Run 1
Run 2
Run 3
Run 4 - 5...
LS1
EYETS
LS2
LS3
7 TeV
8 TeV
13 TeV
13 - 14 TeV
14 TeV
energy
splice consolidation
button collimators
R2E project
Diodes Consolidation
LIU Installation
P7 11 T dip. coll.
Civil Eng. P1-P5
cryolimit
interaction
regions
HL-LHC
installation
5 to 7.5 x
nominal
luminosity
2011
2012
2013
2014
2015
2016
2017
2018
2019
2020
2021
2022
2023
2024
2025
2026
2038
experiment
beam pipes
ATLAS - CMS
upgrade phase 1
ALICE - LHCb
upgrade
radiation
damage
ATLAS - CMS
HL upgrade
75%
nominal
luminosity
nominal luminosity
2 x nom. luminosity
2 x nominal luminosity
30 fb-1
190 fb-1
350 fb-1
integrated
luminosity
3000 fb-1
4000 (ultimate)
discovery
of H boson
now

ATLAS Phase-I Upgrade

(i) Liquid Argon Calorimeter Electronics

Aim to improve the Level-1 calorimeter decision for Run 3 and beyond
(enhanced jet-rejection and pile-up subtraction)

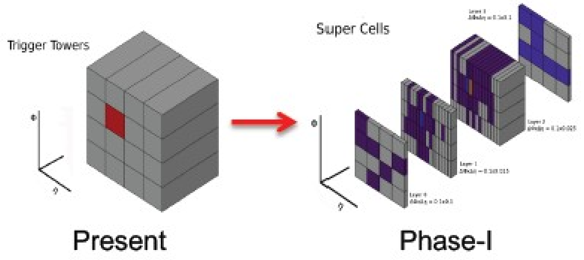

(ii) Trigger / DAQ upgrade

Take full advantage of the finer segmentation available with LAr electronics upgrade, and improved muon trigger information (NSW)

(iii) Muon System: New Small Wheel

Replacement of the inner muon stations in the endcap regions of the detector;
→ reduced muon fake trigger rate, preserve position resolution and efficiency at HL-LHC

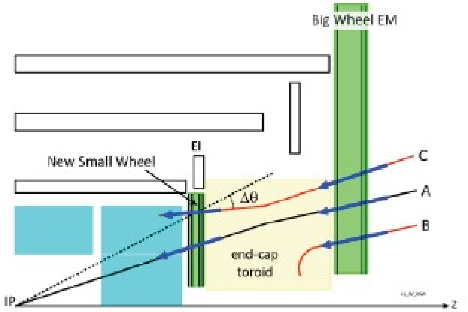

ATLAS Phase-II Upgrade

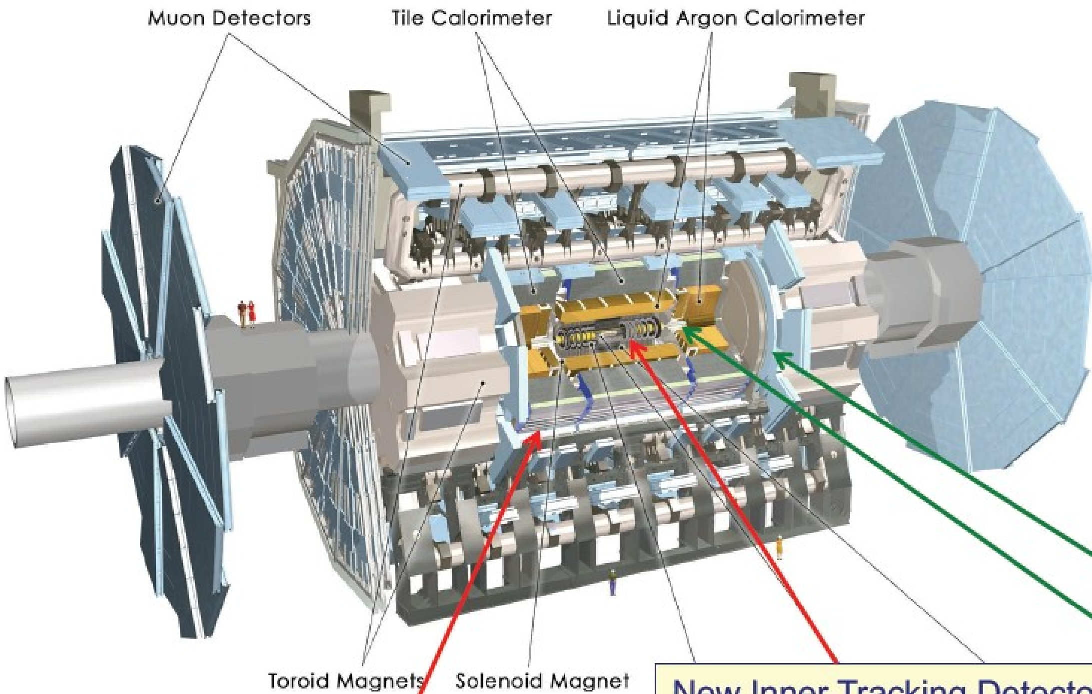

Upgraded Trigger and Data Acquisition System:

- L0: 1 MHz
- Improved High-Level Trigger

Electronics Upgrade :

- LAr Calorimeter
- Tile Calorimeter
- Muon system

New Inner Tracking Detector
(all silicon tracker, up to $|\eta| = 4$)

New muon chambers
in the inner barrel region

Options:
- High granularity timing detector (forward region)
- High-η muon tagger

It is very hard to predict, especially the future.

N.Bohr

arXiv:1902.00134

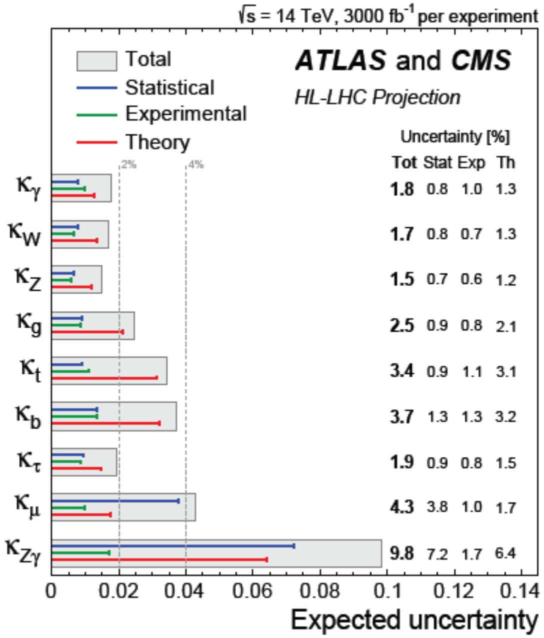

$$\kappa_j^2 = \sigma_j / \sigma_j^{SM}$$

H

Sensitivity to hh direct search

50% uncertainty on $\kappa_3 \equiv \frac{\lambda_3}{\lambda_3^{SM}}$

self coupling normalized to SM

3000 fb^{-1}

arXiv:1905.03764

HH

Δ m_W

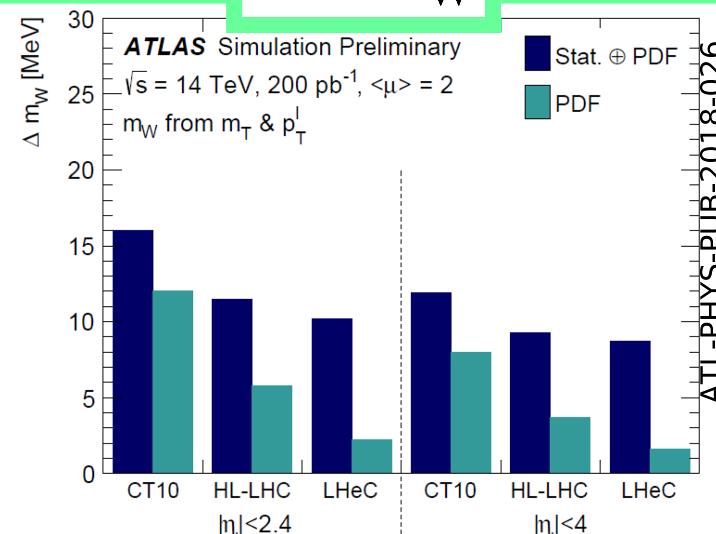

will require special runs

- ♪ *Historical introduction , Setting the stage*
- ♪ *Results from (run 1 and) run 2*
- ♪ *Future of ATLAS , run 3 , HL-LHC*
- ♪ ***Conclusions***
- ♪ *Backup*

- **Fantastic Run-2 dataset , thanks to the outstanding performance of the LHC and ATLAS**
- **During Run-3 emphasis on precision**
- **< 5% of the data that will be delivered by HL-LHC**
  ⇒ a lot to do !

Thanks for your attention

- ♪ *Historical introduction , Setting the stage*
- ♪ *Results from (run 1 and) run 2*
- ♪ *Future of ATLAS , run 3 , HL-LHC*
- ♪ *Conclusions*
- ♪ ***Backup***

- ♪ ***Historical introduction , Setting the stage***
- ♪ ***Results from (run 1 and) run 2***
- ♪ ***Future of ATLAS , run 3 , HL-LHC***
- ♪ ***Conclusions***
- ♪ ***Backup***

♪ ***Historical introduction , Setting the stage***

♪ ***Results from (****Run-1 and* ***) Run-2***

♪ ***Future of ATLAS , run 3 , HL-LHC***

♪ ***Conclusions***

♪ ***Backup***

♪ ***Results from (run 1 and) run 2***

- ***detector***
- ***SM***
- ***BSM***
- ***(B-E)H***
- ***Vector-boson scattering***

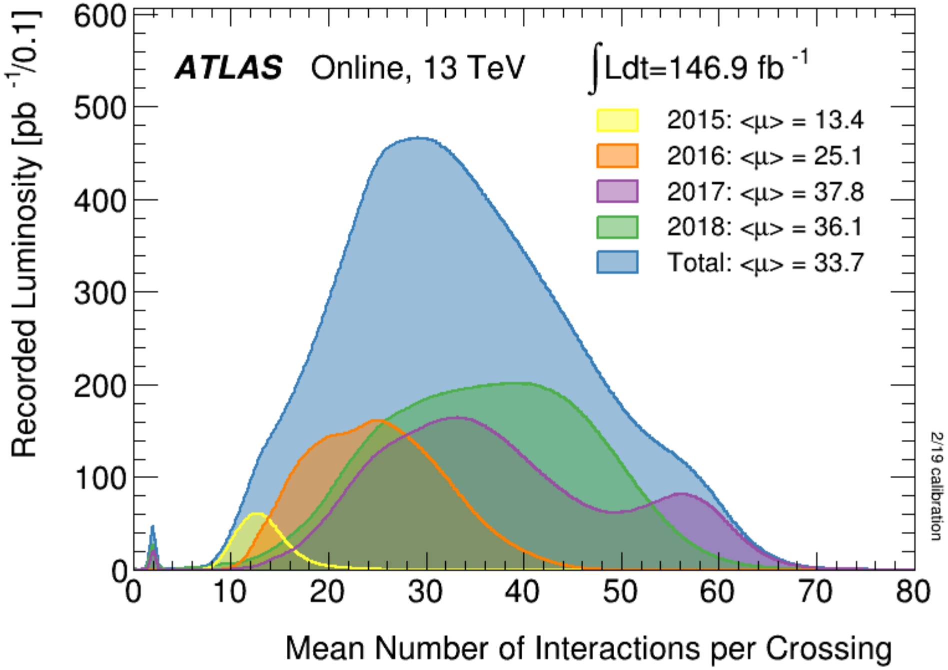

Δt= 25 ns

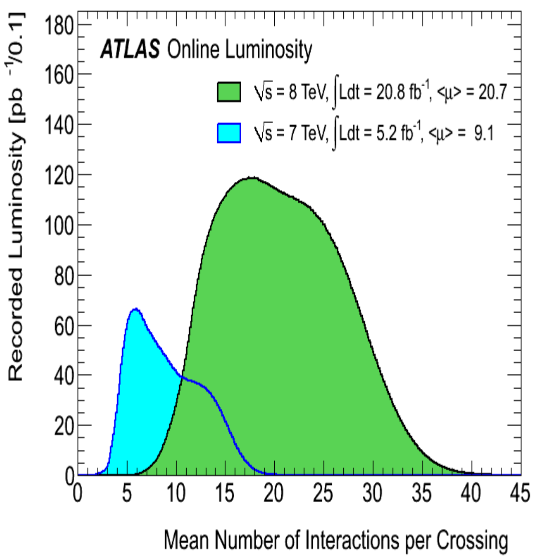

Δt= 50 ns

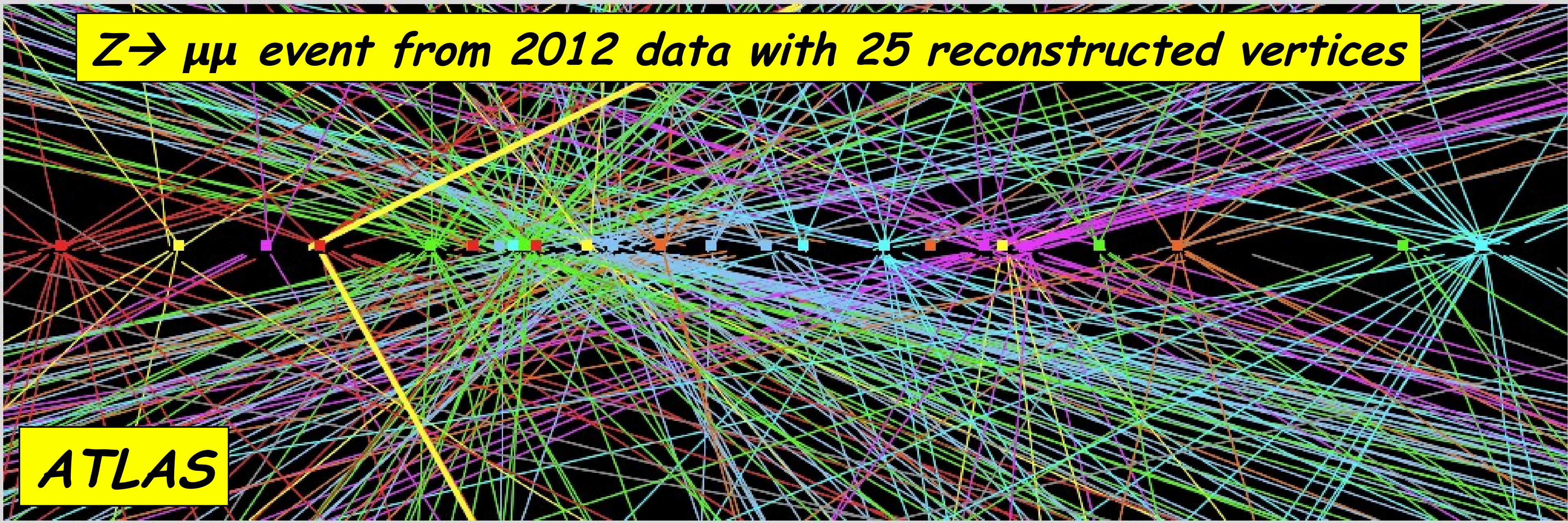

Pile up increases at higher energy (higher luminosity + higher cross sections)
→
Experiments have requested 25 ns (instead of 50 ns) operation at 13 TeV

But if the time constant is larger than 50 ns (i.e integrating time of the LAr calorimeter) then the pile-up is independent of the bunch spacing (for a given luminosity)

M. Lamont, IPAC'13

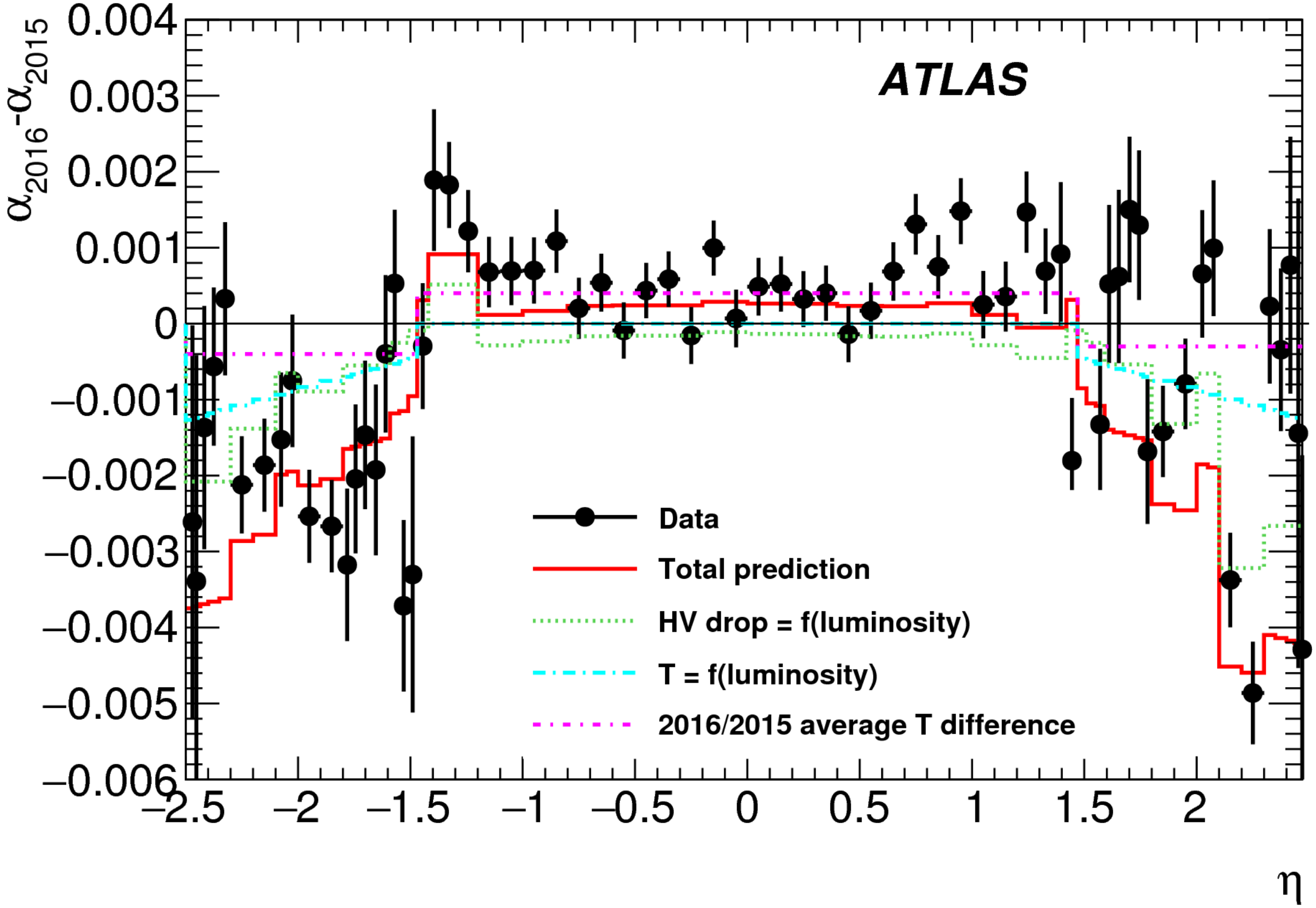

JINST 14 (2019) no.03, P03017

Comparison between the energy scale corrections derived from Z→ ee events in 2015 and 2016 as a function of η. *The difference of the energy scales measured in the data are compared with predictions taking into account the luminosity-induced high-voltage reduction and LAr temperature changes as well as the small overall difference in LAr temperature between 2015 and 2016*

additional constant term c as a function of eta

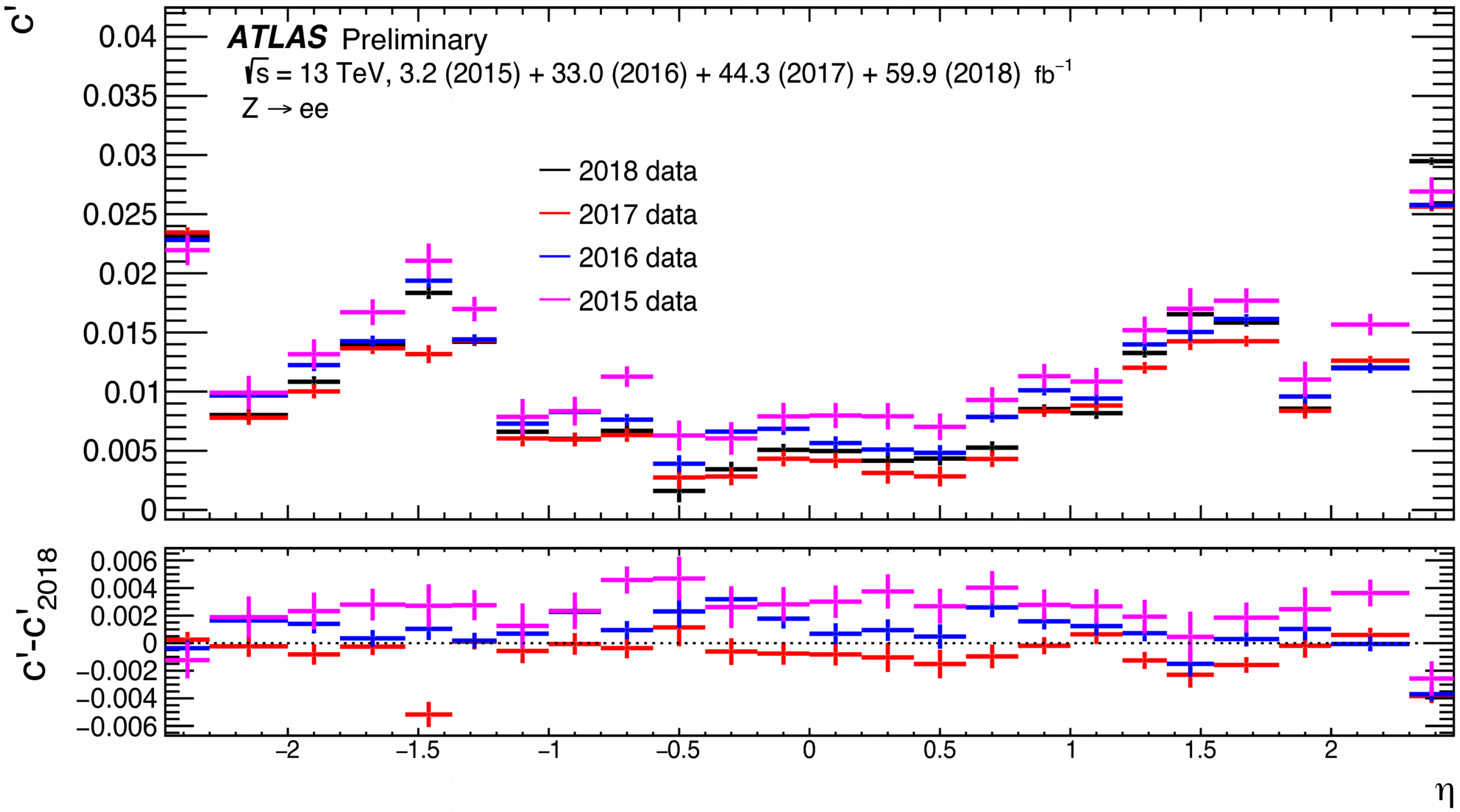

https://atlas.web.cern.ch/Atlas/GROUPS/PHYSICS/PLOTS/EGAM-2019-01/fig_02b.png

Data driven energy calibraton of standard particle flow jets w.r.t p_T

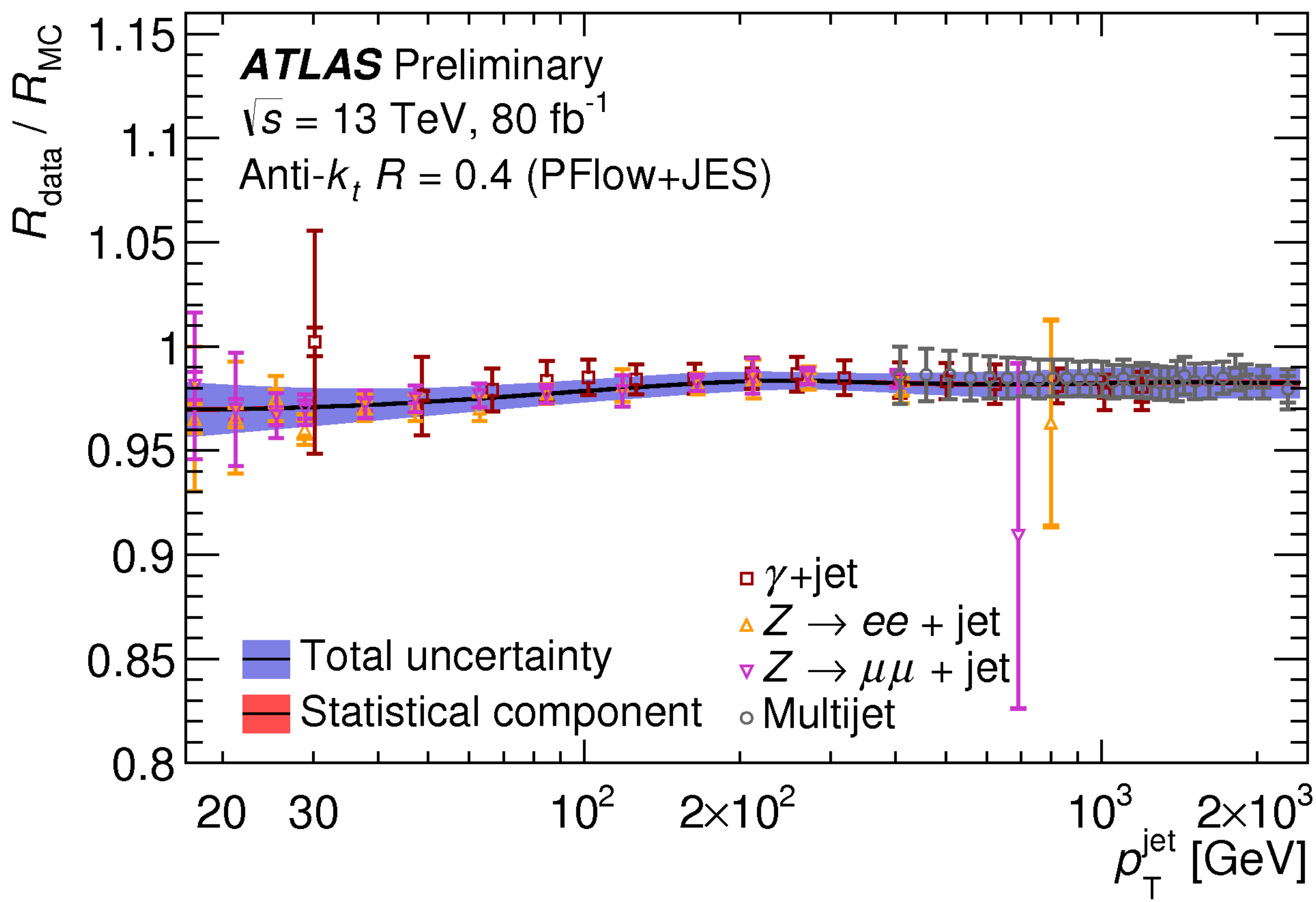

https://atlas.web.cern.ch/Atlas/GROUPS/PHYSICS/PLOTS/JETM-2018-006/fig_01a.png

Data driven b-jet tagging efficiency w.r.t p_T

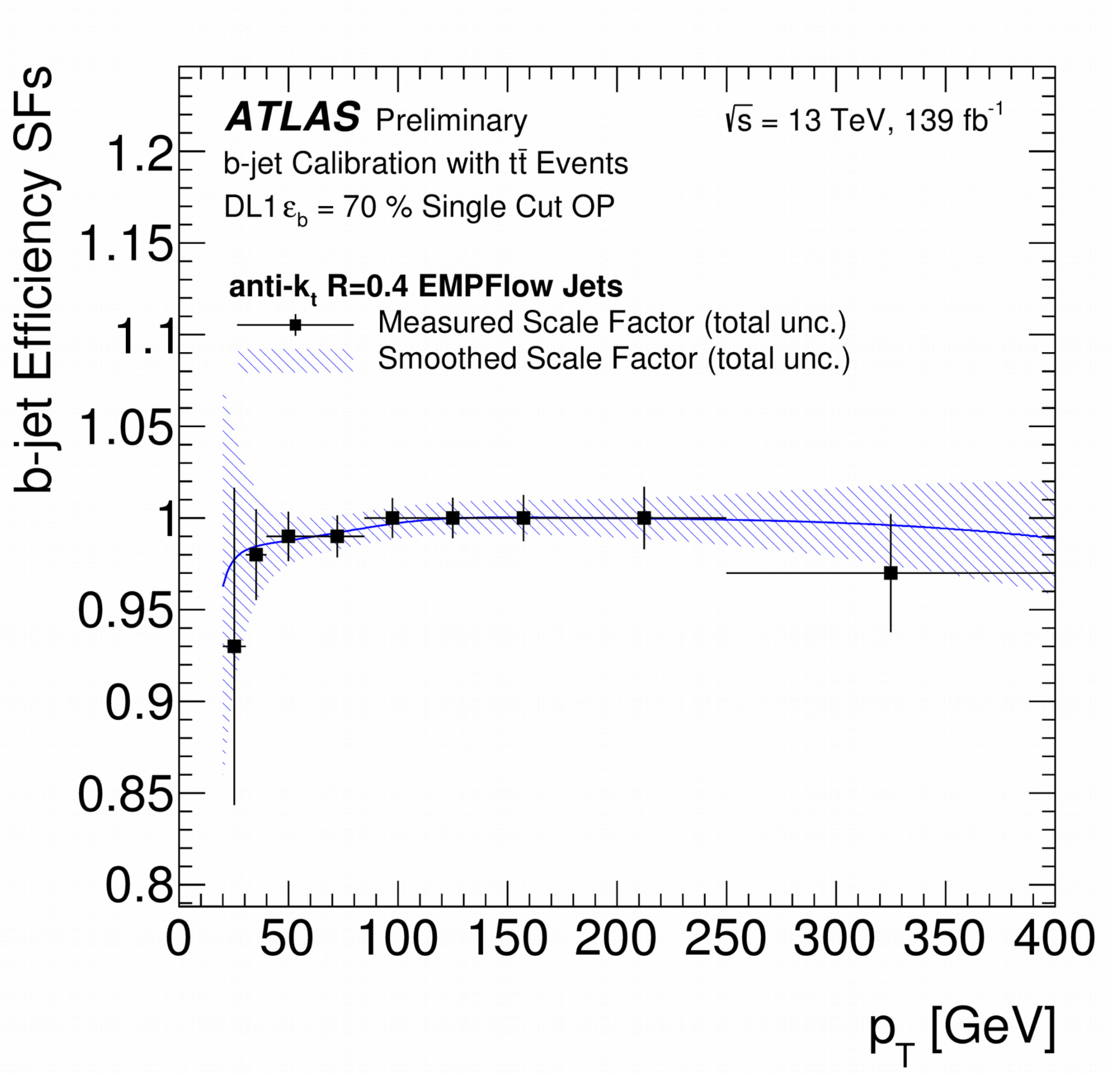

http://atlas.web.cern.ch/Atlas/GROUPS/PHYSICS/PLOTS/FTAG-2019-004/fig_07.png

♪ ***Results from (run 1 and) run 2***

- ***detector***
- ***SM***
- ***BSM***
- ***(B-E)H***
- ***Vector-boson scattering***

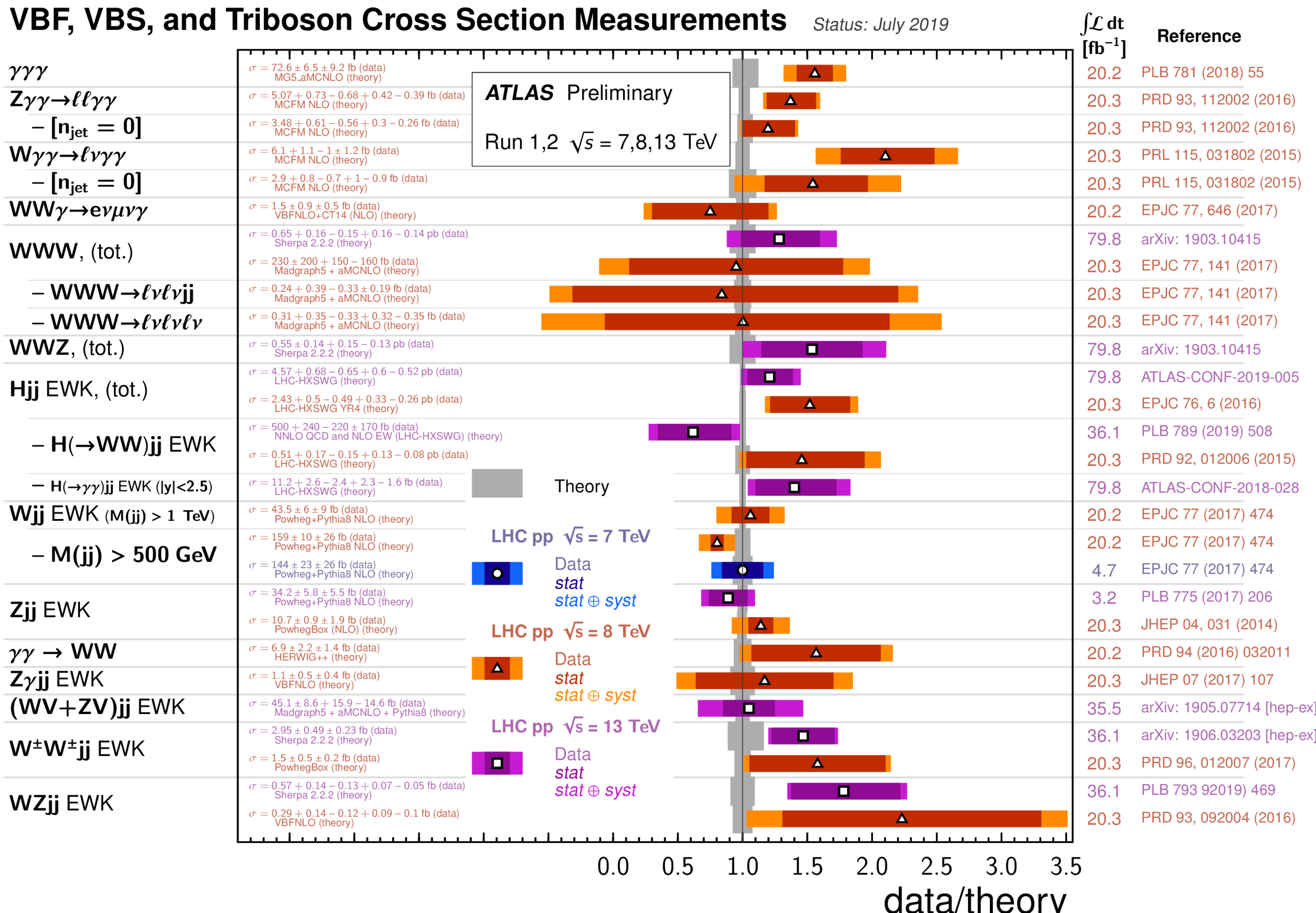

https://atlas.web.cern.ch/Atlas/GROUPS/PHYSICS/PUBNOTES/ATL-PHYS-PUB-2019-024/fig_19.png

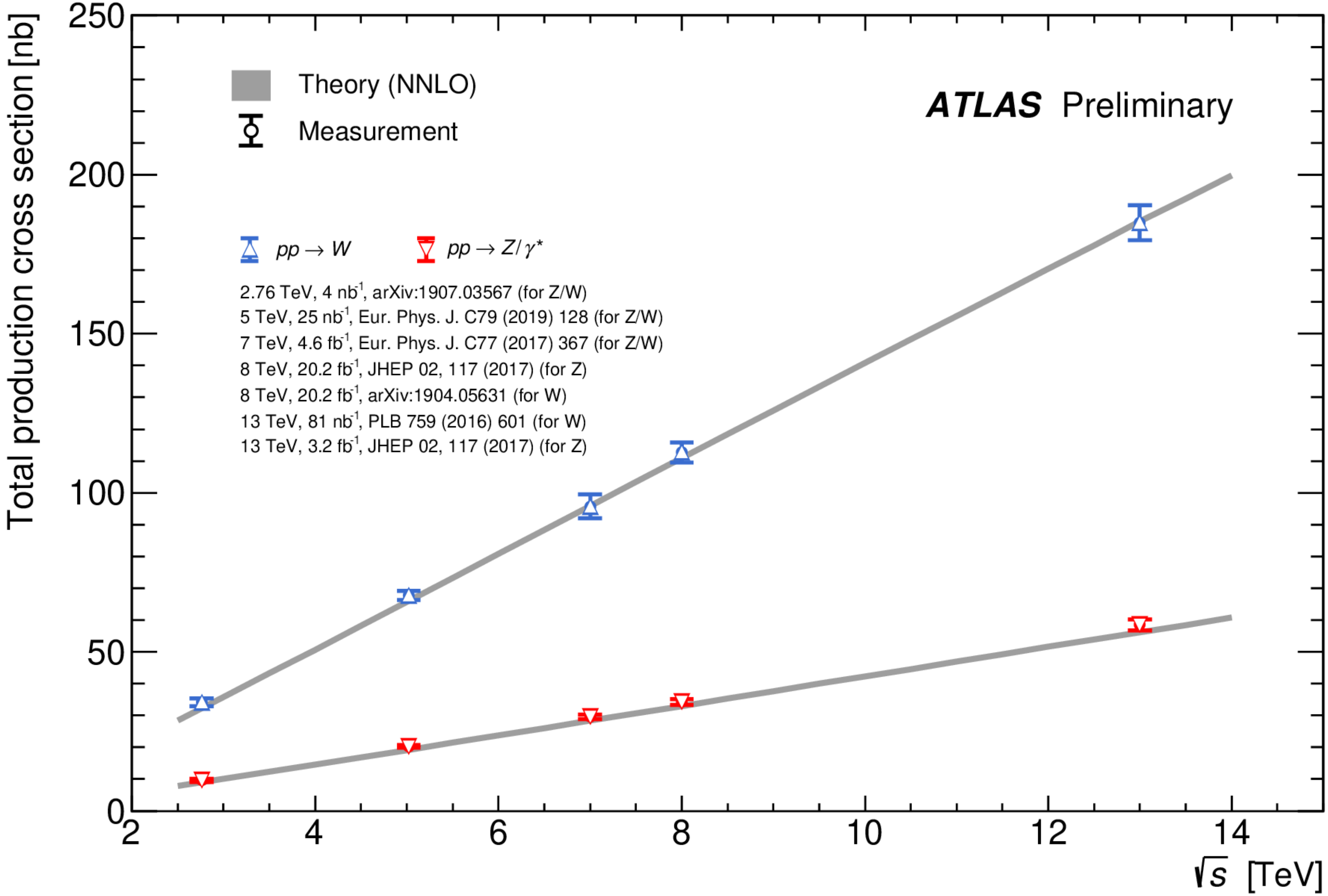

https://atlas.web.cern.ch/Atlas/GROUPS/PHYSICS/PUBNOTES/ATL-PHYS-PUB-2019-024/fig_25.png

4σ evidence for weak triboson production using 2015-2017 data

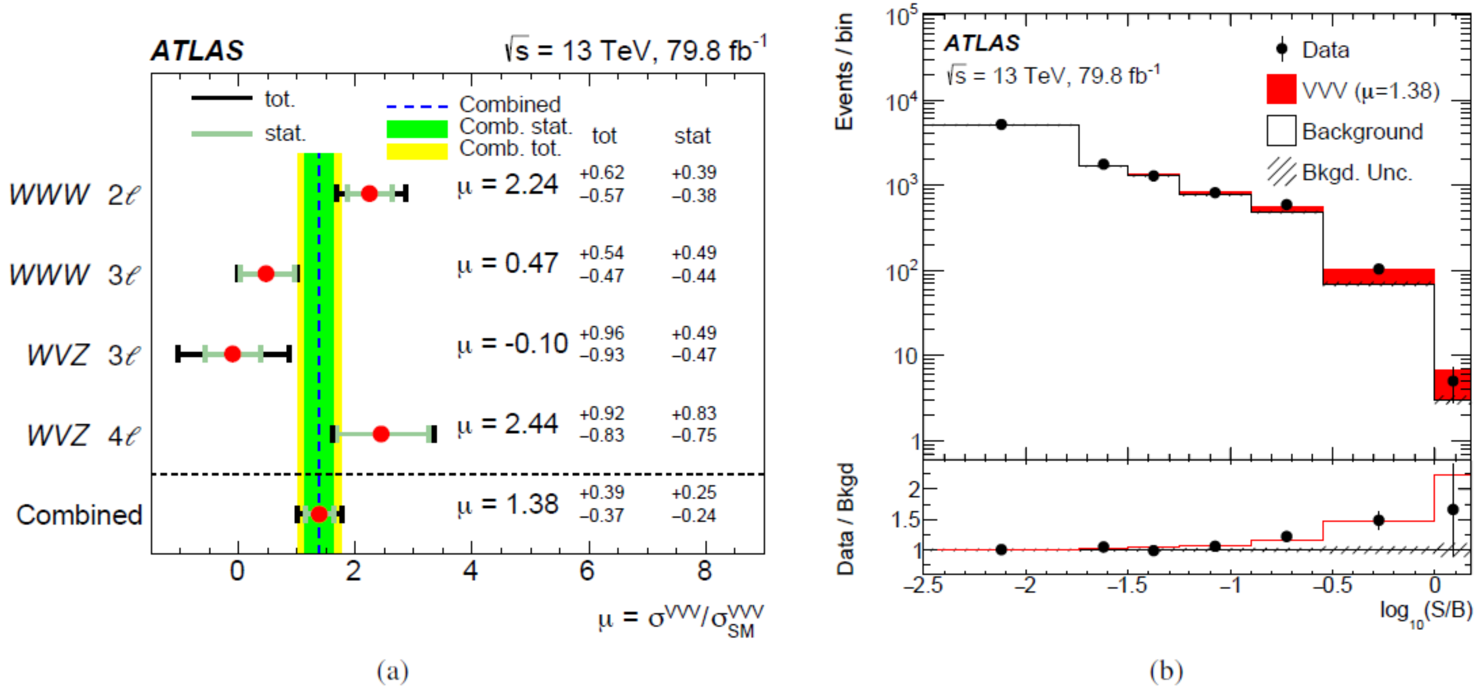

Figure 5: (a) Extracted signal strengths μ for the four analysis regions and for the combination. (b) Event yields as a function of $\log_{10}$ (S/B) for data, background B and the signal S. Events in all eleven signal regions are included. The background and signal yields are shown after the global signal-plus-background fit. The hatched band corresponds to the systematic uncertainties, and the statistical uncertainties are represented by the error bars on the data points. The lower panel shows the ratio of the data to the expected background estimated from the fit, compared to the expected distribution including the signal (red line).

arXiv:1903.10415

Measurement of fiducial and differential W+ W- production
cross-section ... ector

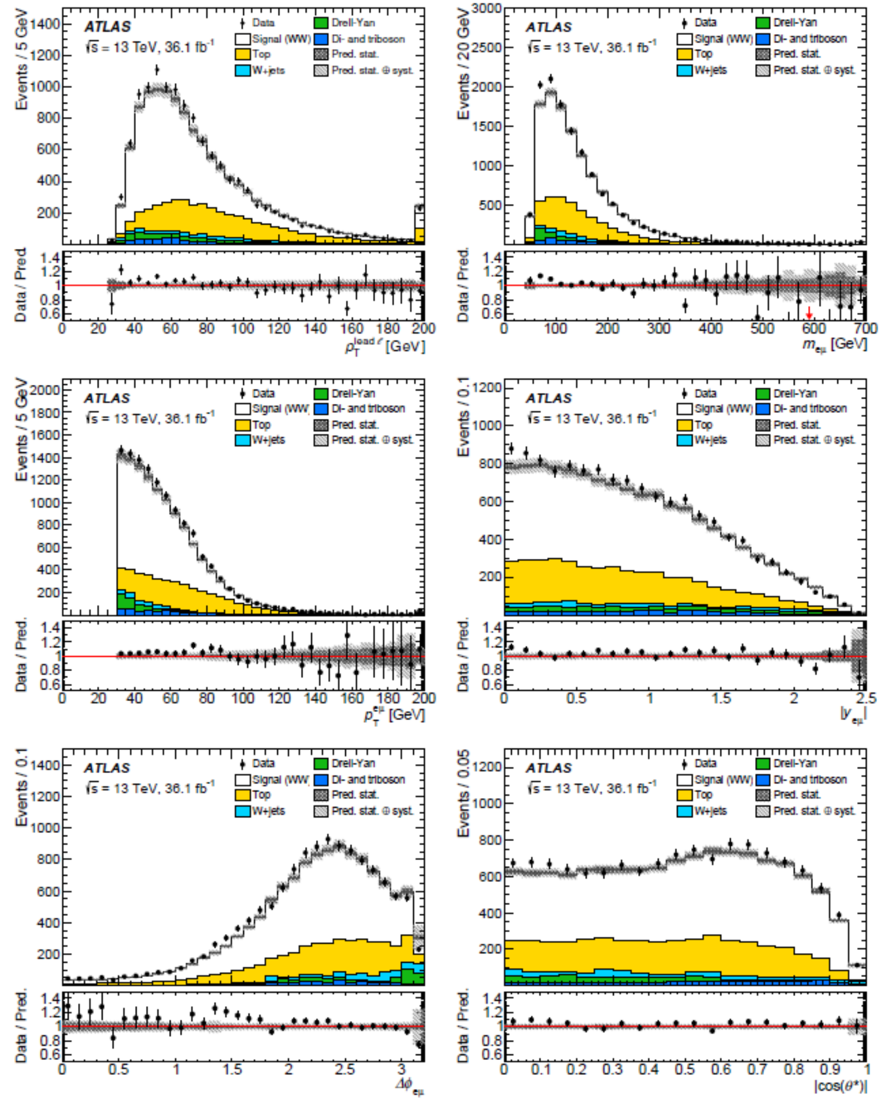

Figure 4: Kinematic distributions of the selected data events after the full event selection (from left to right and top to bottom): $p_T^{\text{lead}\,\ell}$, $m_{e\mu}$, $p_T^{e\mu}$, $|y_{e\mu}|$, $\Delta\phi_{e\mu}$ and $|\cos\theta^*|$. Data are shown together with the predictions of the signal and background production processes. Statistical and systematic uncertainties in the predictions are shown as hatched bands. The lower panels show the ratio of the data to the total prediction. An arrow indicates that the point is off-scale. The last bin includes the overflow.

arXiv:1905.04242

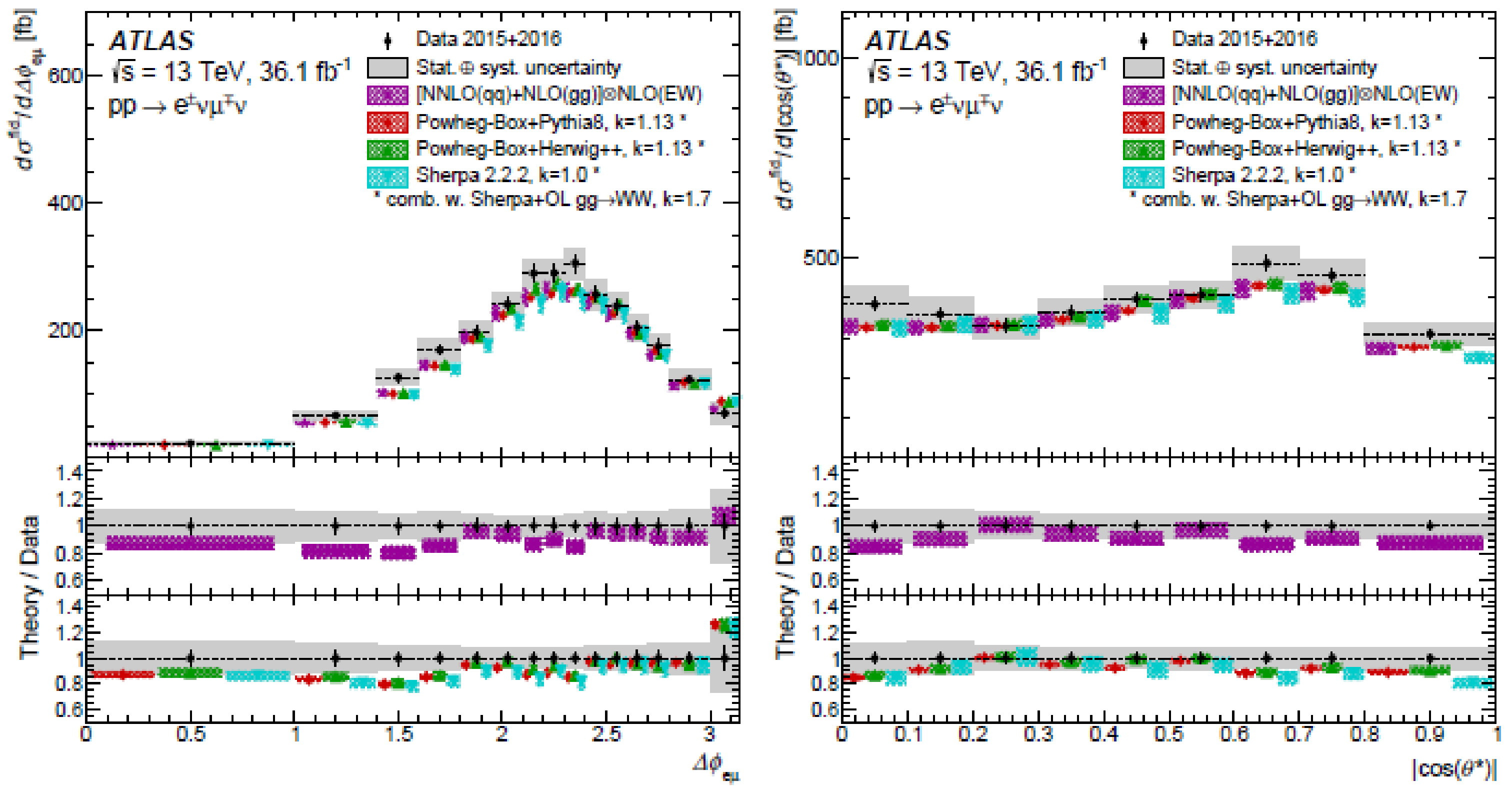

Figure 8: Measured fiducial cross-sections of $WW \to e\mu$ production for two of the six observables: $\Delta\phi_{e\mu}$ and $|\cos\theta^*|$. The measured cross-section values are shown as points with error bars giving the statistical uncertainty and solid bands indicating the size of the total uncertainty. The results are compared with the NNLO prediction with extra NLO EW corrections and NLO corrections for $gg \to WW$ production, and with NLO+PS predictions from Powheg-Box+Pythia 8, Powheg-Box+Herwig++ and Sherpa 2.2.2 for $q\bar{q}$ initial states, combined with Sherpa+OpenLoops (LO+PS) for the gg initial states. All three $q\bar{q}$ NLO+PS predictions are normalized to the NNLO theoretical prediction for the total cross-section, with the gg LO+PS contribution normalized to NLO. Theoretical predictions are indicated as markers with hatched bands denoting PDF+scale uncertainties.

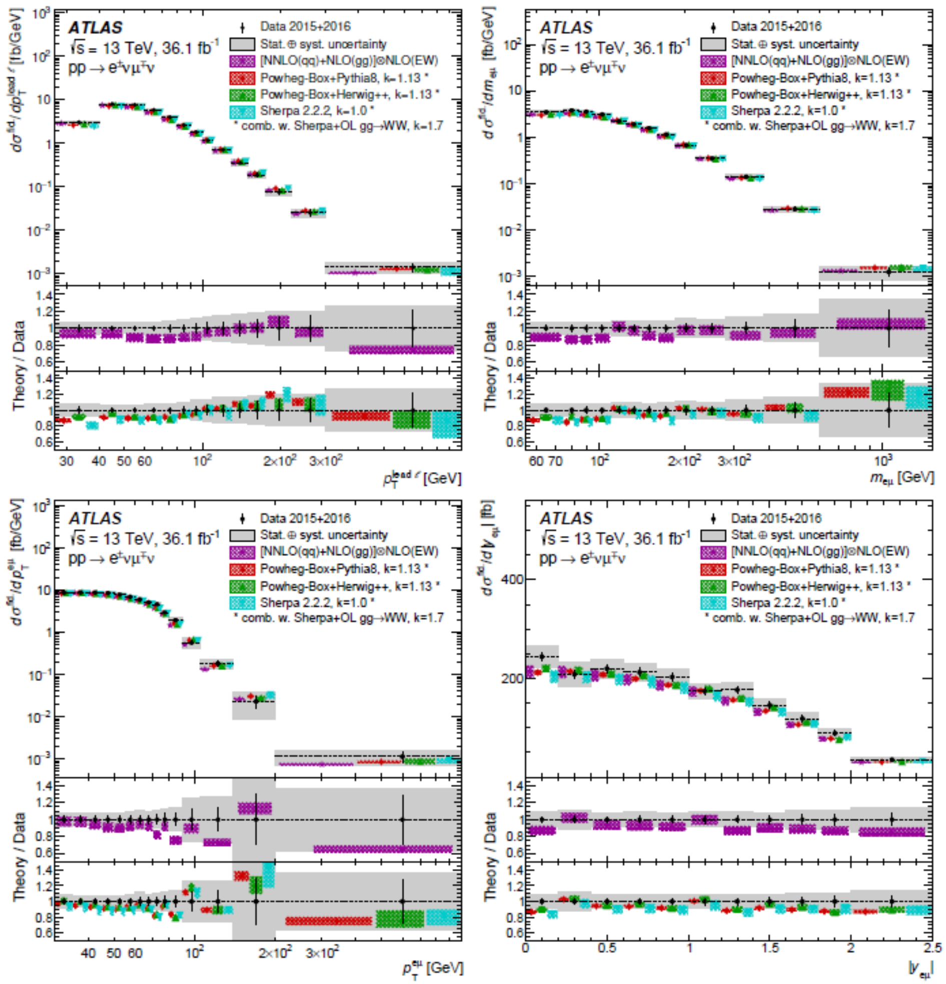

Figure 7: Measured fiducial cross-sections of $WW \to e\mu$ production for four of the six observables (from left to right and top to bottom): $p_{\mathrm{T}}^{\mathrm{lead}\,\ell}$, $m_{e\mu}$, $p_{\mathrm{T}}^{e\mu}$, and $|y_{e\mu}|$. The measured cross-section values are shown as points with error bars giving the statistical uncertainty and solid bands indicating the size of the total uncertainty. The results are compared with the NNLO prediction with extra NLO EW corrections and NLO corrections for $gg \to WW$ production, and with NLO+PS predictions from Powheg-Box+Pythia 8, Powheg-Box+Herwig++ and Sherpa 2.2.2 for $q\bar{q}$ initial states, combined with Sherpa+OpenLoops (LO+PS) for the gg initial states. All three $q\bar{q}$ NLO+PS predictions are normalized to the NNLO theoretical prediction for the total cross-section, with the gg LO+PS contribution normalized to NLO. Theoretical predictions are indicated as markers with hatched bands denoting PDF+scale uncertainties.

Measurement of $Z(\rightarrow l^+l^-)\,\gamma$ differential cross-sections in pp collisions at $\sqrt{s} = 13$ TeV with the ATLAS detector

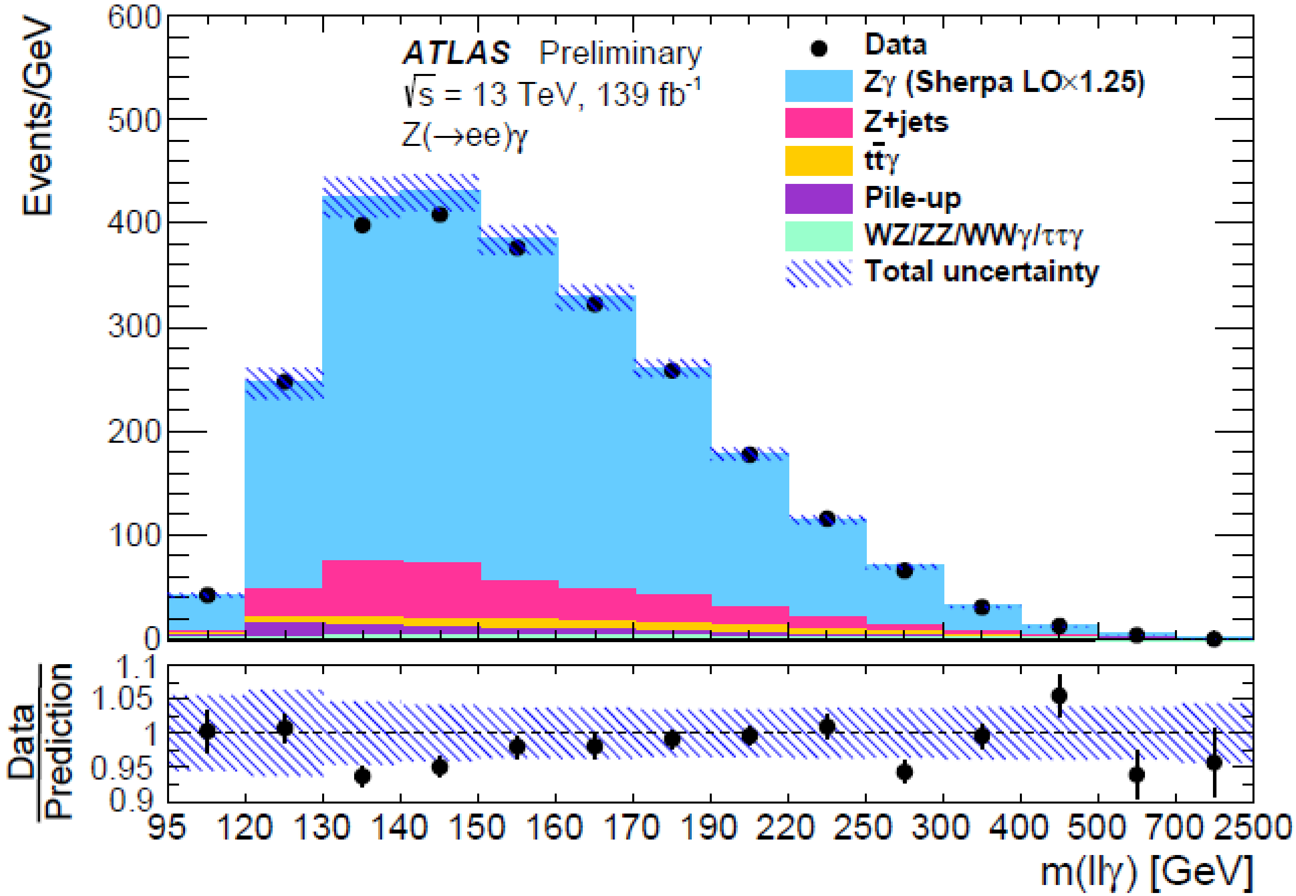

ATLAS-CONF-2019-034

Inclusive and differential measurements of the charge asymmetry in t t eve ... TLAS detector

$$p\bar{p}$$

$$A_{FB} = \frac{N(\Delta y > 0) - N(\Delta y < 0)}{N(\Delta y > 0) + N(\Delta y < 0)}$$

$$\Delta y = y_t - y_{\bar{t}}$$

different from 0 because of interference

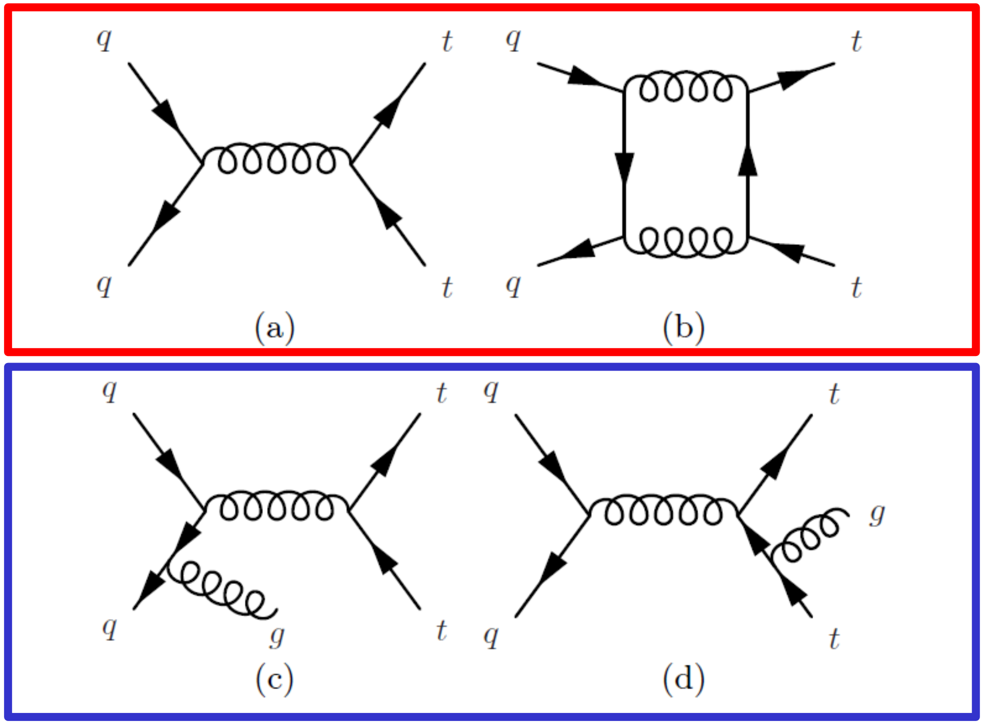

positive asymmetry

negative asymmetry

in pp collisions a FB asymmetry with a fixed $\hat{z}$ axis vanishes

$$A_C = \frac{N(\Delta|y| > 0) - N(\Delta|y| < 0)}{N(\Delta|y| > 0) + N(\Delta|y| < 0)}$$

$$\Delta|y| = |y_t| - |y_{\bar{t}}|$$

J.Aguilar-Saavedra et al. Rev.Mod.Phys. 87 (2015) 421-455

Observation of light-by-light scattering in ultraperipheral Pb+Pb collisions with the ATLAS detector

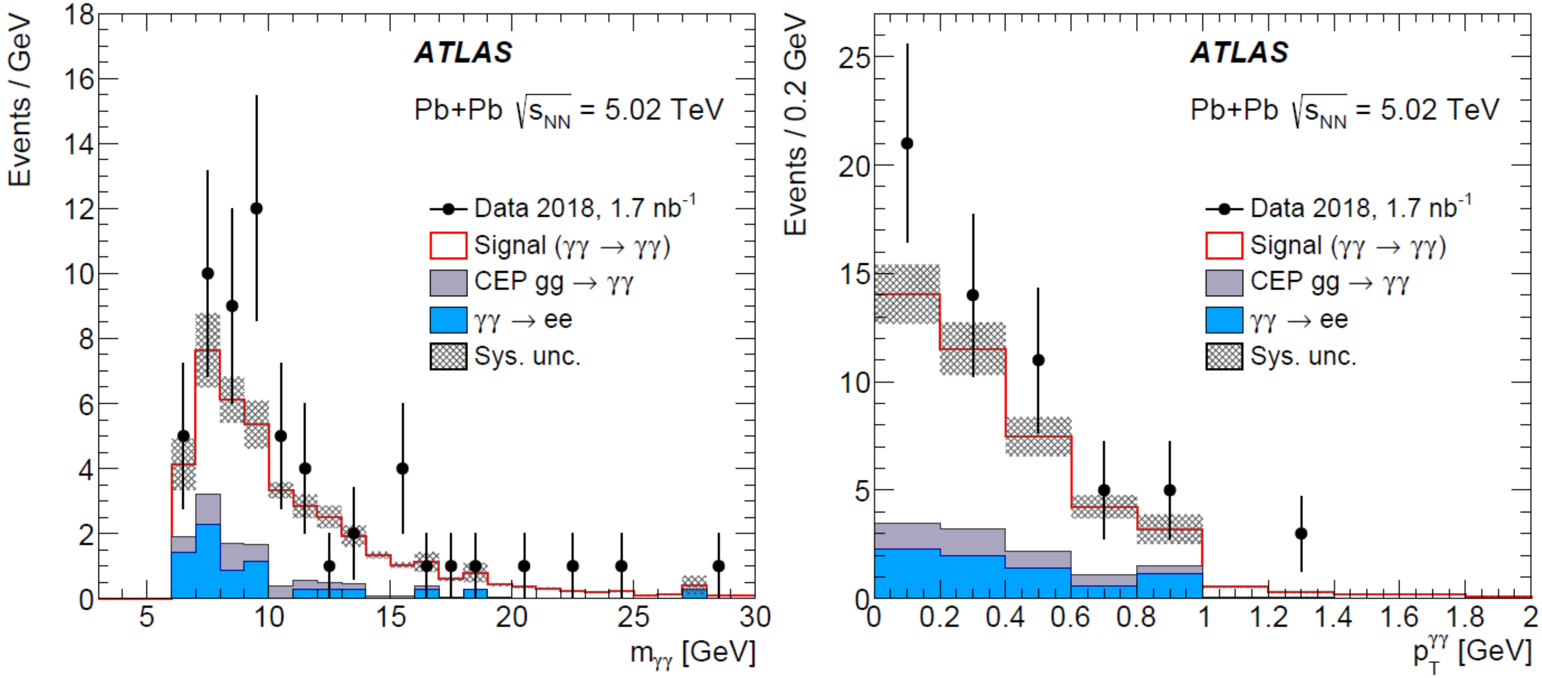

(a) (b)

Figure 3: Kinematic distributions for $\gamma\gamma \to \gamma\gamma$ event candidates: (a) diphoton invariant mass, (b) diphoton transverse momentum. Data (points) are compared with the sum of signal and background expectations (histograms). Systematic uncertainties of the signal and background processes, excluding that of the luminosity, are shown as shaded bands.

$$A_\phi = (1 - |\Delta\phi_{\gamma\gamma}|/\pi) < 0.01$$

Phys.Rev.Lett. 123 (2019) no.5, 052001

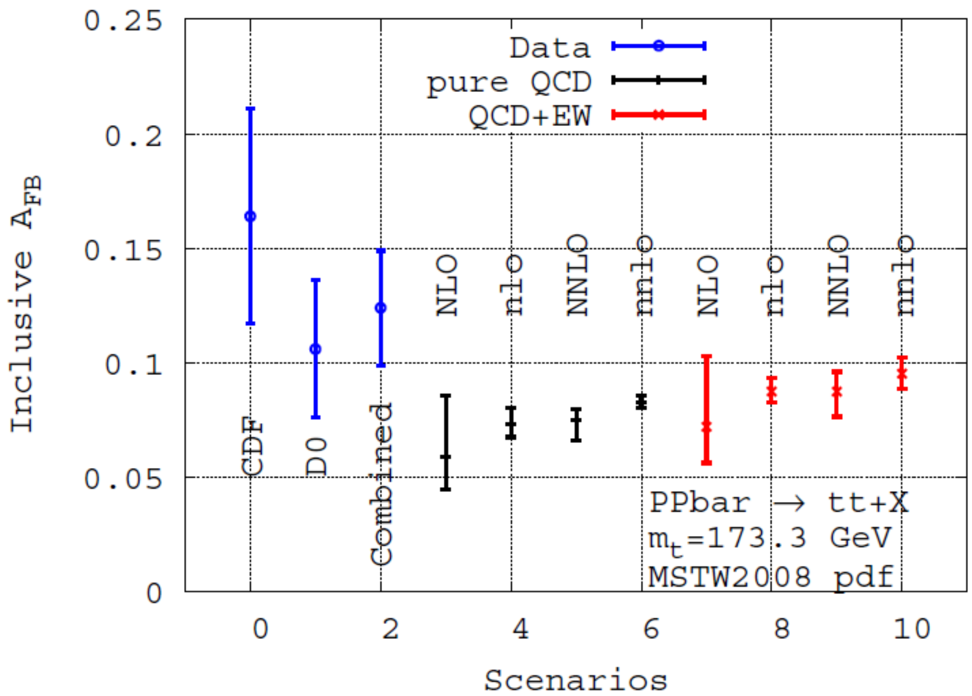

FIG. 1: The inclusive asymmetry in pure QCD (black) and QCD+EW[28] (red). Capital letters (NLO, NNLO) correspond to the unexpanded definition (2), while small letters (nlo, nnlo) to the definition (3). The CDF/DØ (naive) average is from Ref. [29]. Error bands are from scale variation only. Our final prediction corresponds to scenario 10.

M.Czakon et al. Phys.Rev.Lett. 115 (2015) no.5, 052001

FCNC (Flavour-Changing Neutral Current)

arXiv:1908.08461

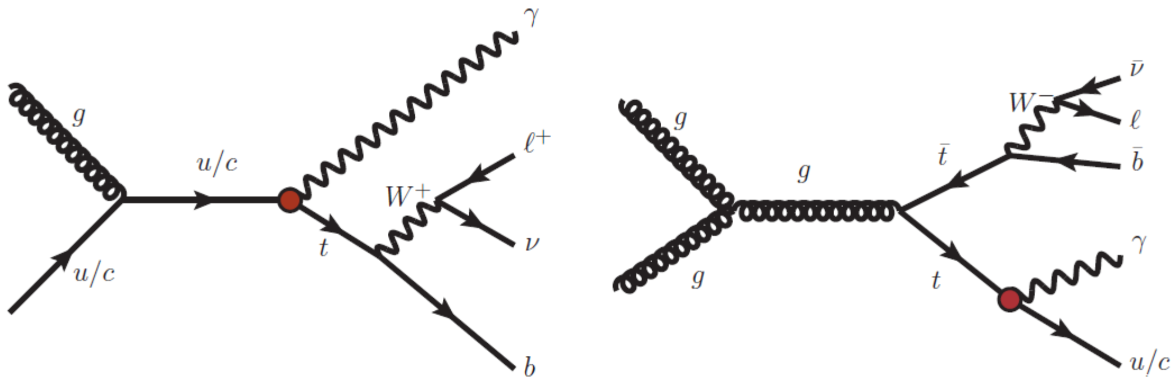

Figure 1: Tree-level Feynman diagrams for top-quark production (left) and decay (right) via FCNCs. The $tq\gamma$ vertex, which is not present in the SM, is highlighted.

Table 1: Observed (expected) 95% CL limits on the effective coupling strengths for different vertices and couplings, the production cross section, and the branching ratio. For the former, the energy scale is assumed to be $\Lambda = 1$ TeV.

Observable	Vertex	Coupling	Obs.	Exp.
$\left\lvert C_{\mathrm{uW}}^{(13)*} + C_{\mathrm{uB}}^{(13)*}\right\rvert$	$tu\gamma$	LH	0.19	$0.22^{+0.04}_{-0.03}$
$\left\lvert C_{\mathrm{uW}}^{(31)} + C_{\mathrm{uB}}^{(31)}\right\rvert$	$tu\gamma$	RH	0.27	$0.27^{+0.05}_{-0.04}$
$\left\lvert C_{\mathrm{uW}}^{(23)*} + C_{\mathrm{uB}}^{(23)*}\right\rvert$	$tc\gamma$	LH	0.52	$0.57^{+0.11}_{-0.09}$
$\left\lvert C_{\mathrm{uW}}^{(32)} + C_{\mathrm{uB}}^{(32)}\right\rvert$	$tc\gamma$	RH	0.48	$0.59^{+0.12}_{-0.09}$
$\sigma(pp \to t\gamma)$ [fb]	$tu\gamma$	LH	36	52^{+21}_{-14}
$\sigma(pp \to t\gamma)$ [fb]	$tu\gamma$	RH	78	75^{+31}_{-21}
$\sigma(pp \to t\gamma)$ [fb]	$tc\gamma$	LH	40	49^{+20}_{-14}
$\sigma(pp \to t\gamma)$ [fb]	$tc\gamma$	RH	33	52^{+22}_{-14}
$\mathcal{B}(t \to q\gamma)\,[10^{-5}]$	$tu\gamma$	LH	2.8	$4.0^{+1.6}_{-1.1}$
$\mathcal{B}(t \to q\gamma)\,[10^{-5}]$	$tu\gamma$	RH	6.1	$5.9^{+2.4}_{-1.6}$
$\mathcal{B}(t \to q\gamma)\,[10^{-5}]$	$tc\gamma$	LH	22	27^{+11}_{-7}
$\mathcal{B}(t \to q\gamma)\,[10^{-5}]$	$tc\gamma$	RH	18	28^{+12}_{-8}

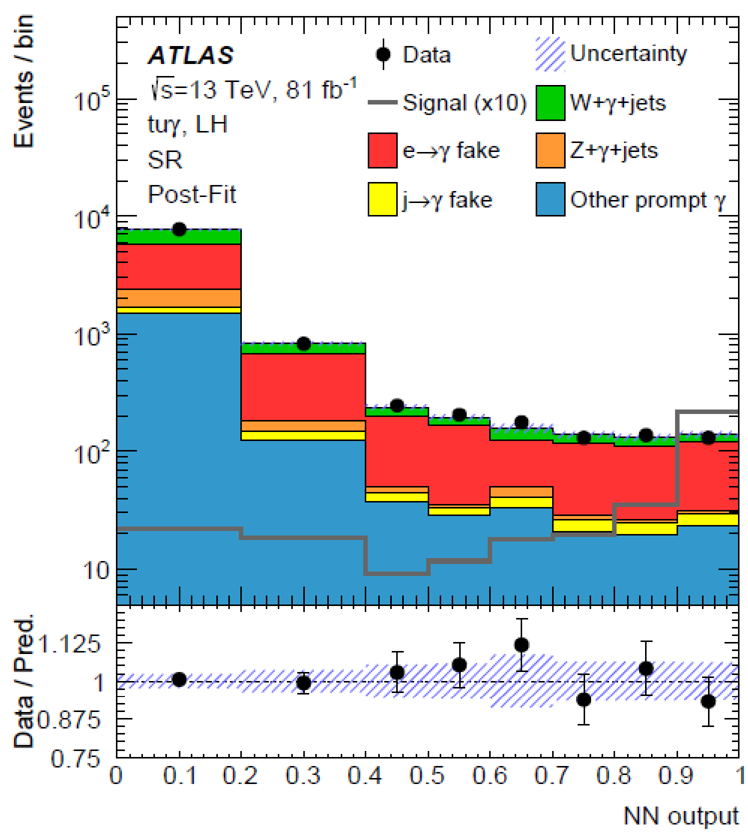

FCNC (Flavour-Changing Neutral Current)

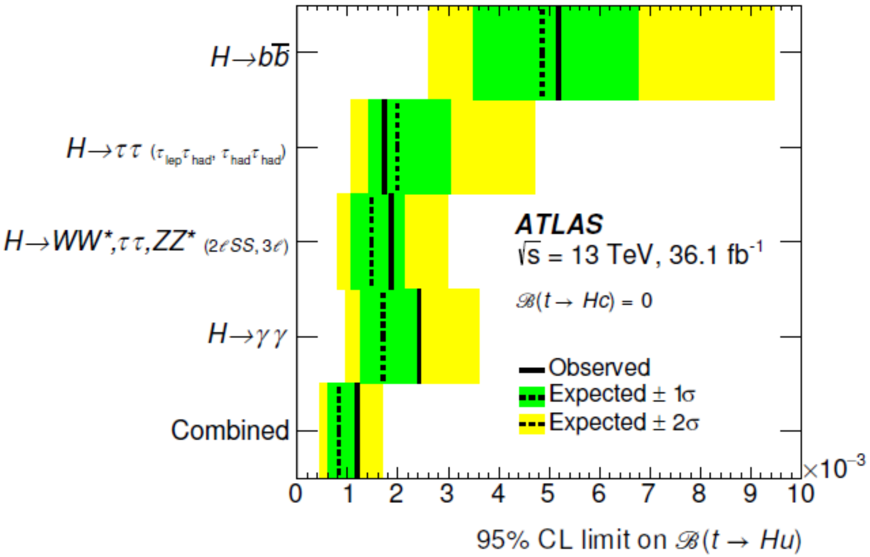

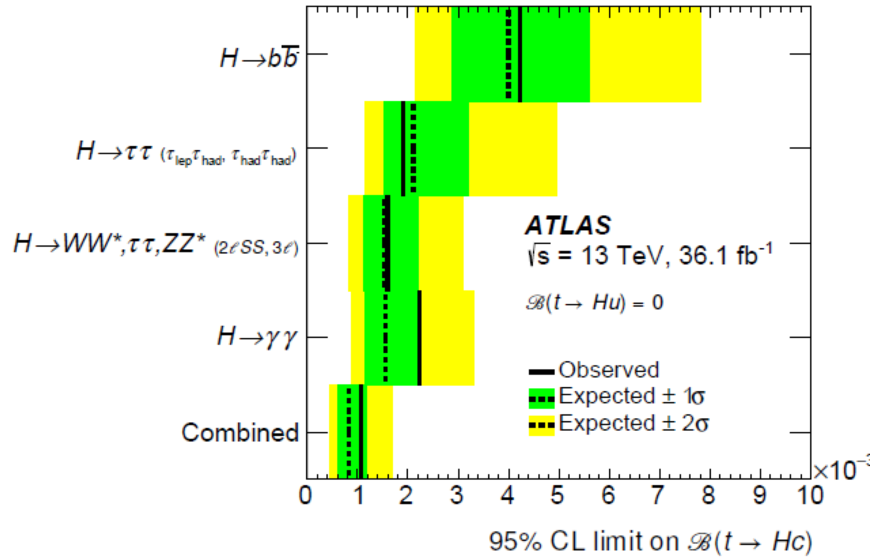

Table 3: Summary of 95% CL upper limits on $\mathscr{B}(t \to Hc)$ and $\mathscr{B}(t \to Hu)$, in each case neglecting the other decay mode. Signatures with two same-charge (three) leptons and no τ_{had} candidates are denoted by 2ℓSS (3ℓ).

	95% CL upper limits on $\mathscr{B}(t \to Hc)$ Observed (Expected)	95% CL upper limits on $\mathscr{B}(t \to Hu)$ Observed (Expected)
$H \to b\bar{b}$	4.2×10^{-3} (4.0×10^{-3})	5.2×10^{-3} (4.9×10^{-3})
$H \to \tau\tau$ ($\tau_{\text{lep}}\tau_{\text{had}}$, $\tau_{\text{had}}\tau_{\text{had}}$)	1.9×10^{-3} (2.1×10^{-3})	1.7×10^{-3} (2.0×10^{-3})
$H \to WW^*, \tau\tau, ZZ^*$ (2ℓSS, 3ℓ) [22]	1.6×10^{-3} (1.5×10^{-3})	1.9×10^{-3} (1.5×10^{-3})
$H \to \gamma\gamma$ [21]	2.2×10^{-3} (1.6×10^{-3})	2.4×10^{-3} (1.7×10^{-3})
Combination	1.1×10^{-3} (8.3×10^{-4})	1.2×10^{-3} (8.3×10^{-4})

JHEP 1905 (2019) 123

ATL-CONF-2018-037

EW precision measurements
Weak angle $\sin^2\theta^l_{eff}$

$$\frac{d\sigma}{dp_T^{\ell\ell}\, dy^{\ell\ell}\, dm^{\ell\ell}\, d\cos\theta\, d\phi} = \frac{3}{16\pi}\frac{d\sigma^{U+L}}{dp_T^{\ell\ell}\, dy^{\ell\ell}\, dm^{\ell\ell}}$$

$$\Big\{(1+\cos^2\theta) + \frac{1}{2} A_0(1-3\cos^2\theta) + A_1 \sin 2\theta \cos\phi$$

$$+\frac{1}{2} A_2 \sin^2\theta \cos 2\phi + A_3 \sin\theta \cos\phi + A_4 \cos\theta$$

$$+A_5 \sin^2\theta \sin 2\phi + A_6 \sin 2\theta \sin\phi + A_7 \sin\theta \sin\phi\Big\}$$

$$\boxed{A_{FB} = 3/8 \times A_4}$$

EW precision measurements

W mass m_W

arXiv:1701.07240

$$m_W = 80369.5 \pm 6.8 \text{ MeV(stat.)} \pm 10.6 \text{ MeV(exp. syst.)} \pm 13.6 \text{ MeV(mod. syst.)}$$
$$= 80369.5 \pm 18.5 \text{ MeV},$$

Combined categories	Value [MeV]	Stat. Unc.	Muon Unc.	Elec. Unc.	Recoil Unc.	Bckg. Unc.	QCD Unc.	EW Unc.	PDF Unc.	Total Unc.	χ^2/dof of Comb.
m_T-p_T^ℓ, $W^\pm$, e-μ	80369.5	6.8	6.6	6.4	2.9	4.5	8.3	5.5	9.2	18.5	29/27

JHEP 04 (2019) 098

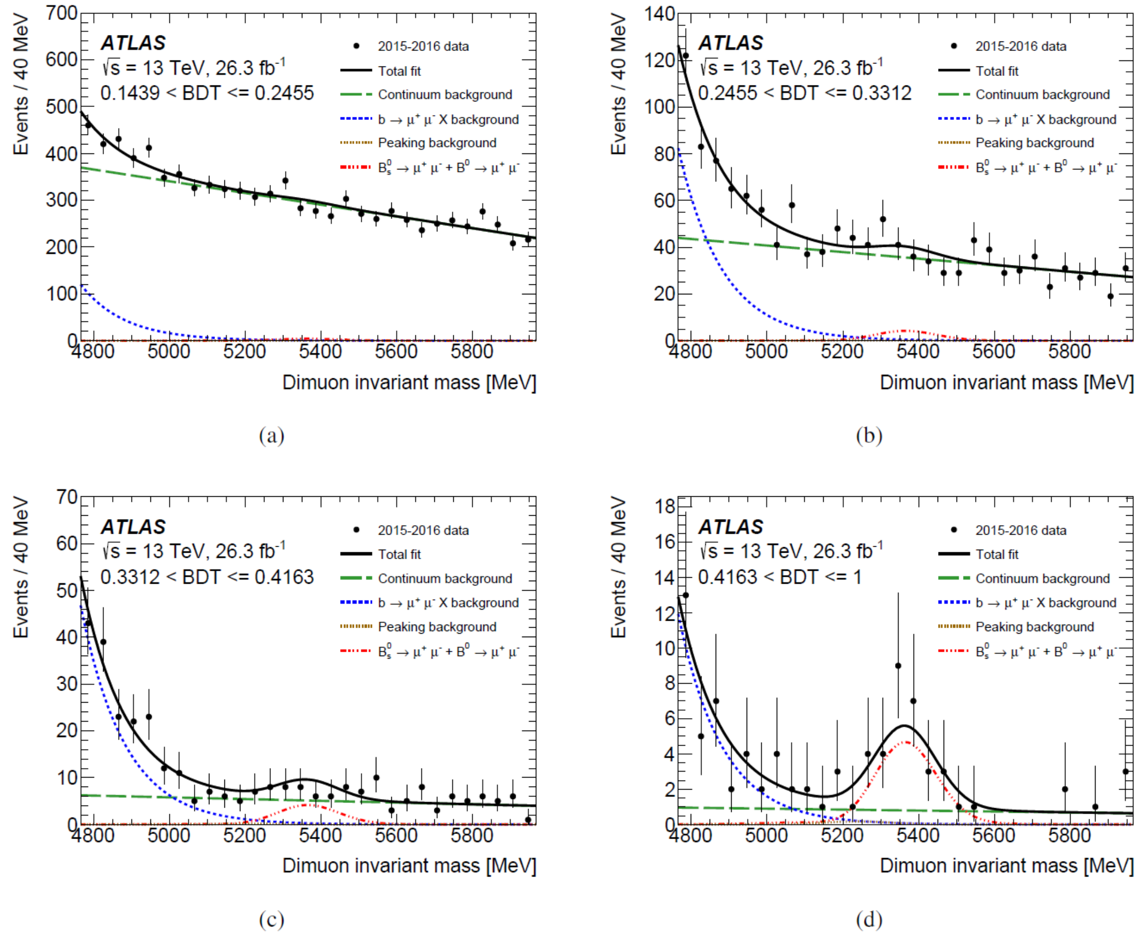

Figure 8: Dimuon invariant mass distributions in the unblinded data, in the four intervals of BDT output. Superimposed is the result of the maximum-likelihood fit. The total fit is shown as a continuous line, with the dashed lines corresponding to the observed signal component, the $b \to \mu\mu X$ background, and the continuum background. The signal components are grouped in one single curve, including both the $B_s^0 \to \mu^+\mu^-$ and the (negative) $B^0 \to \mu^+\mu^-$ component. The curve representing the peaking $B_{(s)}^0 \to hh'$ background lies very close to the horizontal axis in all BDT bins.

B physics

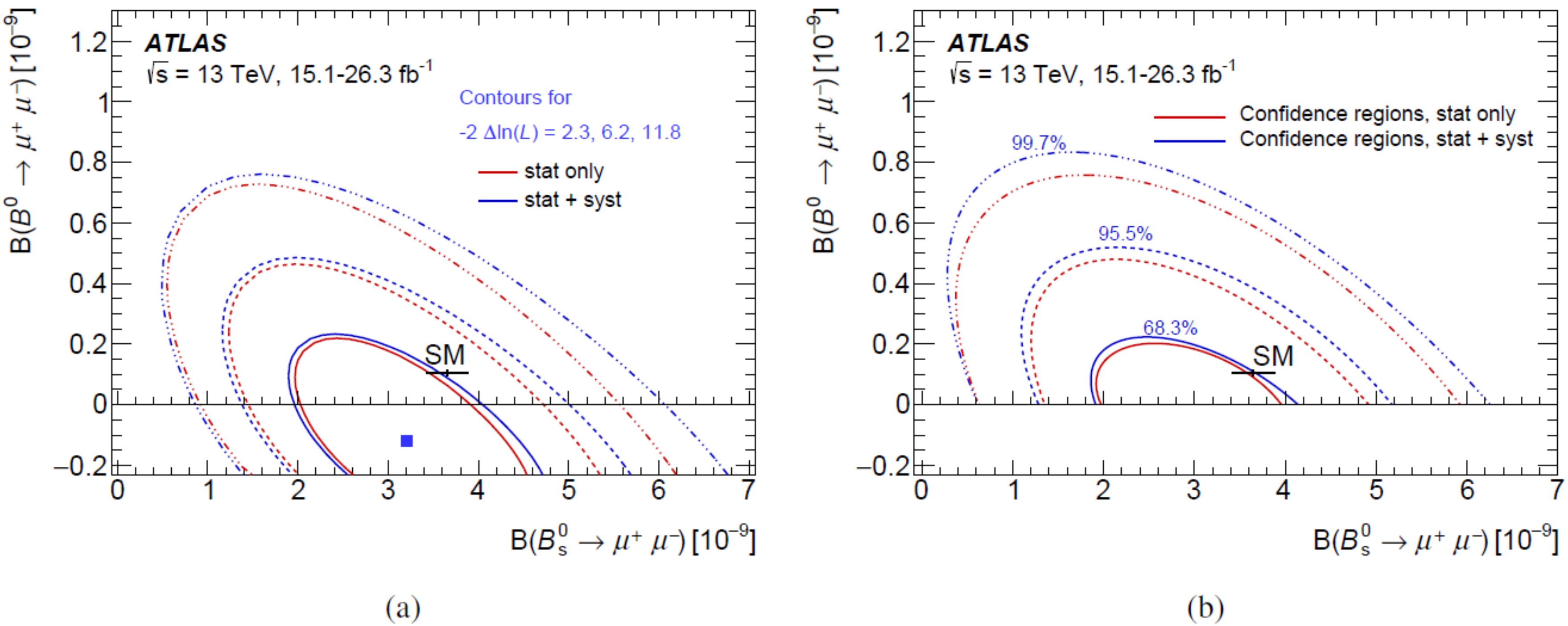

Figure 9: (a) Likelihood contours for the simultaneous fit to $\mathcal{B}(B_s^0 \to \mu^+\mu^-)$ and $\mathcal{B}(B^0 \to \mu^+\mu^-)$, for values of $-2\Delta\ln(\mathcal{L})$ equal to 2.3, 6.2 and 11.8. The SM prediction with uncertainties is indicated. (b) Neyman contours in the $\mathcal{B}(B_s^0 \to \mu^+\mu^-)$–$\mathcal{B}(B^0 \to \mu^+\mu^-)$ plane for 68.3%, 95.5% and 99.7% coverage. At each $-2\Delta\ln(\mathcal{L})$ or coverage value, the inner contours are statistical uncertainty only, while the outer ones include statistical and systematic uncertainties. The construction of these contours makes use of both the dimuon (26.3 fb^{-1}) and the reference channel (15.1 fb^{-1}) datasets.

B physics

$$\phi_s = -0.076 \pm 0.034\,(\text{stat.}) \pm 0.019\,(\text{syst.})\ \text{rad}$$
$$\Delta\Gamma_s = 0.068 \pm 0.004\,(\text{stat.}) \pm 0.003\,(\text{syst.})\ \text{ps}^{-1}$$
$$\Gamma_s = 0.669 \pm 0.001\,(\text{stat.}) \pm 0.001\,(\text{syst.})\ \text{ps}^{-1}$$

Measurement of $\Delta\Gamma_s$ and φ_s in $B_s \rightarrow J/\psi(\mu\mu)\ \varphi(KK)$

- CP violation in $B_s \rightarrow J/\psi\ \varphi$ occurs through the interference in mixing and decay.
- The time evolution of flavour tagged is very sensitive New Physics
- B_s mixing:
  - Mass difference
  - $\Delta m = m_H - m_L$
  - Mixing phase ϕs
  - Decay width difference $\Delta\Gamma s = \Gamma_L - \Gamma_H$
- 9 Physics parameters describe $B_s \rightarrow J/\psi\ \varphi$ decay:

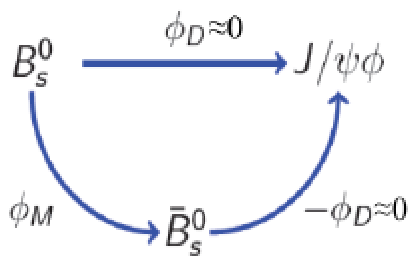

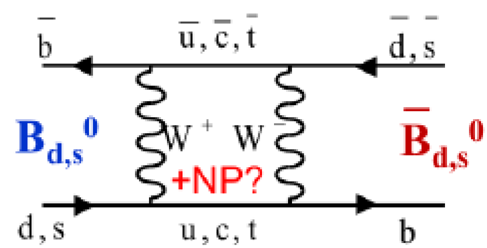

Γ_s, $\Delta\Gamma_s$	decay with and decay width difference
ϕ_s ($\approx 2\beta_s$)	CP violating phase
$\lvert A_0\rvert^2$, $\lvert A_{\parallel}\rvert^2$	CP state amplitudes
$\delta_{\parallel}$, $\delta_{\perp}$	Strong phases
$\lvert A_s\rvert^2$, δ_s	S-wave parameters

ATLAS-CONF-2019-009 Barton@EPS2019

♪ *Results from (run 1 and) run 2*

- *detector*
- *SM*
- ***BSM***
- *(B-E)H*
- *Vector-boson scattering*

Search for Physics BSM

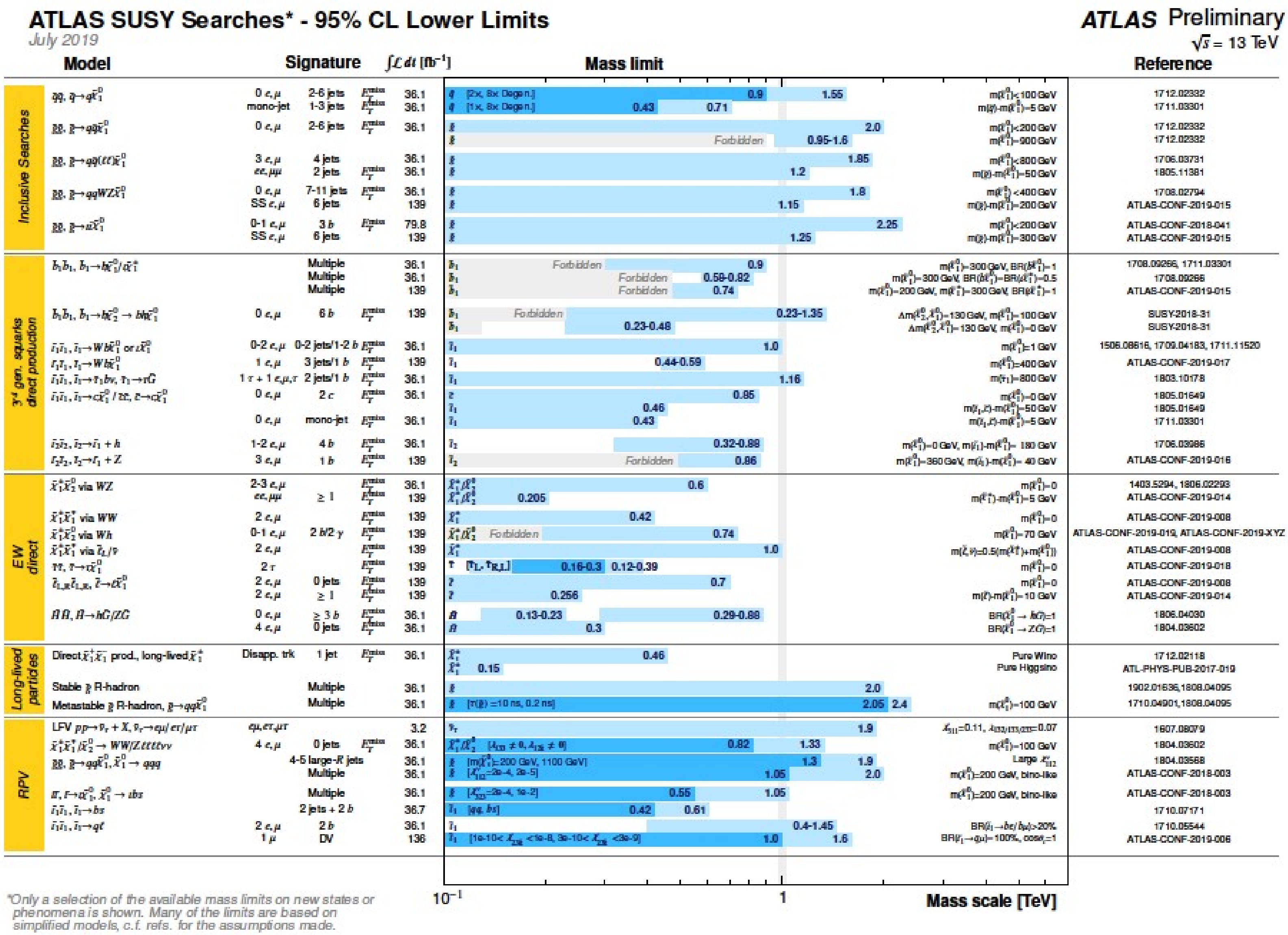

Search for Physics BSM

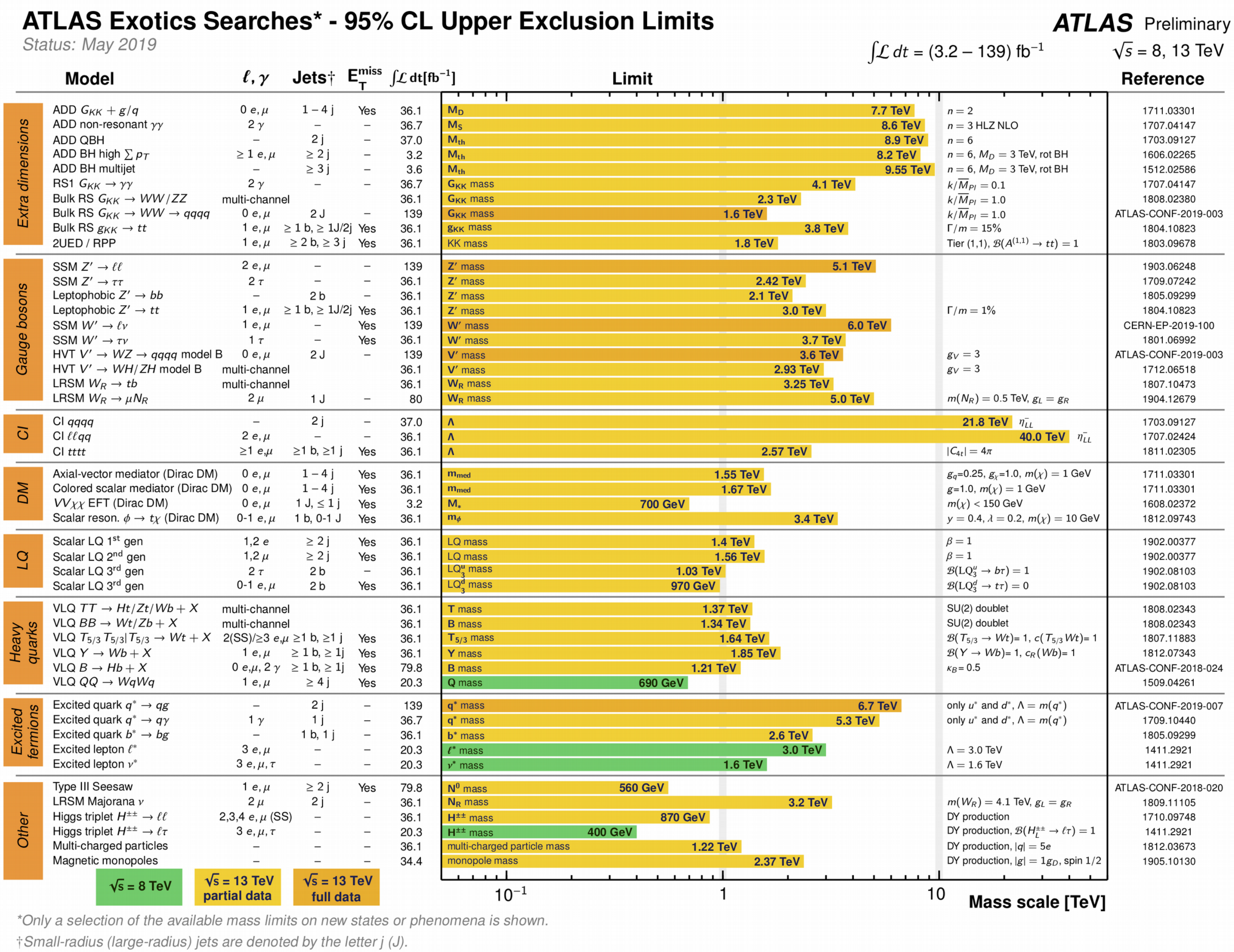

Search for Physics BSM

Full Run-2

parton-level generators assuming spin-½ excited quarks with the same coupling constants as SM quarks

the intrinsic width of the q^* signals is comparable to the detector resolution

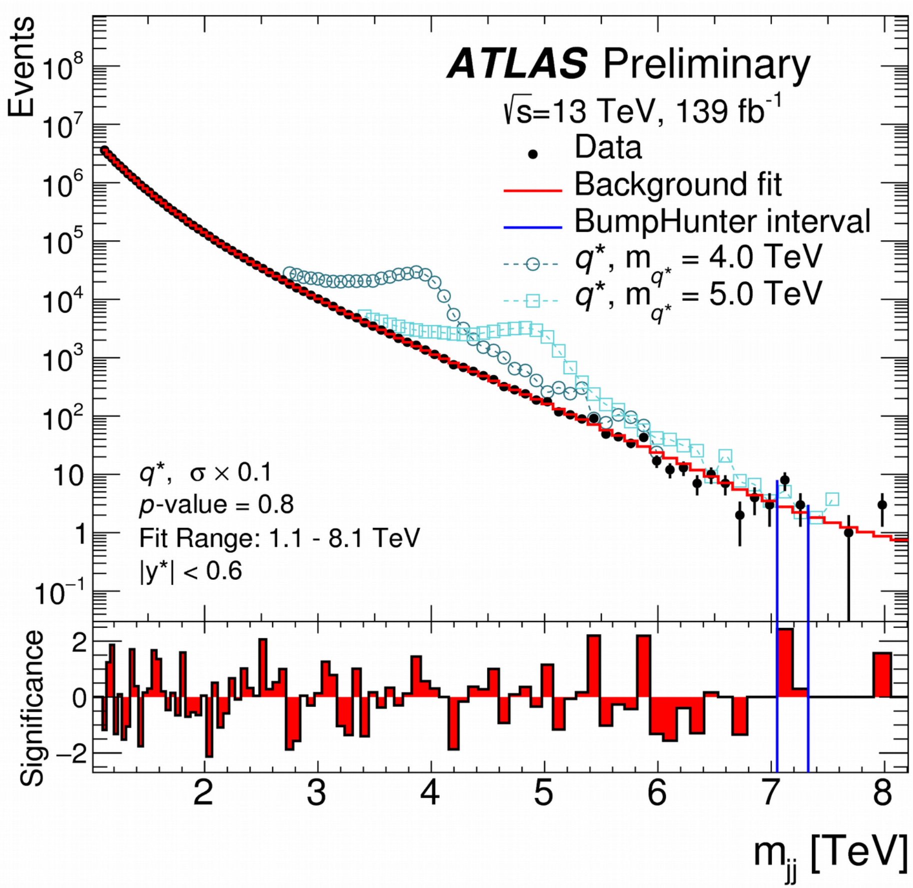

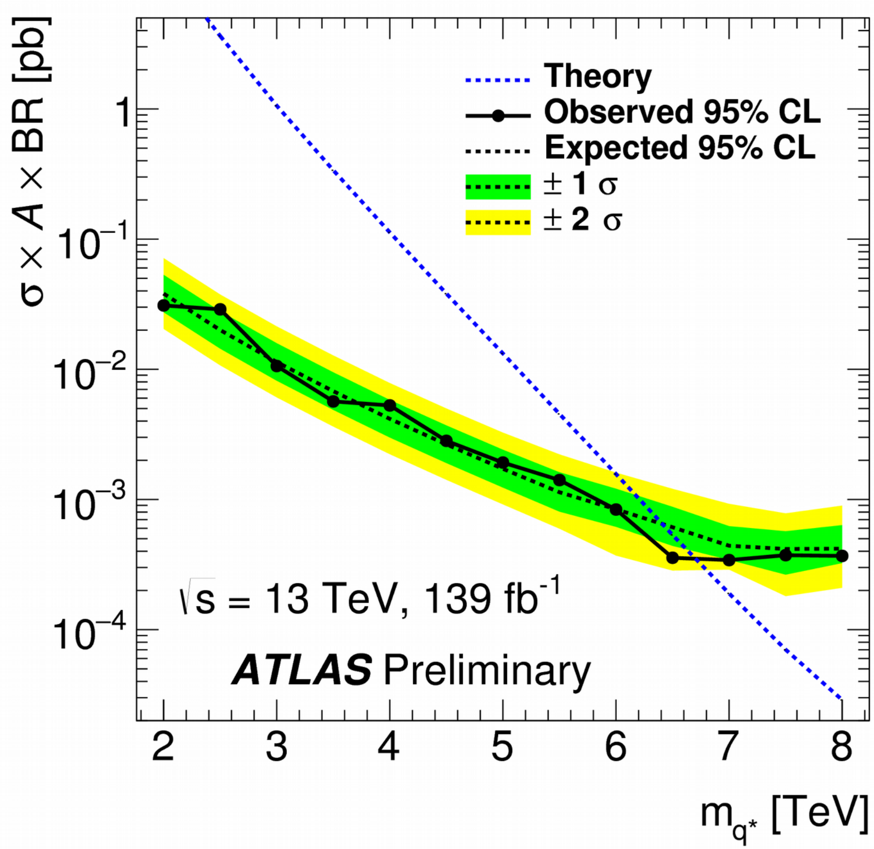

_AS-CONF-2019-007

Search for Physics BSM

Full Run-2

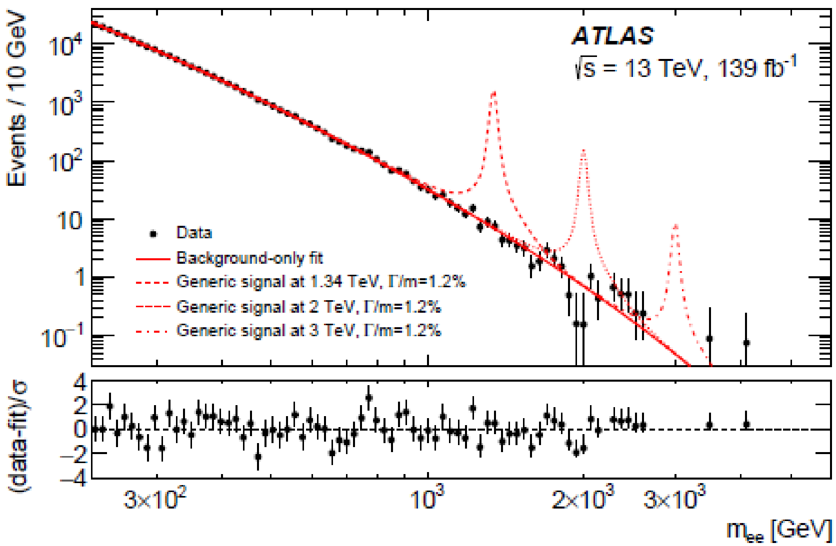

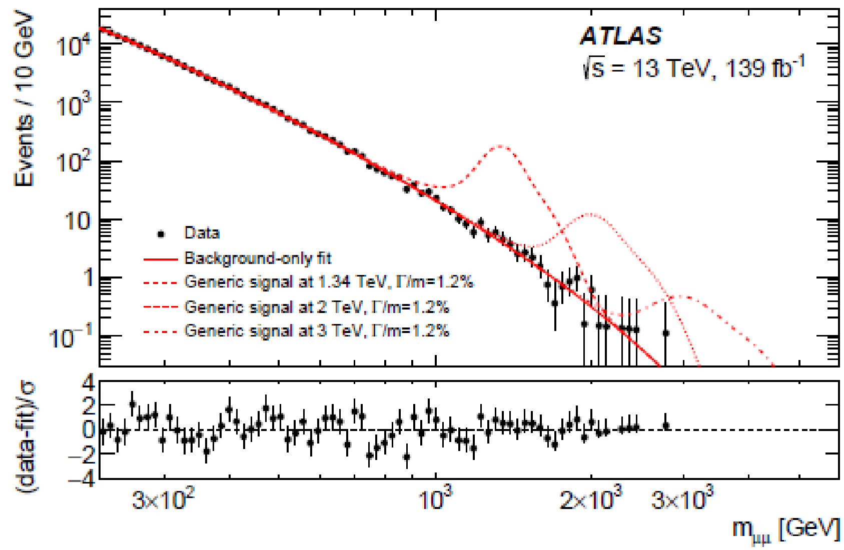

arXiv:1903.06248

Observed and expected 95% CL lower limits on $m_{Z'}$ for three Z' gauge boson models

Model	Lower limits on $m_{Z'}$ [TeV]					
	ee		$\mu\mu$		$\ell\ell$	
	obs	exp	obs	exp	obs	exp
Z'_ψ	4.3	4.3	4.0	3.8	4.5	4.5
Z'_χ	4.6	4.6	4.2	4.1	4.8	4.7
Z'_{SSM}	4.9	4.9	4.5	4.4	5.1	5.0

Search for Physics BSM

Full Run-2

arXiv:1906.05609

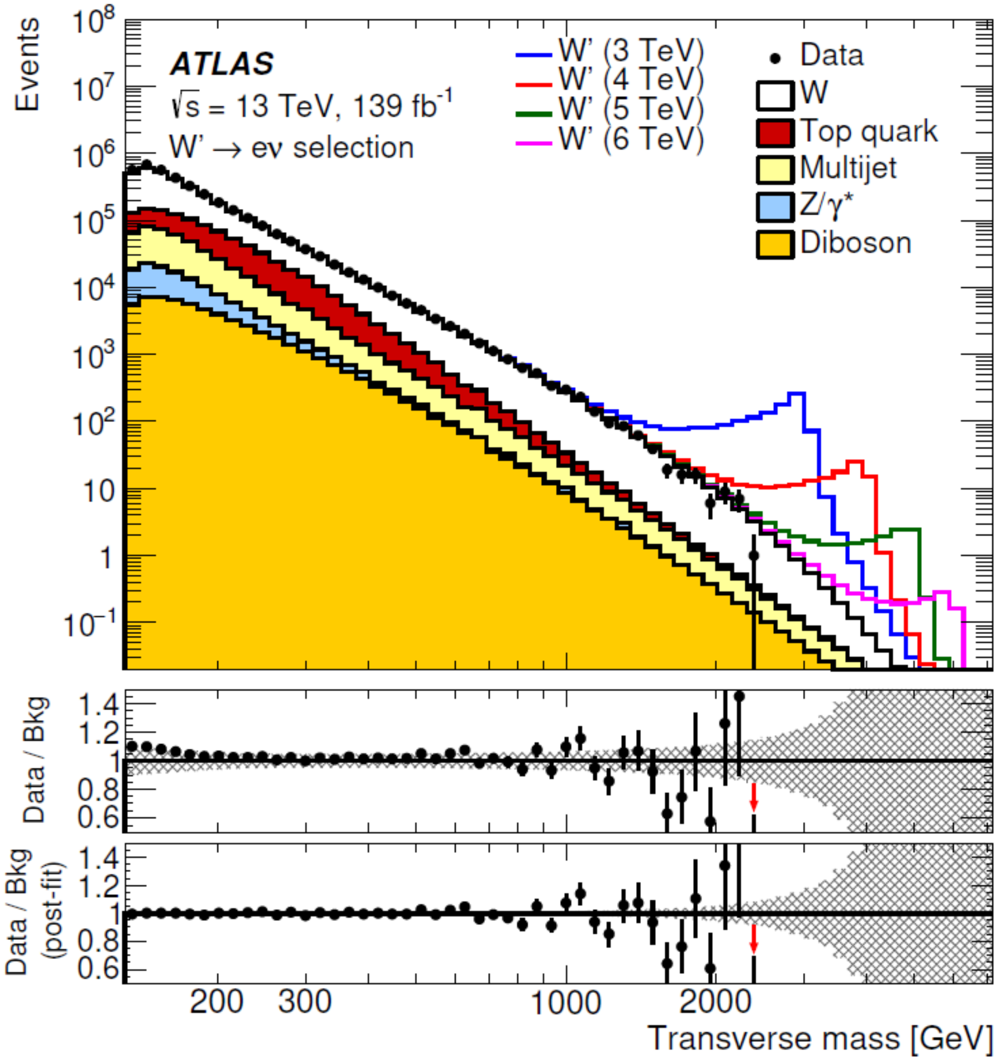

Observed and expected 95% CL lower limits on the W' mass

	$m(W')$ lower limit [TeV]	
Decay	Observed	Expected
$W' \rightarrow e\nu$	6.0	5.7
$W' \rightarrow \mu\nu$	5.1	5.1
$W' \rightarrow \ell\nu$	6.0	5.8

Search for Physics BSM

Full Run-2

arXiv:1906.08589

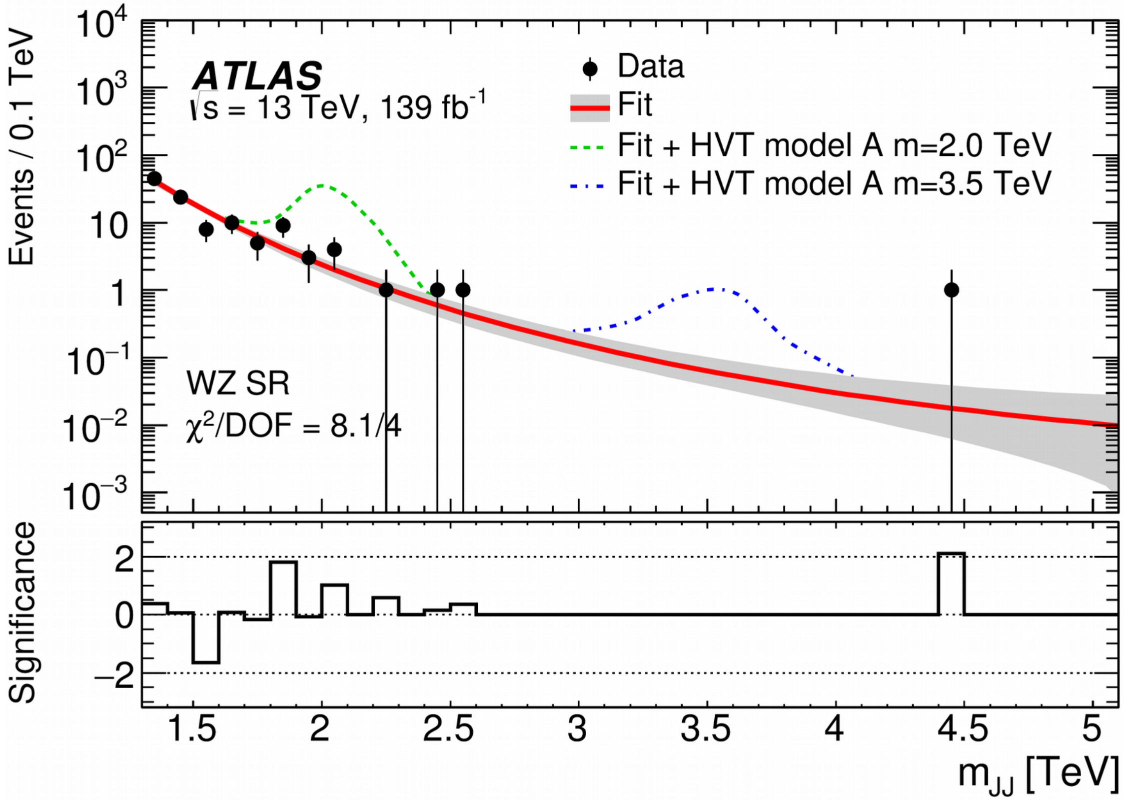

Search for Physics BSM

Full Run-2

arXiv:1906.08589

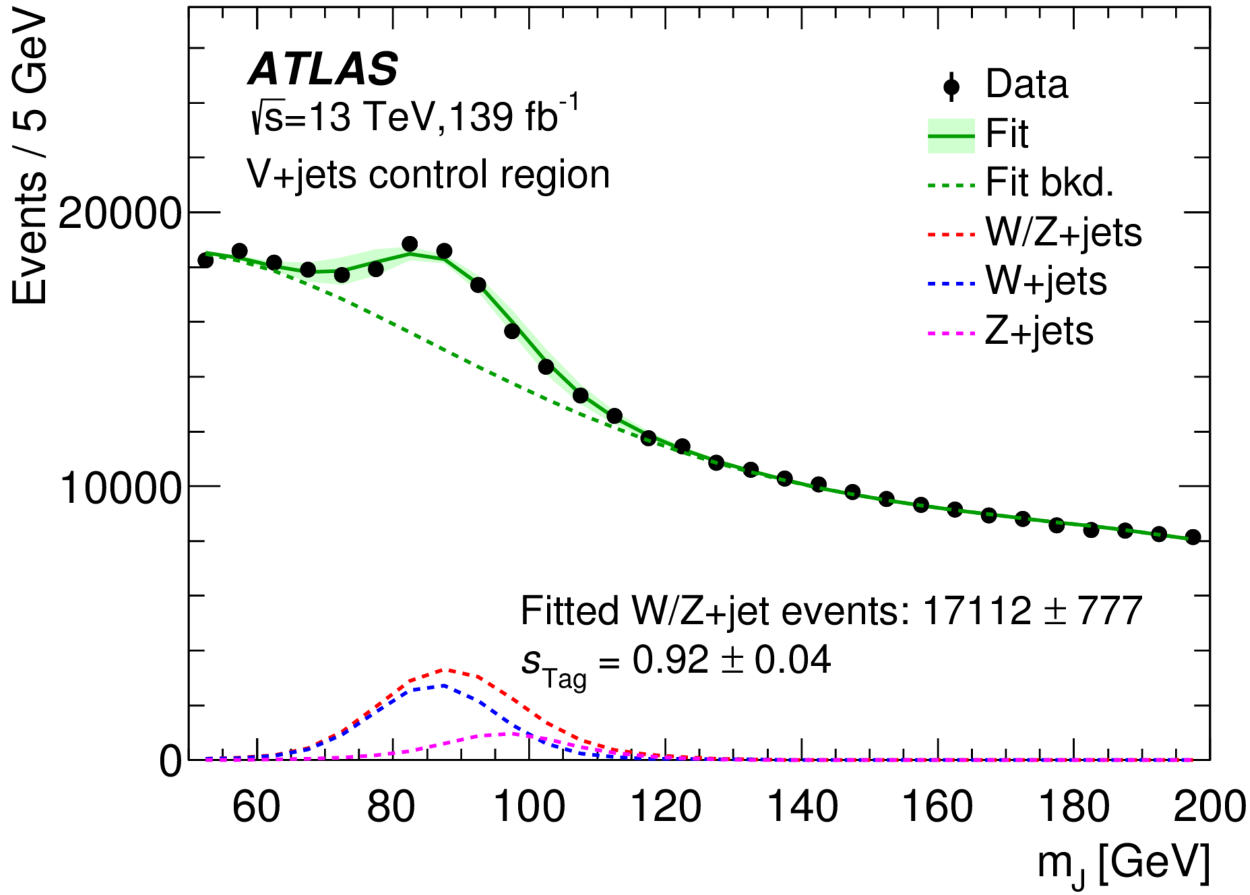

Jet mass distribution for data in the region enhanced in V+jets events after boson tagging

Search for Physics BSM

ATLAS-CONF-2019-008

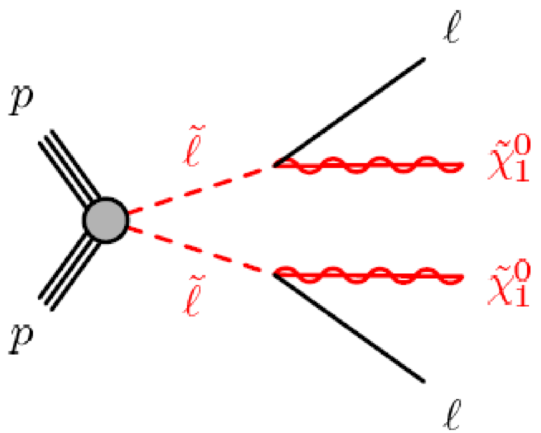

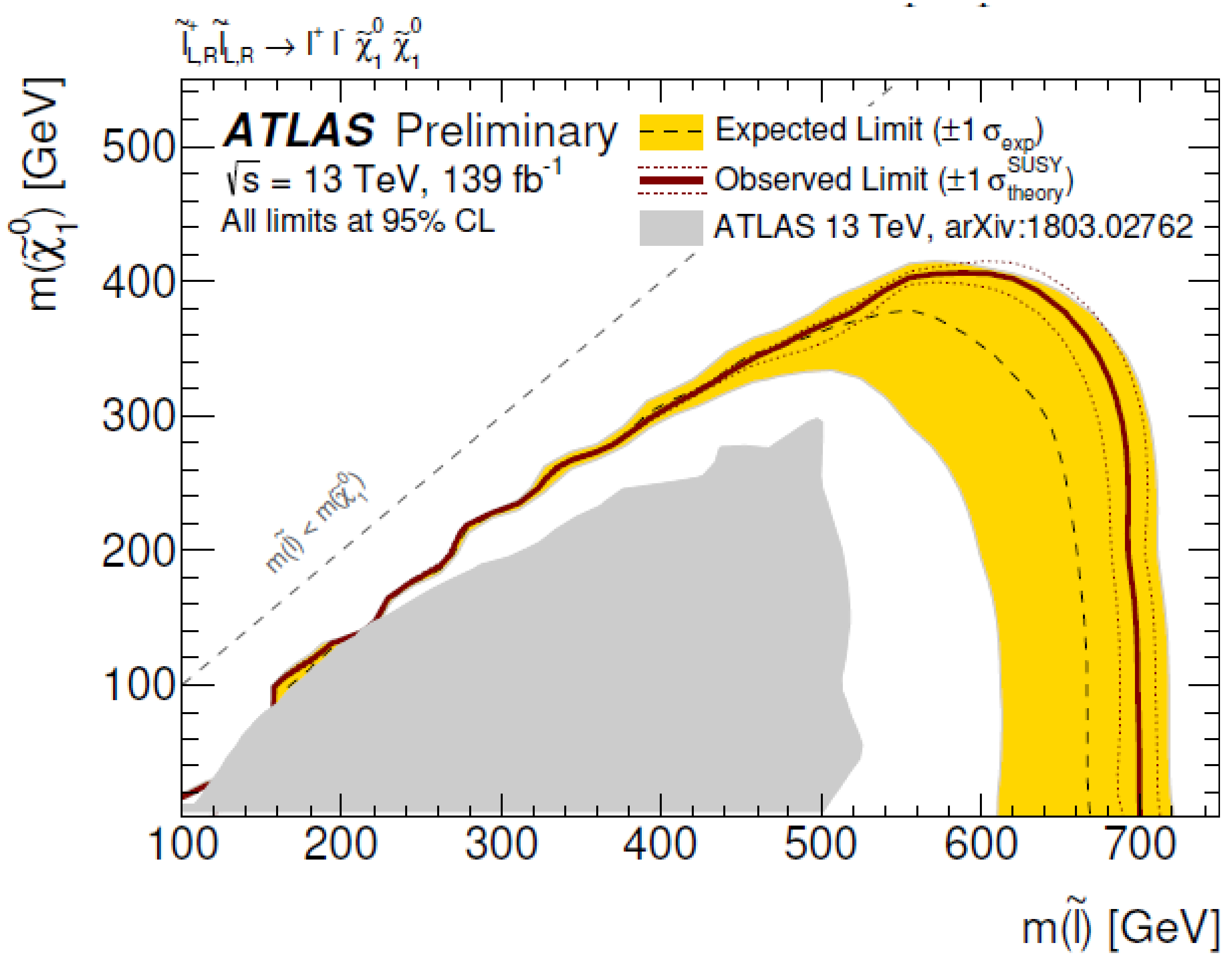

Search for Physics BSM

ATLAS-CONF-2019-040

	MB-SSd	MB-GGd	MB-C
N_{j}	≥ 2	≥ 4	≥ 2
$p_{\mathrm{T}}(j_1)$ [GeV]	> 200	> 200	> 600
$p_{\mathrm{T}}(j_{i=2,\ldots,N_{\mathrm{j_{min}}}})$ [GeV]	> 100	> 100	> 50
$\lvert\eta(j_{i=1,\ldots,N_{\mathrm{j_{min}}}})\rvert$	< 2.0	< 2.0	< 2.8
$\Delta\phi(j_{1,2,(3)}, \boldsymbol{p}_{\mathrm{T}}^{\mathrm{miss}})$ min	> 0.8	> 0.4	> 0.4
$\Delta\phi(j_{i>3}, \boldsymbol{p}_{\mathrm{T}}^{\mathrm{miss}})$ min	> 0.4	> 0.2	> 0.2
Aplanarity	-	> 0.04	-
$E_{\mathrm{T}}^{\mathrm{miss}}/\sqrt{H_{\mathrm{T}}}$ [GeV$^{1/2}$]	> 10	> 10	> 10
m_{eff} [GeV]	> 1000	> 1000	> 1600

Table 3: Summary of preselection criteria used for the multi-bin search.

Search for Physics BSM

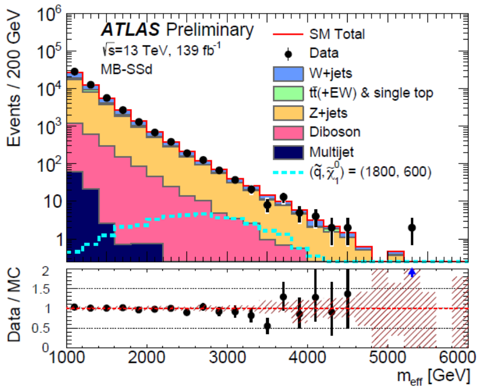

(a)

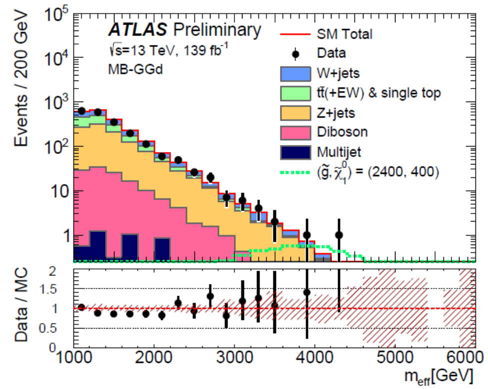

(b)

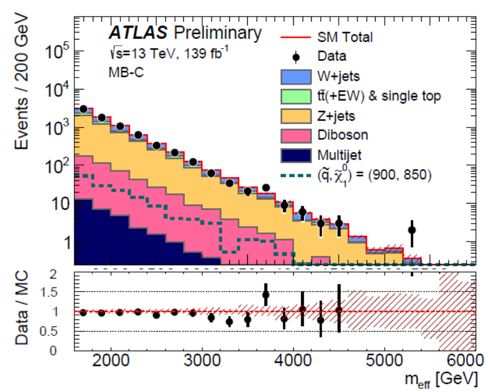

(c)

Figure 8: Observed m_{eff} distributions for the (a) MB-SSd, (b) MB-GGd and (c) MB-C regions obtained after applying the selection criteria from Table 3, before the final binning selections on this quantity. The histograms show the MC background predictions prior to the fits described in the text, normalized to the cross-section times integrated luminosity. The hatched (red) error bands indicate the combined experimental and MC statistical uncertainties. Expected distributions for benchmark signal model points, normalized using NLO+NLL cross-section (Section 3) times integrated luminosity, are also shown for comparison (masses in GeV).

Search for Physics BSM

Table 1: Event selection in the two search regions. A dash means that the variable is not used for selection.

Event category	SR1 Additional forward jet	SR2 Additional central jet
Muons	OS, $p_T > 25\,GeV, \lvert\eta\rvert < 2.1$	
$m_{\mu\mu}$	$m_{\mu\mu} > 12\,GeV$	
b-tagged jet	$p_T > 30\,GeV, \lvert\eta\rvert \leq 2.4$	
Additional jet	$p_T > 30\,GeV, 2.4 < \lvert\eta\rvert < 4.7$	$p_T > 30\,GeV, \lvert\eta\rvert \leq 2.4$
Jet veto	No other jets $p_T > 30\,GeV, \lvert\eta\rvert \leq 2.4$	No jets $p_T > 30\,GeV, 2.4 < \lvert\eta\rvert < 4.7$
p_T^{miss}	—	<40 GeV
$\Delta\phi(\mu\mu, jj)$	—	>2.5 rad

Table 3: The local significances, the measured fiducial signal cross sections with ±1 s.d. uncertainties, and the upper limits at 95% CL, together with the values of N_S for the two SRs and two collision energies. The reconstruction efficiencies and the integrated luminosities are also listed.

$\sqrt{s}$ (TeV)	8		13	
Event category	SR1	SR2	SR1	SR2
Local significance (s.d.)	4.2	2.9	2.0	1.4 deficit
N_S	22.0 ± 7.6	22.8 ± 9.5	14.5 ± 9.3	-14.9 ± 10.1
N_S observed upper limit at 95% CL	40.4	44.7	36.9	32.2
N_S expected upper limit at 95% CL	18.3	27.6	27.6	35.6
ε^{reco}	0.27 ± 0.01		0.28 ± 0.01	
Integrated luminosity, $\mathcal{L}$ (fb^{-1})	19.7 ± 0.5		35.9 ± 0.9	
σ_{fid} (fb)	4.1 ± 1.4	4.2 ± 1.7	1.4 ± 0.9	-1.5 ± 1.0
Observed upper limit at 95% CL (fb)	7.6	8.4	3.7	3.2
Expected upper limit at 95% CL (fb)	3.4	5.2	2.7	3.5

JHEP 1811 (2018) 161

Search for Physics BSM

Full Run-2

ATLAS-CONF-2019-036

	8 TeV		13 TeV	
Region	SR1	SR2	SR1	SR2
Local significance (28 GeV)	0.5	0.5	0.7	0.2
Max. significance	0.9 (29.5 GeV)	1.1 (29.5 GeV)	0.8 (27.5 GeV)	2.1 (26 GeV)

Table 2: Local significance for a dimuon excess at 28 GeV in each signal region and the maximum observed significance in the dimuon invariant mass probed from 26 to 30 GeV in steps of 0.5 GeV are quoted.

Search for Physics BSM   dark matter

If produced at the LHC, DM interactions will be mediated by particles that can also be directly searched for — complementarity

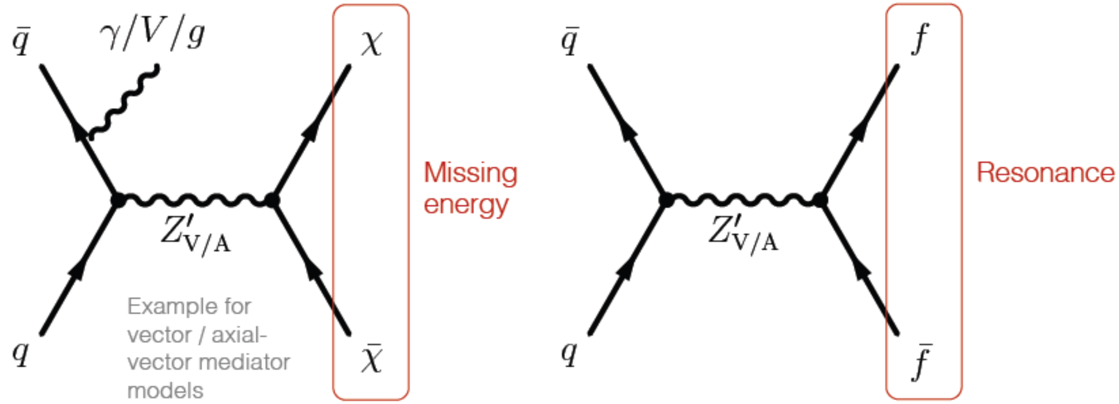

ATLAS released combination of $E_{T,\text{miss}}$ based DM searches involving $E_{T,\text{miss}}$ + X, X = jet, γ, W, Z, H, b(b), t(t) using large number of models

arXiv:1903.01400, up to 37 fb^{-1}

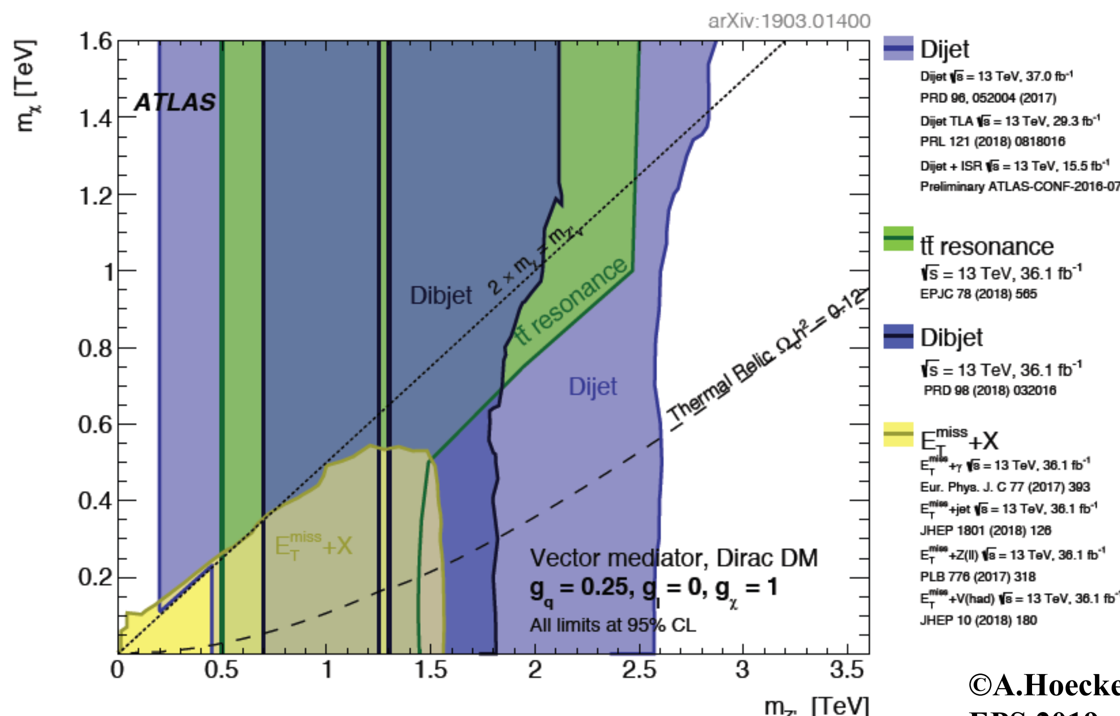

If light enough, Higgs boson can decay to DM (H → invisible)
ATLAS combination:
BR(H → invisible) < 0.26
(0.17 expected)

arXiv:1904.05105, 36 fb^{-1}

♪ *Results from (run 1 and) run 2*

- *detector*
- *SM*
- *BSM*
- ***(B-E)H***
- *Vector-boson*

1 Additional BEH bosons

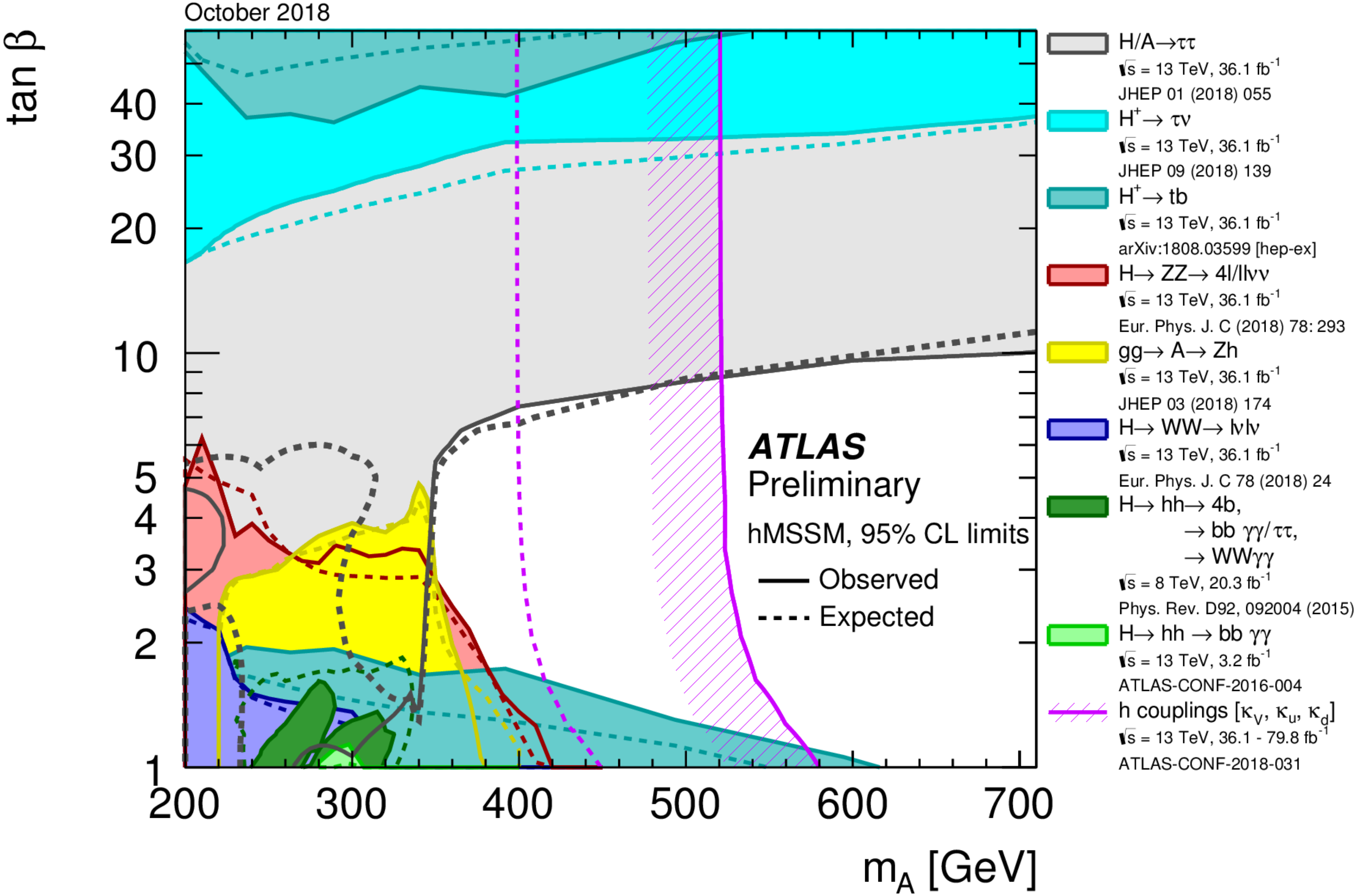

https://atlas.web.cern.ch/Atlas/GROUPS/PHYSICS/CombinedSummaryPlots/HIGGS/

1 Additional BEH bosons

JHEP 1511 (2015) 206

$$\kappa_V = \frac{s_d(m_A, \tan\beta) + \tan\beta\ s_u(m_A, \tan\beta)}{\sqrt{1+\tan^2\beta}}$$

$$\kappa_u = s_u(m_A, \tan\beta)\frac{\sqrt{1+\tan^2\beta}}{\tan\beta}$$

$$\kappa_d = s_d(m_A, \tan\beta)\sqrt{1+\tan^2\beta} \quad ,$$

where the functions s_u and s_d are given by:

$$s_u = \frac{1}{\sqrt{1+\frac{\left(m_A^2+m_Z^2\right)^2 \tan^2\beta}{\left(m_Z^2+m_A^2\tan^2\beta - m_h^2\left(1+\tan^2\beta\right)\right)^2}}}$$

$$s_d = \frac{\left(m_A^2+m_Z^2\right)\tan\beta}{m_Z^2+m_A^2\tan^2\beta - m_h^2\left(1+\tan^2\beta\right)}\ s_u$$

1 Additional BEH bosons

ATLAS-CONF-2018-31

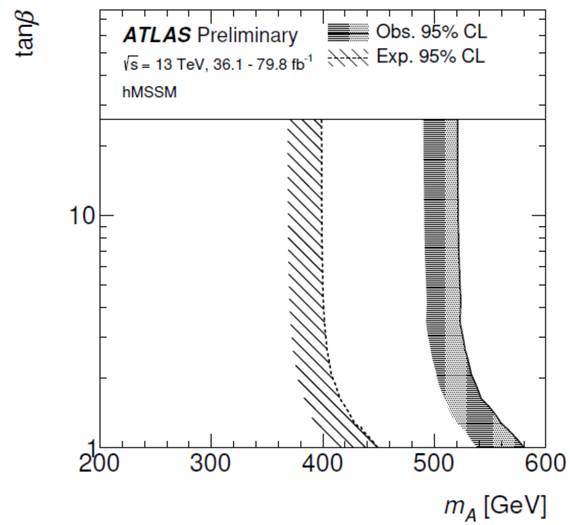

Figure 14: Regions of the $[m_A, \tan\beta]$ plane in the hMSSM excluded by fits to the measured rates of Higgs boson production and decays. Likelihood contours at 95% CL, defined in the asymptotic approximation by $-2\log\Lambda = 5.99$, are drawn for both the data and the expectation of the SM Higgs sector. The regions to the left of the solid contour are excluded. The decoupling limit, in which all Higgs boson couplings tend to their SM value, corresponds to $m_A \to \infty$. The hMSSM is a good approximation of the MSSM only for moderate values of $\tan\beta$. For $\tan\beta \gtrsim 10$ the scenario is approximate due to missing supersymmetry corrections in the Higgs boson coupling to b-quarks, and for $\tan\beta$ of $O(1)$ the precision of the approximation depends on m_A [34].

The Higgs boson couplings to vector bosons, up-type fermions and down-type fermions relative to the corresponding SM predictions are expressed as functions of the ratio of the vacuum expectation values of the Higgs doublets, $\tan\beta$, and the masses of the CP-odd scalar (m_A), the Z boson, and of h.

1 Additional BEH bosons

Charged Higgs searches

$H^{\pm}$ predicted by 2HDM, Higgs triplets,...

In Type II 2HDM:

- Main production in association with a top quark
- At high mass $H^{\pm} \rightarrow tb$ is the dominant decay mode
- $BR(H^{\pm} \rightarrow \tau\nu)$ significant for a large range of masses for high $\tan\beta$

$(m_{H+} < m_{top})$

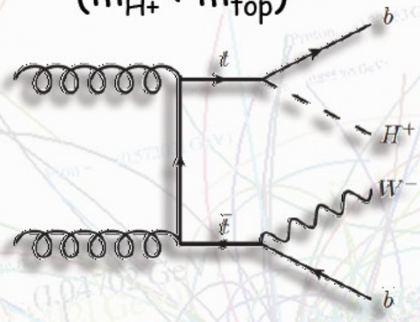

$(m_{H+} > m_{top})$

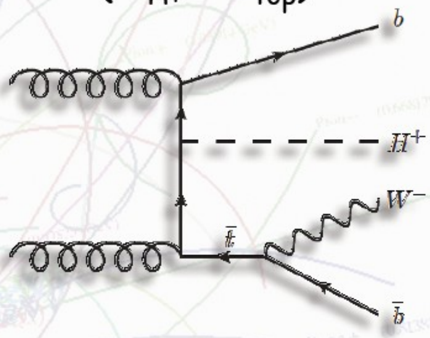

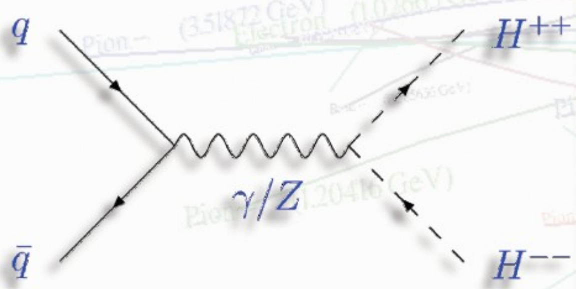

$H^{\pm\pm}$ predicted by Left-Right Symmetric Models (LRSM), Higgs Triplet Model (HTM), Zee-Babu and Georgi-Machacek models

In LRSM and HTM:

- Dominant production at the LHC: DY pair production
- Decays: $H^{\pm\pm} \rightarrow l^{\pm}l^{\pm}$ or $H^{\pm\pm} \rightarrow W^{\pm}W^{\pm}$
  - BR ~ f($m_{H\pm\pm}$, vev of Higgs triplet)
  - Low $m_{H\pm\pm}$ and low vev : $H^{\pm\pm} \rightarrow l^{\pm}l^{\pm}$ dominates

- $H^{\pm} \rightarrow \tau\nu$ JHEP 09 (2018) 139
- $H^{\pm} \rightarrow tb$ JHEP 11 (2018) 085
- $H^{\pm\pm}H^{\mp\mp} \rightarrow 4W$ Eur. Phys. J. C (2019) 79
- $H^{\pm\pm}H^{\mp\mp} \rightarrow 4l$ Eur. Phys. J. C78 (2018) 199

- $H^{\pm} \rightarrow W^{\pm}Z$ Phys. Lett. B 787 (2019) 68
- $H^{\pm} \rightarrow cs$ Eur. Phys. J. C, 73 6 (2013) 2465, Run1

1 Additional BEH bosons γγ excess at 95 GeV

CMS PAS HIG-17-013

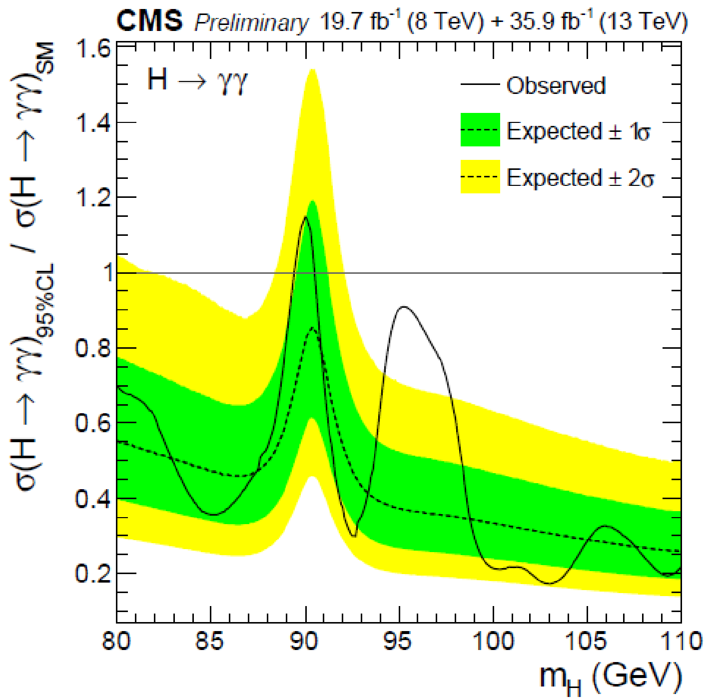

these yield an excess with approximately 2.8σ local (1.3σ global) significance for the same hypothesis mass as for the 13 TeV dataset alone, mass of 95.3 GeV.

1 Additional BEH bosons   γγ excess at 95 GeV

CMS PAS HIG-17-013

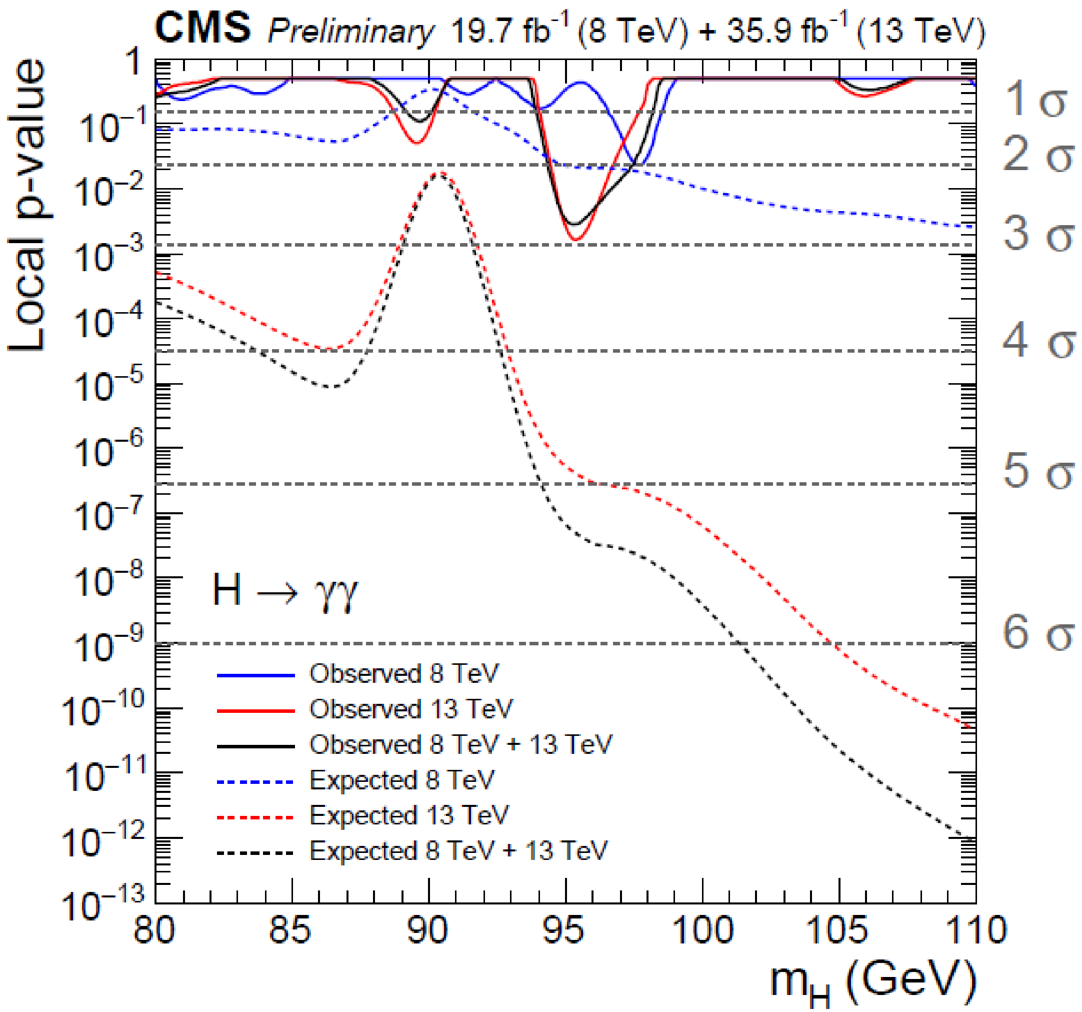

1 Additional BEH bosons γγ excess at 95 GeV

CMS PAS HIG-17-013

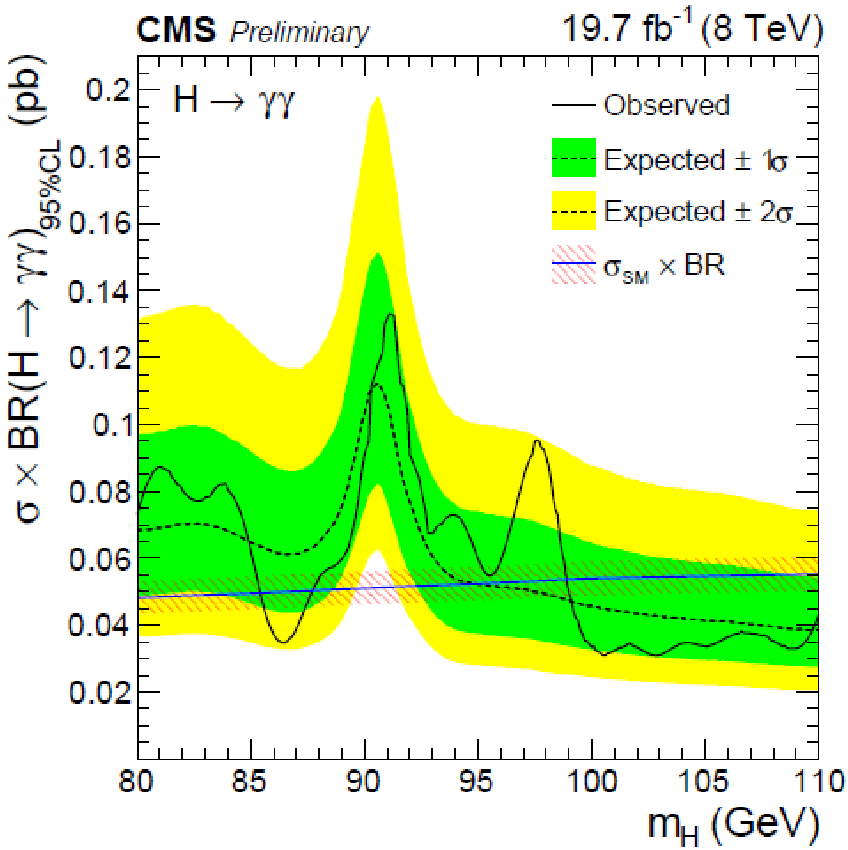

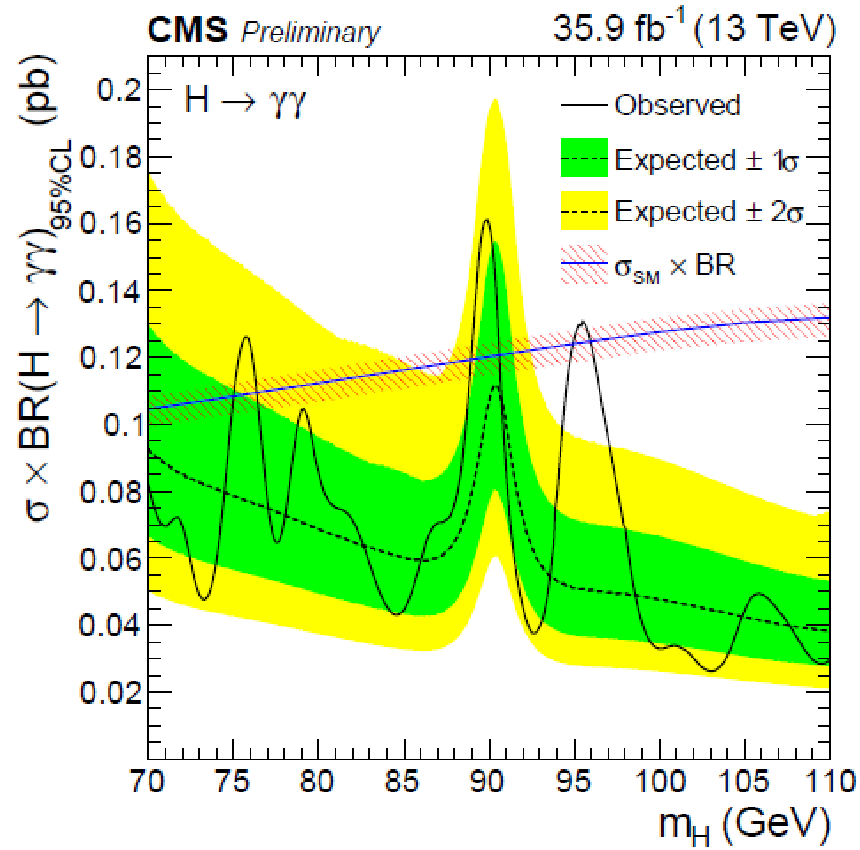

1 Additional BEH bosons γγ excess at 95 GeV

CMS PAS HIG-17-013

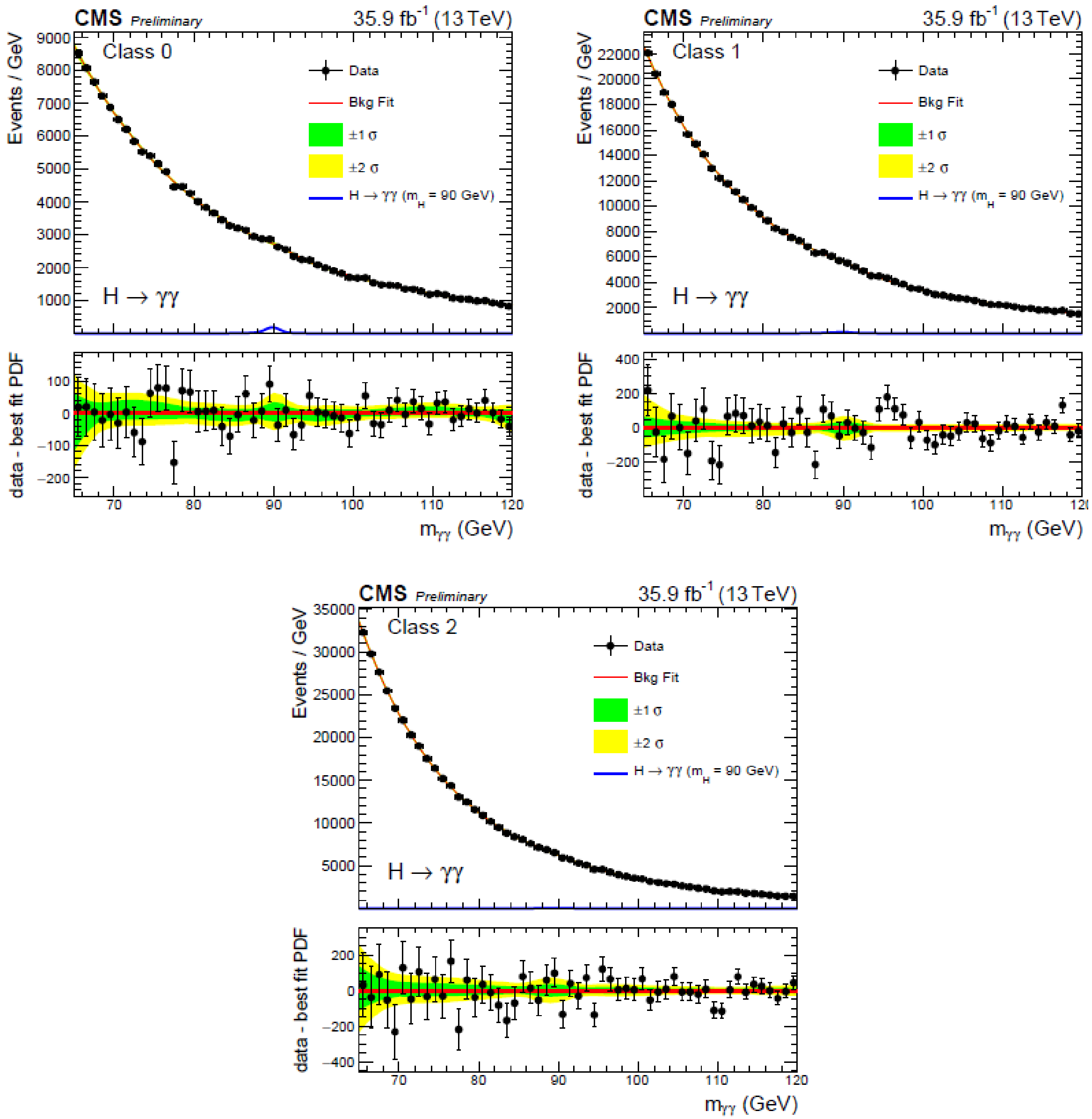

1 Additional BEH bosons γγ excess at 95 GeV

CMS PAS HIG-17-013

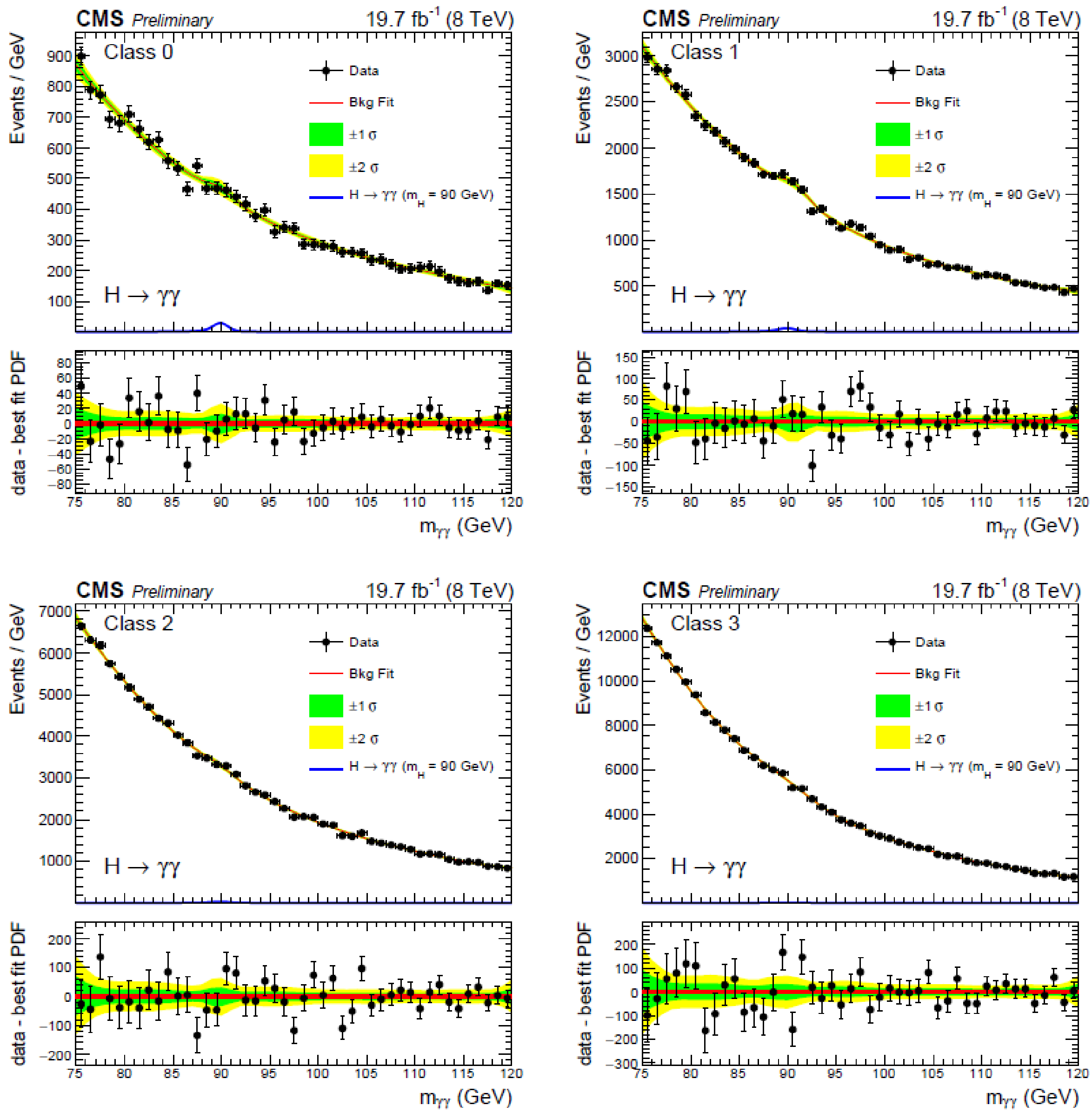

1 Additional BEH bosons γγ excess at 95 GeV

Search for the standard model Higgs boson at LEP

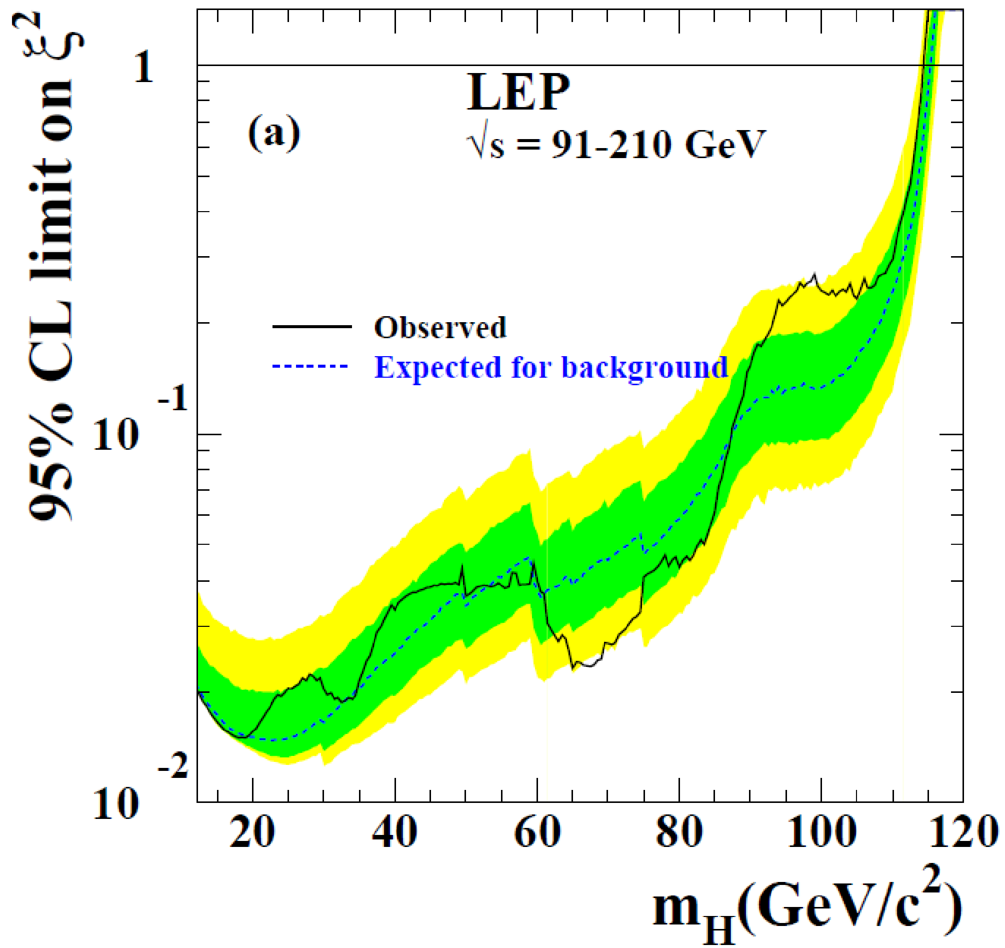

Phys.Lett. B565 (2003) 61-75

1 Additional BEH bosons γγ excess at 95 GeV

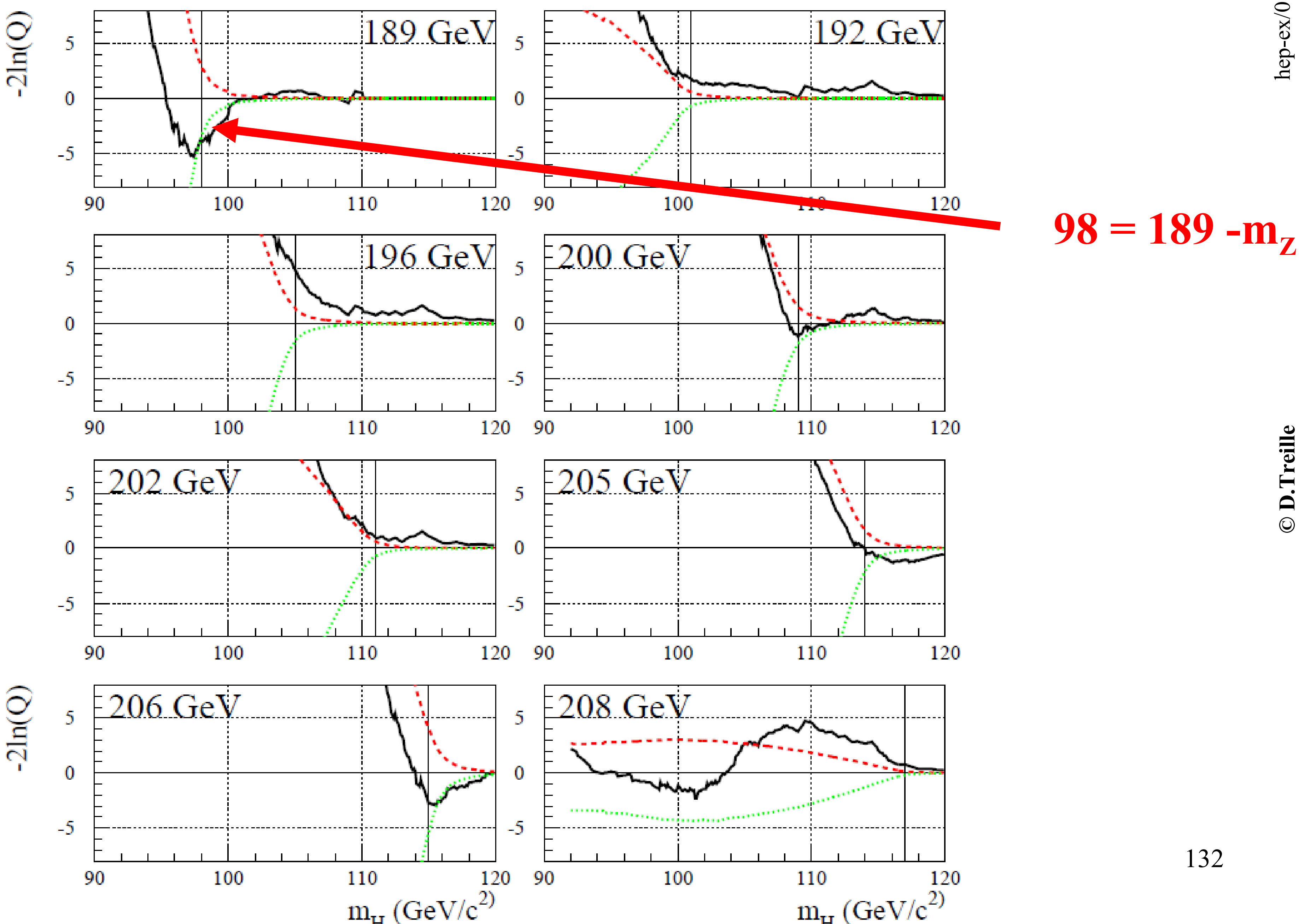

hep-ex/0107029

1 Additional BEH bosons γγ excess at 95 GeV

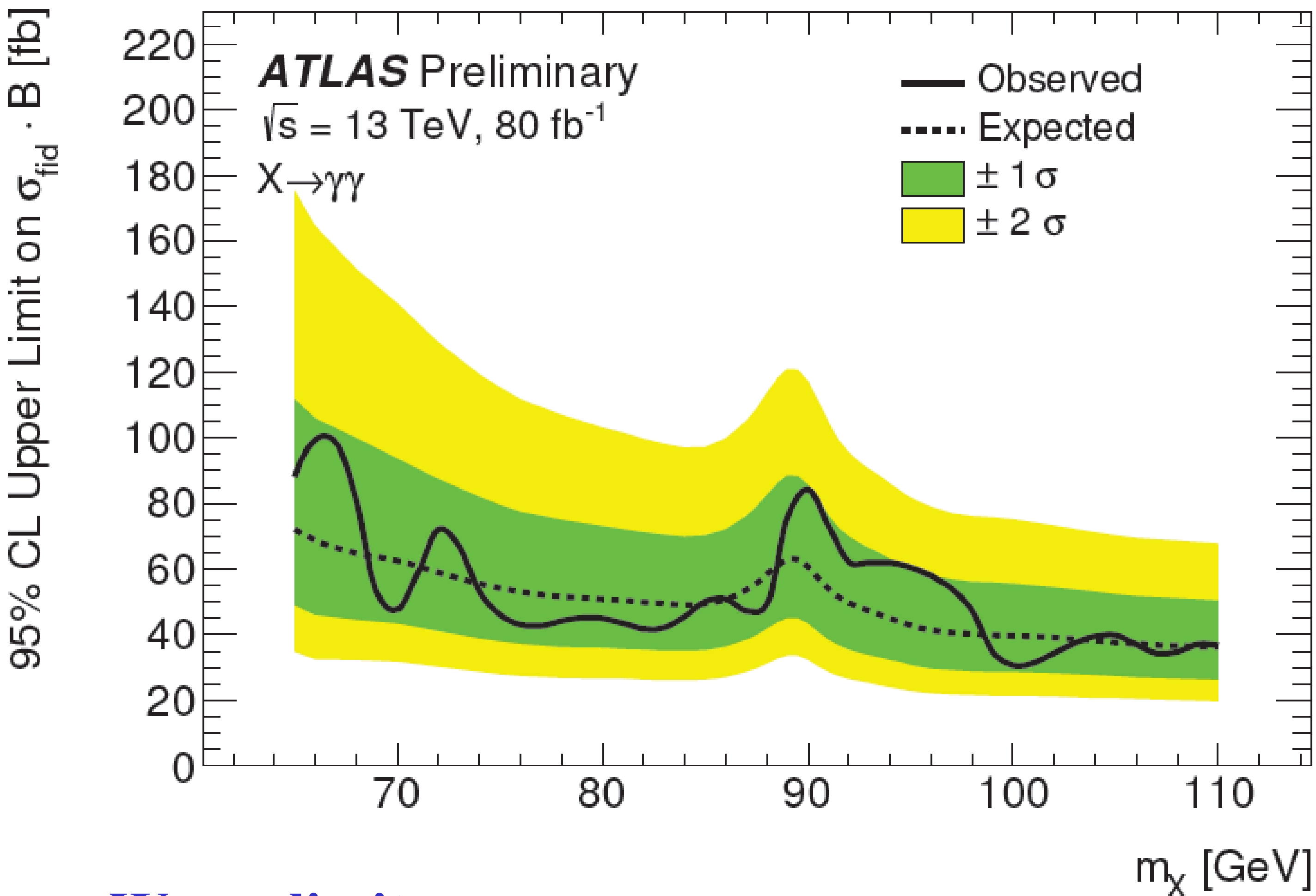

ATLAS-CONF-2018-025

.. **Worse limit**

2 The SM BEH boson

arXiv:1610.07922

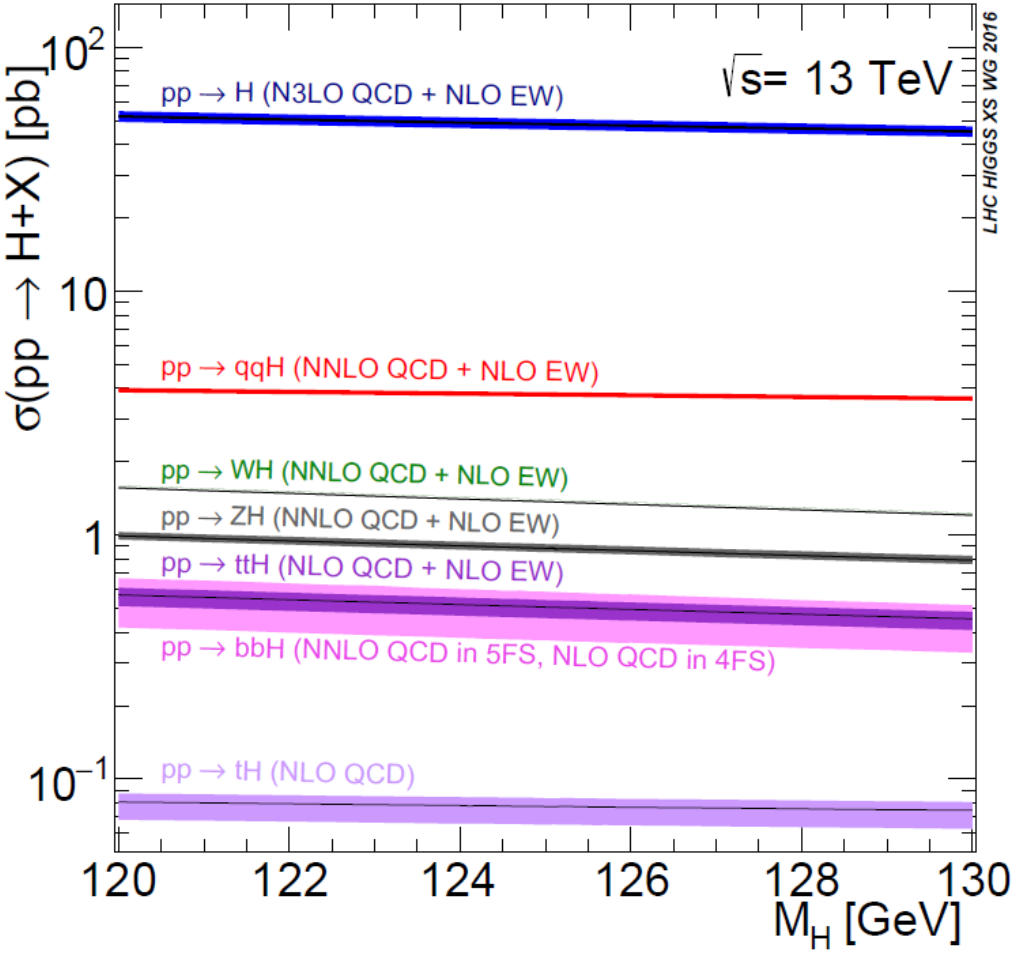

2 The SM BEH boson

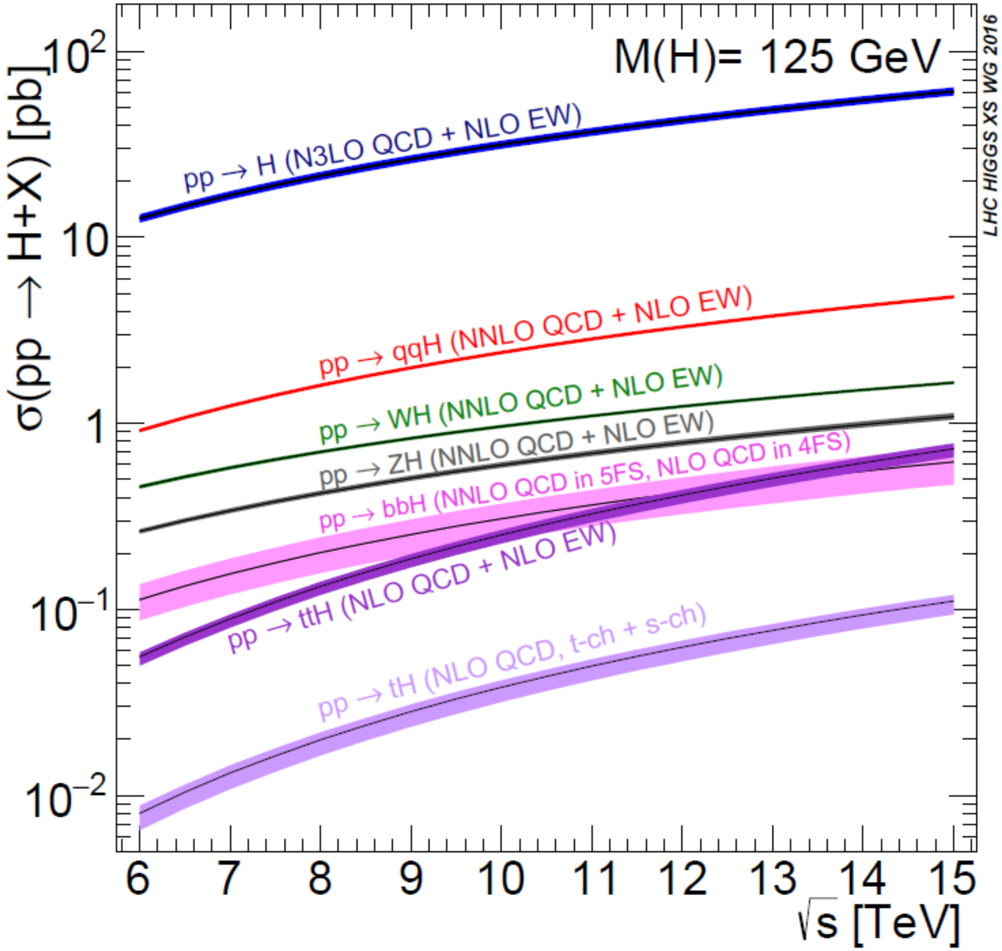

arXiv:1610.07922

2 The SM BEH boson

arXiv:1610.07922

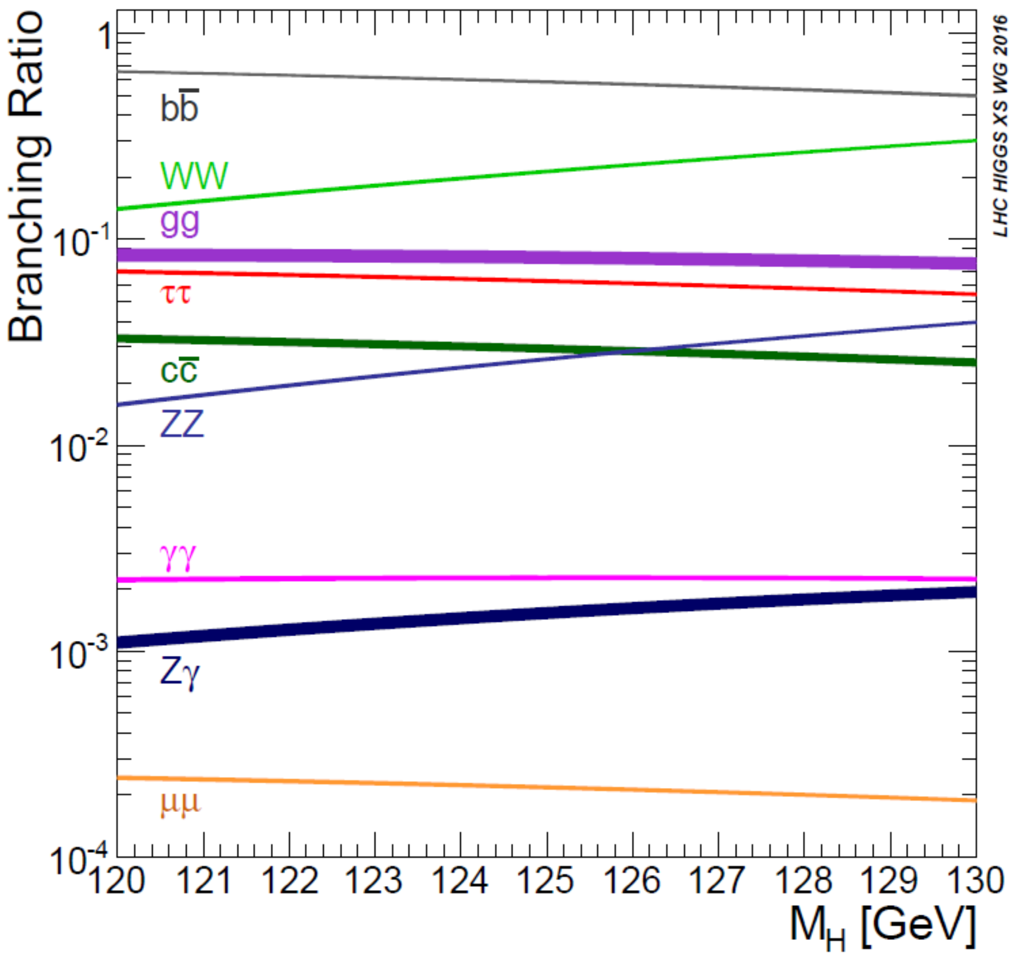

2 The SM BEH boson (final Run-1 ATLAS + CMS result)

PRL 114, 191803 (2015)

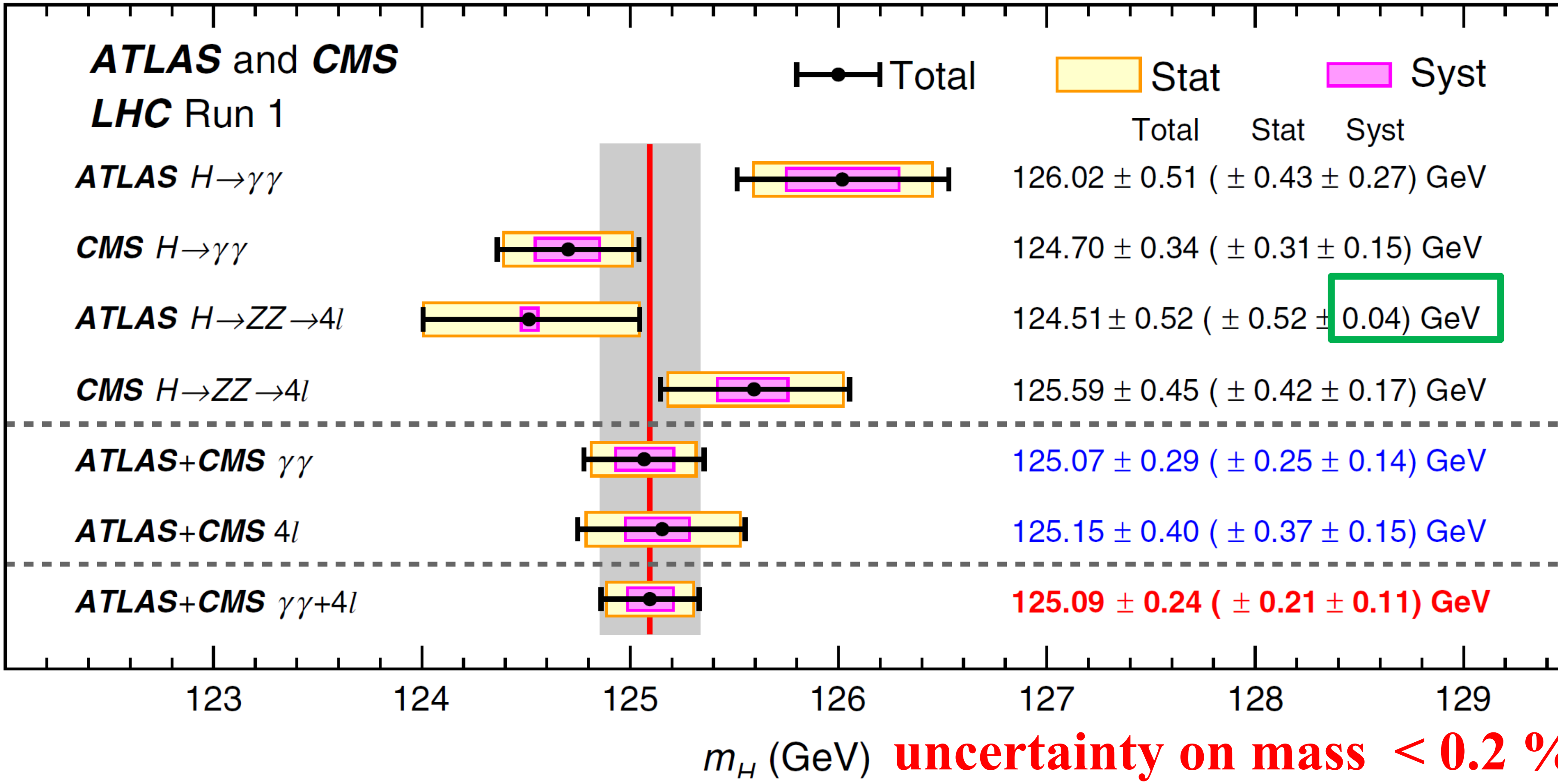

uncertainty on mass < 0.2 %

Remember ATLAS has an uncertainty on W mass of 19 MeV Eur.Phys.J. C78 (2018) no.2, 110

note that $\Delta m_H = 0.1$ GeV → Δ (BR(H→ ZZ)) / BR(H→ ZZ) ~ 1%

At longer term uncertainty will be dominated by 4l

(for H→ γγ : need to extrapolate from e to γ !)

2 The SM BEH boson ($H \to \tau\tau$)

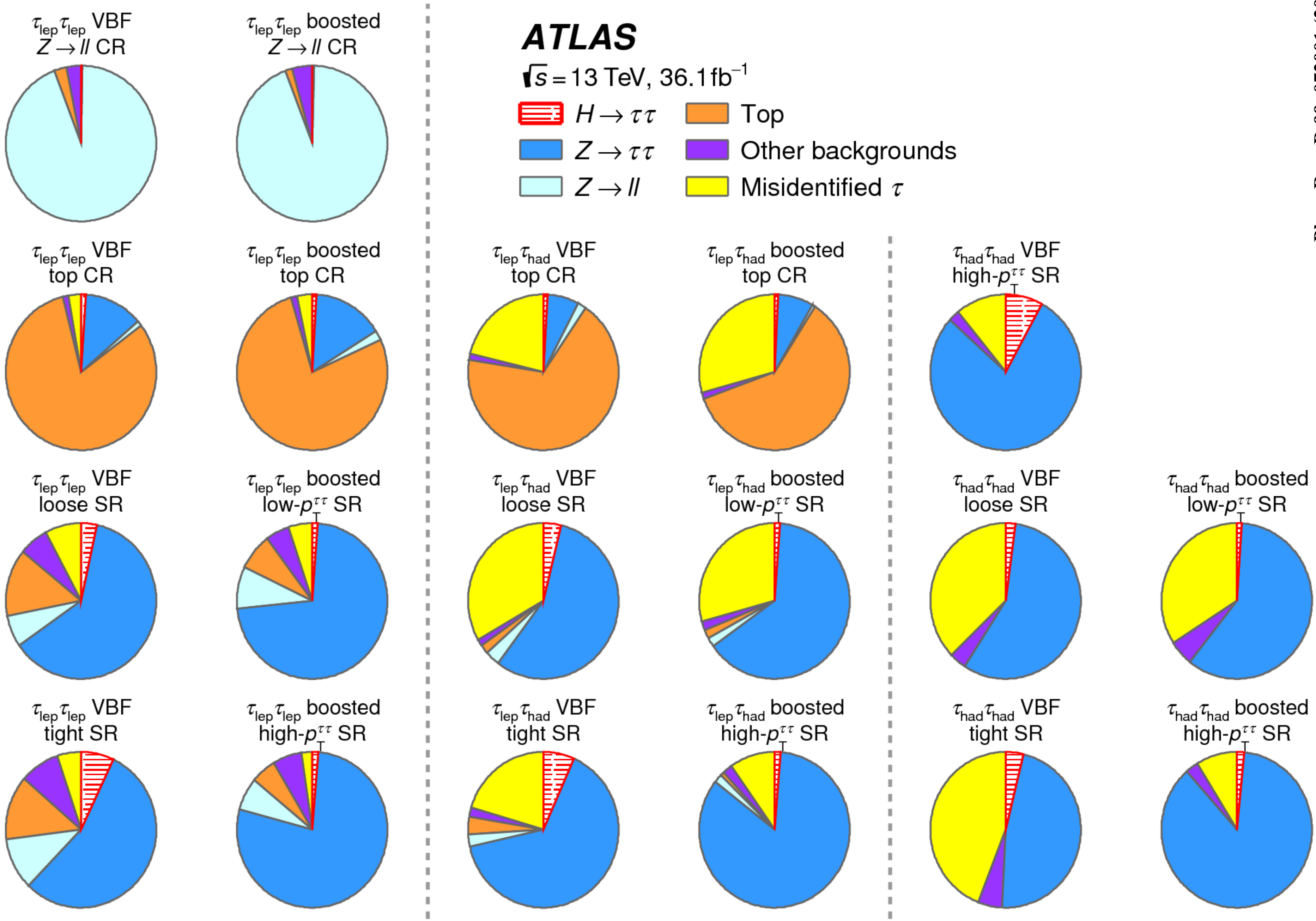

Phys. Rev. D 99, 072001 (2019)

2 The SM BEH boson (H→ττ)

Phys. Rev. D 99, 072001 (2019)

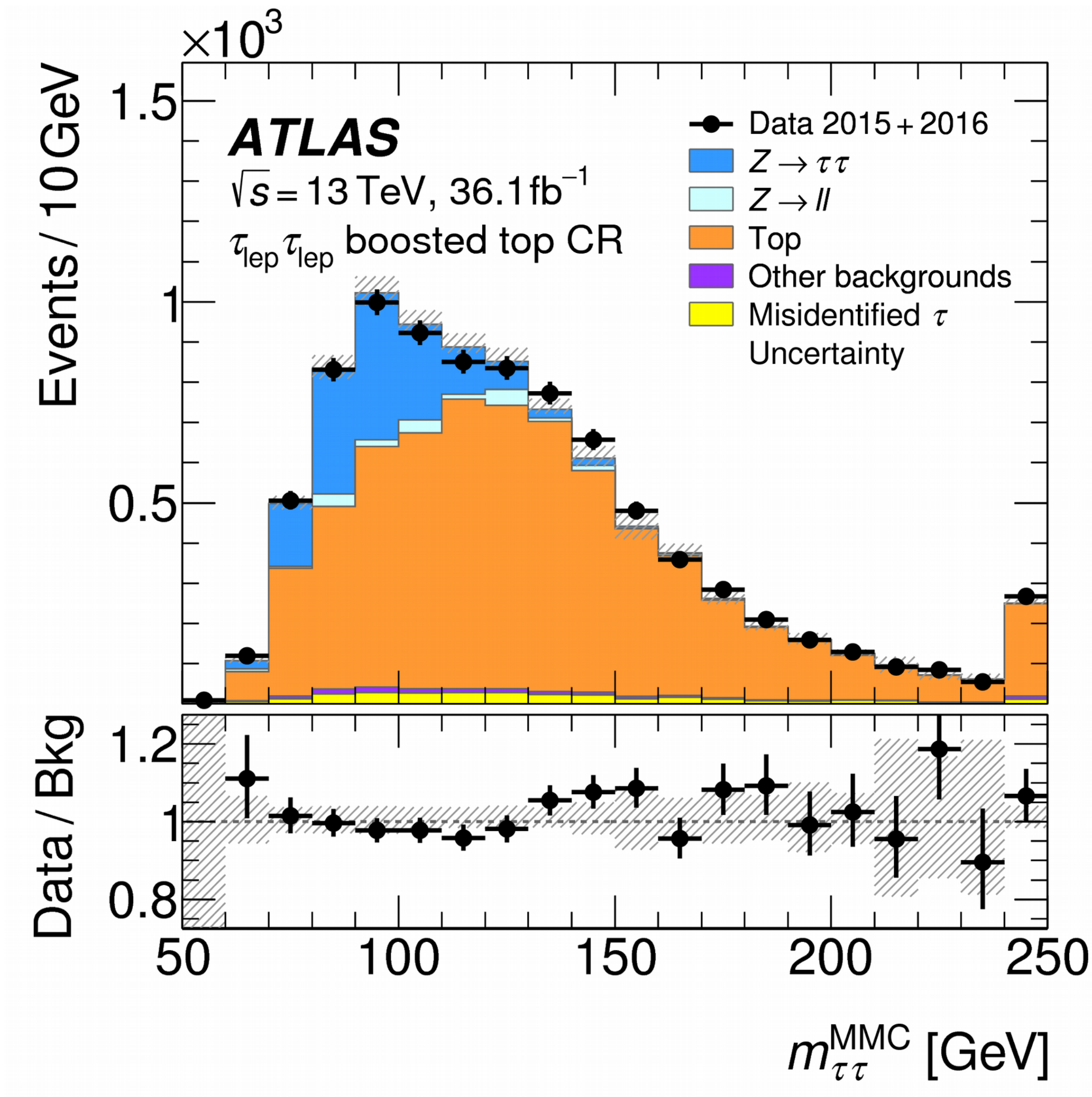

2 The SM BEH boson (H→ττ)

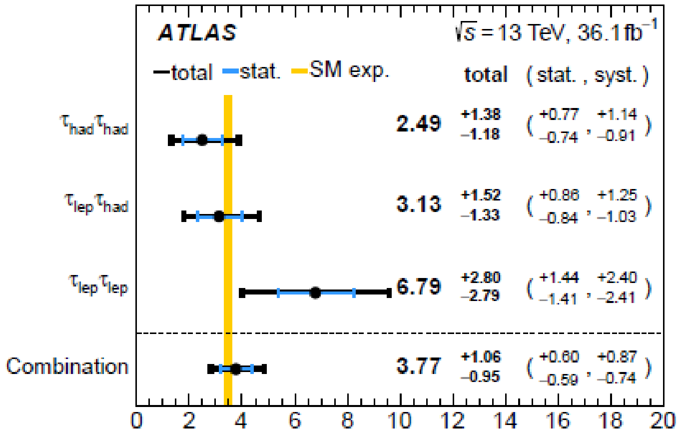

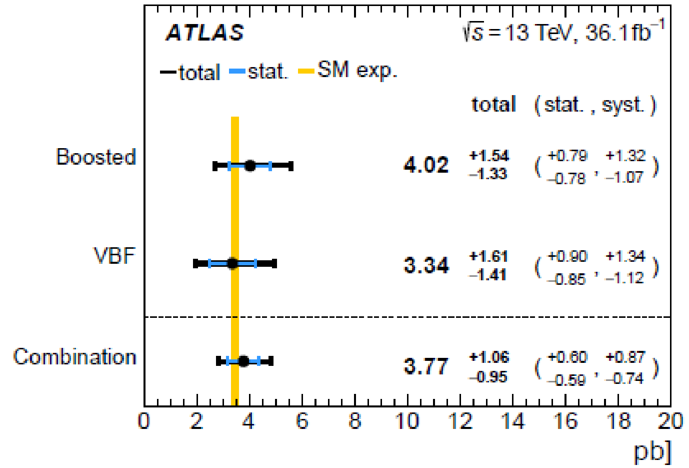

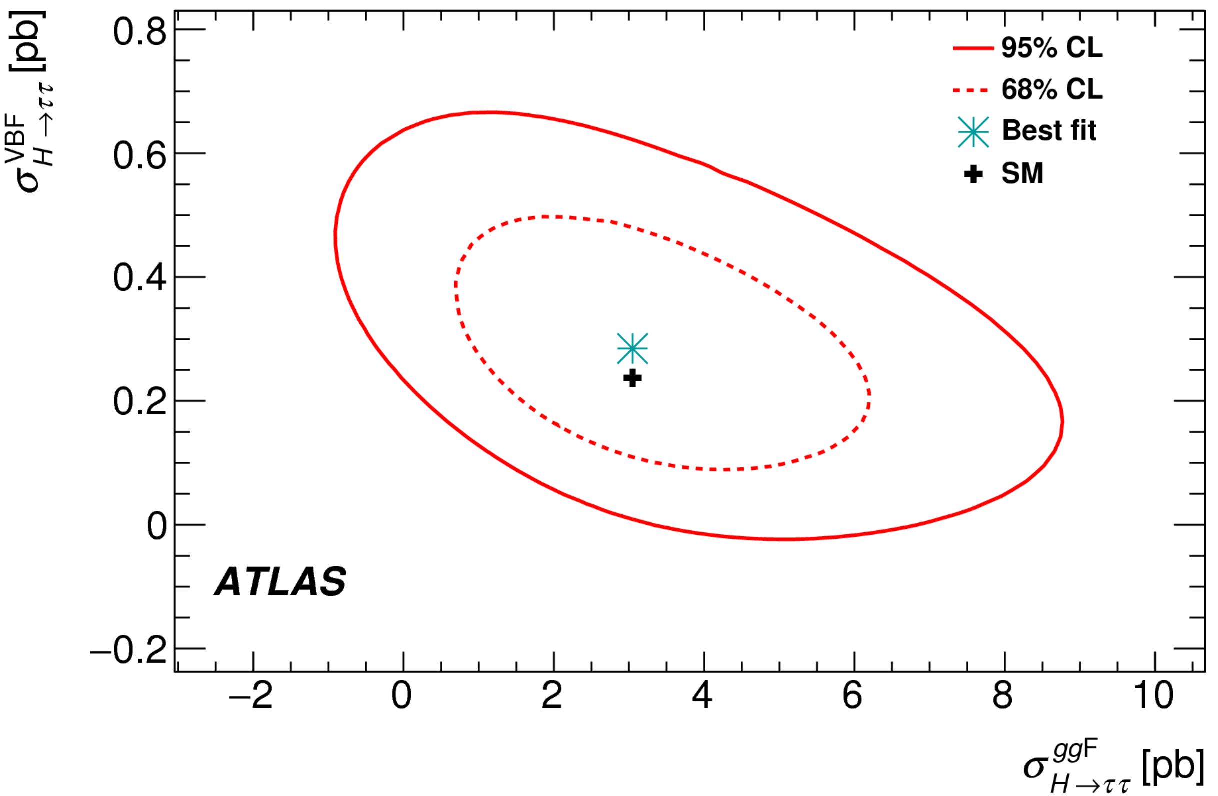

Phys. Rev. D 99, 072001 (2019)

2 The SM BEH boson (H→ττ) τ reconstruction

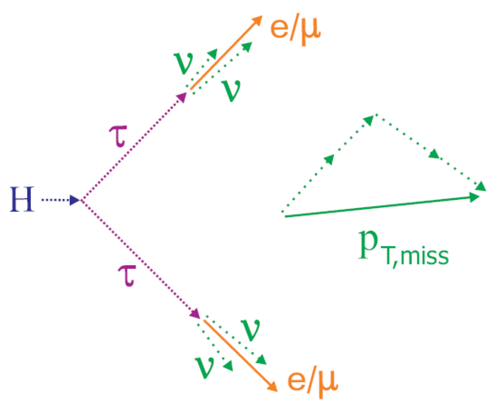

reconstruction of Higgs mass with collinear approximation and angle between the two τ

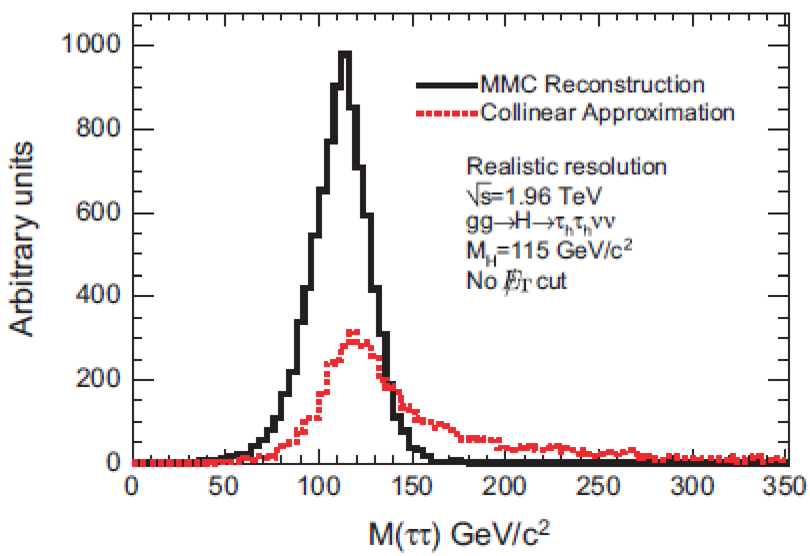

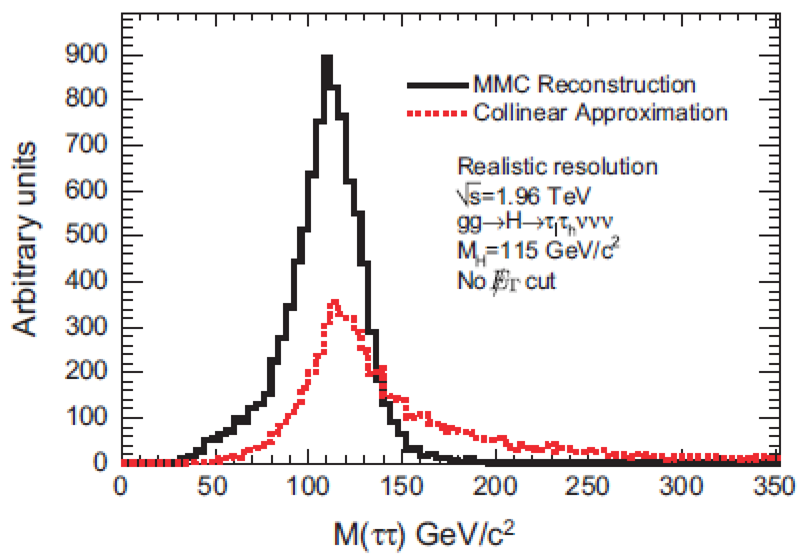

Nucl.Instrum.Meth. A654 (2011) 481-489

Improvement comes from requiring that the relative orientations of the neutrinos and other decay products are consistent with the mass and kinematics of a τ lepton decay

2 The SM BEH boson (H→bb) targetting VBF

Phys.Rev. D98 (2018) no.5, 052003

- Three analysis channels:
  - 2 b-tagged jets + forward jet(s)
  - 2 b-tagged jets + 2 central jets
  - 2 b-tagged jets + 2 forward jets + central high-p_T γ
- Use BDT to select signal regions (Total of 9)

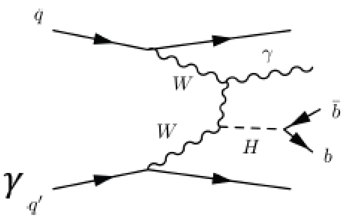

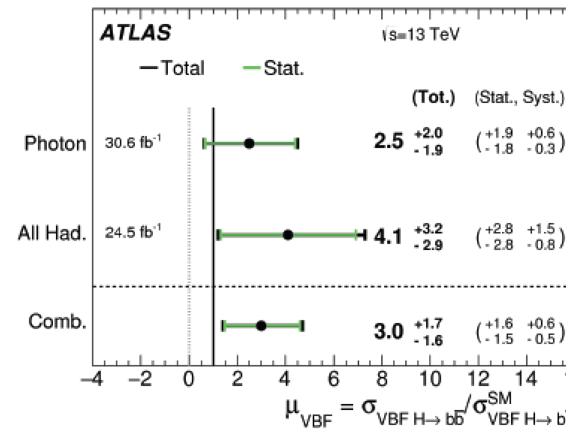

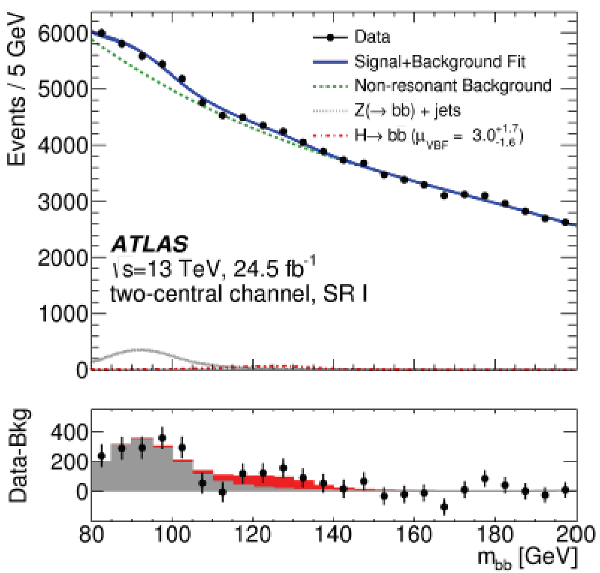

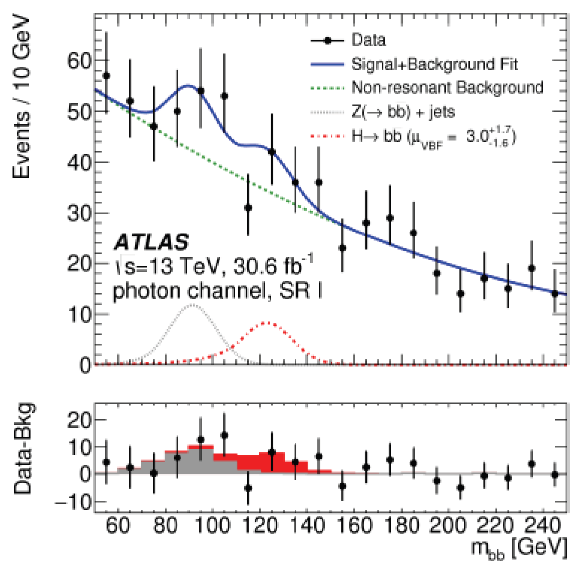

- Fit to the m_{bb} spectrum
- Significance: 1.9σ obs. (0.7σ exp.)
- Observed signal strength for the Higgs boson: $\mu_H = 2.5 \pm 1.3(stat.)\ ^{+0.6}_{-0.4}(syst.)$
- Statistically limited, more data needed

2 The SM BEH boson (H→bb) targetting gg→H J

- Boosted analysis: 2 large-R jets
- 2 b-tagged track jets in one large R-jet
- Higgs-candidate jet: p_T > 480 GeV
- Fit to the jet-mass spectrum

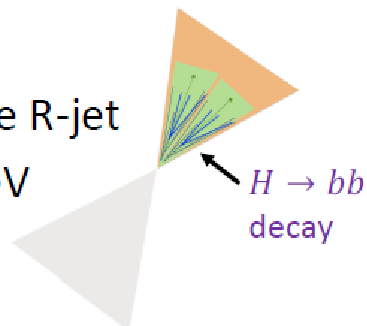

ATLAS-CONF-2018-052

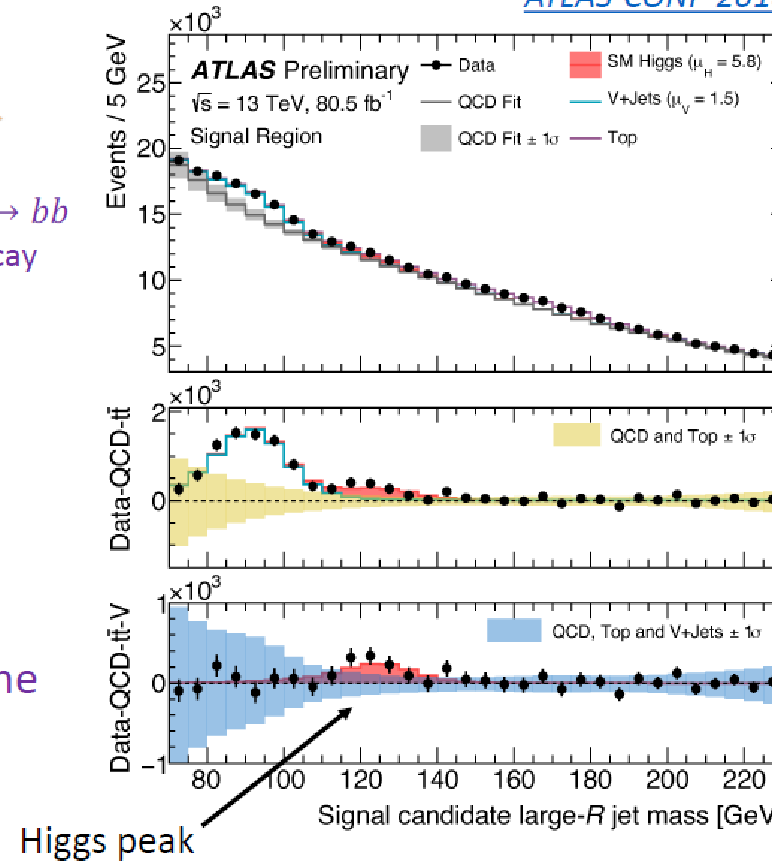

- Significance: 1.6σ obs. (0.28σ exp.)
- Needs more data

- Analysis is sensitive to $p_T^H > 480\ GeV$
- Promising analysis to test for deviations from the SM and to include in STXS cross sections!

2 The SM BEH boson STXS = simplified template cross sections

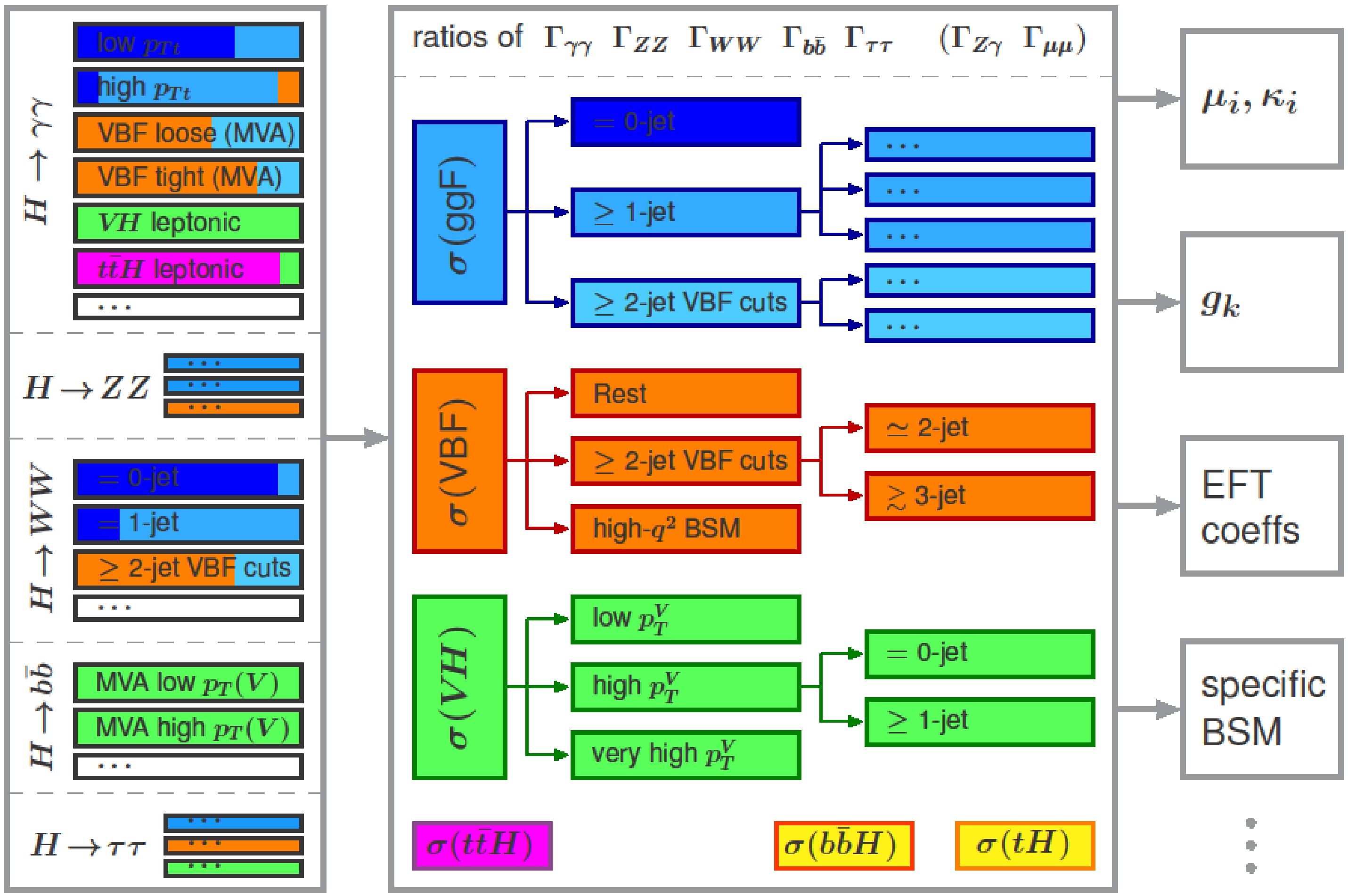

https://twiki.cern.ch/twiki/pub/LHCPhysics/LHCHXSWGFiducialAndSTXS/simplifiedXS.pdf

2 The SM BEH boson STXS = simplified template cross sections

designed to measure the different Higgs boson production processes in specific regions of phase space and in a way that can be easily combined with other decay channels

Compared to the signal strength measurements they provide finer granularity

theory uncertainties are smaller

In fact there are 31 STXS , but measure 9 (lack of statistics)

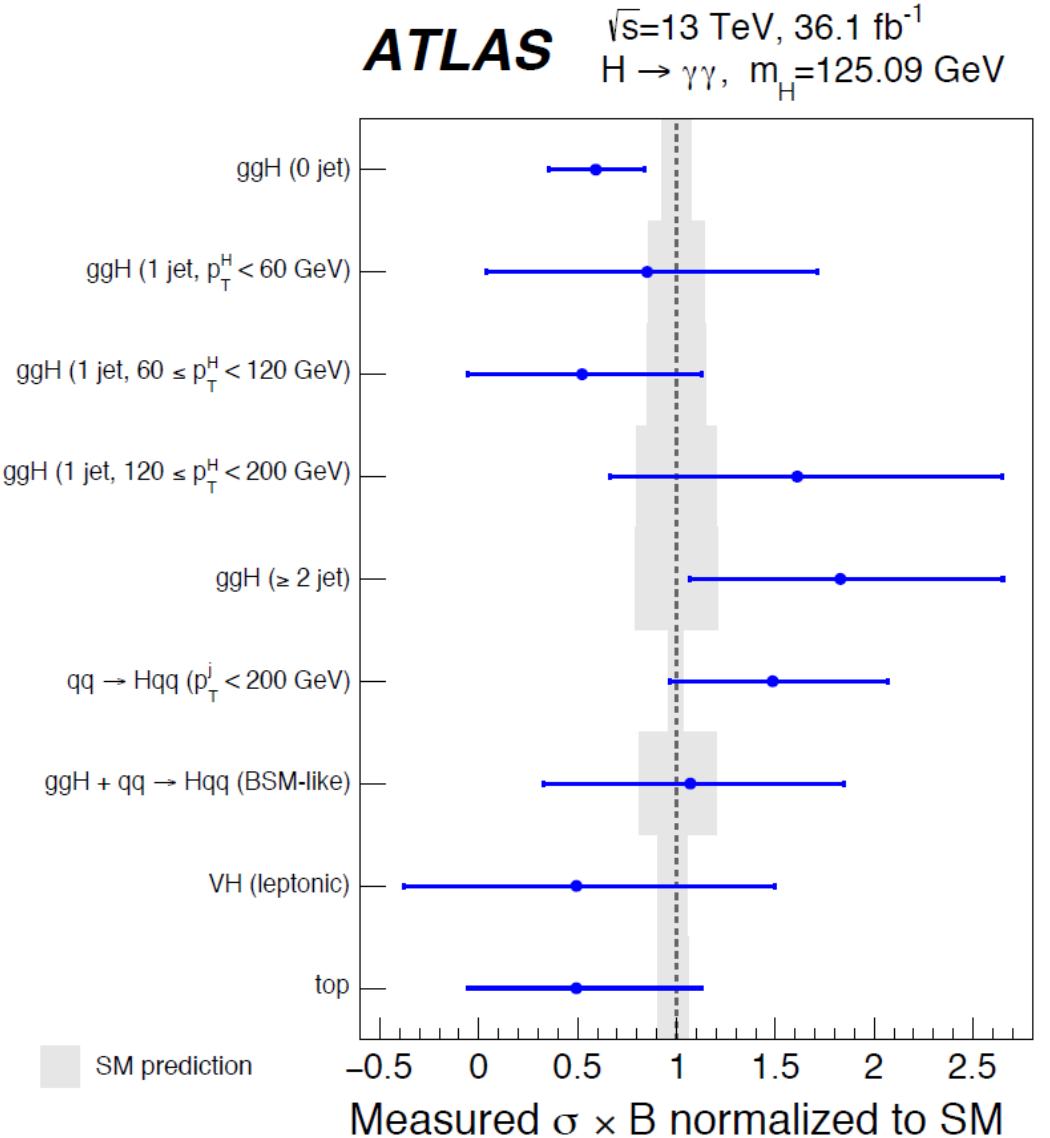

arXiv:1802.04146

2 The SM BEH boson (H→bb) STXS

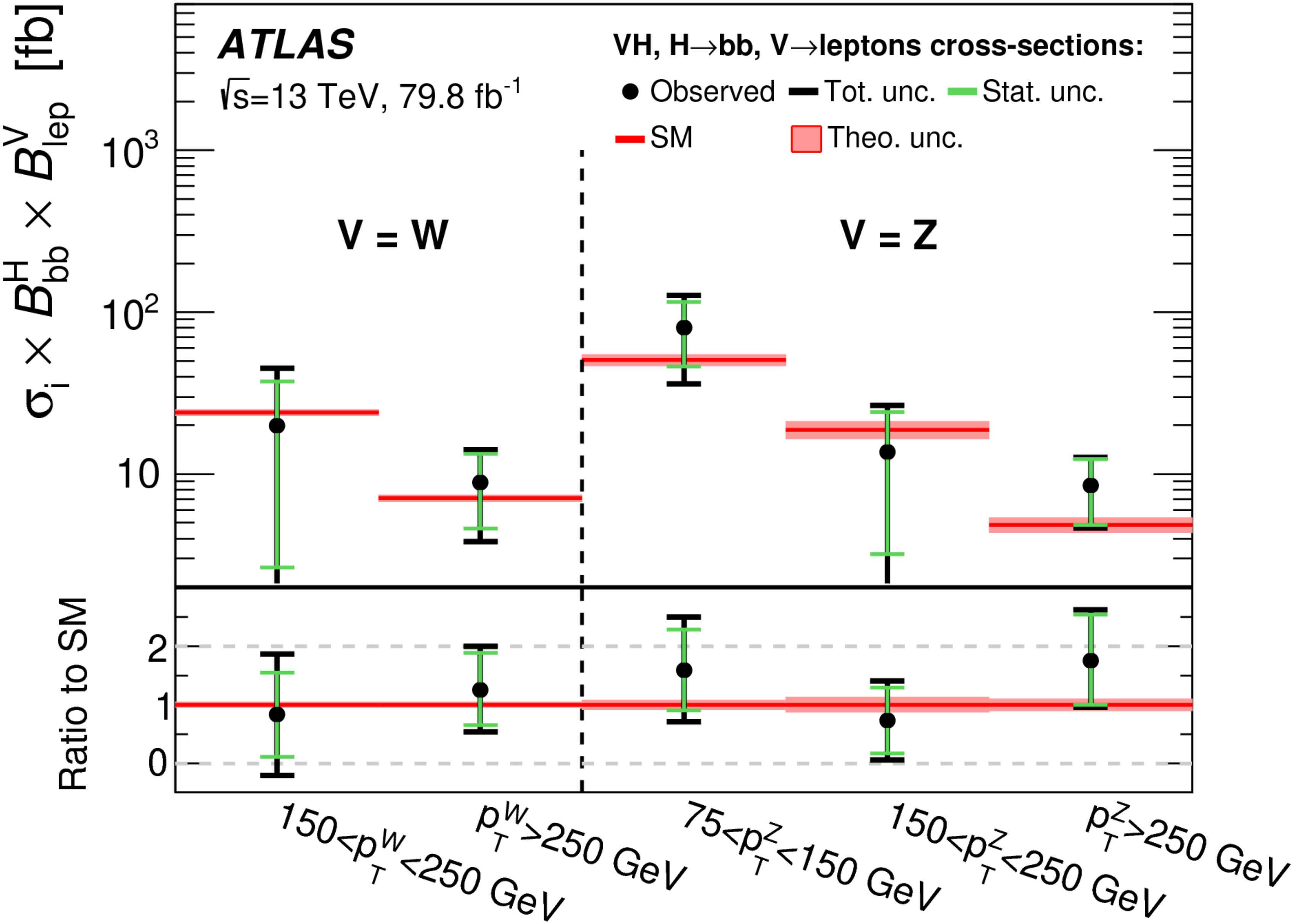

JHEP 05 (2019) 141

2 The SM BEH boson V (Z→bb)

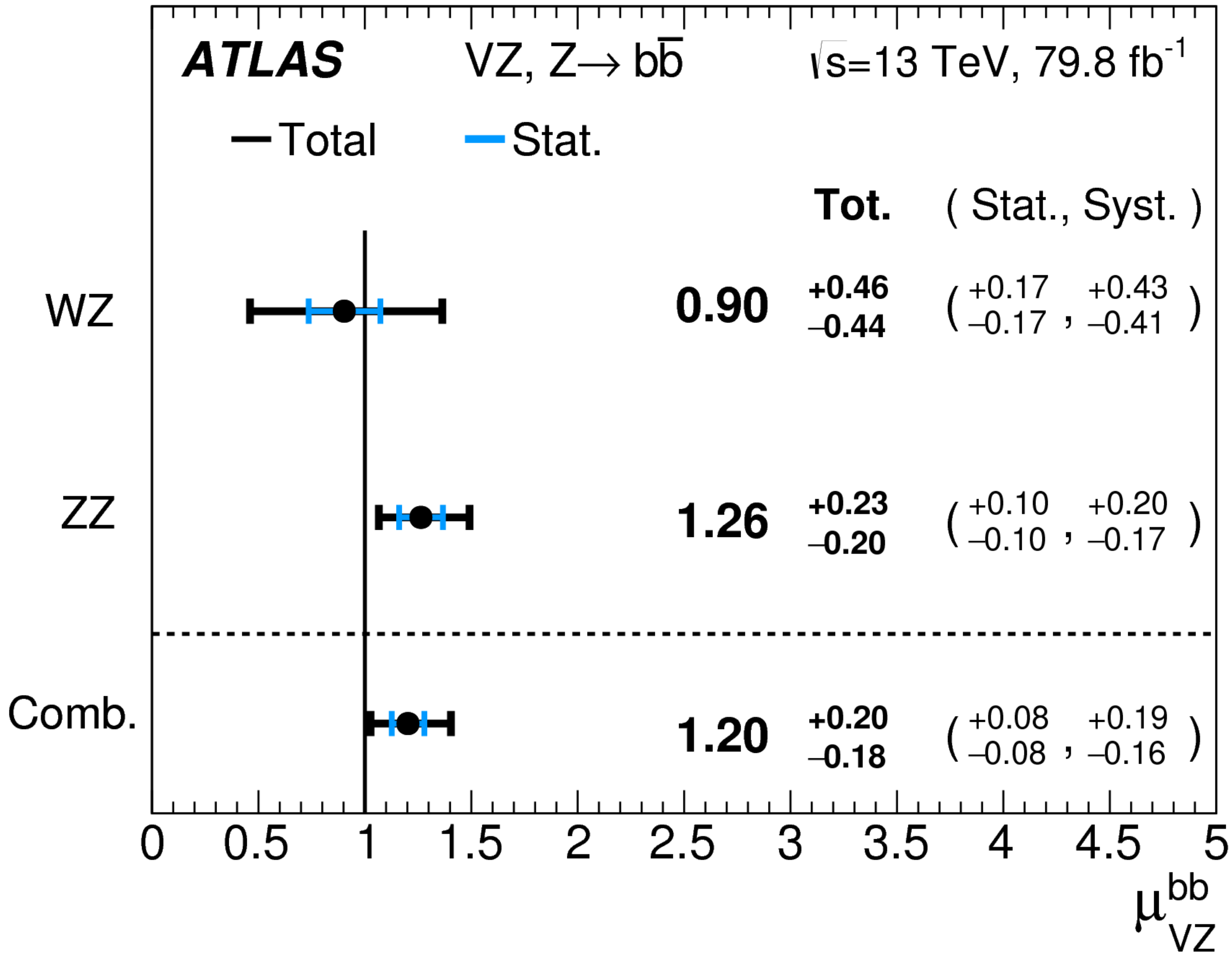

Phys.Lett. B786 (2018) 59-86

2 The SM BEH boson V (H→bb)

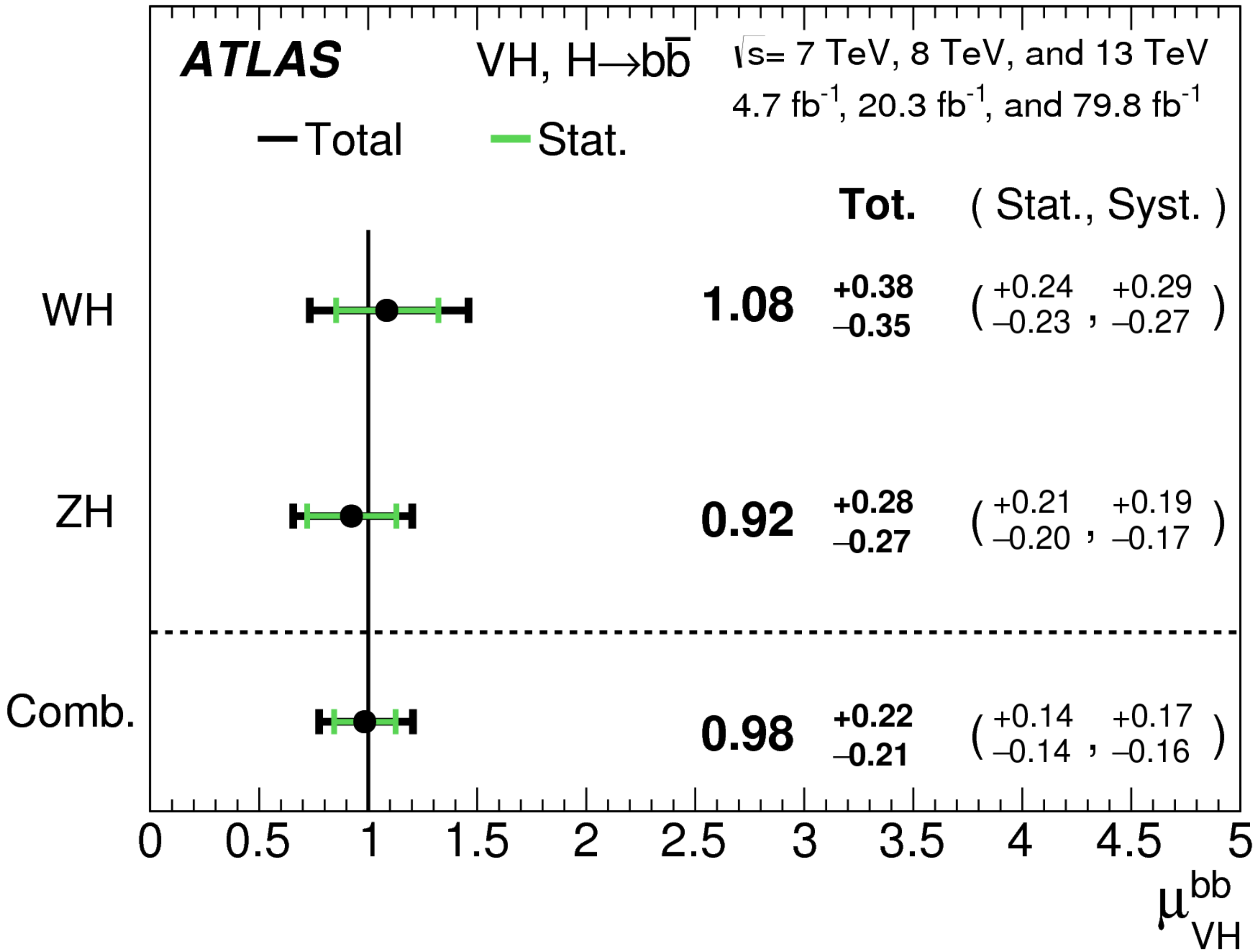

Phys.Lett. B786 (2018) 59-86

2 The SM BEH boson (H→bb)

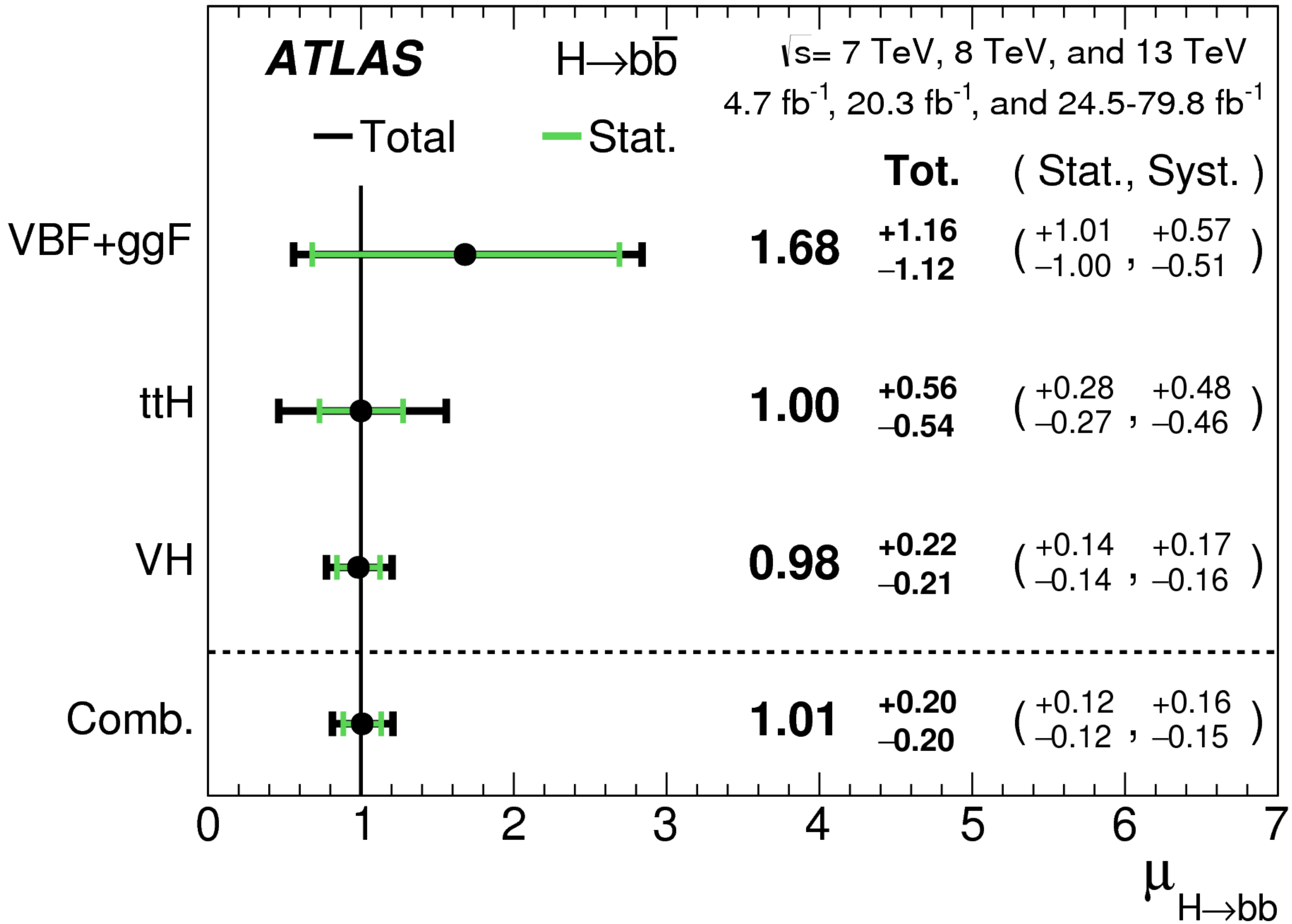

Phys.Lett. B786 (2018) 59-86

2 The SM BEH boson VH

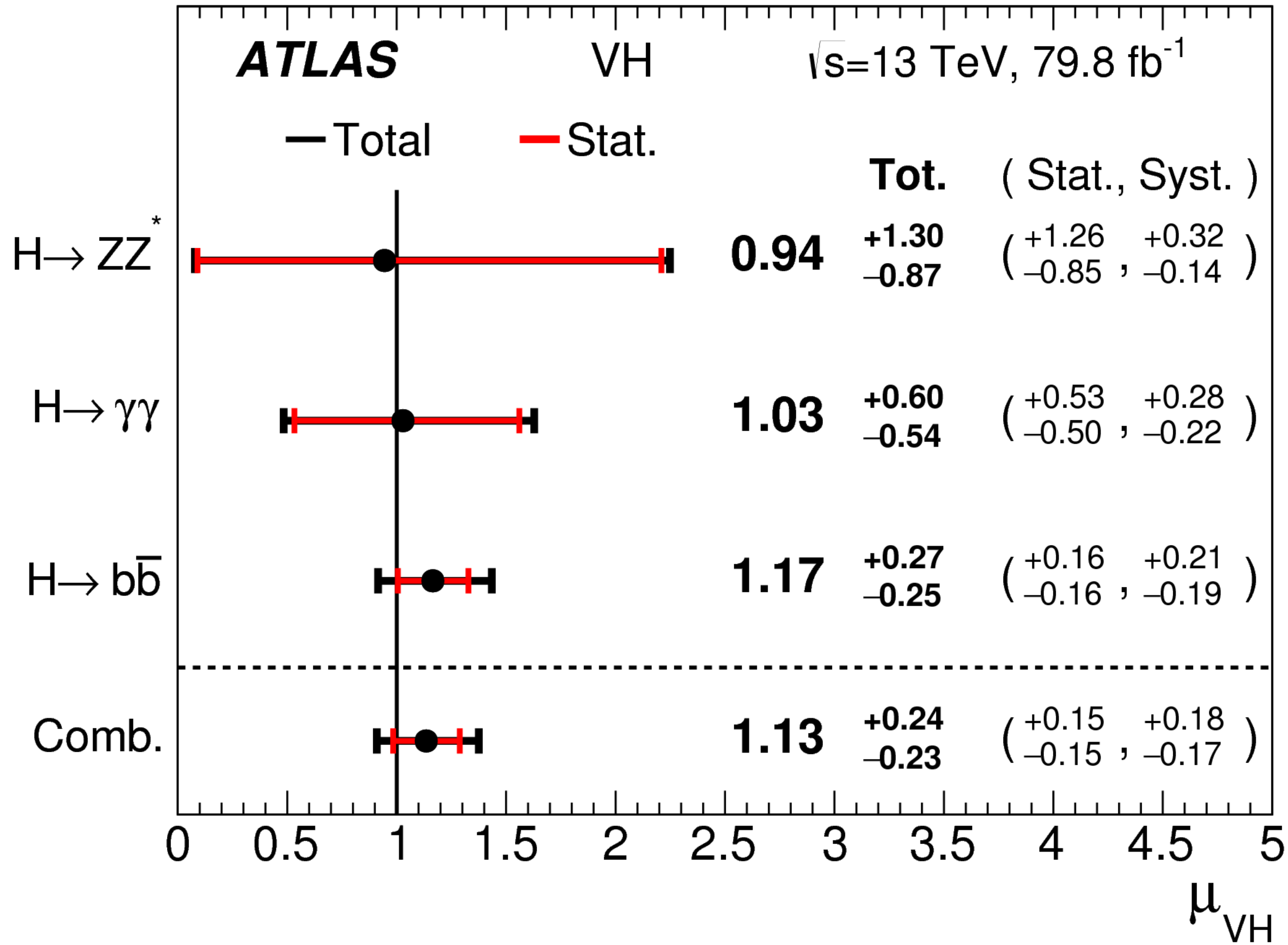

Phys.Lett. B786 (2018) 59-86

2 The SM BEH boson ttH

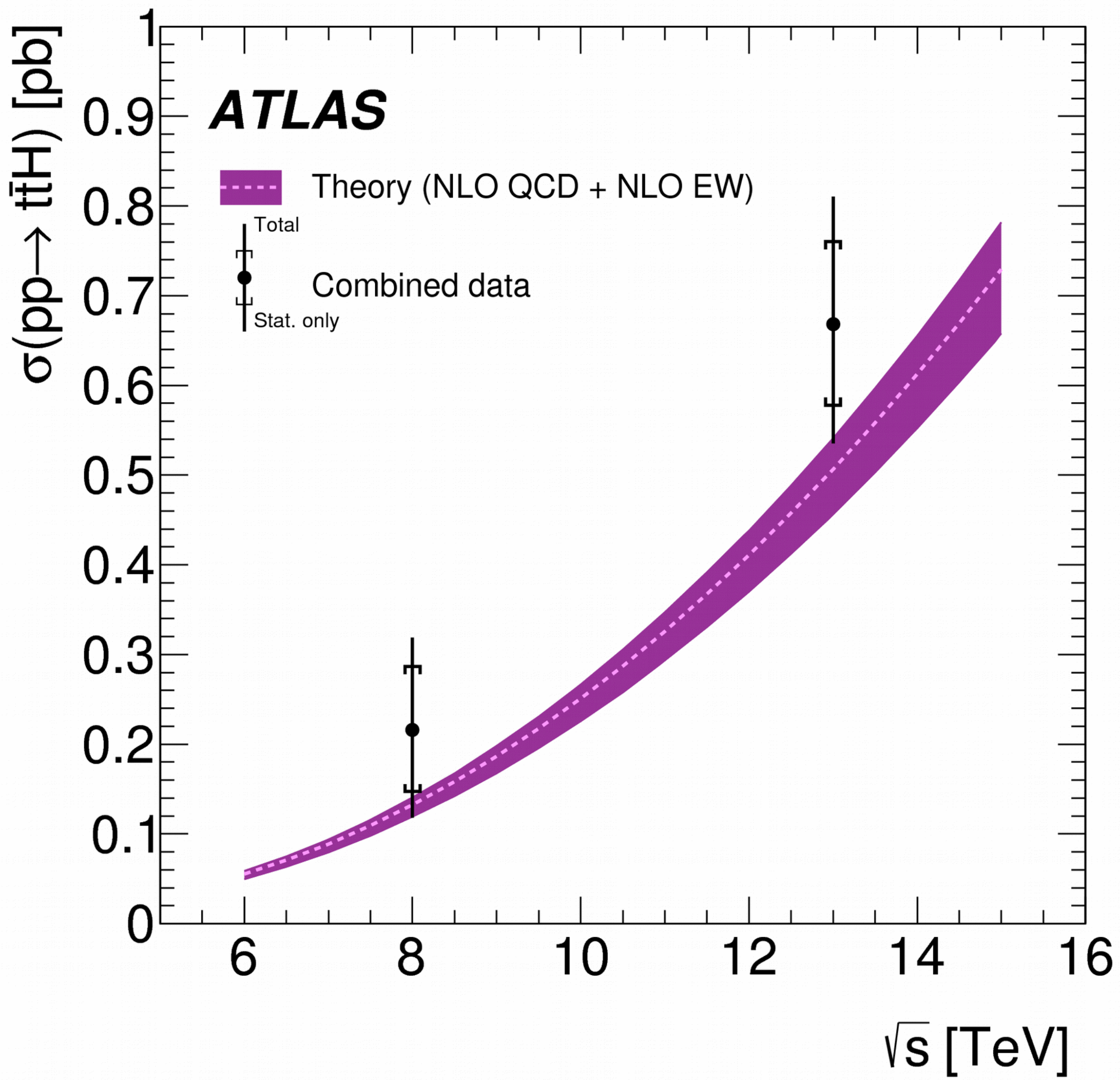

Phys.Lett. B784 (2018) 173-191

2 The SM BEH boson ttH ($\to\gamma\gamma$)

Category	σ_{68} (GeV)	σ_{90} (GeV)
"Lep" Category 1	1.56	2.80
"Lep" Category 2	1.75	3.13
"Lep" Category 3	1.85	3.30
"Had" Category 1	1.39	2.48
"Had" Category 2	1.58	2.84
"Had" Category 3	1.65	2.96
"Had" Category 4	1.67	3.00

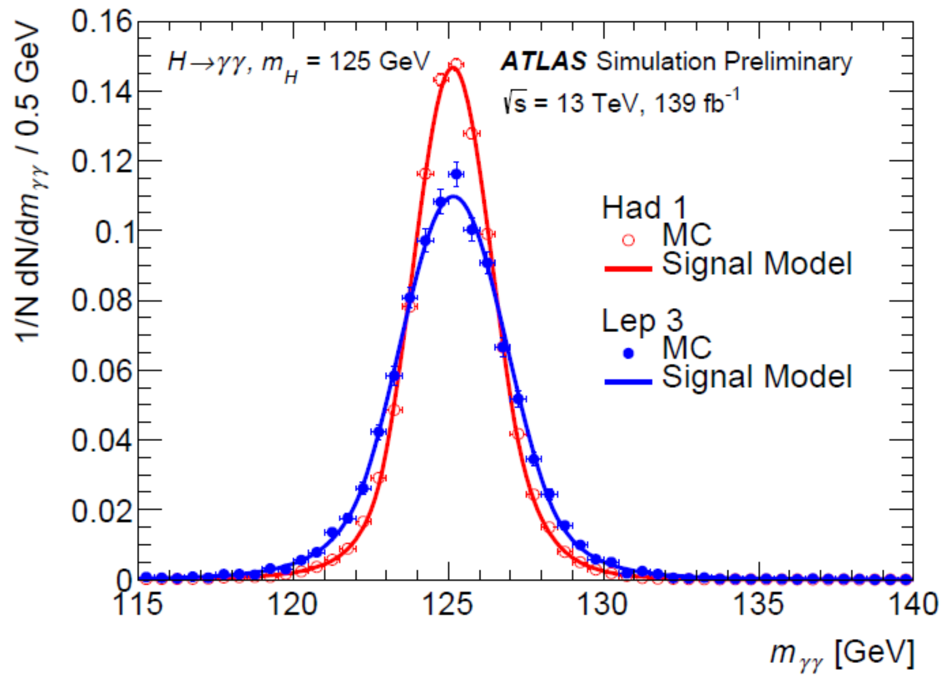

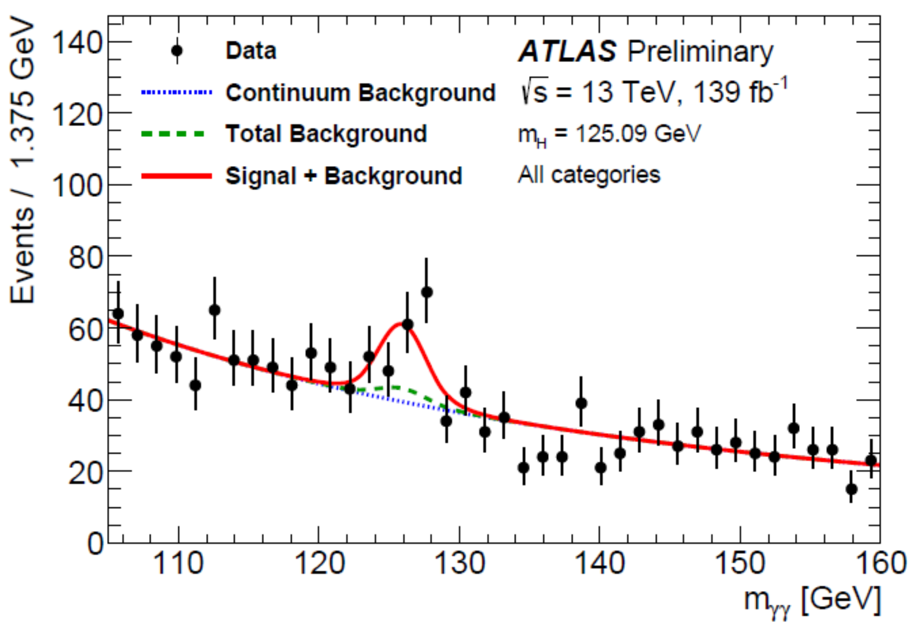

ATLAS-CONF-2019-004

2 The SM BEH boson categories

Several categories are made in order to enhance the sensitivity in order to have different S/B , based on

- **number of jets**
- **different resolutions**
- **different kinematics giving different S/B**

S/B has to be different for various categories

This is needed if we want to gain in statistical significance

if $S_1 / B_1 = S_2 / B_2$

then $S_1 / \sqrt{B_1} \oplus S_2 / \sqrt{B_2} = (S_1+S_2) / \sqrt{(B_1+B_2)}$

and one does not gain making categories

(one of) the work of the experimentalist is to find categories with different S/B !

2 The SM BEH boson invisible H decays

three bins of m_{jj} defined by
boundaries at [1, 1.5, 2, -] TeV

For the SR, an event is required to have

- no isolated electron or muon,
- a leading jet with $p_T > 80$ GeV,
- a subleading jet with $p_T > 50$ GeV,
- no additional jets with $p_T > 25$ GeV,
- $E_T^{miss} > 180$ GeV,
- $H_T^{miss} > 150$ GeV.

The two jets are required to have the following properties:

- not be aligned with $\vec{E}_T^{miss}$, $|\Delta\phi_{j\text{-MET}}| > 1$,
- not be back-to-back, $|\Delta\phi_{jj}| < 1.8$,
- be well separated in η, $|\Delta\eta_{jj}| > 4.8$,
- be in opposite η hemispheres, $\eta_{j_1} \cdot \eta_{j_2} < 0$,
- $m_{jj} > 1$ TeV.

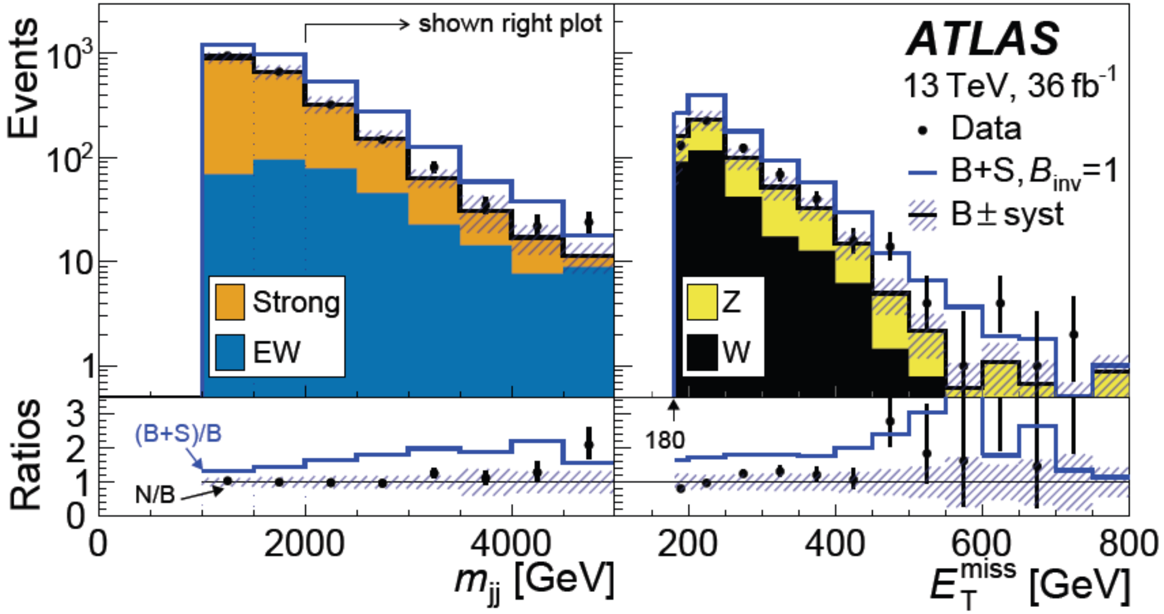

2 The SM BEH boson $H\to \mu\mu$

Category	Data	S_{SM}	S	B	$S/\sqrt{B}$	S/B [%]
VBF High	40	4.5	2.3	34	0.39	6.6
VBF Medium	109	5.5	2.8	100	0.28	2.8
VBF Low	450	9.6	4.9	420	0.24	1.2
2-jet High	3400	38	19	3440	0.33	0.6
2-jet Medium	13938	70	35	13910	0.30	0.3
2-jet Low	40747	75	38	40860	0.19	0.1
1-jet High	2885	32	16	2830	0.31	0.6
1-jet Medium	24919	107	54	24890	0.35	0.2
1-jet Low	77482	134	68	77670	0.24	0.1
0-jet High	24777	85	43	24740	0.27	0.2
0-jet Medium	85281	155	79	85000	0.27	0.1
0-jet Low	180478	144	73	180000	0.17	<0.1

ATLAS-CONF-2019-028

2 The SM BEH boson H→ 4l

ATLAS-CONF-2019-025

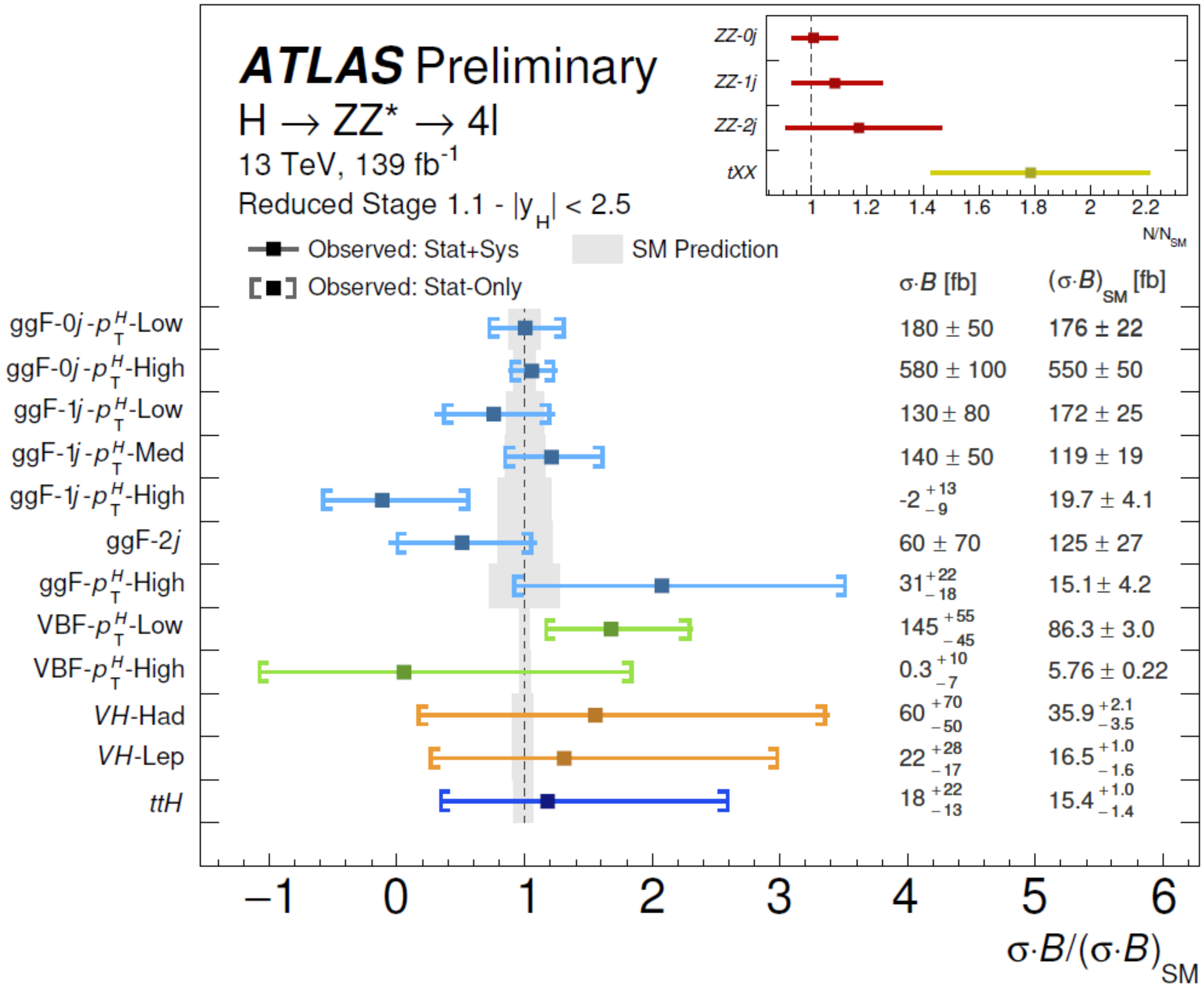

2 The SM BEH boson $H \to \gamma\gamma$

Table 3: The breakdown of uncertainties on the inclusive diphoton fiducial cross section measurement. The uncertainties from the statistics of the data and the systematic sources affecting the signal extraction are shown. The remaining uncertainties are associated with the unfolding correction factor and luminosity.

Source	Uncertainty (%)
Statistics	6.9
Signal extraction syst.	7.9
Photon energy scale & resolution	4.6
Background modelling (spurious signal)	6.4
Correction factor	2.6
Pile-up modelling	2.0
Photon identification efficiency	1.2
Photon isolation efficiency	1.1
Trigger efficiency	0.5
Theoretical modelling	0.5
Photon energy scale & resolution	0.1
Luminosity	1.7
Total	11.0

ATLAS-CONF-2019-029

139 fb^{-1}

Source	Uncertainty (%)
Fit (stat.)	10
Fit (syst.)	8.3
Photon energy scale & resolution	4.0
Background modeling (spurious signal)	7.3
Correction factor	5.2
Photon isolation efficiency	4.6
Pileup	1.9
Photon ID efficiency	1.3
Trigger efficiency	0.7
Dalitz Decays	0.4
Theoretical modeling	$^{+0.3}_{-0.4}$
Diphoton vertex selection	0.1
Photon energy scale & resolution	0.1
Luminosity	2.0
Total	14

ATLAS-CONF-2018-028 **80 fb^{-1}**

Uncertainty in fiducial cross section

Source	Diphoton
Fit (stat.)	17%
Fit (syst.)	6%
Photon energy scale & resolution	4.3%
Background modelling	4.2%
Photon efficiency	1.8%
Jet energy scale/resolution	-
b-jet flavor tagging	-
Lepton selection	-
Pileup	1.1%
Theoretical modeling	0.1%
Signal composition	0.1%
Higgs boson p_T^H & $\|y_H\|$	0.1%
UE/PS	-
Luminosity	3.2%
Total	18%

Uncertainty Group	$\sigma_\mu^{\text{syst.}}$
Theory (QCD)	0.041
Theory ($B(H \to \gamma\gamma)$)	0.028
Theory (PDF+α_S)	0.021
Theory (UE/PS)	0.026
Luminosity	0.031
Experimental (yield)	0.017
Experimental (migrations)	0.015
Mass resolution	0.029
Mass scale	0.006
Background shape	0.027

Phys.Rev. D98 (2018) 052005 **36 fb^{-1}**

2 The SM BEH boson H→ γγ

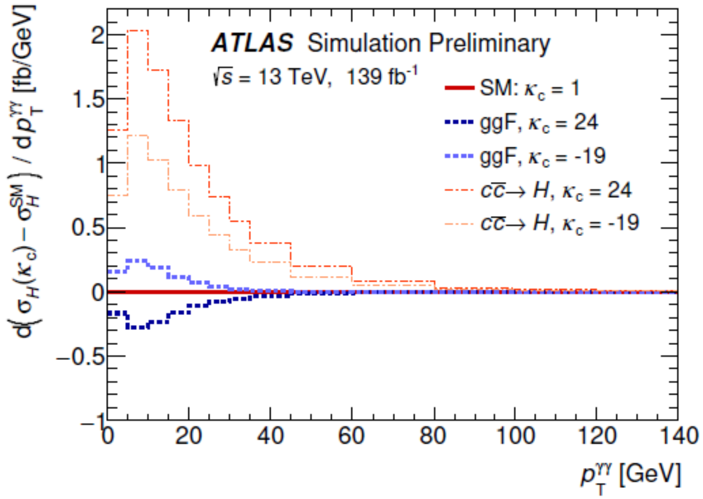

Figure 14: The modification of the $p_T^{\gamma\gamma}$ differential cross section for different values of κ_c, shown separately for the cross sections of the ggF and $c\bar{c} \to H$ production modes. As expected, for a given value of κ_c, the effect on the $c\bar{c} \to H$ production cross section is larger than that on the ggF production.

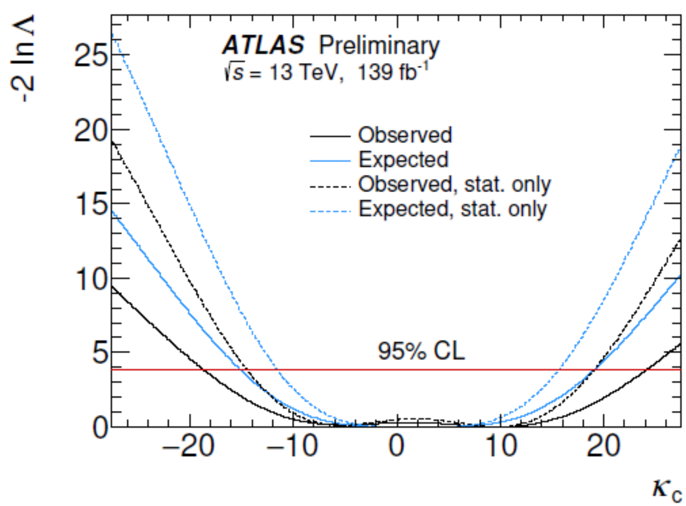

Figure 15: The profile likelihood ratio, λ, shown as a function of κ_c for the fit to the $p_T^{\gamma\gamma}$ distribution. The intersection of the $-2\ln\Lambda$ curve with the horizontal line provides the 95% confidence intervals.

ATLAS-CONF-2019-029

3 Search for a pair of BEH bosons constraint of the H self-coupling from H differential production and decay mesurements

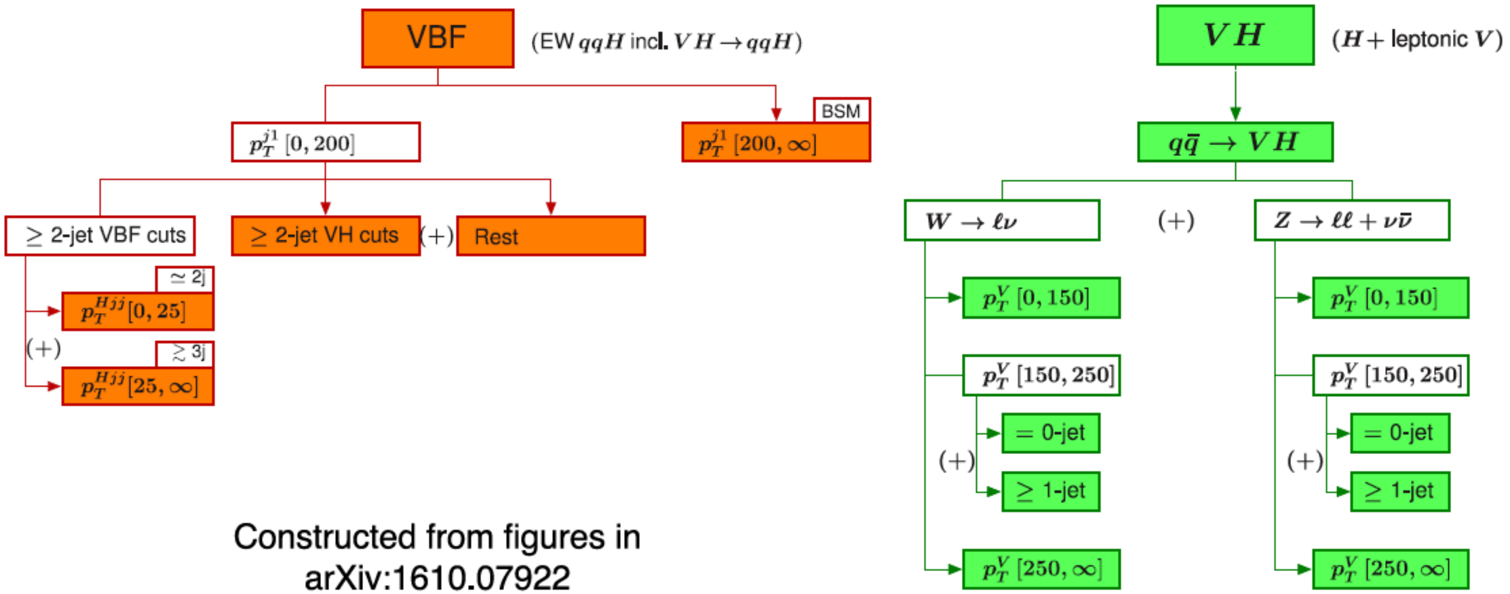

Constructed from figures in arXiv:1610.07922

Figure 3: Schematic diagram of the VBF + V(had)H (left) and V(lep)H (right) STXS regions. $p_{\rm T}^{Hjj}$ is the $p_{\rm T}$ of the Higgs boson plus two jets system, $p_{\rm T}^{V}$ is the $p_{\rm T}$ of the vector boson V in the VH production mode, $p_{\rm T}^{j1}$ is the $p_{\rm T}$ of the jet with the highest $p_{\rm T}$. In the VH, $H \to b\bar{b}$ analysis, the separation in jet number of the $p_{\rm T}^{V}$ [150, 250] region in the VH production mode has been ignored, merging the 0 and the ≥ 1 jet regions. The diagrams are obtained from Ref. [14].

♪ ***Results from (run 1 and) run 2***

- ***detector***
- ***SM***
- ***BSM***
- ***(B-E)H***
- ***Vector-boson scattering***

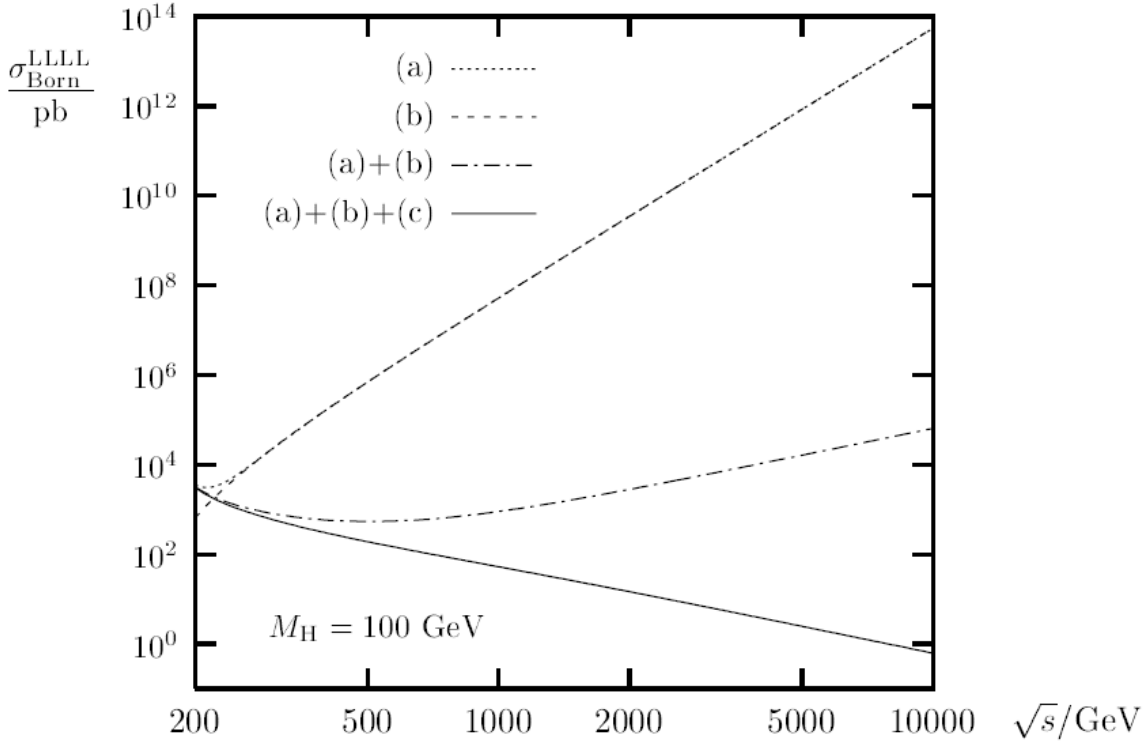

Denner Hahn Nucl.Phys. B525 (1998) 27-50

Figure 2: The cross-sections for longitudinal gauge-boson scattering resulting from subsets of the tree-level diagrams: (a) diagrams involving only three-gauge-boson couplings, (b) diagram involving only four-gauge-boson couplings, (c) diagrams involving Higgs bosons.

- ♪ *Historical introduction , Setting the stage*
- ♪ *Results from (run 1 and) run 2*
- ♪ ***Future of ATLAS , run 3 , HL-LHC***
- ♪ *Conclusions*
- ♪ *Backup*

- ♪ *Historical introduction , Setting the stage*
- ♪ *Results from (run 1 and) run 2*
- ♪ *Future of ATLAS , run 3 , HL-LHC*
- ♪ ***Conclusions***
- ♪ *Backup*